Philipps Universität Marburg

Nejire/dCBP-mediated control of H3 acetylation and transcriptional regulation by testis-specific Plus3 domain proteins during *Drosophila* spermatogenesis

Dissertation

zur Erlangung des Doktorgrades

der Naturwissenschaften

(Dr. rer. nat.)

Dem Fachbereich Biologie

der Philipps-Universität Marburg

vorgelegt von

Tim Hundertmark

aus Extertal/Lippe

Marburg/Lahn 2018

Vom Fachbereich Biologie der Philipps-Universität Marburg als Dissertation angenommen am:
02.11.2018

Erstgutachterin: Prof. Dr. Renate Renkawitz-Pohl
Zweitgutachterin: Dr. Christina Pütz-Rathke

Tag der mündlichen Prüfung:
07.12.2018

Table of contents

Chapter 1

1 Statement of candidate's contribution

According to § 9, paragraph 1 of the "Doctoral regulations of the departments of mathematics and natural sciences and the department of medicine for its mathematics and natural sciences disciplines (dated 15 July 2009)" publications may be accepted as dissertation work "[…] that have emerged from the doctoral study and have been published in, or submitted to, highly regarded journals […]. In such cases, […] a separate declaration must provide a statement on the contribution that the doctoral candidate has made to the publications." The contribution to the publications presented in this dissertation is described in detail before the respective publications in Chapters 5-9.

Chapter 2: Zusammenfassung

2 Zusammenfassung

Die Spermatogenese beschreibt den Prozess der Entwicklung von Keimbahnstammzellen hin zu hochspezialisierten Spermien. Die Spermatogenese von *Drosophila melanogaster* eignet sich sehr gut als Modell zur Analyse von Umstrukturierungen des Chromatins in männlichen Keimzellen, da die zugrundeliegenden Prozesse in Säugetieren und Fliegen sehr ähnlich sind. Histon-Modifikationen sind beispielsweise eine Voraussetzung für den Austausch von Histonen durch Protamine in postmeiotischen Stadien der Spermatogenese, aber auch Prozesse auf Transkriptionsebene früheren Keimzellstadien lassen sich vergleichen. Im Rahmen dieser Arbeit wurde die Histonacetyltransferase Nejire/dCBP, die für die Modifikation von Histon H3 an Lysin 18 und Lysin 27 sowohl während der postmeiotischen Keimzellentwicklung als auch im Spermatozytenstadium verantwortlich ist, näher charakterisiert. Durch einen RNAi-vermittelten knock-down von Nejire/dCBP konnte gezeigt werden, dass dessen Funktion essentiell für die Fertilität männlicher Fliegen ist. Die effiziente Synthese von mRNAs postmeiotisch exprimierter Chromatinkomponenten scheint durch Nejire/dCBP reguliert zu werden. Der Einbau von Protaminen in das Chromatin scheint jedoch nicht direkt von der Funktion von Nejire/dCBP anhängig zu sein. Die *Drosophila* Spermatogenese zeichnet sich durch eine besondere Regulation der Transkription und der Translation aus. Während die meisten Transkripte in Spermatozyten hergestellt werden, muss ein Großteil davon translational reprimiert werden, um in späteren Stadien der Keimzellentwicklung zur Verfügung zu stehen. Die Regulation der Transkription in Spermatozyten wird von Testis-spezifischen Varianten der generellen Transkriptionsmaschinerie unterstützt. Dazu gehören unter anderem die tTAFs, der tMAC Komplex und Bromodomänen-Proteine. Bromodomänen-Proteine sind in der Lage, acetylierte Lysine an N-terminalen Histonketten zu erkennen und an diese zu binden. Die in Spermatozyten exprimierten Bromodomänenproteine tBRD-1 und tBRD-2 können mit tTAFs interagieren und schaffen so möglicherweise eine Möglichkeit für die Rekrutierung des TFIID Komplexes an bestimmte Bereiche des Chromatins.

Weitere Testis-spezifische Varianten ubiquitär exprimierter Proteine stellen die Plus3-Domänenproteine dar. Im Rahmen dieser Arbeit wurde die Expression und die Funktion der im Testis angereicherten Proteine tPlus3a und tPlus3b untersucht. Diese Proteine besitzen eine konservierte Plus3-Domäne. Mit Hilfe einer RNAseq Analyse von RNA aus Testes von Mutanten konnte gezeigt werden, dass tPlus3a und tPlus3b wahrscheinlich zur Regulation der Transkription in Spermatozyten beitragen. Zudem wurden dabei Gene identifiziert die ebenfalls durch tBRD-1 reguliert werden. Unsere Hypothese ist, dass tPlus3a und tPlus3b eine Gruppe von Genen regulieren, die zwar mit denen der tBRD-1-abhängigen Gene überlappen, jedoch kaum mit den tTAF-abhängigen Genen. tPlus3a und tPlus3b könnten so zur Diversifizierung der Transkriptionsregulation in Spermatozyten beitragen.

Chapter 3: Summary

3 Summary

Spermatogenesis describes the development from germ line stem cells to highly specialized sperm. *Drosophila melanogaster* spermatogenesis is a good model system for chromatin remodelling processes as many of these processes are similar in mammals and in flies. Histone modifications are a prerequisite for the exchange of histones by protamines during these chromatin remodelling processes but also transcription processes in earlier germ cell stages can be compared.

In this thesis, the histone acetyltransferase Nejire/dCBP has been characterised as being responsible for the modification of histone H3 at lysine 18 and lysine 27 during post-meiotic germ cell development as well as in the spermatocyte stage. An RNAi-mediated knock-down revealed that the function of Nejire/dCBP is essential for fertility of male flies. Efficient mRNA synthesis of post-meiotic chromatin components depends on Nejire/dCBP whereas incorporation of protamines into the chromatin does not seem to depend on Nejire/dCBP function.

Drosophila spermatogenesis is featured by a special regulation of transcription and translation. While most transcripts are synthesised in spermatocytes, a large portion has to be translationally repressed until required in later stages of germ cell development. Transcriptional regulation is supported by testis-specific variants of the general transcription machinery. This includes among others the tTAFs, the tMAC complex and bromodomain proteins. Bromodomain proteins are able to recognise and bind acetylated lysine residues on N-terminal histone chains. The bromodomain proteins tBRD-1 and tBRD-2 are expressed in spermatocytes and can interact with tTAFs, this might facilitate recruitment of the TFIID complex to certain chromatin areas.

Further testis-specific variants of ubiquitously expressed proteins are the Plus3 domain proteins. Here, the expression and function of the testis-enriched proteins tPlus3a and tPlus3b have been examined. Both proteins share the conserved Plus3 domain of Rtf1. RNAseq analysis using RNA from mutant testes revealed that tPlus3a and tPlus3b likely contribute to the regulation of transcription in spermatocytes. Furthermore, genes which also depend on tBRD-1 function were identified. We hypothesise that tPlus3a and tPlus3b regulate a group of genes overlapping with tBRD-1-depending genes but not with genes depending on tTAFs. tPlus3a and tPlus3b might therefore contribute to diversification of transcriptional regulation in spermatocytes.

Chapter 4: Introduction

4 Introduction

Spermatogenesis describes the developmental process from diploid germ line stem cells (GSCs) to haploid sperm. Impaired sperm production can ultimately cause infertility; 20 to 70 percent of cases of infertility in couples are affiliated to male factors (reviewed in Agarwal et al., 2015). *Drosophila melanogaster* (hereafter referred to as *Drosophila*) is an excellent model organism to study spermatogenesis, as many characteristic features of sperm development are conserved between mammals and flies. The development of male germ cells in *Drosophila* takes place in two paired testes, shaped as curls in the adult fly. Accompanied by histone modifications, chromatin reorganisation takes place in post-meiotic germ cell stages. During this reorganization, histones are exchanged by transition proteins and eventually by protamines. Additionally, the morphology of germ cells, including the nuclei, is changing dramatically, resulting in a needle-like shape of the nucleus. Both mammals and flies share specific mechanisms to ensure correct development in post-meiotic male germ cells. For example, in *Drosophila*, the majority of transcripts is synthesised in the spermatocyte stage, even though many transcripts are first needed in the post-meiotic phase. Therefore, many mRNAs are translationally repressed after synthesis and released later in development. Like spermatocytes in *Drosophila*, round spermatids in mammals exhibit a high transcriptional activity, which decreases in later stages (reviewed in Rathke et al., 2014).

4.1 Spermatogenesis in *Drosophila melanogaster*

Drosophila spermatogenesis (reviewed in Fuller, 1993) starts in the apical testis tip. There, the hub region comprises GSCs as well as somatic cells, which provide a signalling source for the GSC differentiation. Somatic cells in the hub region also contribute to the formation of cyst cells, two of which surround the germ cells during their whole development to mature sperm forming a cyst. A cyst first contains a spermatogonium, originating from a GSC. In the cyst, the spermatogonium undergoes four mitotic divisions, resulting in 16 primary spermatocytes. Cytokinesis is incomplete so that primary spermatocytes stay connected through cytoplasmic bridges. The 16 spermatocytes of one cyst show an enormous growth leading to a 25-fold increase in size of the nucleus during G2 phase (Lindsley and Tokayasu, 1980). Apart from an increasing size, a peak in transcriptional activity is characteristic for the spermatocyte stage until prophase of meiosis I. Right after this prolonged meiotic prophase transcription decreases and the cells enter meiotic divisions. Hardly any transcription is detectable in post-meiotic stages (Olivieri and Olivieri, 1965) except for some rare transcripts, which are newly synthesised and abundant in elongating spermatids (Barreau et al., 2008). In spermatocytes, the two large autosomes and the X- and Y-chromosomes are disposed in distinct chromatin regions in the nucleus. After two meiotic divisions, 64 haploid spermatids emerge from the spermatocytes. Spermatids are still connected via cytoplasmic bridges within the cyst. Initially, these spermatids are round and the chromatin appears to be in a relaxed state. The following development of the initially round spermatids to mature sperm is called spermiogenesis. It is characterised by enormous

morphological changes, e.g. the formation of the sperm flagellum or nuclear elongation and the reorganisation of chromatin. For changes of morphology, different stages can be defined: the nucleus starts to elongate while cellular organelles are re-configured to adapt to a smaller volume of elongating spermatids. Therefore, the mitochondria merge to form the Nebenkern, which is then elongating alongside the spermatid nucleus. As the nucleus further stretches, the axoneme of the future flagellum is forming from the basal body and the so-called canoe stage is reached, named for its canoe shaped nuclei. The flagella are mainly built from microtubules, mitochondria and outer dense fibers, their components represent a large portion of all proteins in the testis. The flagella are very long - flagella of spermatids near the basal end of the testis even reach the apical region. At the end of spermiogenesis, the morphology of the spermatid nucleus obtains a thin, needle-like shape. An actin-based structure, called individualization complex (IC), forms to separate the 64 spermatids of a cyst from each other. Finally, mature sperm are released from the testis and reach the seminal vesicles (reviewed in Fuller, 1993).

4.2 Chromatin dynamics during spermatogenesis

Whilst the morphological changes of nucleus and organelles are clearly visible in phase contrast microscopy or with Hoechst staining of spermatid nuclei, reorganisation of chromatin is at first glance inconspicuous even though it occurs in parallel to nuclear shaping. The chromatin structure in spermatocytes and in round spermatids is - as in somatic cells - histone based. As the nucleus becomes smaller, the chromatin in spermatids is being compacted. Histones are gradually exchanged by transition proteins represented by TP1 and TP2 in mice (Brewer et al., 2002), and Tpl94D in *Drosophila*, respectively (Rathke et al., 2007), which contribute to the compaction of chromatin. Transition proteins are in turn replaced by very basic protamines, ProtamineA and ProtamineB, and Mst77F (Jayaramaiah Raja and Renkawitz-Pohl, 2005). Protamine and Mst77F incorporation enables an even tighter compaction of chromatin (Doyen et al., 2015; Eren-Ghiani et al., 2015; Kost et al., 2015; Kimura and Loppin, 2016). Additionally, protamine-like proteins like Prtl99C are also part of the chromatin in mature sperm (Eren-Ghiani et al., 2015). The most prominent stage for the switch from histones to protamines is the canoe stage, the change takes place within about 5 hours as shown by *in vivo* imaging (Awe and Renkawitz-Pohl, 2010; Gärtner et al., 2014). The early canoe stage is defined by the presence of remaining histones, while in the late canoe stage protamines are incorporated into the chromatin and histones cannot be detected anymore. In addition to the proteins mentioned above, some histone variants are known, that are stable or transient components of chromatin in germ cells. The histone variants H2A.X, H2A.Z and H3.3 are part of the nucleosomes in spermatocytes and in early post-meiotic stages and are removed from chromatin in the same manner like canonical H2A or H3 (Rathke et al., 2007). HILS1 is a histone variant known to be part of post-meiotic chromatin in mammals (Yan et al., 2003). The *Drosophila* homologue of HILS1, Mst77F, is likewise expressed exclusively in post-meiotic germ cell stages and can even be found in mature sperm (Rathke et al., 2010). Several modifications of histones accompany chromatin reorganisation in

spermatocytes as well as in post-meiotic stages. SUMOylation, ubiquitination, phosphorylation, methylation and acetylation of histones can have various functions for chromatin remodelling and other processes (reviewed in Rathke et al., 2014).

4.2.1 Objective of this study: Visualisation of chromatin-associated proteins in *Drosophila* spermatogenesis

Spermatid chromatin is organised in a dynamic way and multiple steps have to be passed until the final compaction by protamines, Mst77F and Prtl99C is reached. As several homologous proteins are involved in both mammals and fly, *Drosophila* can serve as an excellent model to study the modification of histones and the replacement with transition proteins and protamines in immunofluorescence stainings. For some proteins an antibody-based detection might appear insufficient when used for highly compact chromatin. Therefore, a modified method for decondensation of chromatin prior to immunofluorescence staining was used to detect chromatin components in mature sperm (Eren-Ghiani et al., 2015).

The aim of this study was the elaboration of a detailed protocol for immunofluorescence stainings of *Drosophila* testis squash preparations. Different requirements for fixation and staining regarding spermatocytes or post-meiotic germ cell stages are included and should help with first immunostainings in fly testes. An alternative protocol (modified after Li et al., 2008) is given for decondensation before immunofluorescence stainings to enable detection of proteins also on compacted chromatin (see Chapter 5).

4.2.2 Objective of this study: Regulation of acetylation marks on H3K18 and H3K27 by Nejire/dCBP

Alongside chromatin compacting proteins, the modification of histones is likewise an expression of dynamic chromatin changes. Methylation of histones at H3K4 and H3K79 is assumed to open the chromatin structure (Rathke et al., 2014; Dottermusch-Heidel et al., 2014 a;b) while H3K9 and H3K27 methylation in transcriptionally silent post-meiotic germ cell stages in *Drosophila* suggests a contribution of these modifications to a repressed chromatin configuration (Rathke et al. 2007). Histone acetylation seems to be required for progression of spermiogenesis and is a prerequisite for histone removal as is was shown in histone acetyltransferase (HAT) inhibitor cultures with *Drosophila* testes (Awe and Renkawitz-Pohl, 2010). Furthermore, a correlation of different modifications is assumed, like the ubiquitination of H2A and a hyper-acetylation event of histone H4 in *Drosophila* (Rathke et al., 2007). Tan et al. discovered lysine crotonylation (Kcr) as mark of sex chromosome linked active genes. Alongside of Kcr, various other new modifications have been described to occur during spermiogenesis (Tan et al., 2011), making clear that further investigation of histone modifications is crucial for a full understanding of chromatin dynamics during *Drosophila* spermatogenesis.

This study reveals timing and localisation of several histone modifications, especially for H3 and H4. We describe the dependence of these modifications on HAT activity and incorporation of protamines using testis inhibitor culture. Furthermore, the inhibitor studies also reveal that crotonylation of histones in post-meiotic stages is depending on histone acetylation as Kcr is not detectable anymore when HATs are inhibited. Supporting an interdependence of histone acetylation and crotonylation the inhibition of histone deacetylases (HDACs) leads to a premature detection of Kcr. Interestingly, premature incorporation of protamines cannot be observed upon inhibition of HDACs. We characterised the HAT Nejire/dCBP as a key regulator of H3K18 and H3K27 acetylation in spermatocytes and in post-meiotic germ cells. Knock-down of Nejire/dCBP does not lead to a complete lack of protamines or other post-meiotic chromatin-associated proteins but to sterility in male (see Chapter 6).

4.3 mRNA expression profiles of the *Drosophila* testis

Spermatogenesis in animals is driven by a unique regulatory programme. Transcription, both in mammals and *Drosophila*, ceases at a certain point in male germ cell development. Although mice show transcription in post-meiotic stages of spermatogenesis (Kierszenbaum and Tres, 1975; Schultz et al., 2003) the synthesis of new mRNAs stops upon compaction of chromatin by protamines in late germ cell stages and further development relies on stored transcripts (Steger, 2001). The majority of transcription in *Drosophila* germ cells takes place during the spermatocyte stage. After meiosis, newly synthesised transcripts are barely detectable (Olivieri and Olivieri, 1965; Gould-Somero and Holland, 1975). Only a small number of genes have been described to be transcribed during elongation of spermatids (Barreau et al., 2008). The absence of active transcriptional processes in late stages of spermatogenesis suggests a storage of transcripts in earlier stages. These transcripts are translationally repressed and released from repression at the required time (White-Cooper, 2010) as exemplarily shown for example for protamine and Mst77F transcripts (Barckmann et al., 2013). So far, many transcriptome analyses have been carried out using either microarray or RNAseq approaches. In *Drosophila*, about 50% of genes are transcribed in adult testis tissue (Chintapalli et al., 2007; Graveley et al., 2010). Different factors influence the usability of these transcriptome data. Due to translational repression of transcripts in spermatocytes, protein expression cannot be deduced directly from the abundance of a transcript. Furthermore, a distinction between transcripts expressed in germ cells and transcripts expressed in the testis sheath is difficult and has to be examined for each gene in detail. Data on protein expression can further strengthen gene expression models and will help to interpret transcriptome data.

4.4 Objective of this study: the proteome of *Drosophila* testis

The generation of proteome data can be implemented in different approaches concerning accuracy and effectiveness. A separation of peptide mixtures with 2D gelelectrophoresis and excision of single peptide spots from the gel can be followed by mass spectrometry (MS) analysis. This approach was used for the identification of 342 proteins from isolated *Drosophila* sperm (Dorus et al., 2006). An analysis of other isolated germ cell stages in the same way is difficult due to the presence of different germ cell stages next to each other in the testis tube of flies. Isolation of cyst cells and subsequent *in vitro* culture is a valid method to visualise germ cell development as well as for the application of functional studies using inhibitors (Gärtner et al., 2014). However, the isolation of cysts which contain a defined germ cell stage for large-scale proteome analyses might be time consuming and a contamination with other germ cell stages during cyst isolation is likely. Proteome analyses of whole testes from adult flies revealed that 1108 proteins are expressed in testis tissue (Takemori et al., 2009; Wasbrough et al., 2010). Taking into account that transcriptome data suggest an expression of many thousands of genes (Chintapalli et al., 2007; Graveley et al., 2010), these results may fall too short.

This study aims to complement the testis proteome of *Drosophila* and to identify proteins, which might not have been detected in previous large-scale proteomic approaches. We use a high throughput mass-spectrometry (MS) analysis to identify proteins from protein extracts of whole testis tissue. Preparation of protein extracts from different developmental stages enables us to examine the protein in a developmental context. The proteome of testes from third instar larvae contains only germ cell stages up to the spermatocyte stage so that a proteome from cells before the meiotic divisions can be evaluated. Furthermore, proteins from the testis sheath are less abundant in larval testes, as the formation of the testis sheath occurs earliest in the pupa (Bodenstein, 1950; Susic-Jung et al., 2012). The testis muscles might first contribute to the proteome of pupal testes. We isolated testes from pupae, in which germ cell stages up to the elongation of spermatids are expected to be enriched. The pupal proteome might therefore cover especially proteins involved in chromatin reorganisation and sperm morphogenesis. Finally, the proteome for adult testis tissue will contain all germ cell stages but will also represent proteins needed for fully elongated flagella. Taken together, the proteomics data for larval, pupal and adult testes identified over 6000 proteins. We also describe expression pattern and function of several newly identified proteins for different developmental stages, illustrating how our proteome data can contribute to a better understanding of germ cell development (see Chapter 7).

4.5 Transcriptional regulation in *Drosophila* spermatocytes

In general, synthesis of protein-coding transcripts is accompanied by an association of RNA Polymerase II (Pol II) with promoter regions. Several protein complexes, the general transcription factors (GTFs), define the promoters for basal transcription through RNA Pol II. Activation or repression of transcription is often mediated by binding of activators or repressors to subunits of the GTFs, which influence the transcriptional initiation or the rate at which Pol II is recruited to a

promoter. One of the GTF subunits, TFIID, is a critical regulator for RNA Pol II binding as it contains the TATA box-binding protein (TBP), which directly recognizes the TATA-box motif. Fourteen TBP-associated factors (TAFs) contribute to the TFIID complex and can be targeted by transcriptional activators to facilitate recruitment of Pol II to promoter regions (reviewed in Burley and Roeder, 1996). TFIID forms the pre-initiation complex together with other GTF subunits, TFIIA, TFIIB, TFIIE, TFIIF and TFIIH. Both TFIIA and TFIID are evolutionary conserved from yeast to human and therefore play a crucial role in the regulation of transcription by serving as a binding platform for activator or repressor proteins in many species (reviewed in Freiman, 2009).

4.5.1 Germ cell-specific variants of general transcription factors

The occurrence of germ cell-specific variants for somatic GTF subunits across many species of vertebrates suggests a regulatory exception for the germ line (Xiao et al., 2006; reviewed in Freiman, 2009). Examples for germ line-enriched paralogues of the somatic TAFs in mammals are TAF4b and TAF7L. TAF4b maintains self-renewal of spermatogonia (Falender et al., 2005) while TAF7L replaces the function of TAF7 in the germ cell stages with high transcriptional activity (Pointud et al., 2003). In *Drosophila*, the testis-specific variants of general TAFs, the tTAFs, comprise Cannonball (Can, TAF5 paralogue), Meiosis I Arrest (Mia, TAF6 paralogue), Spermatocyte Arrest (Sa, TAF8 paralogue), No Hitter (Nht, TAF4 paralogue) and Ryan Express (Rye, TAF12 paralogue; Hiller et al., 2001; Hiller et al., 2004). They can be allocated to the *can*-class of meiotic arrest genes, which comprise genes functioning in spermatocytes and which are important for meiosis and onset of spermatogenesis. Meiotic arrest mutants cease developmental progression during the spermatocyte phase and do not show emergence of spermatids (Lin et al., 1996; reviewed in White-Cooper and Davidson, 2011). tTAFs have been shown to be structural similar to the general TAFs and also form heterodimers with each other (reviewed in Kolthur-Seetharam et al., 2008). Several spermiogenesis-relevant genes, like don juan (*dj)*, don juan like (*djl)*, *Mst77F*, *Mst87F*, *protB* and fuzzy onions (*fzo)* have been shown to be regulated by tTAFs (Chen et al., 2005; Hempel et al., 2006; Barckmann et al., 2013; Lu et al., 2013). With microarray analyses on tTAF mutants it could be shown that several thousand genes seem to be regulated by meiotic arrest genes (Lu et al., 2013; Lu and Fuller, 2015; White-Cooper and Davidson, 2011).

Apart from tTAFs, the *can*-class also includes a gene coding for Mip40, which has been shown to co-purify with Always early (Aly) and Tombola (Tomb). These are components of the tMAC complex, a testis-specific variant of the dREAM complex and belong to the *aly*-class of genes (Beall et al., 2007; Jiang et al., 2007). Together with Comr (Jiang and White-Cooper, 2003) and Topi (Perezgasga et al., 2004), other components of tMAC, they are supposed to regulate transcription with their DNA-binding capability (White-Cooper and Davidson, 2011). Over 1000 genes are indeed negatively regulated in *aly* mutants according to microarray data (Doggett et al., 2011). Taken together, tTAFs and components of the tMAC complex have the potential to regulate a large set of genes, emphasising the role of tissue specific variants for germ cell development.

4.6 Bromodomain proteins as epigenetic readers of histone acetylations

Active transcription is often connected with an open chromatin structure. Acetylation of N-terminal histone chains is suggested to be a crucial factor for activation of chromatin (Marushige, 1976). It was shown that transcribed genes are associated with nearby acetylated histones (Hebbes et al., 1988) but also the higher order structure of chromatin can be influenced by single histone acetylations (Shogren-Knaak et al., 2006). The recognition of acetylated histones is a known feature of bromodomain (BRD)-containing proteins. Bromodomains are conserved domains and appear in various proteins featuring different functions, for example by contributing to the function of HATs in regulation of gene activity (Dhalluin et al., 1999). It was also shown that bromodomains are part of chromatin remodellers like Brahma (Elfring et al., 1998) or even of proteins functioning in transcriptional repression (Tae et al., 2011). For the human $TAF_{II}250$, which contains tandem bromodomains, binding to acetylated H4 is supposed to target the TFIID complex to certain chromatin targets (Jacobson et al., 2000). Furthermore, bromodomains are the eponymous feature of bromodomain and extra-terminal (BET) family proteins, which always contain an extra-terminal (ET) domain in addition to one or two bromodomains (reviewed in Florence and Faller, 2001). The yeast BET family member Bdf1 needs its ET domain for protein interactions. It is moreover assumed to interact with components of yeast TFIID complex to ensure gene expression (Matangkasombut et al., 2000). The mammalian bromodomain proteins BRD2, BRD3 and BRD4 have a variety of functions in many different tissues, underscoring their importance for regulation of gene expression by recruiting other proteins (reviewed in Josling et al., 2012).

Mammalian BRDT was long known as testis-specific, double bromodomain protein with expression from spermatocytes to elongating spermatids (Jones et al., 1997; Gaucher et al., 2012). However, other studies suggested expression also in oocytes (Paillisson et al., 2007). A variety of functions have been described for BRDT, e.g. it is able to remodel chromatin (Pivot-Pajot et al., 2003; Gaucher et al., 2012) or it can be a component of spliceosome complexes to contribute to mRNA splicing (Berkovits et al., 2012). Deletion of the first bromodomain of BRDT causes severe defects in spermiogenesis, like malformed spermatid nuclei or defects in formation of the chromocenter, it is also not capable anymore of targeting certain promoters in spermatids (Shang et al., 2007; Berkovits and Wolgemuth, 2011). A *brdt* null mutant shows defects in earlier germ cell development and 1864 genes are down-regulated in testes of mutant mice (Gaucher et al., 2012). This indicates a major role for BRDT in gene regulation during spermatogenesis. In *Drosophila*, tBRD-1 was the first discovered BET family protein showing testis-specific expression (Leser et al., 2012).

4.6.1 Objective of this study: The function of the bromodomain protein tBRD-1 in transcriptional regulation during spermatogenesis

tBRD-1 is exclusively expressed in the testis and localises to the nucleus of spermatocytes. It is important for male fertility as *tbrd-1* mutants are sterile and show defects in spermiogenesis (Leser et

al., 2012). This study examines a possible connection between tBRD-1 and the tTAFs in *Drosophila* testes. tBRD-1 localisation depends on tTAF function which was shown for *sa* mutants. It is also able to physically interact with some of the tTAFs in yeast two-hybrid assays (Y2H). We also newly characterised tBRD-2 and tBRD-3 as bromodomain proteins, which are expressed in a testis-specific manner similar to tBRD-1. An interaction of tBRD-1 and tBRD-2 in the Y2H system indicates that they might act together as reader proteins of histone acetylation. A microarray analysis of RNA from adult testes revealed a mis-regulation of several hundred of genes in *tbrd-1* mutants compared to wild-type flies. Compared to microarray data for *sa* mutants, tBRD-1-regulated genes partially overlap with those regulated by Sa. *sa* mutants show the typical meiotic arrest phenotype, ceasing germ cell development in the spermatocyte stage (Hiller et al., 2004). *tbrd-1* mutants show first defects in spermiogenesis where spermatid nuclei do not elongate properly. These findings together with the knowledge about a much larger set of target genes for Sa than for tBRD-1 led us to hypothesise a cooperation between tBRD-1 and the tTAFs to regulate a subset of target genes (see Chapter 8).

4.7 Paf1C is conserved in many species and plays a role in transcriptional regulation

The BRD proteins give a hint how the immense amount of different transcripts in male germ cells can be differentiated in subsets through testis-specifically expressed variants by supporting the general transcription machinery. Lu and Fuller showed that the Mediator complex is a further candidate for refinement of the transcriptional program in *Drosophila* spermatocytes (Lu and Fuller, 2015). Mediator is conserved in most species (reviewed in Boube et al., 2002) and moreover does not necessarily need GTFs for its recruitment to promoters, as it is itself associated with RNA Pol II (Rani et al., 2004). However, the potential of Mediator as a transcriptional regulator in spermatocytes is immense as over 1500 genes are down-regulated in testes of *Mediator* knock-down flies. In addition, a co-regulation with tMAC has been described for many target genes of Mediator (Lu and Fuller, 2015). It seems likely that there is still a great number of yet unidentified proteins, which can diversify the transcriptional regulation achieved by complexes, like Mediator, tMAC or the testis-specific TFIID variant.

In search for further candidates, which could play a role in the regulation of transcription, we found that the ubiquitously expressed Rtf1 is also present in male germ cells (Dottermusch-Heidel, unpublished data). Rtf1 is a component of the Paf1 complex (Paf1C), which is conserved among all eukaryotes with its subunits Paf1, Cdc73, Leo1, Ctr9 and Rtf1 (reviewed in Tomson and Arndt, 2013). Paf1C is physically associated with RNA Pol II in yeast and human (Wade et al., 1996; Kim et al., 2010), indicating a role in transcriptional regulation. Across eukaryotes, many studies on Paf1C function have been carried out. Two major roles for the complex stand out: the modification of chromatin and the regulation of transcription-related processes. Chromatin modifications, like ubiquitination of H2B or methylation of H3K4 and H3K79, depend on the function of Paf1C (Ng et

al., 2003; Wood et al., 2003). These modifications are often connected to transcriptional elongation by RNA Pol II (Xiao et al., 2005; Warner et al., 2007). The association of Cdc73 and Paf1 with 3' mRNA processing factors is an example for the connection of Paf1C with transcription-related processes (Rozenblatt-Rosen et al., 2009; Penheiter et al., 2005). In *Drosophila*, Paf1C and especially its component Rtf1 was shown to be important for histone modification, Notch signalling and also for the regulation of transcription (Tenney et al., 2006; Adelman et al., 2006).

4.7.1 Various functions of the Plus3 domain protein Rtf1

Like other Paf1C components, Rtf1 is a very conserved protein and can be found in yeast, mammals and flies. Rtf1 has several protein domains whose functions have been examined in different species. However, the results might be transferable to other species due to the conservation of Rtf1. The histone modification domain (HMD) was shown to be essential for histone modification in cooperation with the chromatin remodeller Chd1 in yeast. The C-terminus of Rtf1 is needed for the interaction with other components of Paf1C (Warner et al., 2007). The most interesting structural domain is the Plus3 domain of Rtf1. Across all higher eukaryotes only few Plus3 domain-containing proteins are known and often only a single gene coding a Plus3 domain can be found, which makes Rtf1 a protein with unique properties. Plus3 domains have a conserved secondary structure, which is determined by several conserved amino acids. Three positively charged amino acids are eponymous for the Plus3 domain and provide a binding capacity for negatively charged nucleotides. Indeed it has been demonstrated for human Rtf1 that it can bind single-stranded DNA *in vitro* (De Jong et al., 2008). The Plus3 domain of yeast Rtf1 is important for association with open reading frames and for recruitment of the Paf1C to chromatin (Warner et al., 2007; Wier et al., 2013). Interestingly, several groups report that Rtf1 is not always tightly associated with all other components of the Paf1C (Rozenblatt-Rosen et al., 2005; Adelman et al., 2006; Kim et al., 2010). Knock-down of *Rtf1* yields numerous mis-regulated genes but the overlap with regulated genes upon knock-down of other Paf1C components was only minor, indicating that Rtf1 can contribute to transcriptional regulation outside of Paf1C (Cao et al., 2015).

4.7.2 Objective of this study: The expression and function of the testis-enriched Plus3 domain proteins tPlus3a and tPlus3b

Like many other species, *Drosophila* has a homologue for Rtf1. Strikingly, there are three other genes in flies, which have potential to code for Plus3 domain proteins. Microarray data suggest that *CG12498*, *CG31702* and *CG31703* transcripts are enriched in the fly testis (Chintapalli et al., 2007). In this study, we focus on expression and function of CG31702 (named tPlus3a) and CG31703 (named tPlus3b) in search for further proteins taking part in transcriptional regulation in germ cells. As previously mentioned, the testis-specific BRD proteins are candidates for refining transcriptional regulation in the testis. Taking into account that there are thousands of genes expressed in male germ cells, the contribution of BRD proteins seems to be insufficient to explain how a specialised transcription like in spermatocytes can be accomplished. Here, we show that tPlus3a and tPlus3b have

a conserved Plus3 domain comparable to Rtf1 and that they are expressed in spermatocytes. Mutants show a severely reduced fertility and defects during the individualisation of sperm. Comparative RNAseq analyses of testes from *tplus3a/tplus3b* mutants and *tbrd-1* mutants reveals a large set of genes regulated in both mutants. When we compared the microarray data of *tplus3a/tplus3b* mutants to microarray data for a *tbrd-2* knock-down the overlap of regulated genes was only minor. We therefore conclude that tPlus3a and tPlus3b co-regulate a subset of target genes with tBRD-1 but not with tBRD-2. We hypothesise that Plus3 domain proteins in the testis further contribute to the diversification of transcriptional regulation in spermatocytes (see Chapter 9).

4.8 References

Adelman, K., Wei, W., Ardehali, M.B., Werner, J., Zhu, B., Reinberg, D. and Lis, J.T. (2006). *Drosophila* Paf1 modulates chromatin structure at actively transcribed genes. Mol Cell Biol. 2006 Jan; 26(1):250-60

Agarwal, A., Mulgund, A., Hamada, A. and Chyatte, M.R. (2015). A unique view on male infertility around the globe. Reprod Biol Endocrinol. 2015 Apr; 13:37. doi: 10.1186/s12958-015-0032-1

Awe, S. and Renkawitz-Pohl R. (2010). Histone H4 acetylation is essential to proceed from a histone- to a protamine-based chromatin structure in spermatid nuclei of *Drosophila melanogaster*. Syst. Biol. Reprod. Med. 2010 Feb; 44–61

Barckmann, B., Chen, X., Kaiser, S., Jayaramaiah-Raja, S., Rathke, C., Dottermusch-Heidel, C., Fuller, M.T. and Renkawitz-Pohl, R. (2013). Three levels of regulation lead to protamine and Mst77F expression in *Drosophila*. Dev Biol. 2013 May; 377(1):33-45. doi: 10.1016/j.ydbio.2013.02.018

Barreau, C., Benson, E., Gudmannsdottir, E., Newton, F. and White-Cooper, H. (2008). Post-meiotic transcription in *Drosophila* testes. Development. 2008 Apr; 1897-1902. doi:10.1242/dev.021949

Beall, E.L., Lewis, P.W., Bell, M., Rocha, M., Jones, D.L. and Botchan, M.R. (2007). Discovery of tMAC: a *Drosophila* testis-specific meiotic arrest complex paralogous to Myb-Muv B. Genes Dev. 2007 Apr; 21(8):904-19

Berkovits, B.D. and Wolgemuth, D.J. (2011). The first bromodomain of the testis-specific double bromodomain protein Brdt is required for chromocenter organization that is modulated by genetic background. Dev Biol. 2011 Dec; 360(2):358-68. doi: 10.1016/j.ydbio.2011.10.005

Berkovits, B.D., Wang, L., Guarnieri, P., Wolgemuth, D.J. (2012). The testis-specific double bromodomain-containing protein BRDT forms a complex with multiple spliceosome components and is required for mRNA splicing and 3'-UTR truncation in round spermatids. Nucleic Acids Res. 2012 Aug; 40(15):7162-75. doi: 10.1093/nar/gks342

Bodenstein, D. (1950). The postembryonic development of *Drosophila*. In Biology of *Drosophila*, New York: John Wiley & Sons, Inc. (ed. Demerec, M., editor); 275-367

Boube, M., Joulia, L., Cribbs, D.L. and Bourbon, H.M. (2002). Evidence for a mediator of RNA polymerase II transcriptional regulation conserved from yeast to man. Cell. 2002 Jul; 110(2):143-51

Brewer, L., Corzett, M. and Balhorn, R. (2002). Condensation of DNA by spermatid basic nuclear proteins. J Biol Chem. 2002 Oct; 277(41):38895-900

Burley, S.K. and Roeder, R.G. (1996). Biochemistry and structural biology of transcription factor IID (TFIID). Annu Rev Biochem. 1996; 65:769-99

Cao, Q.F., Yamamoto, J., Isobe, T., Tateno, S., Murase, Y., Chen, Y., Handa, H. and Yamaguchi, Y. (2015). Characterization of the Human Transcription Elongation Factor Rtf1: Evidence for Nonoverlapping Functions of Rtf1 and the Paf1 Complex. Mol Cell Biol. 2015 Oct; 35(20):3459-70. doi: 10.1128/MCB.00601-15

Chen, X., Hiller, M., Sancak, Y. and Fuller, M.T. (2005). Tissue-specific TAFs counteract Polycomb to turn on terminal differentiation. Science. 2005 Nov; 310(5749):869-72

Chintapalli, V.R., Wang, J. and Dow, J.A. (2007). Using FlyAtlas to identify better *Drosophila* models of human disease. Nature Genetics. 2007 Jun; 39:715–720

Deeney, J.T., Belkina, A.C., Shirihai, O.S., Corkey, B.E., Denis, G.V. (2016). BET bromodomain proteins Brd2, Brd3 and Brd4 selectively regulate metabolic pathways in the pancreatic β-Cell. PLoS One. 2016 Mar; 11(3):e0151329. doi: 10.1371/journal.pone.0151329

De Jong, R.N., Truffault, V., Diercks, T., Ab, E., Daniels, M.A., Kaptein, R. and Folkers, G.E. (2008). Structure and DNA binding of the human Rtf1 Plus3 domain. Structure. 2008 Jan; 16(1):149-59. doi: 10.1016/j.str.2007.10.018

Dhalluin, C., Carlson, J.E., Zeng, L., He, C., Aggarwal, A.K. and Zhou, M.M. (1999). Structure and ligand of a histone acetyltransferase bromodomain. Nature. 1999 Jun; 399(6735):491-6

Doggett, K., Jiang, J., Aleti, G. and White-Cooper, H. (2011). Wake-up-call, a lin-52 paralogue, and Always early, a lin-9 homologue physically interact, but have opposing functions in regulating testis-specific gene expression. Dev Biol. 2011 Jul; 355(2):381-93. doi: 10.1016/j.ydbio.2011.04.030

Dorus, S., Busby, S.A., Gerike, U., Shabanowitz, J., Hunt, D.F. and Karr, T.L. (2006). Genomic and functional evolution of the *Drosophila melanogaster* sperm proteome. Nat Genet. 2006 Dec; 38(12):1440-5

Dottermusch-Heidel, C., Gärtner, S.M., Tegeder, I., Rathke, C., Barckmann, B., Bartkuhn, M., Bhushan, S., Steger, K., Meinhardt, A. and Renkawitz-Pohl, R. (2014a). H3K79 methylation: a new conserved mark that accompanies H4 hyperacetylation prior to histone-to-protamine transition in *Drosophila* and rat. Biol Open. 2014 May 2; 3(6):444-52. doi: 10.1242/bio.20147302

Dottermusch-Heidel, C., Klaus, E.S., Gonzalez, N.H., Bhushan, S., Meinhardt, A., Bergmann, M., Renkawitz-Pohl, R., Rathke, C. and Steger, K. (2014b). H3K79 methylation directly precedes the histone-to-protamine transition in mammalian spermatids and is sensitive to bacterial infections. Andrology. 2014 Sep; 2(5):655-65. doi: 10.1111/j.2047-2927.2014.00248.x

Doyen, C.M., Chalkley, G.E., Voets, O., Bezstarosti, K., Demmers, J.A., Moshkin, Y.M. and Verrijzer C.P. (2015). A testis-specific chaperone and the chromatin remodeler ISWI mediate repackaging of the paternal genome. Cell Rep. 2015 Nov 17; 13(7):1310-1318. doi: 10.1016/j.celrep.2015.10.010

Elfring, L.K., Daniel, C., Papoulas, O., Deuring, R., Sarte, M., Moseley, S., Beek, S.J., Waldrip, W.R., Daubresse, G., DePace, A., Kennison, J.A. and Tamkun, J.W. (1998). Genetic analysis of *brahma*: the *Drosophila* homolog of the yeast chromatin remodeling factor SWI2/SNF2. Genetics. 1998 Jan; 148(1):251-65

Eren-Giani, Z., Rathke, C., Theofel, I. and Renkawitz-Pohl, R. (2015). Prtl99C acts together with protamines and safeguards male fertility in *Drosophila*. Cell Reports. 2015 Dec; 13(11):2327-2335. doi: 10.1016/j.celrep.2015.11.023

Fuller, M.T. (1993). Spermatogenesis. In: The Development of *Drosophila melanogaster*, 71-147. Cold Spring Harbor Laboratory Press

Falender, A.E., Freiman, R.N., Geles, K.G., Lo, K.C., Hwang, K., Lamb, D.J., Morris, P.L., Tjian, R. and Richards, J.S. (2005). Maintenance of spermatogenesis requires TAF4b, a gonad-specific subunit of TFIID. Genes Dev. 2005 Apr; 19(7):794-803

Florence, B. and Faller, D.V. (2001). You bet-cha: a novel family of transcriptional regulators. Front Biosci. 2001 Aug; 6:D1008-18. Review

Freiman, R.N. (2009). Specific variants of general transcription factors regulate germ cell development in diverse organisms. Biochim Biophys Acta. 2009 March; 1789(3):161–166. doi:10.1016/j.bbagrm.2009.01.005

Gärtner, S.M., Rathke, C., Renkawitz-Pohl, R. and Awe, S. (2014). Ex vivo culture of *Drosophila* pupal testis and single male germ-line cysts: dissection, imaging, and pharmacological treatment. J Vis Exp. 2014 Sep; (91):51868. doi: 10.3791/51868

Gaucher, J., Boussouar, F., Montellier, E., Curtet, S., Buchou, T., Bertrand, S., Hery, P., Jounier, S., Depaux, A., Vitte, A.L., Guardiola, P., Pernet, K., Debernardi, A., Lopez, F., Holota, H., Imbert, J.,

Wolgemuth, D.J., Gérard, M., Rousseaux, S. and Khochbin, S. (2012). Bromodomain-dependent stage-specific male genome programming by Brdt. EMBO J. 2012 Oct; 31(19):3809-20. doi: 10.1038/emboj.2012.233

Gould-Somero, M. and Holland, L. (1974). The timing of RNA synthesis for spermiogenesis in organ cultures of *Drosophila melanogaster* testes. Wilhelm Roux Arch Entwickl Mech Org. 1974 Jun; 174(2):133-148. doi: 10.1007/BF00573626

Graveley, B.R., Brooks, A.N., Carlson, J.W., Cherbas, L., Choi, J., Davis, C.A., Dobin, A., Duff, M., Eads, B., Hansen, K.D., Landolin, J., Langton, L., Malone, J., Miller, D., Roberts, J., Sandler, J., Sturgill, D., Tang, H., van Baren, M.J., Wan, K.H., Xiao, S., Yang, L., Zhang, D., Zhang, Y., Zou, Y., Andrews, J., Brenner, S.E., Brent, M., Cherbas, P., Dudoit, S., Gingeras, T.R., Hoskins, R., Kaufman, T., Oliver, B, Celniker, S.E. (2010.03.15). The *D. melanogaster* transcriptome: modENCODE RNA-Seq data

Hebbes, T.R., Thorne, A.W. and Crane-Robinson, C. (1988). A direct link between core histone acetylation and transcriptionally active chromatin. EMBO J. 1988 May; 7(5):1395-402

Hempel, L.U., Rathke, C., Raja, S.J. and Renkawitz-Pohl, R. (2006). In *Drosophila*, *don juan* and *don juan like* encode proteins of the spermatid nucleus and the flagellum and both are regulated at the transcriptional level by the TAF II80 cannonball while translational repression is achieved by distinct elements. Dev Dyn. 2006 Apr; 235(4):1053-64

Hiller, M., Chen, X., Pringle, M.J., Suchorolski, M., Sancak, Y., Viswanathan, S., Bolival, B., Lin, T.Y., Marino, S. and Fuller, M.T. (2004). Testis-specific TAF homologs collaborate to control a tissue-specific transcription program. Development. 2004 Nov; 131(21):5297-308

Hiller, M.A., Lin, T.Y., Wood, C. and Fuller, M.T. (2001). Developmental regulation of transcription by a tissue-specific TAF homolog. Genes Dev. 2001 Apr; 15(8):1021-30

Jacobson, R.H., Ladurner, A.G., King, D.S. and Tjian, R. (2000). Structure and function of a human TAFII250 double bromodomain module. Science. 2000 May; 288(5470):1422-5

Jayaramaiah Raja, S. and Renkawitz-Pohl, R. (2005). Replacement by *Drosophila melanogaster* protamines and Mst77F of histones during chromatin condensation in late spermatids and role of sesame in the removal of these proteins from the male pronucleus. Mol Cell Biol. 2005 Jul; 25(14):6165-77

Jiang, J. and White-Cooper, H. (2003). Transcriptional activation in *Drosophila* spermatogenesis involves the mutually dependent function of *aly* and a novel meiotic arrest gene *cookie monster*. Development. 2003 Feb; 130(3):563-73

Jiang, J., Benson, E., Bausek, N., Doggett, K., White-Cooper, H. (2007). Tombola, a tesmin/TSO1-family protein, regulates transcriptional activation in the *Drosophila* male germline and physically interacts with always early. Development. 2007 Apr; 134(8):1549-59

Jones, M.H., Numata, M. and Shimane, M. (1997). Identification and characterization of *BRDT*: A testis-specific gene related to the bromodomain genes *RING3* and *Drosophila fsh*. Genomics. 1997 Nov; 45(3):529-34

Josling, G.A., Selvarajah, S.A., Petter, M. and Duffy, M.F. (2012). The role of bromodomain proteins in regulating gene expression. Genes (Basel). 2012 May; 3(2):320-43. doi: 10.3390/genes3020320. Review

Kierszenbaum, A.L. and Tres, L.L. (1975). Structural and transcriptional features of the mouse spermatid genome. J Cell Biol. 1975 May; 65(2):258-70

Kim, J., Guermah, M. and Roeder, R.G. (2010). The human PAF1 complex acts in chromatin transcription elongation both independently and cooperatively with SII/TFIIS. Cell. 2010 Feb; 140(4):491-503. doi: 10.1016/j.cell.2009.12.050

Kimura, S. and Loppin, B. (2016). The *Drosophila* chromosomal protein Mst77F is processed to generate an essential component of mature sperm chromatin. Open Biol. 2016 Nov; 6(11). pii: 160207

Kolthur-Seetharam, U., Martianov, I. and Davidson, I. (2008). Specialization of the general transcriptional machinery in male germ cells. Cell Cycle. 2008 Nov; 7(22):3493-8

Kost, N., Kaiser, S., Ostwal, Y., Riedel, D., Stützer, A., Nikolov, M., Rathke, C., Renkawitz-Pohl, R. and Fischle, W. (2015). Multimerization of *Drosophila* sperm protein Mst77F causes a unique condensed chromatin structure. Nucleic Acids Res. 2015 Mar 31; 43(6):3033-45. doi: 10.1093/nar/gkv015

Leser, K., Awe, S., Barckmann, B., Renkawitz-Pohl, R. and Rathke, C. (2012). The bromodomain-containing protein tBRD-1 is specifically expressed in spermatocytes and is essential for male fertility. Biol Open. 2012 Jun; 1(6):597-606. doi: 10.1242/bio.20121255

Li, Y., Lalancette, C., Miller, D. and Krawetz, S.A. (2008). Characterization of nucleohistone and nucleoprotamine components in the mature human sperm nucleus. Asian J Androl. 2008 Jul; 10(4):535-41

Lin, T.Y., Viswanathan, S., Wood, C., Wilson, P.G., Wolf, N. and Fuller, M.T. (1996). Coordinate developmental control of the meiotic cell cycle and spermatid differentiation in *Drosophila* males. Development. 1996 Apr; 122(4):1331-41

Lindsley, D.L. and Tokuyasu, K.T. (1980). Spermatogenesis. In: Ashburner, M. and Wright, T.R.F., Eds.; The Genetics and Biology of *Drosophila* Vol. 2 d. Academic Press; 225-294

Lu, C. and Fuller, M.T. (2015). Recruitment of Mediator complex by cell type and stage-specific factors required for tissue-specific TAF dependent gene activation in an adult stem cell lineage. PLoS Genet. 2015 Dec; 11(12):e1005701. doi: 10.1371/journal.pgen.1005701

Lu, C., Kim, J., Fuller, M.T. (2013). The polyubiquitin gene *Ubi-p63E* is essential for male meiotic cell cycle progression and germ cell differentiation in *Drosophila*. Development. 2013 Sep; 140(17):3522-31. doi: 10.1242/dev.098947

Marushige, K. (1976). Activation of chromatin by acetylation of histone side chains. Proc Natl Acad Sci USA. 1976 Nov; 73(11):3937-41

Matangkasombut, O., Buratowski, R.M., Swilling, N.W. and Buratowski, S. (2000). Bromodomain factor 1 corresponds to a missing piece of yeast TFIID. Genes Dev. 2000 Apr; 14(8):951-62

Ng, H.H., Dole, S. and Struhl, K. (2003). The Rtf1 component of the Paf1 transcriptional elongation complex is required for ubiquitination of histone H2B. J Biol Chem. 2003 Sep; 278(36):33625-8

Olivieri, G. and Olivieri, A. (1965). Autoradiographic study of nucleic acid synthesis during spermatogenesis in *Drosophila melanogaster*. Mutation Research. 1965 Apr; 366-380

Paillisson, A., Levasseur, A., Gouret, P., Callebaut, I., Bontoux, M., Pontarotti, P. and Monget, P. (2007). Bromodomain testis-specific protein is expressed in mouse oocyte and evolves faster than its ubiquitously expressed paralogs BRD2, -3, and -4. Genomics. 2007 Feb; 89(2):215-23

Pattabiraman, S., Baumann, C., Guisado, D., Eppig, J.J., Schimenti, J.C. and De La Fuente, R. (2015). Mouse BRWD1 is critical for spermatid postmeiotic transcription and female meiotic chromosome stability. J Cell Biol. 2015 Jan; 208(1):53-69. doi: 10.1083/jcb.201404109

Penheiter, K.L., Washburn, T.M., Porter, S.E., Hoffman, M.G. and Jaehning, J.A. (2005). A posttranscriptional role for the yeast Paf1-RNA polymerase II complex is revealed by identification of primary targets. Mol Cell. 2005 Oct; 20(2):213-23

Perezgasga, L., Jiang, J., Bolival, B.Jr., Hiller, M., Benson, E., Fuller, M.T. and White-Cooper, H. (2004). Regulation of transcription of meiotic cell cycle and terminal differentiation genes by the testis-specific Zn-finger protein matotopetli. Development. 2004 Apr; 131(8):1691-702

Philipps, D.L., Wigglesworth, K., Hartford, S.A., Sun, F., Pattabiraman, S., Schimenti, K., Handel, M., Eppig, J.J. and Schimenti, J.C. (2008). The dual bromodomain and WD repeat-containing mouse protein BRWD1 is required for normal spermiogenesis and the oocyte-embryo transition. Dev Biol. 2008 May; 317(1):72-82. doi: 10.1016/j.ydbio.2008.02.018

Pivot-Pajot, C., Caron, C., Govin, J., Vion, A., Rousseaux, S. and Khochbin, S. (2003). Acetylation-dependent chromatin reorganization by BRDT, a testis-specific bromodomain-containing protein. Mol Cell Biol. 2003 Aug; 23(15):5354-65

Pointud, J.C., Mengus, G., Brancorsini, S., Monaco, L., Parvinen, M., Sassone-Corsi, P. and Davidson, I. (2003). The intracellular localisation of TAF7L, a paralogue of transcription factor TFIID subunit TAF7, is developmentally regulated during male germ-cell differentiation. J Cell Sci. 2003 May; 116(Pt 9):1847-58

Rani, P.G., Ranish, J.A. and Hahn, S. (2004). RNA polymerase II (Pol II)-TFIIF and Pol II-mediator complexes: the major stable Pol II complexes and their activity in transcription initiation and reinitiation. Mol Cell Biol. 2004 Feb; 24(4):1709-20

Rathke, C., Baarends, W.M., Awe, S. and Renkawitz-Pohl, R. (2014). Chromatin dynamics during spermiogenesis. Biochim Biophys Acta. 2014 Mar; 1839(3):155-68. doi:10.1016/j.bbagrm. 2013.08.004

Rathke, C., Baarends, W.M., Jayaramaiah-Raja, S., Bartkuhn, M., Renkawitz, R. and Renkawitz-Pohl, R. (2007). Transition from a nucleosome-based to a protamine-based chromatin configuration during spermiogenesis in *Drosophila*. J Cell Sci. 2007 May; 120(Pt 9):1689-700

Rathke, C., Barckmann, B., Burkhard, S., Jayaramaiah-Raja, S., Roote, J. and Renkawitz-Pohl, R. (2010). Distinct functions of Mst77F and protamines in nuclear shaping and chromatin condensation during *Drosophila* spermiogenesis. Eur J Cell Biol. 2010 Apr; 89(4):326-38. doi: 10.1016/j.ejcb.2009.09.001

Rozenblatt-Rosen, O., Nagaike, T., Francis, J.M., Kaneko, S., Glatt, K.A., Hughes, C.M., LaFramboise, T., Manley, J.L. and Meyerson, M. (2009). The tumor suppressor Cdc73 functionally associates with CPSF and CstF 3' mRNA processing factors. Proc Natl Acad Sci USA. 2009 Jan; 106(3):755-60. doi: 10.1073/pnas.0812023106

Schultz, N., Hamra, F.K. and Garbers, D.L. (2003). A multitude of genes expressed solely in meiotic or postmeiotic spermatogenic cells offers a myriad of contraceptive targets. Proc Natl Acad Sci USA. 2003 Oct; 100(21):12201-6

Shang, E., Nickerson, H.D., Wen, D., Wang, X. and Wolgemuth, D.J. (2007). The first bromodomain of Brdt, a testis-specific member of the BET sub-family of double-bromodomain-containing proteins, is essential for male germ cell differentiation. Development. 2007 Oct; 134(19):3507-15

Shang, E., Salazar, G., Crowley, T.E., Wang, X., Lopez, R.A., Wang, X. and Wolgemuth, D.J. (2004). Identification of unique, differentiation stage-specific patterns of expression of the bromodomain-containing genes Brd2, Brd3, Brd4, and Brdt in the mouse testis. Gene Expr Patterns. 2004 Sep; 4(5):513-9.

Shogren-Knaak, M., Ishii, H., Sun, J.M., Pazin, M.J., Davie, J.R. and Peterson, C.L. (2006). Histone H4-K16 acetylation controls chromatin structure and protein interactions. Science. 2006 Feb; 311(5762):844-7

Steger, K. (2001). Haploid spermatids exhibit translationally repressed mRNAs. Anat Embryol (Berl). 2001 May; 203(5):323-34

Susic-Jung, L., Hornbruch-Freitag, C., Kuckwa, J., Rexer, K.-H., Lammel, U. and Renkawitz-Pohl, R. (2012). Multinucleated smooth muscles and mononucleated as well as multinucleated striated muscles develop during establishment of the male reproductive organs of *Drosophila melanogaster*. Dev Biol. 2012 Oct; 370(1):86-97. doi: 10.1016/j.ydbio.2012.07.022

Tae, S., Karkhanis, V., Velasco, K., Yaneva, M., Erdjument-Bromage, H., Tempst, P. and Sif, S. (2011). Bromodomain protein 7 interacts with PRMT5 and PRC2, and is involved in transcriptional repression of their target genes. Nucleic Acids Res. 2011 Jul; 39(13):5424-38. doi: 10.1093/nar/gkr170

Takemori, N. and Yamamoto, M.T. (2009). Proteome mapping of the *Drosophila melanogaster* male reproductive system. Proteomics. 2009 May; 9(9):2484-93. doi: 10.1002/pmic.200800795

Tan, M., Luo, H., Lee, S., Jin, F., Yang, J. S., Montellier, E., Buchou, T., Cheng, Z., Rousseaux, S., Rajagopal, N., Lu, Z., Ye, Z., Zhu, Q., Wysocka, J., Ye, Y., Khochbin, S., Ren, B. and Zhao, Y. (2011). Identification of 67 histone marks and histone lysine crotonylation as a new type of histone modification. Cell. 2011 Sep; 146(6):1016-28

Tenney, K., Gerber, M., Ilvarsonn, A., Schneider, J., Gause, M., Dorsett, D., Eissenberg, J.C. and Shilatifard, A. (2006). *Drosophila* Rtf1 functions in histone methylation, gene expression, and Notch signaling. Proc Natl Acad Sci USA. 2006 Aug; 103(32):11970-4

Tomson, B.N. and Arndt, K.M. (2013). The many roles of the conserved eukaryotic Paf1 complex in regulating transcription, histone modifications, and disease states. Biochim Biophys Acta. 2013 Jan; 1829(1):116-26. doi: 10.1016/j.bbagrm.2012.08.011. Review

Wade, P.A., Werel, W., Fentzke, R.C., Thompson, N.E., Leykam, J.F., Burgess, R.R., Jaehning, J.A. and Burton, Z.F (1996). A novel collection of accessory factors associated with yeast RNA polymerase II. Protein Expr Purif. 1996 Aug; 8(1):85-90

Warner, M.H., Roinick, K.L. and Arndt, K.M. (2007). Rtf1 is a multifunctional component of the Paf1 complex that regulates gene expression by directing cotranscriptional histone modification. Mol Cell Biol. 2007 Sep; 27(17):6103-15

Wasbrough, E.R., Dorus, S., Hester, S., Howard-Murkin, J., Lilley, K., Wilkin, E., Polpitiya, A., Petritis, K. and Karr, T.L. (2010). The *Drosophila melanogaster* sperm proteome-II (DmSP-II). J Proteomics. 2010 Oct; 73(11):2171-85. doi: 10.1016/j.jprot.2010.09.002

White-Cooper, H. (2010). Molecular mechanisms of gene regulation during *Drosophila* spermatogenesis. Reproduction. 2010 Jan; 139(1):11-21. doi: 10.1530/REP-09-0083. Review

White-Cooper, H. and Davidson, I. (2011). Unique aspects of transcription regulation in male germ cells. Cold Spring Harb Perspect Biol. 2011 Jul; 3(7). pii: a002626. doi: 10.1101/cshperspect.a002626. Review

Wier, A.D., Mayekar, M.K., Héroux, A., Arndt, K.M. and VanDemark, A.P. (2003). Structural basis for Spt5-mediated recruitment of the Paf1 complex to chromatin. Proc Natl Acad Sci USA. 2013 Oct; 110(43):17290-5. doi: 10.1073/pnas.1314754110

Wood, A., Schneider, J., Dover, J., Johnston, M. and Shilatifard, A. (2003). The Paf1 complex is essential for histone monoubiquitination by the Rad6-Bre1 complex, which signals for histone methylation by COMPASS and Dot1p. J Biol Chem. 2003 Sep; 278(37):34739-42

Xiao, T., Kao, C.F., Krogan, N.J., Sun, Z.W., Greenblatt, J.F., Osley, M.A. and Strahl, B.D. (2005). Histone H2B ubiquitylation is associated with elongating RNA polymerase II. Mol Cell Biol. 2005 Jan; 25(2):637-51

Xiao, L., Kim, M. and DeJong, J. (2006). Developmental and cell type-specific regulation of core promoter transcription factors in germ cells of frogs and mice. Gene Expr Patterns. 2006 Apr; 6(4):409-19

Yan, W., Ma, L., Burns, K.H. and Matzuk, M.M. (2003). HILS1 is a spermatid-specific linker histone H1-like protein implicated in chromatin remodeling during mammalian spermiogenesis. Proc Natl Acad Sci USA. 2003 Sep; 100(18):10546-51

Chapter 5: Analysis of chromatin dynamics during *Drosophila* spermatogenesis

Hundertmark, T.*, Theofel, I.*, Eren-Ghiani, Z., Miller, D. and Rathke, C. (2017). Published in Stuart D. (eds) Meiosis. Methods in Molecular Biology, vol 1471. Humana Press, New York, NY

* These authors contributed equally to this work

Candidate's contribution:

- Immunofluorescence (Figure 4)
- Production of microscopic images (Figures 2, 4)
- Proofreading the manuscript

Chapter 17

Analysis of Chromatin Dynamics During *Drosophila* Spermatogenesis

Tim Hundertmark*, Ina Theofel*, Zeynep Eren-Ghiani, David Miller, and Christina Rathke

Abstract

In the course of spermatogenesis, germ cells undergo dramatic morphological changes that affect almost all cellular components. Therefore, it is impossible to study the process of spermatogenesis in its entirety without detailed morphological analyses. Here, we describe a method to visualize chromatin dynamics in differentiating *Drosophila* male germ cells using immunofluorescence staining. In addition, we demonstrate how to treat *Drosophila* sperm before immunofluorescence staining to help reveal epitopes in the highly condensed sperm chromatin that otherwise may be inaccessible to antibodies.

Key words *Drosophila*, Spermatogenesis, Chromatin, Immunofluorescence, Sperm decondensation

1 Introduction

Male germ cell differentiation represents one of the most dramatic examples of cell plasticity in metazoans. This involves transformation of nearly every subcellular organelle right up to the final condensation of sperm chromatin [1].

Drosophila spermatogenesis is an excellent model to study chromatin changes in differentiating cells that can be roughly divided into three phases: a mitotic, a meiotic, and a postmeiotic phase. Characteristic features of meiotic spermatocytes are high transcriptional activity and vigorous cell growth [2], accompanied by a fivefold enlargement of the spermatocyte nucleus in diameter in comparison to a typical mitotic cell nucleus (compare Fig. 1a, b). The testis meiotic arrest complex (tMAC), a testis-specific TFIID complex, and the bromodomain proteins tBRD-1, tBRD-2, and tBRD-3 seem to play a central role in gene regulation in spermatocytes [2–4]. After the meiotic divisions, the initially round

*Authors contributed equally.

David T. Stuart (ed.), *Meiosis*, Methods in Molecular Biology, vol. 1471,
DOI 10.1007/978-1-4939-6340-9_17, © Springer Science+Business Media New York 2017

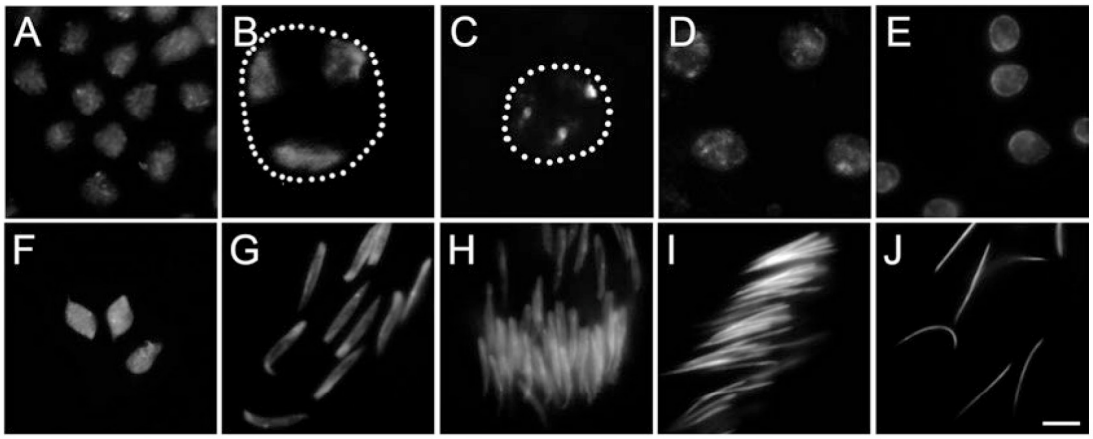

Fig. 1 Male germ cell nuclei at different stages of spermatogenesis visualized by Hoechst staining. (**a**) Several nuclei of spermatogonia. (**b**) One primary spermatocyte nucleus (*circled*). Three distinct chromosomal regions are visible. (**c**) One prometaphase nucleus (first meiotic division). (**d**) Two late anaphases (first meiotic division). (**e**) Nuclei of round haploid spermatids. (**f**) Three spermatid nuclei starting to elongate. (**g**) Elongating spermatid nuclei in the so-called early canoe stage. (**h**) Several parallel arranged elongating spermatid nuclei in the so-called late canoe stage. (**i**) Several parallel arranged needle-shaped spermatid nuclei ready for individualization. (**j**) Needle-shaped mature sperm nuclei. Scale bar, 5 μm

nucleus (Fig. 1e) elongates and becomes thinner (Fig. 1f–j). In parallel to the nuclear transformation, a unique reorganization of chromatin takes place whereby most of the histone-based nucleosomes are replaced by a protamine-like structure [5]. In addition to protamines, other DNA-binding proteins, including Mst77F and Prtl99C, are detectable in sperm nuclei by immunofluorescence microscopy [6, 7].

Useful tools to study chromatin changes during spermatogenesis are transgenic flies expressing fluorescence-tagged fusion proteins under the control of their native gene regulatory regions. These fly strains have been used to analyze the localization of a given nuclear protein without antibodies, e.g., protamines [8], the transition protein-like 94D (Tpl94D) [9], the testis-enriched HMG-box-containing protein-1 (tHMG-1) [10], or the testis-enriched HMG-box-containing protein-2 (tHMG-2) [10]. Moreover, fluorescence-tagged fusion proteins have been used for live imaging, testis culture, or inhibitor experiments [11, 12]. In combination with different antibodies (raised in different animals), these strains allow the simultaneous visualization of several chromatin components.

Here, we focus on chromatin changes in spermatocytes and in postmeiotic spermatids as well as on sperm chromatin. In this protocol, we explain how to (1) separate male and female *Drosophila*, (2) dissect testes and seminal vesicles, (3) decondense sperm chromatin, (4) perform immunofluorescence staining on germ cells and sperm, and (5) evaluate and depict immunofluorescence stainings.

2 Materials

The following materials, buffers, and solutions were calculated for a total number of eight preparations using vertical glass (coplin) staining jars for eight microscope slides with a capacity of 50 mL.

2.1 General Laboratory Equipment

1. Micropipettes (1–10 µL, 2–20 µL; 20–200 µL and 100–1000 µL).
2. Corresponding tips for the micropipettes.
3. Gloves.
4. Safety glasses.
5. Paper towels.
6. Pair of scissors.
7. Reaction tubes (1.5 mL).
8. Polythene tubes (15 mL).
9. Laboratory glass bottles.
10. Measuring cylinder (1000 mL).
11. Glass pipettes (10 mL).
12. Pipette ball or other vacuum assistive device for pipetting.
13. Microscales.
14. pH meter.
15. Stereo microscope.
16. Fume hood.

2.2 Buffers and Solutions

Please note the safety data sheets for the corresponding chemicals.

1. Phosphate-buffered saline (PBS): For 1 L of 1× solution, dissolve 7.6 g NaCl, 0.99 g Na_2HPO_4, and 0.36 g NaH_2PO_4 in 800 mL distilled water. Adjust the pH to 7.2 with HCl. To reach a final concentration of 130 mM NaCl, 7 mM Na_2HPO_4, and 3 mM NaH_2PO_4, add distilled water to a total volume of 1 L. PBS can be stored at room temperature.
2. 10 mL freshly prepared F-PBS (3.7%): Dilute 1 mL formaldehyde solution (37% (w/w) in H_2O) in 9 mL 1× PBS to obtain a 3.7% dilution.
3. 100 mL PBSTD: Dissolve 0.3 mL Triton X-100 and 0.3 g sodium deoxycholate in 100 mL 1× PBS (*see* **Note 1**). PBSTD can be stored at room temperature.
4. 600 mL PBT: Dissolve 0.6 mL Tween 20 in 600 mL 1× PBS (*see* **Note 1**). PBT can be stored at room temperature.

5. 500 mL freshly prepared 3% BSA/PBT: Dissolve 15 g bovine serum albumin (BSA) fraction V (≥98%, lyophilized powder) in 500 mL PBT. 3% BSA/PBT can be stored for a few days at 4 °C.
6. 50 mL ice-cooled 95% ethanol (please note the safety instructions) (*see* **Note 2**).
7. Freshly prepared decondensation solution (for staining seminal vesicles only): 0.2% Triton X-100, 10 mM dithiothreitol, 400 U/mL heparin in 1× PBS (please note the safety instructions) [13].

2.3 Fly Strains and Dissection Material

1. Poly-L-lysine solution (0.1% (w/v) in H_2O).
2. Microscope slides (frosted end).
3. Pencil.
4. Newly hatched or 1–2-day-old *Drosophila melanogaster* of the desired genotype maintained on standard medium at 25 °C. Here the following fly strains were used: *w1118* (to visualize spermatocyte and mature sperm nuclei); *protamineB-eGFP* transgenic flies [8] (to depict chromatin dynamics in postmeiotic stages) (*see* **Note 3**).
5. *Drosophila* carbon dioxide (CO_2) station for anesthesia with porous gas pad and foot pedal (please note the safety instructions).
6. Piece of Whatman paper (about 60 × 60 mm).
7. Small brush, e.g., Da Vinci Series 1526y size 1 Harbin Kolinsky Red Sable Brush.
8. One fresh *Drosophila* vial.
9. Block dish (40 × 40 mm) with glass lid.
10. Dissection pad, e.g., the lid of a petri dish or a microscope slide.
11. Two dissection tweezers (Swiss Dumont Inox—5).
12. Dissecting needle (for dissection of seminal vesicles only).
13. Cover slips (18 × 18 mm and 24 × 32 mm).
14. Pieces of paper tissue (about 60 × 60 mm).
15. Gripping tweezer.
16. A small container with liquid nitrogen (please note the safety instructions).
17. Stainless steel scalpel holder with blade.
18. Vertical glass staining jar with glass cover for eight microscope slides (capacity 50 mL).
19. Polystyrene case containing crushed ice (to cool the 95% ethanol).

2.4 Immunofluorescence Staining Components

1. Light-tight humid chamber with lid (*see* **Note 4**).
2. Primary antibodies. Here the following primary antibodies were used: anti-tBRD-1 (dilution 1:5000) [3, 4]; anti-tHMG-2 (dilution 1:500) [10]; and anti-Prtl99C (dilution 1:500) [7]. If alternative primary antibodies are used, their optimal dilution must be empirically determined.
3. Fluorochrome-conjugated secondary antibodies. Here anti-rabbit Cy3-conjugated (dilution 1:100; Dianova) was used.
4. 500 µL Hoechst 33258 staining solution (1 µg/mL): Dilute 0.5 µL of Hoechst 33258 stock solution (1 mg/mL) in 500 µL 3% BSA/PBT (please note the safety instructions).
5. Fluoromount-G® (Southern Biotech).
6. Preparation folder with lid.

2.5 Analysis of Immunofluorescence Stainings

1. Zeiss Axioplan II upright fluorescence microscope with digital camera, 40× and 63× oil objectives, filter cubes for Dapi/Hoechst, FITC/GFP and TRITC/Cy3, and Apotome function.
2. Immersion oil for fluorescence microscopy.
3. Digital image processing microscope software AxioVision (Zeiss) or equivalent.
4. Adobe Photoshop or equivalent.

3 Methods

Carry out all procedures at room temperature unless otherwise specified. This protocol was modified after [14].

3.1 Preparation of Polylysine-Coated Slides

1. Spread out the microscope slides (with frosted end) on the bench.
2. Pipette 8 µL of poly-L-lysine solution (0.1% (w/v) in H_2O) in the middle of each slide and spread the drop with the help of another microscope slide.
3. Mark the frosted end of the coated side with a pencil (*see* **Note 5**).
4. Dry the slides at room temperature. Coated slides can be stored for months if protected from dust.

3.2 Collecting Males

1. Anesthetize newly hatched or 1–2-day-old adult flies, respectively, of the desired genotype on a porous gas pad using carbon dioxide (CO_2).
2. Transfer the anesthetized flies to a piece of Whatman paper (about 60×60 mm), and place under a stereo microscope. Separate males and females with the help of a brush. Sexes can easily be distinguished based on the morphology of their abdomen. Females have a more hastate abdomen with clearly deposed

anal plate (Fig. 2a), and the dark rings of the tergite borders are separately visible up to the last segment [15]. Males have a more rounded abdomen without deposed extension (Fig. 2b), and the dark rings of the last segments are fused to a homogeneous broad band [15]. In addition, males exhibit a so-called sex comb on each prothoracic leg (Fig. 2b, double arrows) [16].

3. For immunofluorescence stainings on seminal vesicles, transfer the males to a new vial, store the vials at 18 °C, and continue with Subheading 3.3.2 after 5–6 days (after 5–6 days, bulging seminal vesicles can be easily dissected). For

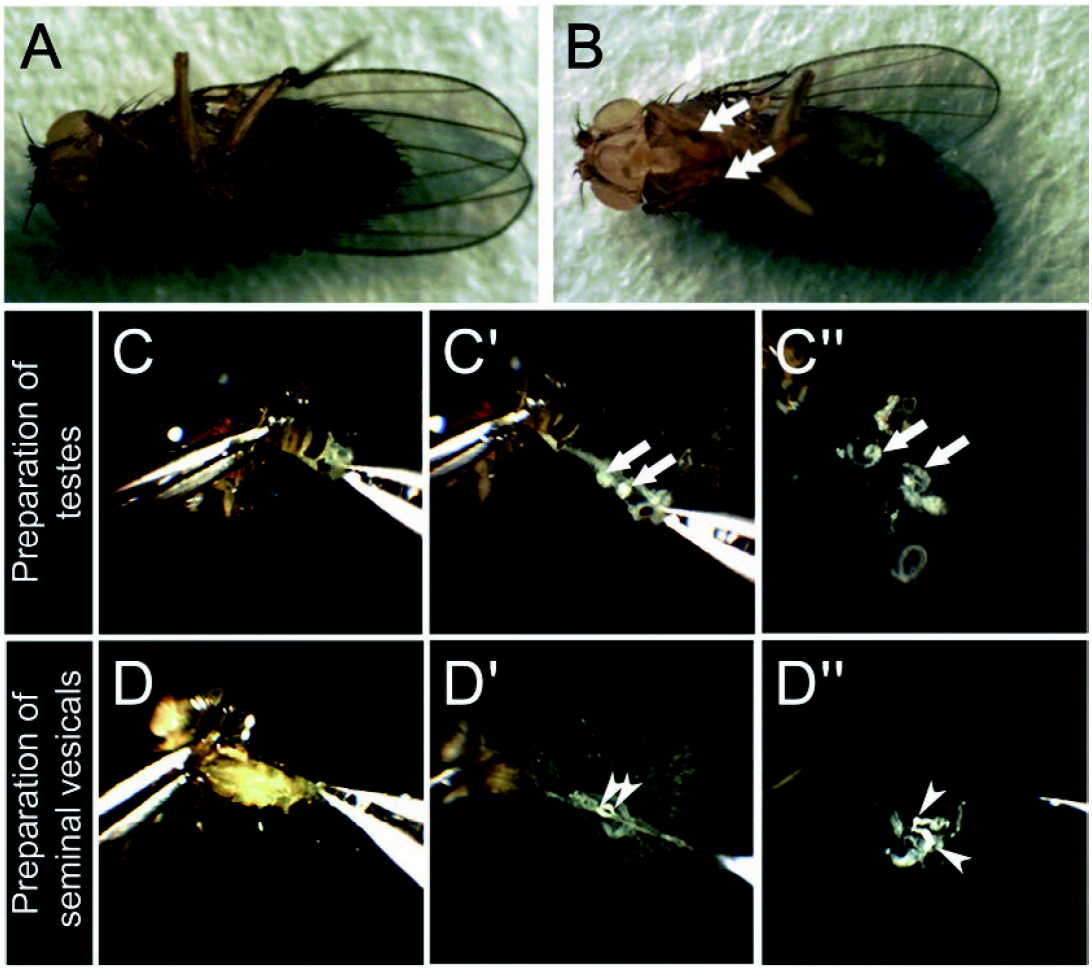

Fig. 2 Preparation of *Drosophila* testis and seminal vesicles from adult flies. (**a**) Adult *Drosophila* female. (**b**) Adult *Drosophila* male. The male-specific sex combs are marked by *double arrows*. (**c**, **d**) Adult males hold in a lateral position (left tweezers), while the last abdominal segments are gripped by a second set of tweezers (right tweezers). (**c′**, **d′**) Dissected males with abdomen torn apart. The genital apparatus including the pair of testes (one *arrow* points to one testis) and the seminal vesicles (one *arrowhead* points to one seminal vesicle), respectively, are visible. (**c″**) Testes partially detached from surrounding tissues (*arrows*). (**d″**) A genital apparatus with bulging seminal vesicles (*arrowheads*) is shown

immunofluorescence stainings on adult testes, collect the separated males in a block dish, cover the block dish with a glass lid to prevent fly away of awaking males, and immediately continue with Subheading 3.3.1.

3.3 Tissue Dissection and Preparation

3.3.1 Testis Dissection and Slide Preparation

1. Pipette a drop of PBS (about 30 µL) on a dissection pad, e.g., the lid of a petri dish or a microscope slide.
2. Place the dissection pad under a stereomicroscope (*see* **Note 6**), and transfer one male, with the help of a dissection tweezer into the drop of PBS.
3. Place the male in a lateral position (the head points to the left) with the help of two dissection tweezers.
4. Use the tweezer in your left hand to hold the fly in this position (place the tweezer between the first and the second abdominal segment) (*see* Fig. 2c).
5. Use the tweezer in your right hand to grip the last abdominal segment (Fig. 2c), and move the tweezer to the right to pull apart the abdomen (Fig. 2c′). In the course of this, the genital apparatus including the pair of testes will be revealed (Fig. 2c′, arrows).
6. Detach the testes (Fig. 2c″, arrows) from the genital apparatus and the surrounding tissues (*see* **Note 7**).
7. Pipette 30 µL of PBS in the middle of a polylysine-coated microscope slide, and transfer the testes with the help of the dissection tweezers into the drop of PBS (four to six testes per slide). Due to poly-L-lysine coating, the testes will stick to the slide.
8. Cover the testes with a cover slip (18 × 18 mm).
9. Apply a piece of paper tissue (60 × 60 mm) onto the cover slip, and gently push to aspirate excess PBS (this is enough to release the germ cells out of the testis tube and to spread them on the slide) (*see* **Note 8**).
10. Check under the stereomicroscope whether the testes are properly squashed (a broad milky spot should be visible now).
11. Hold the slide with a gripping tweezer at the frosted end, and vertically plunge the unfrosted part of the slide into liquid nitrogen. The nitrogen starts to evaporate until the slide is completely frozen (please wear safety glasses and note the safety instructions).
12. As soon as the slide is completely frozen, place it at the bench, and immediately remove the cover slip with the help of a stainless steel scalpel holder with blade.
13. Store the slide on ice in a vertical staining jar containing ice-cooled 95% ethanol for at least 15 min or until all other slides are prepared (*see* **Note 9**).
14. Continue with Subheading 3.4.1 when all slides are prepared.

3.3.2 Seminal Vesicle Dissection and Slide Preparation

1. Pipette a drop of PBS (about 30 µL) on a dissection pad, e.g., the lid of a petri dish or a microscope slide.
2. Place the dissection pad under a stereo microscope (*see* **Note 6**), and transfer one male, with the help of a dissection tweezer into the drop of PBS.
3. Place the male in a lateral position (the head points to the left) with the help of two dissection tweezers.
4. Use the tweezer in your left hand to hold the fly in this position (place the tweezer between the first and the second abdominal segment).
5. Use the tweezer in your right hand to grip the last abdominal segment (Fig. 2d), and move the tweezer to the right to pull apart the abdomen (Fig. 2d′). In the course of this, the genital apparatus including the pair of bulging seminal vesicles will be revealed (Fig. 2d′, arrowheads).
6. Detach the seminal vesicles (Fig. 2d″, arrowheads) from the genital apparatus and the surrounding tissues (*see* **Note 7**).
7. Pipette 30 µL of PBS in the middle of a polylysine-coated microscope slide, and transfer the seminal vesicles with the help of the dissection tweezers into the drop of PBS (two to four seminal vesicles per slide). Due to coating with poly-L-lysine, the seminal vesicles will stick to the slide.
8. Grab the seminal vesicles on one side with the help of dissection tweezers, and spread the sperm with the help of a dissecting needle.
9. Cover the testes with a cover slip (18 × 18 mm).
10. Apply a piece of paper tissue (60 × 60 mm) onto the cover slip and gently dab to blot away excess PBS (*see* **Note 8**).
11. Hold the slide with a gripping tweezer at the frosted end and vertically plunge the unfrosted part of the slide into liquid nitrogen. The nitrogen starts to evaporate until the slide is completely frozen (please wear safety glasses and note the safety instructions).
12. As soon as the slide is completely frozen, place it at the bench, and immediately remove the cover slip with the help of a stainless steel scalpel holder with blade.
13. Store the slide on ice in a vertical staining jar containing 95 % ethanol for at least 15 min or until all other slides are prepared (*see* **Note 9**).
14. Continue with Subheading 3.3.3 when all slides are prepared.

3.3.3 Decondensation of Sperm Nuclei

1. Incubate the slides for 1 min in a vertical staining jar containing PBS.
2. Deposit the slides horizontally in a humid chamber (the side of the slide containing the sperm points upward).

3. Pipette 80 µL of decondensation solution (*see* Subheading 2.2, **item 7**) in the middle of each slide.
4. Cover the solution with a cover slip (24 × 32 mm), close the humid chamber, and incubate the slides for 20–30 min (*see* **Note 10**).
5. Carefully remove the cover slip by hand and continue with Subheading 3.4.1.

3.4 Staining Slides for Immunofluorescence

3.4.1 Immunofluorescence Stainings: Day 1

1. Incubate the slides for 1 min in a vertical staining jar containing PBS.
2. Deposit the slides horizontally on a sheet of paper towel under the fume hood (the side of the slide containing the germ cells or sperm points upward).
3. For the fixation of the germ cells, pipette 1 mL of 3.7% F-PBS in the middle of each slide (make sure that the F-PBS covers the parts containing germ cells or sperm).
4. Incubate for 7 min (*see* **Note 11**).
5. For permeabilization, incubate the slides twice for 15 min in a vertical staining jar containing PBSTD.
6. Transfer the slides to a vertical staining jar containing PBT and incubate for 10 min.
7. Transfer the slides to a vertical staining jar containing 3% BSA/PBT, and incubate for at least 30 min to block nonspecific binding sites.
8. Deposit the slides horizontally in a humid chamber (the side of the slide containing the germ cells or sperm points upward).
9. Pipette 60 µL of primary antibody (diluted in 3% BSA/PBT) or a mixture of different primary antibodies (raised in different animals) in the middle of each slide (*see* **Note 12**).
10. Cover the antibody dilution with a cover slip (24 × 32 mm) (prevent air bubbles), close the humid chamber, and incubate over night at 4 °C (at least 16 h).

3.4.2 Immunofluorescence Stainings: Day 2

1. Carefully remove the cover slip by hand.
2. Wash the slides four times for 15 min in a vertical staining jar containing 3% BSA/PBT.
3. Deposit the slides horizontally in a humid chamber (the side of the slide containing the germ cells or sperm points upward).
4. Pipette 60 µL of fluorochrome-conjugated secondary antibody (diluted in 3% BSA/PBT) or a mixture of different secondary antibodies in the middle of each slide.
5. Cover the secondary antibody dilution with a cover slip (24 × 32 mm) (prevent air bubbles), close the humid chamber, and incubate for 90 min in the dark.
6. Carefully remove the cover slip by hand.

7. Wash the slides once for 15 min in the dark in a vertical staining jar containing 3% BSA/PBT.
8. Deposit the slides horizontally in a humid chamber (the side of the slide containing the germ cells or sperm points upward).
9. Pipette 60 µL of Hoechst solution (1 µg/mL diluted in 3% BSA/PBT) in the middle of each slide (please note the safety instructions).
10. Cover the Hoechst solution with a cover slip (24×32 mm), close the humid chamber, and incubate for 20 min in the dark.
11. Carefully remove the cover slip by hand.
12. Wash the slides three times for 15 min in the dark in a vertical staining jar containing 3% BSA/PBT.
13. Deposit the slides horizontally on a sheet of paper towel on the bench (the side of the slide containing the germ cells or sperm points upward) (*see* **Note 13**).
14. Pipette approximately 30 µL of Fluoromount-G on the middle of each slide (*see* **Note 14**), and cover with a cover slip (24×32 mm). Try to avoid air bubbles during embedding.
15. Store the slides horizontally in a preparation folder with lid at 4 °C.

3.5 Evaluation of Immunofluorescence Stainings

1. Before evaluation, store the slides in the closed preparation folder at room temperature for about 30 min.
2. Clamp one slide on the microscope stage, and use the fluorescence light produced by TRITC/Cy3 to locate the region containing the germ cells on the slide and to bring it to the right position beneath the objective. The region can be easily seen by just looking at the slide surface with the naked eye.
3. Apply a drop of immersion oil to this region.
4. Raise the microscope stage to bring the slide and the 40× objective into close proximity.
5. Switch to the Dapi/Hoechst filter, and adjust the microscope stage until the male germ cells come into a sharp focus.
6. First, get yourself an overview of the different stages of spermatogenesis by carefully looking at the differently shaped nuclei (Fig. 1). For the analysis of primary spermatocytes, it is important to note that the nucleus is characterized by three distinct Hoechst-positive areas (Fig. 3). Two of these represent the paired second and third chromosomes (Fig. 3, arrows). The third area represents the nucleolus (Fig. 3, arrowheads) formed by the nucleolus organizer region on the X and the Y chromosomes that encodes the ribosomal RNA (rRNA) [17]. Switch to phase contrast to ensure that the spermatocyte cells you are looking at are undamaged. In the course of postmeiotic spermatid differentiation, the nuclei change their shape from round to needle shaped. In parallel,

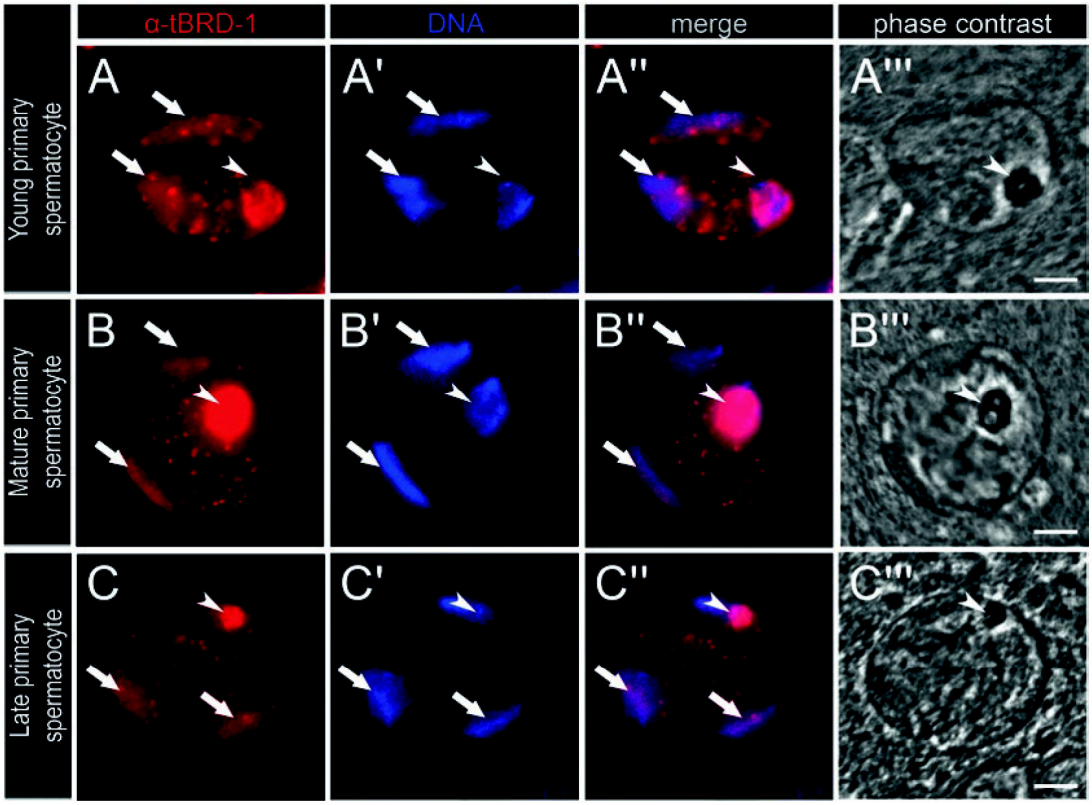

Fig. 3 tBRD-1 expression in growing spermatocytes. (**a**–**c**‴) Single primary spermatocyte nuclei stained with anti-tBRD-1 antibody. (**a**–**a**‴) In young primary spermatocyte nuclei, tBRD-1 diffusely localizes to regions of the autosomal bivalents (*arrows*) and to the nucleolus (*arrowheads*). (**b**–**b**‴) In mature primary spermatocyte nuclei, tBRD-1 is distinctly visible at the autosomal bivalents (*arrows*) and at the nucleolus (*arrowheads*). (**c**–**c**‴) In late primary spermatocyte nuclei, albeit reduced tBRD-1 is still detectable at the regions of the autosomal bivalents (*arrows*). High amounts of tBRD-1 co-localize with the shrinking nucleolus (*arrowheads*). (**a**′, **b**′, **c**′) Hoechst DNA staining. (**a**‴–**c**‴) Corresponding phase-contrast images. Scale bars, 5 μm

an exchange of histones by protamines occurs in canoe stage nuclei. This exchange is accompanied by the expression of further chromatin components, e.g., tHMG-2 (Fig. 4). Besides protamines, Prtl99C represents a further component of sperm chromatin (Fig. 5).

7. Carefully analyze the corresponding stages you are interested in, and record single-channel images (do not forget to label the images with relevant information, e.g., genotype, kind of antibody, magnification, exposure time, scale bar).
8. Before carrying out any image processing, save the original, unprocessed raw versions, and work on copies thereafter.
9. If necessary, mindfully process images using, e.g., AxioVision, Adobe Photoshop, etc.
10. Repeat your experiments to validate your results.

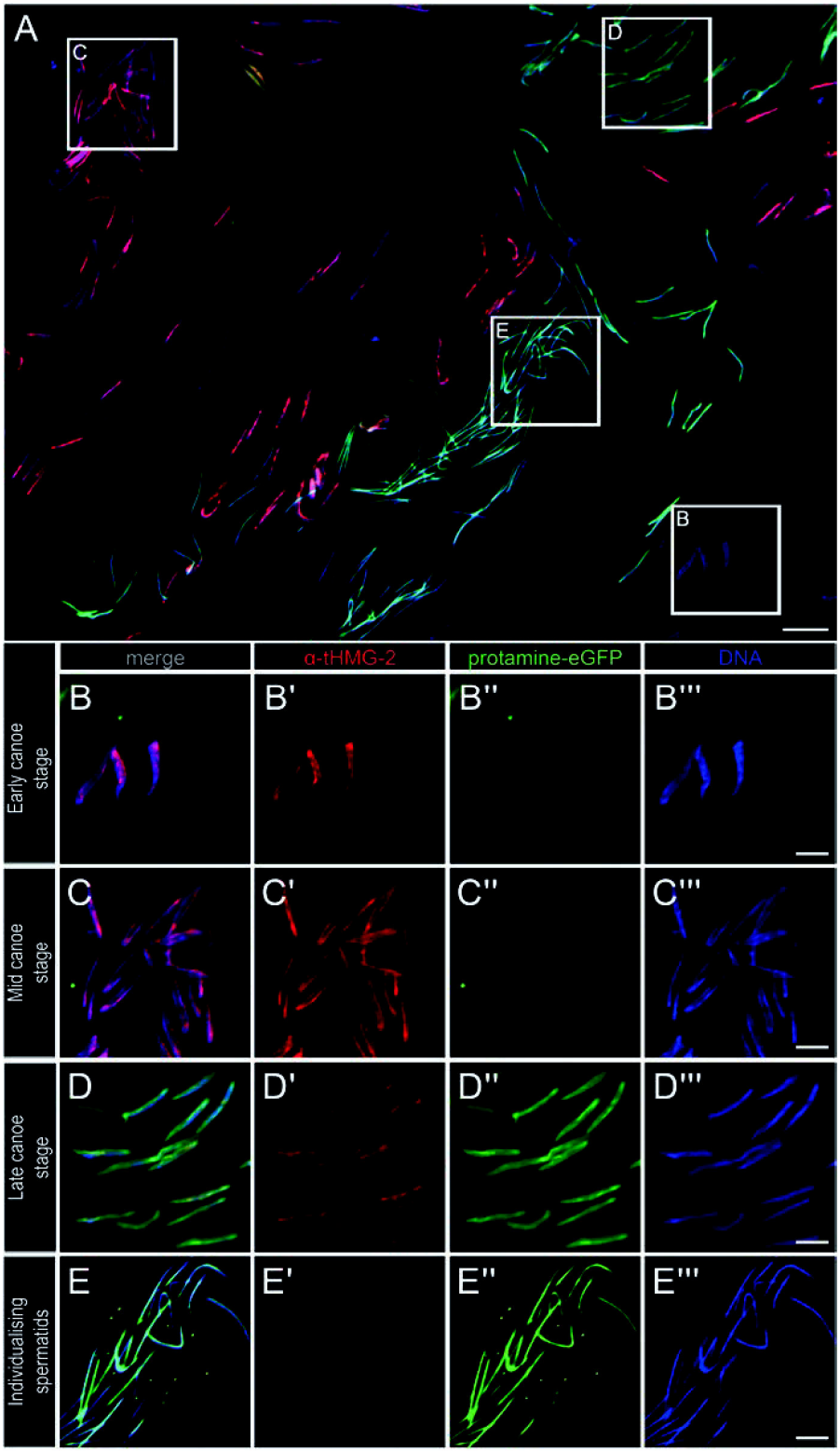

Fig. 4 Postmeiotic chromatin dynamics. (**a**) Postmeiotic haploid spermatid nuclei of transgenic flies expressing protamine B-eGFP (*green*) labeled with anti-tHMG-2 antibody (*red*) and counter stained with Hoechst (*blue*). (**b**–**b**‴) In early canoe stage spermatid nuclei, the chromatin component tHMG-2 (**b**′) is visible but no protamines (**b**″). (**c**–**c**‴) Mid canoe stage spermatid nuclei expressing tHMG-2 (**c**′). Protamines (**c**″) are hardly detectable.

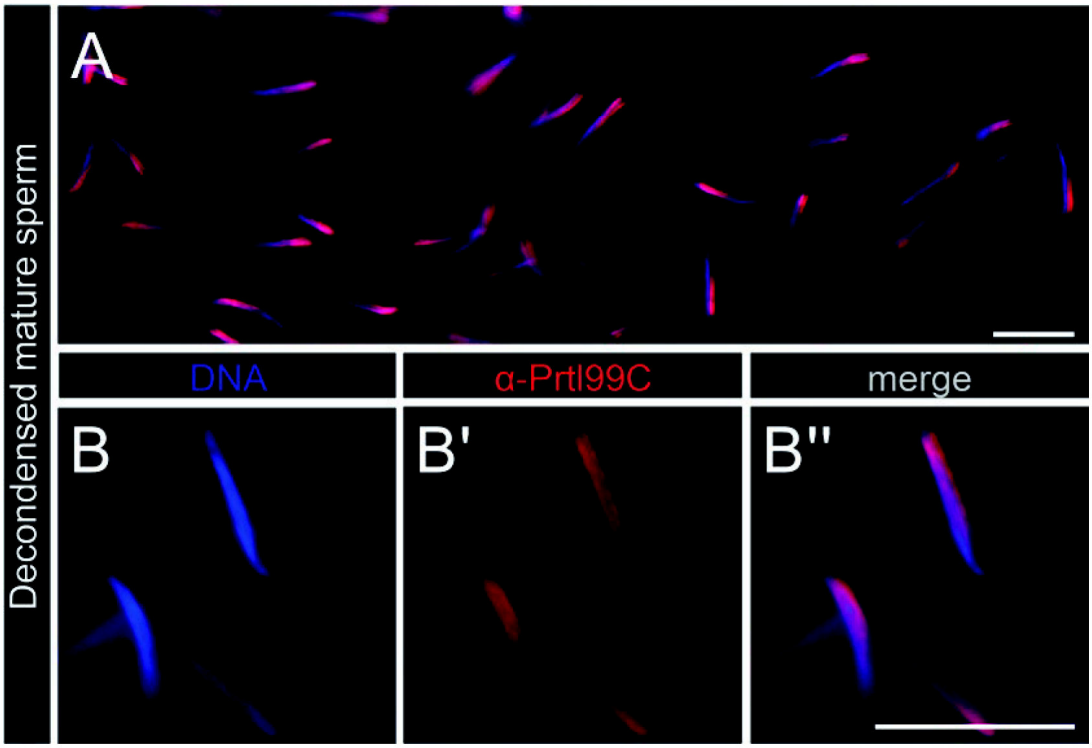

Fig. 5 The chromatin component Prtl99C in decondensed mature sperm nuclei. (**a**) Decondensed mature sperm nuclei labeled with anti-Prtl99C antibody (*red*) and counter stained with Hoechst (*blue*). (**b**–**b**″) Mature sperm nuclei expressing Prtl99C (**b**′). DNA visualized via Hoechst staining (**b**). Merge (**b**″). Scale bars, 10 μm

4 Notes

1. A pH value higher than 8.0 is required for dissolution. Triton X-100 and Tween 20 are both highly viscous chemicals. Cut the end of the micropipette tip with the help of a pair of scissors or scalpel to facilitate pipetting.
2. Ethanol is used to dehydrate the slides and can be used several times. Do not forget to label the stored ethanol, e.g., 95% ethanol for tissue dehydration.
3. Use newly hatched males to follow chromatin dynamics in spermatocytes and 1–2-day-old males to analyze chromatin in post-meiotic stages. For immunofluorescence stainings on seminal vesicles, separate newly hatched *Drosophila* males from females (*see* Subheading 3.2), and keep them at 18 °C for 5–6 days.

Fig. 4 (continued) (**d**–**d**‴) In late canoe stage spermatid nuclei, tHMG-2 (**d**′) and protamines (**d**″) are detectable. (**e**–**e**‴) Spermatid nuclei during individualization express high amounts of protamines (**e**″). Scale bars, 10 μm in **a**; 5 μm in **b**–**e**

4. You can easily build a humid chamber by yourself. Use a rectangular bake dish with lid and completely wrap the dish and the lid with aluminum foil. Cover the dish with several layers of water-moisturized paper tissue, and close the lid.
5. Do not use a marker to label your slides because you have to store your slides in ethanol later. Only use a pencil.
6. A black pad facilitates dissection.
7. Be careful to ensure that the testes or seminal vesicles do not dehydrate during dissection.
8. During squash preparation, do not push too hard; otherwise, you may destroy the cells. Also ensure that the cover slip is not slipping out of position.
9. Do not forget to label (e.g., genotype) the slide using a pencil before you proceed with the next slide. Clean the dissection pad and tweezers before you continue with the preparation of the next slide; cleaning is especially important in case you continue with another genotype.
10. The optimal time for chromatin decondensation depends on the antibodies used and has to be empirically determined accordingly.
11. When focusing your attention on spermatocyte chromatin, reduce the fixation time to 6 min.
12. To rule out nonspecific binding of the secondary antibodies, mock incubations with 3% BSA/PBT (without primary antibody) are recommended. We recommend that the specificity of the primary antibody should be validated using a mutant fly line and an antibody competition assay.
13. Be careful to ensure that the slides do not dehydrate during embedding.
14. Cut the end of the micropipette tip with the help of a pair of scissors or scalpel; this will facilitate pipetting of the viscous Fluoromount media.

Acknowledgment

This work was supported by the German Research Foundation (DFG) within the TRR 81 and a research grant to CR (RA 2150/2-1). DM and ZE-G were supported by REPRO-TRAIN Marie Curie Initial Training Network (PITN-2011-289880).

References

1. Fuller M (1993) Spermiogenesis. In: Bate M, Martinez-Arias A (eds) The development of Drosophila melanogaster. Cold Spring Harbor Laboratory Press, Cold Spring Harbor, NY, pp 71–147
2. White-Cooper H (2010) Molecular mechanisms of gene regulation during Drosophila spermatogenesis. Reproduction 139:11–21
3. Leser K, Awe S, Barckmann B, Renkawitz-Pohl R, Rathke C (2012) The bromodomain-containing protein tBRD-1 is specifically expressed in spermatocytes and is essential for male fertility. Biol Open 1:597–606
4. Theofel I, Bartkuhn M, Hundertmark T, Boettger T, Gärtner SMK, Leser K, Awe S, Schipper M, Renkawitz-Pohl R, Rathke C (2014) tBRD-1 selectively controls gene activity in the *Drosophila* testis and interacts with two new members of the bromodomain and extra-terminal (BET) family. PLoS One 9:e108267
5. Rathke C, Baarends WM, Awe S, Renkawitz-Pohl R (2014) Chromatin dynamics during spermiogenesis. Biochim Biophys Acta 1839:155–168
6. Rathke C, Barckmann B, Burkhard S, Jayaramaiah-Raja S, Roote J, Renkawitz-Pohl R (2010) Distinct functions of Mst77F and protamines in nuclear shaping and chromatin condensation during *Drosophila* spermiogenesis. Eur J Cell Biol 89:326–338
7. Eren-Ghiani Z, Rathke C, Theofel I, Renkawitz-Pohl R (2015) Prtl99C acts together with protamines and safeguards male fertility in *Drosophila*. Cell Rep 13:1–9
8. Jayaramaiah-Raja S, Renkawitz-Pohl R (2005) Replacement by *Drosophila melanogaster* protamines and Mst77F of histones during chromatin condensation in late spermatids and role of sesame in the removal of these proteins from the male pronucleus. Mol Cell Biol 25:6165–6177
9. Rathke C, Baarends WM, Jayaramaiah-Raja S, Bartkuhn M, Renkawitz R, Renkawitz-Pohl R (2007) Transition from a nucleosome-based to a protamine-based chromatin configuration during spermiogenesis in *Drosophila*. J Cell Sci 12:1689–1700
10. Gärtner SMK, Rothenbusch S, Buxa MK, Theofel I, Renkawitz R, Rathke C, Renkawitz-Pohl R (2015) The HMG-box-containing proteins tHMG-1 and tHMG-2 interact during the histone-to-protamine transition in *Drosophila* spermatogenesis. Eur J Cell Biol 94:46–59
11. Awe S, Renkawitz-Pohl R (2010) Histone H4 acetylation is essential to proceed from a histone- to a protamine-based chromatin structure in spermatid nuclei of *Drosophila melanogaster*. Syst Biol Reprod Med 56:44–61
12. Gärtner SMK, Rathke C, Renkawitz-Pohl R, Awe S (2014) Dissection of *Drosophila* pupal testis and single male germ line cysts for *ex vivo* culture, pharmacological treatment and imaging of developing male germ cells. J Vis Exp 91:e51868
13. Li Y, Lalancette C, Miller D, Krawetz SA (2008) Characterization of nucleohistone and nucleoprotamine components in the mature human sperm nucleus. Asian J Androl 10:535–541
14. Hime GR, Brill JA, Fuller MT (1996) Assembly of ring canals in the male germ line from structural components of the contractile ring. J Cell Sci 109:2779–2788
15. Mainx F (1949) Das kleine Drosophila-Praktikum. Springer, Wien
16. Hannah-Alavah A (1958) Morphology and chaetotaxy of the legs of *Drosophila melanogaster*. J Morph 103:281–310
17. Ritossa FM, Spiegelman S (1965) Localization of DNA complementary to ribosomal RNA in the nucleolus organizer region of Drosophila melanogaster. Proc Natl Acad Sci U S A 53:737–745

Chapter 6: Nejire/dCBP-mediated histone H3 acetylation during spermatogenesis is essential for male fertility in *Drosophila melanogaster*

Hundertmark, T., Gärtner, S.M.K., Rathke, C. and Renkawitz-Pohl, R. (2018). PLoS One. 2018 Sep 7;13(9):e0203622

Candidate's contribution:

- Immunofluorescence (Figure 4, 5, 7, 8)
- Fertility tests
- Production of microscopic images and figures (Figures 4, 5, 7, 8)
- Proofreading the manuscript
- Experiments for revision of the manuscript

PLOS ONE

RESEARCH ARTICLE

Nejire/dCBP-mediated histone H3 acetylation during spermatogenesis is essential for male fertility in *Drosophila melanogaster*

Tim Hundertmark, Stefanie M. K. Gärtner, Christina Rathke, Renate Renkawitz-Pohl*

Philipps University of Marburg, Department of Biology, Developmental Biology, Marburg, Germany

* renkawit@biologie.uni-marburg.de

OPEN ACCESS

Citation: Hundertmark T, Gärtner SMK, Rathke C, Renkawitz-Pohl R (2018) Nejire/dCBP-mediated histone H3 acetylation during spermatogenesis is essential for male fertility in *Drosophila melanogaster*. PLoS ONE 13(9): e0203622. https://doi.org/10.1371/journal.pone.0203622

Editor: Mary Bryk, Texas A&M University, UNITED STATES

Received: April 16, 2018

Accepted: August 23, 2018

Published: September 7, 2018

Data Availability Statement: All relevant data are within the paper and its Supporting Information files.

Funding: This work was supported by the Deutsche Forschungsgemeinschaft (SFB TRR81 "Chromatin Changes in Differentiation and Malignancies" to C.R. and R. R.-P.).

Competing interests: The authors have declared that no competing interests exist.

Abstract

Spermatogenesis in many species including *Drosophila melanogaster* is accompanied by major reorganisation of chromatin in post-meiotic stages, involving a nearly genome-wide displacement of histones by protamines, Mst77F and Protamine-like 99C. A proposed prerequisite for the histone-to-protamine transition is massive histone H4 hyper-acetylation prior to the switch. Here, we investigated the pattern of histone H3 lysine acetylation and general lysine crotonylation in *D. melanogaster* spermiogenesis to elucidate a possible role of these marks in chromatin reorganisation. Lysine crotonylation was strongest prior to remodelling and the deposition of this mark depended on the acetylation status of the spermatid chromatin. In contrast to H4 acetylation, individual H3 acetylation marks displayed surprisingly distinct patterns during the histone-to-protamine transition. We observed that Nejire, a histone acetyl transferase, is expressed during the time of histone-to-protamine transition. Nejire knock down led to strongly reduced fertility, which correlated with misshaped spermatid nuclei and a lack of mature sperm. *protA* and *prtl99C* transcript levels were reduced after knocking down Nejire. ProtB-eGFP, Mst77F-eGFP and Prtl99C-eGFP were synthesized at the late canoe stage, while histones were often not detectable. However, in some cysts histones persist in parallel to protamines. Therefore, we hypothesize that complete histone removal requires multiple histone modifications besides H3K18ac and H3K27ac. In summary, H3K18 and H3K27 acetylation during *Drosophila* spermatogenesis is dependent on Nejire or a yet uncharacterized acetyl transferase. We show that Nejire is required for male fertility since Nejire contributes to efficient transcription of *protA* and *prtl99C*, but not *Mst77F*, in spermatocytes, and to maturation of sperm.

Introduction

One of the most dramatic processes of chromatin remodelling occurs during the post-meiotic phase of spermatogenesis. The previously histone-based chromatin becomes a highly compact structure due to the nearly genome-wide replacement of histones, first by transition proteins, which are then replaced by small basic proteins called protamines. The general aspects and other characteristic features of this large-scale chromatin compaction are conserved from fly

to man (reviewed in [1–4]. However, the molecular processes that finally lead to histone replacement and chromatin condensation remain largely unknown.

One mechanism proposed to be a prerequisite for the histone-to-protamine transition is a genome-wide hyper-acetylation of histones occurring in the total absence of transcription (Braun 2001; Sassone-Corsi 2002). In mouse and *D. melanogaster*, hyper-acetylation of histone H4 is observed in elongating spermatids and gradually disappears in parallel with histone degradation [5–7]. A lack of histone hyper-acetylation correlates with male infertility in mouse and man [8, 9]. Furthermore, histones lack hyper-acetylation in species where histones are not replaced by protamines [10]. Similarly, histone hyper-acetylation is essential for chromatin reorganisation in *D. melanogaster* spermiogenesis, since inhibition of acetylation after the pre-meiotic transcriptional phase blocks further spermatid differentiation, and the chromatin remains histone bound (Awe and Renkawitz-Pohl, 2010). These data clearly demonstrate that hyper-acetylation is tightly linked to histone replacement. Simultaneously with H4 hyper-acetylation, H3K9 acetylation, lysine crotonylation and H3K4, H3K9 and H3K79 methylation are described to increase prior to the transition from histones to protamines [7, 11–13]. As in mammals, in *D. melanogaster* histones are successively replaced by protamines (ProtA and ProtB) and in *Drosophila* by two additional abundant sperm chromatin components, Mst77F [14–17] and Protamine-like99C (Prtl99C) [18].

How H4 hyper-acetylation and other histone modifications regulate the histone-to-protamine transition in elongating spermatids is poorly understood. According to the histone code hypothesis, modifications could define specific signals and serve as an interface language between histones and chromatin modifying activities [19]. As part of the histone code, acetylated lysine residues, as well as other post-translational histone modifications, provide binding sites for specific protein interactions. Since both the assembly and removal of histones in somatic cells during replication, DNA repair and transcription involve specialized machineries (reviewed in [20], histone hyper-acetylation by distinct histone acetyl-transferases in elongating spermatids could serve as a signal to recruit the machinery displacing histones. Part of such a machinery could be bromodomain-containing proteins, since the bromodomain is a motif that specifically binds to acetylated lysine residues [21] (for review see [22]). In *D. melanogaster*, blocking histone acetylation specifically in the post-meiotic phase by inhibitors led to loss of protamine deposition. As in mice, *D. melanogaster* histone hyper-acetylation cannot be the sole inducer of the switch since premature histone hyper-acetylation does not lead to a premature protamine-based chromatin structure [23].

Here, we identified post-translational histone modifications accompanying histone-to-protamine transition in *D. melanogaster* with the focus on histone H3 acetylation. In addition, we searched for enzymes mediating histone modifications, such as histone acetyl-transferases, which may function as "writer factors" in the histone-protamine-transition phase. We show that histone H3 acetylation displays a highly diverse pattern compared to H4 acetylation. Remarkably, after meiosis H3K18ac and H3K27ac are limited to the early canoe stage just prior to the histone-to-protamine transition. We postulate Nejire or an enzyme with the same specificity as a putative "writer" of these post-meiotic H3 histone acetylations. Germ line-specific knock down of Nejire led to a lack of mature sperm, demonstrating a function of Nejire in proper spermatid differentiation.

Materials and methods

Fly stock and maintenance

D. melanogaster strains were maintained on standard medium at 25˚C. w^{1118} was used as the wild-type strain. Protamine B-mCherry (ProtB-mCherry) transgenic flies were generated by

modifying the ProtamineB-eGFP construct of [15]. For *nejire* functional studies the RNAi line v105115 (Vienna Drosophila Resource Center) was combined with ProtB-GFP, Mst77F-eGFP [15] and Prtl99C-eGFP [18] transgenic fly lines. For the *nejire* knock down, v105115 protB-GFP males were crossed against virgin females of bam-Gal4/bam-Gal4; Sp/CyO; bam-Gal4-VP16/MKRS. Crossings for knock down experiments were maintained at 30˚C.

Culture of pupal testes and inhibitor treatment

Pupal testes cultures of transgenic flies carrying ProtB-mCherry were established as described in [23]. In short, pupal testes were dissected in Shields and Sang M3 insect culture medium (Sigma- Aldrich Cat#S8398) supplemented with 10% foetal bovine serum (heat inactivated, insect culture tested, Sigma-Aldrich Cat#F3018), 100 U/ml penicillin and 100 mg/ml streptomycin (Gibco-Invitrogen Cat No. 15140–148). The intact testes were transferred to a 25-well plate. For inhibitor treatment, generally, six pupal testes were used for each inhibitor and control per experiment. The experiments were repeated at least three times.

Testes were treated with anacardic acid (AA, Merck Biosciences; 28.69 mM in DMSO stock) and trichostatin A (Cell Signalling Tech.; 4 mM in ethanol stock) in appropriate dilution in culture medium. Control cultures with solvent alone were analysed in parallel. Cultures were incubated for 24 h at 25˚C.

Sterility tests. One adult male of each genotype was placed together with two wild-type virgin females in a vial for 3 days at 25˚C. After 3 days, the parental generation was removed from the vials. After 2 weeks, offspring in each vial were counted.

Antibodies and immunofluorescence staining

For immunofluorescence analysis, adult testes and cultured pupal testes of transgenic flies carrying ProtB-mCherry were squashed and treated essentially as described in Hime et al.[24]. DNA was stained with Hoechst 33258 dye. H3K4ac was probed with Histone H3K4ac antibody (pAb) (active motif, Cat. No. 39382) in 1:100, 1:250, 1:500 and 1:1000 dilutions. Histone H3K9ac was detected with antibody anti-Acetyl-Histone H3 (Ac-Lys9) (Sigma, Cat. No. H9286) at a 1:500 dilution. H3K14ac was detected with Histone H3K14ac antibody (pAb) (active motif, Cat. No. 39698) at a 1:500 dilution. H3K4ac was detected with Histone H3K4ac antibody (pAb) (Millipore) at 1:100, 1:250, 1:500 and 1:1000 dilutions. H3K18ac was detected with Histone H3K18ac antibody (pAb) (active motif, Cat. No. 39756) at a 1:500 dilution. H3K23ac was detected with antibody Histone H3K23ac antibody (pAb) (active motif, Cat. No. 39132) at a 1:600 dilution. H3K27ac was detected with Histone H3K27ac antibody (pAb) (active motif, Cat. No. 39136) at a 1:500 dilution. H3K36ac was detected with Histone H3K36ac antibody (pAb) (active motif, Cat. No. 39380) at a 1:250 dilution. H3K56ac was detected with anti-acetyl-Histone H3 (Lys56) antibody (Millipore, 04–1135) at a 1:1000 dilution. H3K64ac was detected with Histone H3K64ac antibody (pAb) (active motif, Cat. No. 39546) at 1:100, 1:250, 1:500 and 1:1000 dilutions. H4K5ac was detected with Histone H4K5ac antibody (pAb) (active motif, Cat. No. 39170) at a 1:500 dilution. H4K8ac was detected with Histone H4K8ac antibody (pAb) (active motif, Cat. No. 61103) at a 1:500 dilution. H4K12ac was detected with antibody Histone H4K12ac antibody (pAb) (active motif, Cat. No. 39928) at a 1:500 dilution. Kcr was detected with antibody anti-crotonyllysine antibody (PTM Biolabs, Cat.No. PTM-501) at 1:200 dilution. Histones were detected with antibody anti-Histone, F152.C25.WJJ (Millipore) at a 1:1200 dilution. Nejire was detected with antibody anti-CBP [25] at a 1:1000 dilution. These primary antibodies were visualized with anti-rabbit, DyLight488-conjugated secondary antibody (Vector Laboratories) at 1:100 dilutions.

RNA isolation and qPCR

RNA from 300 Bam>>v105115 testes or v105115 undriven testes was extracted using TRIzol (Invitrogen). Extracted total RNA was treated with RNase-free Turbo DNase (Ambion) and purified using an RNeasy mini kit (Qiagen). 1 μg of DNAse treated and purified RNA was used for cDNA synthesis with the Transcriptor First Strand cDNA Synthesis kit (Roche) according to the manual in a 20 μl reaction. qPCR reactions were set up with 10 μl iTaq™ Universal SYBR® Green Supermix (Bio-Rad), 4 μl ddH_2O, 0.5 μl (10 μM) gene-specific primer A, 0.5 μl (10 μM) gene-specific primer B and 5 μl cDNA (1:25 dilution). qPCR was performed in three technical replicates on the Mx3000P qPCR. Ct values were normalized to the mRNA expression level of Rpl32. Mean value and SEM of three biological replicates was calculated using GraphPad PRISM version 5.03. For statistical analysis one-sample t-test with a hypothetical value of 1 was used.

Results

Multiple histone H3 acetylations in early and late canoe stages of the histone-to-protamine transition phase of *D. melanogaster* spermatogenesis

In *D. melanogaster*, the histone-to-protamine transition takes place during the so-called canoe stage. Here, the early canoe stage is defined by the start of histone removal, and the late canoe stage by the start of protamine accumulation [7]. Hyper-acetylation of histone H4 is proposed to be a prerequisite for histone removal during spermiogenesis in flies and mammals. In addition, a simultaneous increase in histone H3 acetylation was shown in mammals [6]. However, little is known about a possible role of H3 acetylation in post-meiotic chromatin remodelling.

Histone H4 acetylation is continuously visible from the spermatocyte stage to the canoe stage, where H4 hyper-acetylation is evident. In contrast, the histone H3 acetylation displayed an unexpected specific pattern within the stages of spermiogenesis (Table 1). We aimed to identify the overall pattern of histone H3 acetylation in spermiogenesis of *D. melanogaster* using specific commercially available antibodies against acetylated lysine residues K4, K9, K14,

Table 1. Acetylation and crotonylation of histones in nuclei at different stages of spermatogenesis.

	Spermatocytes	Round spermatid	Youngelongatingspermatid	Early canoe stagespermatid	Late canoe stagespermatid	Individualizedsperm
Anti-H4K5ac	+	+	+	+	-	-
Anti-H4K8ac	+	+	+	+	-	-
Anti-H4K12ac	+	+	+	+	-	-
Anti-H4K16ac	-	-	-	-	-	-
Anti-H3K4ac	-	-	-	-	-	-
Anti-H3K9ac	+	-	+	+	-	-
Anti-H3K14ac	+	-	-	+	+	-
Anti-H3K18ac	+	-	-	+	-	-
Anti-H3K23ac	+	-	-	+	+	-
Anti-H3K27ac	+	-	-	+	-	-
Anti-H3K36ac	+	-	-	-	+	-
Anti-H3K56ac	+	-	-	-	-	-
Anti-H3K64ac	-	-	-	-	-	-
Anti-Kcr	+	-	-	+	(+)	-

Results are based on immunostaining of squashed testes preparations. Note that samples were analysed in a qualitative manner: +, detectable signals; -, no detectable signals; (+), rarely detectable signals. See the text for explanation of the colours.

https://doi.org/10.1371/journal.pone.0203622.t001

K18, K23 and K27 in the N-terminal domain of histone H3 and K36, K56 and K64 in the globular core domain (summarized in Table 1). Of these antibodies anti-H3K4ac and anti-H3K64ac showed no specific signal in germ cells. H3K56 acetylation was only detectable in primary spermatocytes (data not shown). H3K27ac is present in spermatocytes and prominent later in early canoe stage nuclei (Table 1). In addition to acetylation in primary spermatocytes, the other antibodies displayed characteristic post-meiotic acetylation patterns that for the most part allowed us to group post-meiotic histone H3 lysine acetylation into three classes: (1) acetylation that occurs prior to the histone to protamine transition; (2) acetylation occurring during the time of the transition (late in the early canoe, and beginning of late canoe stage), and (3) acetylation that occurs when most of the chromatin is protamine based (summarized in Table 1; example shown in Fig 1).

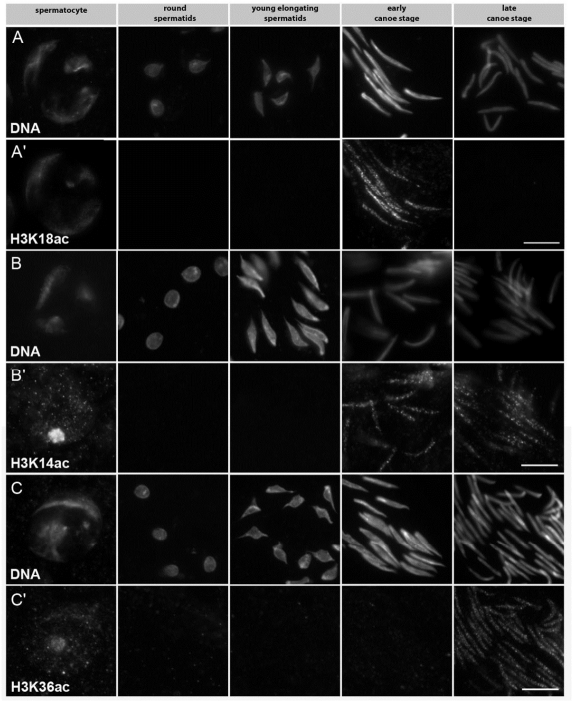

Fig 1. Histone H3 lysine acetylation displays a variable pattern in *Drosophila* spermiogenesis. (A-C′) Immunostaining of squashed preparations of spermatocyte and spermatid nuclei from adult testes of ProtB-mCherry expressing flies. (A, B, C) DNA visualized with Hoechst dye. Expression of the ProtB-mCherry fusion protein (from late canoe stage onward) was used to distinguish early and late canoe stage spermatids (not shown). (A′) H3K18ac detected with an anti-H3K18ac antibody was present prior to the switch from histones to protamines in early canoe stage spermatids in a speckled pattern at the nuclei (column 4). (B′) H3K14ac detected with an anti-H3K14ac antibody in early and late canoe stage spermatids gives a speckled pattern at the nuclei (column 4). (C′) H3K36ac detected with an anti-H3K36ac antibody gives a speckled pattern at the nuclei of late canoe stage spermatids (column 5). Scale bar: 10 μm.

https://doi.org/10.1371/journal.pone.0203622.g001

In the first group, histone H3K9, H3K18 and H3K27 acetylation (Fig 1A′) were detected prior to transition (Table 1, green). H3K9ac was strongest in young elongating and early canoe stage nuclei (Table 1). The signal disappeared in conjunction with histone degradation. H3K18ac (Fig 1A′) and H3K27ac (Table 1, green) are remarkable because of their speckled patterns, which occurred only in early canoe stage nuclei.

The second group comprises H3K14ac (Fig 1B′) and H3K23ac (Table 1, blue); both showed a speckled pattern in early and late canoe stage nuclei. H3K36ac represents a third class, since it was exclusively found in late canoe stage nuclei, clearly visible as a speckled pattern (Fig 1C′ and Table 1, orange).

The histone mark lysine crotonylation is detectable in spermatocytes and canoe stage nuclei

In mouse, a recently discovered new histone mark, lysine crotonylation (Kcr), was reported to show intense labelling during elongating spermatid steps 9–11 ([13] for review see [26]). The intense lysine crotonylation signal coincides with the genome-wide histone hyper-acetylation prior to the switch from histones to protamines shown by [6]. Since lysine crotonylation is an evolutionarily conserved histone mark in *D. melanogaster* and mouse, we investigated the distribution of this histone modification in *Drosophila* spermatogenesis by staining squashed preparations of adult testes using an anti-Kcr antibody. Kcr is detectable in primary spermatocyte nuclei over the chromosome regions (Fig 2, column 1, arrowheads). In post-meiotic stages, Kcr is restricted to canoe stage nuclei where the speckled signal is most prominent in early canoe stage nuclei (Fig 2, column 2; Table 1). Thus, we conclude that Kcr disappears in correlation with histone degradation.

Anacardic acid blocks H3 acetylation and lysine crotonylation whereas TSA induces premature H3 acetylation and lysine crotonylation at the round nuclei stage

As we have shown previously, histone acetylation is essential for the transition from histone-based chromatin to protamine-based chromatin in *D. melanogaster* spermiogenesis [23]. To gain further insights into the role of H3 acetylation and lysine crotonylation during the time of

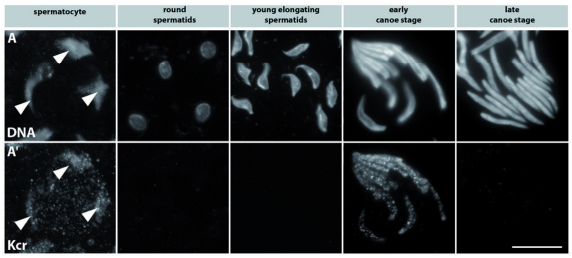

Fig 2. Histone lysines are crotonylated mainly at the early canoe stage shortly before protamine deposition in post-meiotic spermatid nuclei. Immunostaining of squashed testes preparations from ProtB-mCherry expressing flies. Expression of the ProtB-mCherry fusion protein was used to distinguish early and late canoe stage spermatids (not shown). (A) DNA visualized with Hoechst dye. (A′) Lysine-crotonylation detected with an anti-Kcr antibody over the chromosomes in primary spermatocytes (column 1, arrowheads). In early canoe stage nuclei the Kcr signal reappeared and remained until ProtB-mCherry expression had just started in late canoe stage spermatids (column 4–5). Scale bar: 10 μm.

https://doi.org/10.1371/journal.pone.0203622.g002

transition, we used our established culture system for pupal *Drosophila* testes monitored with RFP or GFP tagged protamines [27]. In these cultures, the histone-to-protamine switch takes place as within the intact fly. The time of transition is easily assessed since the first spermatid cysts switch to protamine-based chromatin between 24 and 48 hours after puparium formation (APF). These properties make cultured pupal testes a valuable test system to study the histone to protamine transition using inhibitor treatment.

To study the effect of inhibiting histone acetyl-transferase (HAT) and histone deacetylase (HDAC) on H3 lysine acetylation and lysine crotonylation specifically in the post-meiotic phase, we isolated pupal testes of ProtB-mCherry transgenic flies at around 24 h APF. To block histone acetylation, these testes were subjected in culture to 150 μM of the HAT inhibitor anacardic acid (AA) for about 24 hours. A known inhibitor of several HAT families [28]. AA neither induces apoptosis nor shows cytotoxic effects in cultured testes, but leads to a block in elongating spermatid differentiation [23]. To block HDAC activity we treated cultured testes for 24 h with 50 μM trichostatin A (TSA). TSA inhibits both class I and II HDACs [29, 30] leading to premature H4 acetylation in *Drosophila* spermiogenesis, while showing no obvious effect on histone to protamine transition [23].

Since the behaviour of lysine crotonylation with respect to HATs and HDACs has only been described in cell culture experiments [13] we examined Kcr distribution after AA and TSA treatment in *D. melanogaster* spermatogenesis. In control testes, Kcr was visible at the early canoe stage up until the late canoe stage was reached (Fig 3A′). At this stage protamines are also deposited in cultured testes, as monitored by ProtB-mCherry expressing post-transition spermatids, which were detectable after 24 h of incubation (data not shown).

In testes treated with AA no late canoe stage spermatids had developed (Fig 3B and 3B′). As expected from our studies with H4 acetylation, both H3K14ac and H3K18ac are no longer detectable in AA treated testes (data not shown). For adding and removing Kcr on histones it has been suggested that the enzymes responsible are independent from those mediating lysine acetylation and deacetylation [13]. Thus, we expected no changes in Kcr distribution upon treatment with AA and TSA. Surprisingly, inhibition of HATs led to a complete loss of Kcr in cultured testes (Fig 3B′) compared to control testes (Fig 3A′). TSA treatment increased acetylation at all stages where HDAC activity is required (not shown) and resulted in enhanced and premature Kcr addition in round and young elongating spermatids (Fig 3C′).

In summary, our data further strengthen the role of histone acetylation as being an essential feature in allowing *D. melanogaster* spermatids to develop further, including the transition from histone- to protamine-based chromatin. We identified Kcr as a new histone mark that depends on the acetylation status of the spermatid chromatin and probably plays a role during *D. melanogaster* spermiogenesis.

The histone acetylase Nejire/dCBP is detected in spermatocytes and in the late canoe stage

The extensive reorganisation of chromatin during spermiogenesis requires stage-specific patterns of histone lysine acetylation. Consequently, we searched for enzymes that set these marks and thereby play a putative role in chromatin remodelling and spermatogenesis. H3K18ac and H3K27ac are specifically detected in the early canoe stage (Table 1). These are marks set by the CREB-binding protein (CBP), a lysine acetyl transferase also known as Nejire/dCBP in *Drosophila* [31]. Therefore, we concentrated on analysing Nejire/dCBP. Squashed testes preparations stained with an antibody against Nejire/dCBP revealed expression of Nejire/dCBP in somatic cells of the testes (data not shown) and in the germ line (Fig 4A′). Nejire/dCBP was expressed in primary spermatocytes, then not detected in early post-meiotic stages, but

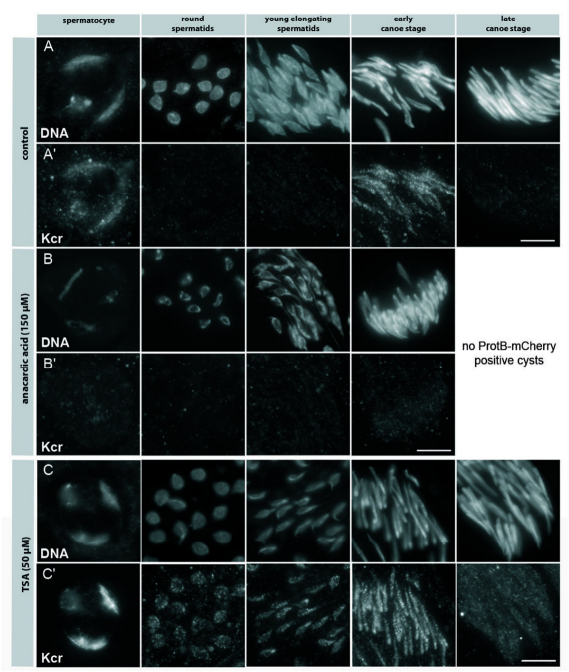

Fig 3. Histone lysine crotonylation depends on histone acetylation. Squashed preparations of spermatid nuclei from pupal testes of ProtB-mCherry expressing flies at 24 h APF incubated for 24 h with either 150 μM AA (B, B′) and 50 μM TSA (C, C′) compared to untreated testes (A, A′). (A, B, C) DNA visualized with Hoechst dye. (A′, B′, C′) Kcr detected with an anti-Kcr antibody. Expression of the ProtB-mCherry fusion protein was used to distinguish early and late canoe stage spermatids (not shown). Treatment with AA led to a complete loss of Kcr (B′) compared to untreated testes (B). In addition, further development of spermatids was blocked (B′). Treatment with TSA (C, C′) led to a strong increase in Kcr at the chromosomal regions in primary spermatocytes (C′, column 1). In post-meiotic stages, premature Kcr occurred in round and young elongating spermatid nuclei (C′, columns 2 and 3). Scale bar: 10 μm.

https://doi.org/10.1371/journal.pone.0203622.g003

reappeared in late canoe stage nuclei (Fig 4A′). Lysine acetylation mediated by Nejire/dCBP, i.e. H3K18ac and H3K27ac, was detected at the early canoe stage (Table 1). This seemed a contradiction to the visibility of Nejire/dCBP at the late canoe stage, were histones are not detectable anymore. We searched in FlyBase for other candidates with the ability to acetylate H3K18 and H3K27. The genome of *D. melanogaster* contains numerous genes with coding capacity for acetyl transferases. Corresponding transcripts were found in testes of adult males for many of them. For some of these acetyl transferases, the targeted histone or a defined lysine residue is known, but none of them was characterized as targeting H3K18 and H3K27 (S1 Table). Thus, we considered that Nejire/dCBP might be the responsible enzyme and only detectable in late canoe stage because Nejire/dCBP is present in chromatin remodelling complexes and not accessible to the antibody during the early canoe stage, while the N-terminal acetylation marks H3K18ac and H3K27ac are accessible to the antibody. At the late canoe stage, histones are not detectable anymore in the already highly condensed chromatin, thus at this time Nejire likely is in the nucleoplasm and therefore might accessible to the antibody at this time. Thus, we

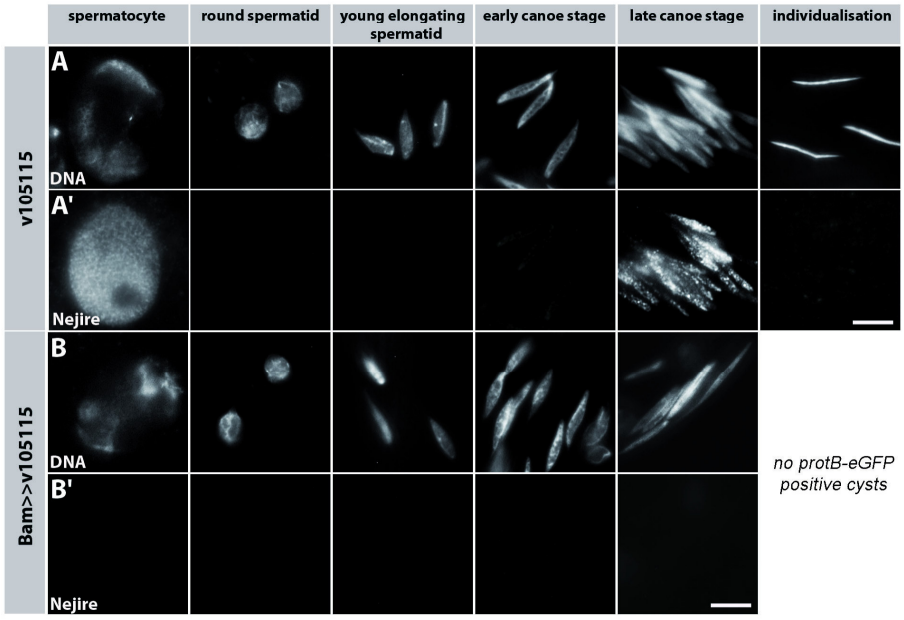

Fig 4. Nejire/dCBP is stage specifically expressed in spermatocytes and spermatid nuclei. Immunostaining of squashed testes preparations from ProtB-mCherry transgenic flies. Expression of the fusion protein was used to distinguish early and late canoe stage spermatids (not shown). (A′) Nejire/dCBP was detected with an anti-dCBP antibody in nuclei of spermatocytes and spermatids, and (A) DNA visualized with Hoechst dye; (column 3–5). B′) Nejire/dCBP is efficiently knocked down by RNAi in spermatocytes in spermatocyte nuclei (column 1) and in late canoe stage spermatids (column 4); (B) DNA was visualized with Hoechst dye. Scale bar: 5 μm.

https://doi.org/10.1371/journal.pone.0203622.g004

approached the role of Nejire/dCBP both by knock down specifically in the male germ line and by specifically inhibiting acetylation during spermiogenesis.

Despite Nejire knock down Prot-eGFP, Mst77F-eGFP and Prtl99C-eGFP are synthesized

Inhibition of all acetylations by inhibitors led to the failure of protamination. Therefore, we asked whether knocking down Nejire/dCBP dependent H3 acetylation is sufficient to abolish protamination.

To obtain a functional insight into the *in vivo* role of Nejire/dCBP in protamination, we applied RNAi-mediated knock down specifically in male germ cells, since Nejire is also expressed in somatic cells of the testis. Knock down of Nejire/dCBP by the germ line limited driver line bamGal4 was efficient in spermatocytes and canoe stage spermatids (Fig 4B′). In *D. melanogaster*, several sperm proteins act additively to compact the paternal genome [18]. Therefore, we analysed the expression of ProtA-eGFP, Mst77F-eGFP, Prtl99C-eGFP in the Nejire/dCBP knock down situation.

In an overview of whole mount testes, it was evident that eGFP-labelled sperm proteins are present in young males (0–6 h after hatching) and three day old males (72–78 h after hatching) (Fig 5). At both stages, the overall morphology of the testes and the presences of elongated

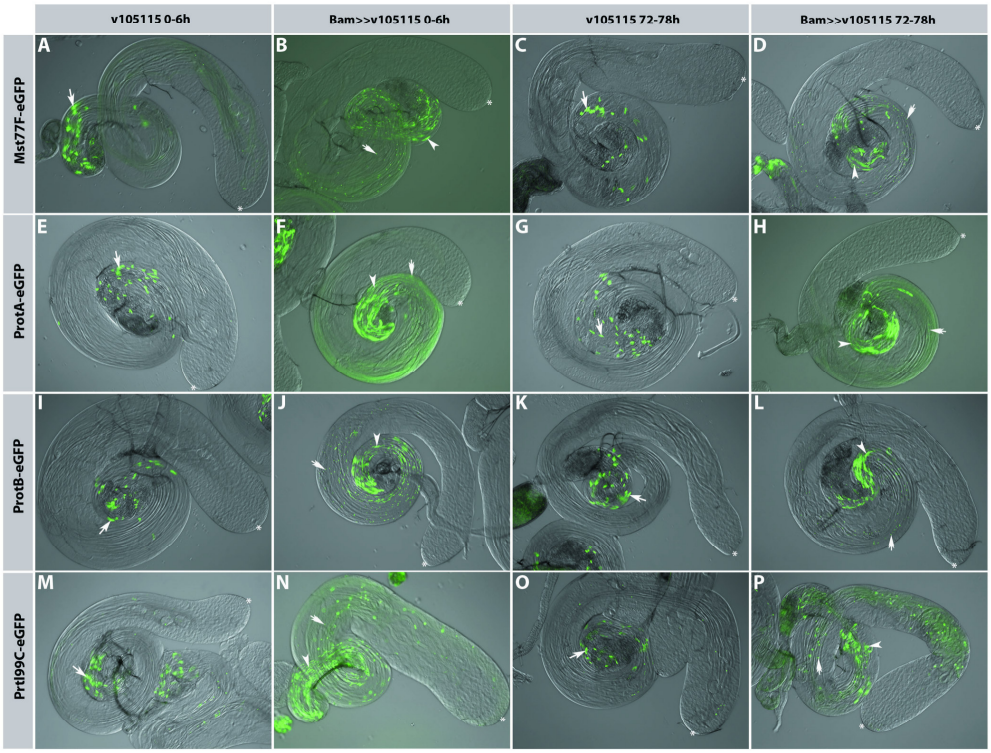

Fig 5. Mst77F, ProtB and Prtl99C are expressed after knock down of Nejire/dCPB. Whole mount preparations (fluorescence and DIG of testes from Mst77F-eGFP (A-D), ProtA-eGFP (E-H), ProtB-eGFP (I-L) and Prtl99C-eGFP (M-P) expressing flies (BamGAl4 strain as the control (A, E, I, M 0–6 h after hatching and C, G, K 72–78 h after hatching), and in the Nejire/dCBP knock down situation (B, F, J, N 0–6 h after hatching and D, G, K, O 72–78 h after hatching). Arrows indicate cysts with elongated spermatid nuclei, arrowheads point to scattered elongated nuclei, double arrows point to scattered small round or oval spermatid nuclei.

https://doi.org/10.1371/journal.pone.0203622.g005

flagella were similar in control and Nejire/dCBP knock down males. Spermatid nuclei expressed Mst77F-eGFP (Fig 5A–5D), ProtA-eGFP (Fig 5E–5H), ProtB-eGFP (Fig 5I–5L) and Prtl99C-eGFP (Fig 5M–5P). In the control (bam GAL4 driver line) eGFP-positive nuclei accumulate towards the seminal vesicles, and the synchronously developing spermatid nuclei of cysts were evident (arrow). However, in the Nejire/dCBP knock down situation additional elongated eGFP-positive nuclei (arrowhead) and small round or oval nuclei (double arrow) were scattered towards the hub region (asterisk). In the whole mounts this is particular visible in Fig 5J,5N and 5P. Therefore, we conclude that Nejire is essential for correct maturation of sperm nuclei.

Post-meiotic *de novo* H3K18 and H3K27 acetylation

We hypothesized that Nejire/dCBP acetylates the histone lysine residues shortly before the time of histone-to-protamine transition. Alternatively, acetylations might persist from the

spermatocyte phase and become visible due to the enormous reduction in the nuclear volume [32]. To test this hypothesis of post-meiotic acetylation, we used our pupal testes culture system (as described above). The histone-to-protamine transition takes place between 50–60 h after meiotic divisions [23]. We treated pupal testes of ProtB-mCherry transgenic flies with the HAT inhibitor anacardic acid and the HDAC inhibitor trichostatin A. We chose an incubation time of 24 h to avoid effects of transcriptional regulation in the spermatocyte stage. Thus spermatids at the canoe stage, between 40 h and 60 h after meiosis, went through the spermatocyte stage before we took the testes into culture.

Immunofluorescence staining with anti-H3K18ac antibody revealed that in contrast to the untreated control testes (Fig 6A′) H3K18ac was almost undetectable in post-meiotic stages in AA-treated testes (Fig 6B′). Testes treated with TSA displayed an increase in the H3K18ac signal (Fig 6C′). Furthermore, H3K18ac was prematurely detected from young elongating spermatid stages onwards (Fig 6C′, columns 3–5). This argues for the activity of a so far uncharacterized

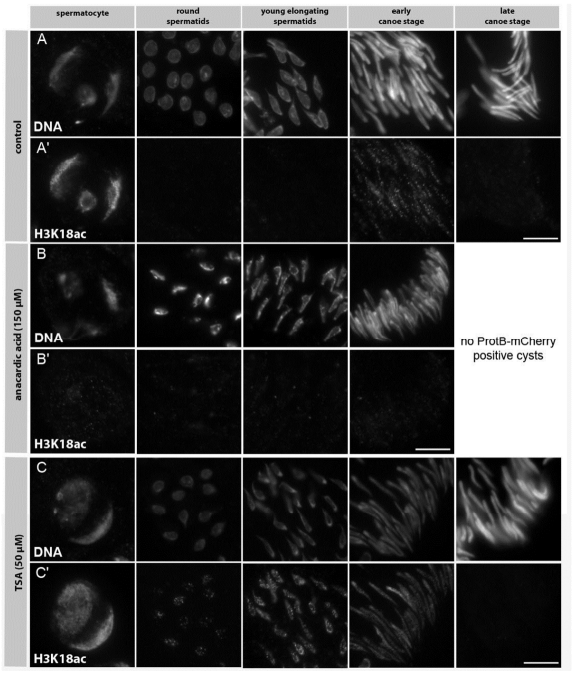

Fig 6. Anacardic acid inhibits post-meiotic acetylation of H3K18. Squashed preparations of spermatid nuclei from pupal testes of ProtB-mCherry expressing flies at 24 h APF incubated for 24 h with either 150 μM AA (B, B′) or 50 μM TSA (C, C′) in comparison to untreated testes (A, A′). (A, B, C) DNA visualized with Hoechst dye. (A′, B′, C′) H3K18ac detected with an anti-H3K18ac antibody. Expression of the ProtB-mCherry fusion protein was used to distinguish early and late canoe stage spermatids (not shown). Treatment with AA leads to a complete absence of H3K18ac signal in post-meiotic spermatid stages (B′, column 4). In comparison to untreated testes (A′, columns 4 and 5) further spermatid differentiation is blocked. In primary spermatocytes H3K18ac was strongly reduced (B′, column 1). Treatment with TSA induced premature H3K18ac appearance in young elongating spermatid nuclei (C′, column 3). TSA also induced increased nuclear H3K18ac levels in primary spermatocytes (C′, column 1). Scale bar: 10 μm.

https://doi.org/10.1371/journal.pone.0203622.g006

enzyme with the same target specificity as Nejire/dCBP. In this experiment differentiating spermatids arrested before or during the histone-to-protamine transition. This might be due to inhibition of more than H3 acetylations in this assay, for example H4 acetylation [23].

Based on these findings we propose that Nejire/dCBP-mediated H3K18 and H3K27 acetylation in spermatids is a specific post-meiotic activity.

Nejire/dCBP is essential for high levels of *protB* and *prtl99C* transcripts

When monitoring Nejire/dCBP (Fig 4A′) and H3K18ac and H3K27ac (Table 1) during the spermatocyte highly active transcriptional phase, these signals were severely reduced after RNAi-mediated *nejire* knock down (Figs 4B′ and 7B′; Panel B′ in S1 Fig). *Mst77F*, *protA*, *protB* and *prtl99C* genes are transcribed in spermatocytes and transcripts are under translational repression until the end of the canoe stage. The corresponding proteins accumulate during the late canoe stage in the spermatid nucleus [18, 33]. It is likely that transcription of these genes depends on Nejire/dCBP. To test this, we isolated RNA from testes of the undriven RNAi line v105115 and *bamGAL4* driven RNAi *(v105115)* to quantify *nejire* transcripts. We determined the relative transcript level of *mst77F*, *protA*, *prtl-99C*, *nejire/dCBP* and *tbrd-1* as controls (Fig 8G).

In the knock down situation, *nejire* transcripts are reduced considerably. The residual *nejire* transcripts were likely due to Nejire expression in somatic cells of the testes, which are not affected by the *bamGAL4* driver line. tBrd1 transcripts and proteins are limited to the spermatocyte stage [34]. We chose *tbrd1* transcripts since *Mst77F*, *prtl99C*, *protA* and *protB* genes do not belong to tBRD1 target genes [35, 36]. *tbrd-1* transcript levels were not significantly changed upon *nejire* knock down. *Mst77F* transcript levels were not severely reduced in the knock down situation in contrast to *protA* and *prtl99C* transcripts, which were reduced to about 40% of the wild-type level (Fig 8G). We conclude that the transcript levels of *protA* and *prtl99C* depend directly or indirectly on Nejire/dCBP, and thus might arrest spermiogenesis due to insufficient synthesis of sperm chromatin components.

Nejire/dCBP is essential for efficient post-meiotic histone degradation and male fertility

We subsequently analysed squash preparations for ProtB-eGFP in the Nejire knock down situation with respect to Nejire/dCBP-dependent H3 acetylation, histone degradation and ProtB-eGFP deposition. Here, the characteristic H3K27 (Fig 7B′) and H3K18 (Panel B′ in S1 Fig) acetylation pattern was missing in spermatocytes and the early canoe stage. In spermatid bundles in cysts, histones were detectable at the early canoe stage (compare Fig 7B″ with Fig 7A″) but undetectable at the late canoe stage, as in the wild-type situation. However, the spermatid nuclei at the early canoe stage seemed less compact (Fig 7B and 7B″) than in wild-type (Fig 7A and 7A″).

The phenotypes presented in Fig 7 were most abundant; however, we also observed highly abnormally shaped spermatid nuclei (Fig 8B and 8C′), in agreement with the aberrantly shaped nuclei in whole mount preparations (Fig 5). The shape of ProtB-eGFP positive nuclei was highly variable (Fig 8A–8C′), although similar in the individual nuclei of one cyst. Some protamine positive and histone negative nuclei appeared in this assay (Fig 8A′, arrow). Strikingly, in contrast to wild-type, several slim nuclei contained both histones and ProtB-eGFP (Fig 8A-8A′, arrowhead), a feature not observed in squash preparations of wild-type testes [23]. In particular, we found histones and ProtB-eGFP in early canoe stage-like nuclei (Fig 8B-8B′) and in tid-shaped nuclei (Fig 8C-C′).

Notably, we found no individualized sperm after Nejire/dCBP knock down in squash preparations (Fig 7). We analysed seminal vesicles of 3-day-old males in the Nejire knock down

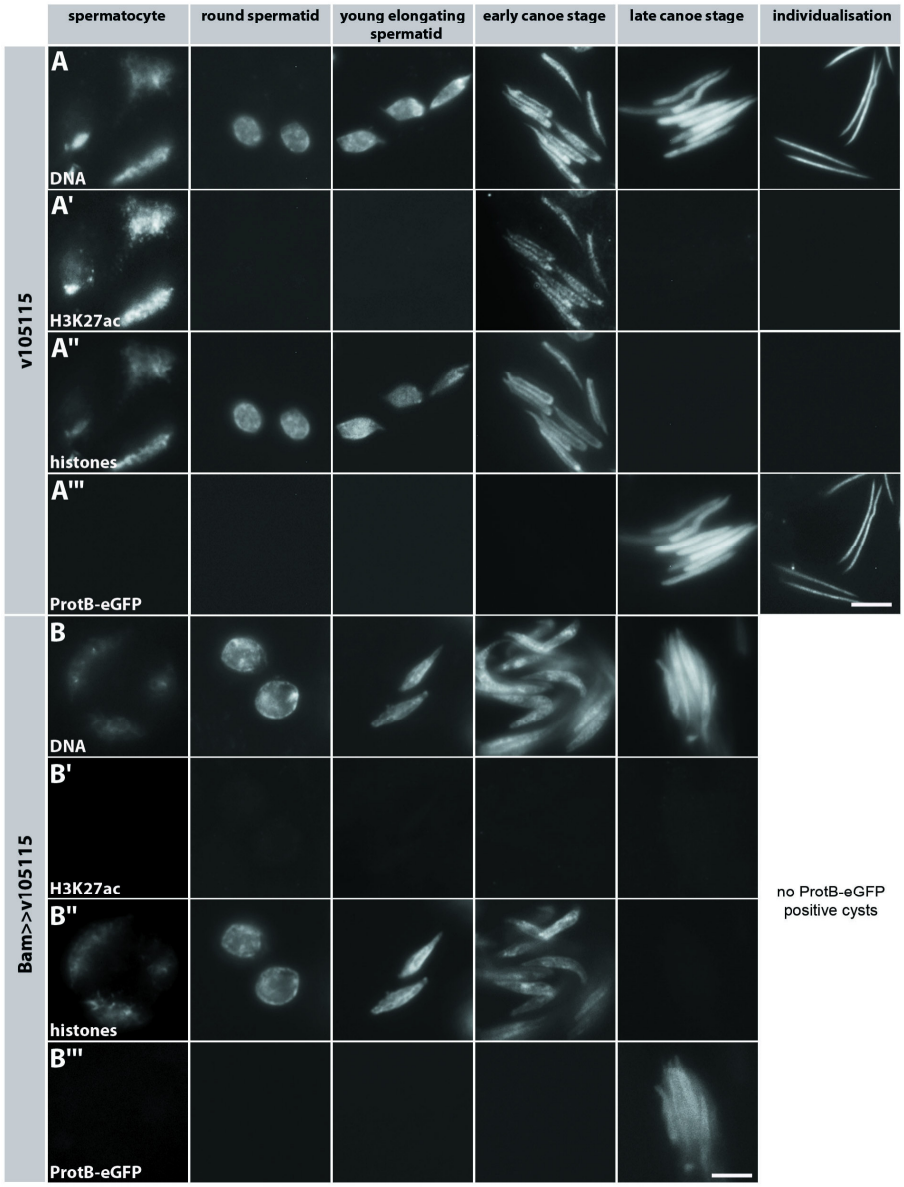

Fig 7. Knocking down Nejire/dCBP *in vivo* results in failure of H3K27 acetylation. Squashed preparations of testes from ProtB-eGFP-expressing wild-type flies (A-A‴) compared to testes of ProtB-eGFP males after Nejire knock down (B-B‴). DNA was visualized with Hoechst dye (A, B). H3K27ac was detected with an anti-H3K27ac antibody (A′, B′); histones were detected with anti-histone-antibody (A″, B″).

ProtB-GFP was used to visualize protamine expression (A‴, B‴). In the wild-type, H3K27ac characterizes the spermatocyte and early canoe stage (A′), histones are detectable until the early canoe stage (A″), ProtB-eGFP characterizes nuclei at the late canoe stage and in individualized sperm (A‴). (B) Knock down of Nejire led to a complete absence of individualized sperm and the H3K27 acetylation signal in both spermatocytes and post-meiotic spermatid stages (B′). After *nejire* knock down histones persist until the early canoe stage and degrade as in wild-type (compare B″ to A″). Residual ProtB-eGFP positive spermatid nuclei are observed at the late canoe stage (B‴). Scale bar: 5 μm.

https://doi.org/10.1371/journal.pone.0203622.g007

situation, and again, we could not detect residual sperm in their seminal vesicles (Fig 8E). In contrast, wild type seminal vesicles were full of protamine-eGFP positive sperm (Fig 8D). In agreement with these phenotypes, fertility tests demonstrated that knock down of Nejire led to male sterility (Fig 8F).

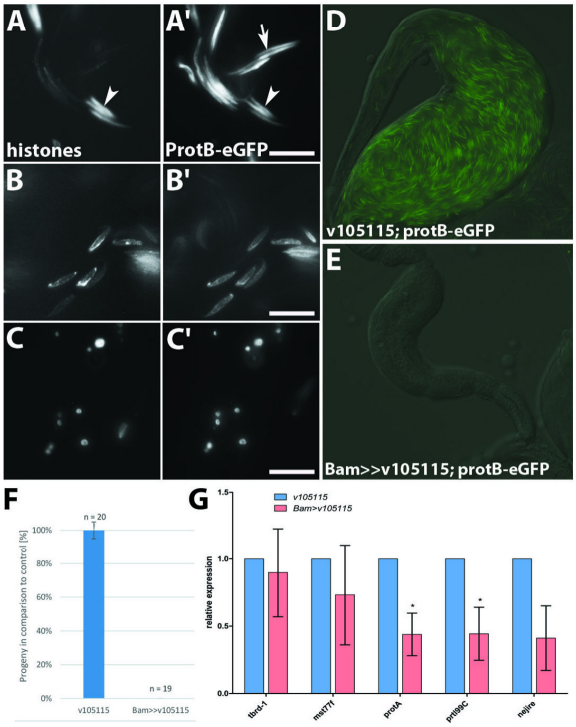

Fig 8. Knock down of Nejire/dCBP reduces transcript levels of ProtB and Prtl99C, and histone degradation, leading to male sterility. Disturbed spermatid nuclei shapes after Nejire/dCBP knock down (A-C′). Distribution of histones was visualized with an antibody against core histones (A-C). ProtB-eGFP distribution in the same nuclei as the core histones (A′-C′, D-E). Elongated spermatid nuclei (A-A′), canoe stage-like nuclei (B-B′), small round and oval nuclei (C-C′). (D-F) Males are sterile after knocking down Nejire/dCBP. Seminal vesicles of v105115 males (control) are filled with ProtB-eGFP positive sperm (D). Seminal vesicles of Bam-GAL4 driven v105115 RNAi males lack ProtB-eGFP positive sperm (E). Bam-GAL4 driven v105115 RNAi males lack progeny (F). *protB* and *prtl99C* transcript levels are significantly reduced after knock down of nejire (* $p < 0.05$) (G). Scale bar: 5 μm.

https://doi.org/10.1371/journal.pone.0203622.g008

In summary, these data indicate that the efficiency of histone degradation and protamination is impaired by Nejire knock down and therefore depends directly or indirectly on H3 acetylation by Nejire/dCBP.

Discussion

Male germ cells in vertebrates and *Drosophila* undergo a striking compaction of their genome in the haploid phase leading to nearly complete replacement of the histone-based chromatin by protamines. For many years, scientists have been trying to unravel the molecular basis of post-meiotic genome reprogramming that ultimately leads to large-scale genome compaction by the deposition of highly basic DNA-interacting non-histone proteins such as transition proteins and protamines.

Histone acetylation is a prerequisite for histone crotonylation in early canoe stage spermatids

A characteristic feature of the post-meiotic chromatin reorganization phase is the deposition of stage-specific histone modifications in flies and mammals. Detailed descriptions of modifications such as acetylation, methylation, phosphorylation, ubiquitination and SUMOylation are available (reviewed in [3, 37]. However, the most striking modification event linked to histone replacement in spermiogenesis is the replication and transcription-independent massive hyper-acetylation of the core histone H4 in early elongating spermatids (Fig 9). Since global histone hyper-acetylation by itself is not enough to mediate removal of histones we tried to identify further modifications playing a putative role in histone-to-protamine transition.

In addition to histone H4 hyper-acetylation and H3K79 methylation [11, 38], we identified lysine crotonylation (Kcr) as another conserved histone modification that precedes removal of histones in the absence of global transcription in *D. melanogaster* spermiogenesis (Fig 9). Histone Kcr occurs in a hyper-crotonylation wave in elongating spermatids, coinciding with histone hyper-acetylation in mice [13]. Like histone acetylation and H3K79 methylation, Kcr is a mark of transcriptionally active chromatin in spermatocytes. Using the histone acetyl-transferase inhibitor anacardic acid in pharmacological assays with cultured testes revealed that lysine crotonylation is dependent on post-meiotic histone hyper-acetylation; thus, we assume that crotonylation marks were set *de novo* in spermatids. Since inhibition of acetylation also strongly reduced H3K79 methylation, these modifications likely depend on histone acetylation. These findings indicate that these histone modifications might act in concert to regulate chromatin remodelling during the histone-to-protamine switch.

A distinct pattern of H3 acetylation characterizes the histone-to-protamine transition phase

In addition, we analysed the distribution of histone H3 acetylation marks in *Drosophila*. In contrast to the conserved H4K5/8/12 acetylation, detectable from spermatocyte stages until histones are removed, H3 lysine acetylation was shown to display a versatile pattern in *Drosophila* spermiogenesis (Fig 9). H3K18, H3K27 and H3K9 acetylation are detectable in stages prior to chromatin remodelling. Here, the observed H3K18 and H3K9 pattern corresponds to the pattern of these acetylation marks in mammals [39]. In *Drosophila* H3K36 acetylation is detectable in late spermatids already loaded with protamines. The vast majority of histones is reported to be replaced by protamines at this stage, but using a specific antibody we showed that at least histone H3 is detectable for longer in canoe stage nuclei than the other core

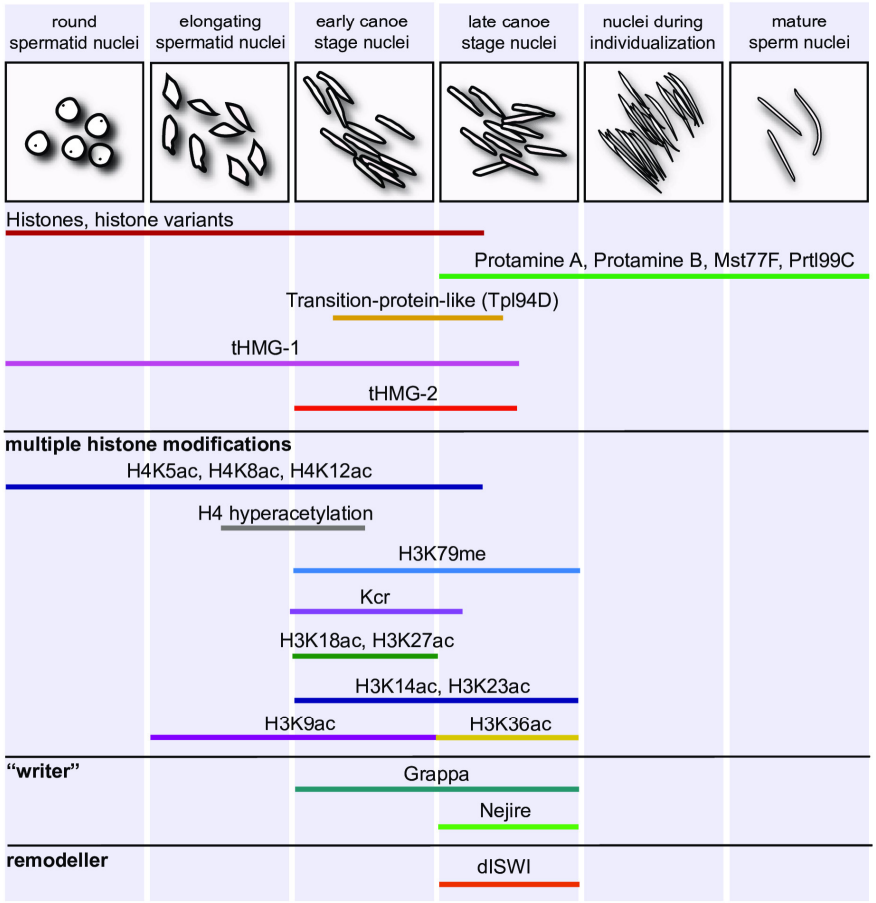

Fig 9. Key chromatin remodelling events and histone modifications in *Drosophila* spermiogenesis. At the top, morphogenesis of the germ cell nuclei is depicted in the order of events after meiosis. Below, histone-to-protamine transition is accompanied by a variety of specific histone modifications associated with Tpl94D, tHMGs, chaperones, Nejire, Grappa and dISWI expression.

https://doi.org/10.1371/journal.pone.0203622.g009

histones [7]. Of interest, a depletion of H3K9 acetylation in mice corresponded to a prolonged retention time of histone H3 on chromatin [12].

A fundamental question is the functional implications of the histone modifications that precede and accompany histone-to-protamine transition. Amalgamating all the stage-specific histone modifications and testis specific histone variants that have been reported, one might generate a testis-specific histone code directing chromatin compaction, histone removal and histone degradation by recruiting a specific machinery acting on modified histones. However, the nature of this histone code remains elusive. In mammals so far, histone hyper-acetylation

was hypothesized to lead to an open chromatin structure that facilitates and induces histone displacement.

Many histone modifications, HMG box proteins, chaperones, Nejire and ISWI characterize the switch from an open nucleosome-based arrangement to highly condensed sperm chromatin

In *D. melanogaster*, at least four proteins of sperm chromatin are known: the very similar ProtA and ProtB (also known as Mst35Ba/Bb) and Mst77F and Prtl99C (Fig 9). Biochemical evidence suggests that Mst77F multimerizes to compact chromatin [17]. Mst77F is deposited independently of protamines [40], while protamine deposition seems to depend on the presence of Mst77F [14]. We proposed that these proteins act additively to compact sperm chromatin [18].

Doyen et al [14] suggest that the chromatin remodeller ATPase ISWI is essential for stable incorporation of Mst77F and protamines. Apparently, different chaperones are needed for the loading of these sperm chromatin components [14, 41]. Several different transient HMG proteins (Tpl94D; tHMG-1, tHMG-2) characterize the histone-to-protamine transition phase [7, 42]. Histone modifications (methylation, crotonylation, acetylation) are striking shortly before (early canoe stage) and during the histone-to-protamine transition (late canoe stage).

Using a combination of *in vitro* cultures and inhibitor studies we show that crotonylation depends on previous acetylation, as already known for methylation of H3K79 by Grappa (*Drosophila* Dot1l) [11, 38]. Strikingly, H3K79 methylation and the responsible Dot1-like methyl transferase Grappa characterize the early and late canoe stage [38]. We proposed that Grappa, in cooperation with Rtf1 and UbcD6, marks sites of DNA strand breaks, e.g. by H3K79 methylation, and recruits DNA repair proteins.

Since histone acetylation seemed crucial for progressing to histone-to protamine transition, we aimed to identify acetyl-transferases, in particular those expressed at the canoe stage. H3 acetylation appears later than H4 hyper-acetylation and very specific in the early canoe stage (H3K18ac and H3K27ac). H3K18ac and H3K27ac acetylation marks are set by the aceyl-tranferease Nejire/dCBP.

Here, we present evidence that H3K18 and H3K27 acetylation depends on Nejire. Nejire is essential for fertility and responsible for efficient *protamine* mRNA synthesis. Hyper-acetylation of H3 at K18 and K27 during the histone-to-protamine transition likely is responsible for efficient histone degradation, since inhibition of histone acetyltransferases in the post-meiotic phase abolished H3K18 and H3K27 acetylation. These data are in agreement with *de novo* acetylation by Nejire/dCBP, if the detection in the early canoe stage indeed failed because of accessibility failure for the antibody. Alternatively, we propose that a so far unknown acetyl transferase with the same target specificity exists and that Nejire/dCBP targets other nuclear proteins during the canoe stage. While *in vitro* cultures of testes allowed us to selectively address the consequence of inhibition on post-meiotic stages, RNAi knock down experiments are only possible in the highly transcriptionally active spermatocyte stage. Thus, the distortions seen after knock down of ISWI [14] and Nejire might reflect in part a consequence of their involvement in transcriptional regulation in the spermatocyte phase.

Expression of Nejire during the late canoe stage and the loss of H3K18 and H3K27 acetylation after stage-specific inhibitor application led us to hypothesise that Nejire has dual functions in transcription in spermatocytes and H3 acetylation shortly before and during the histone-to-protamine transition. Nejire/dCBP contains a bromodomain, a protein motif known to specifically bind acetyl-lysine residues (reviewed in [43]. We postulate that Nejire/

dCBP is recruited via its bromodomain to already existing histone acetylations and then acetylates H3K18 and H3K27.

Nejire regulates transcript levels of Prtl99C and protamines as well as efficient histone degradation

Nejire/dCBP is already expressed in spermatocytes, the major transcriptionally active phase ([44] for review see [45]) and later in addition during the phase of protamine loading. This might argue for a dual role of Nejire during spermatogenesis. The knock down of Nejire/dCBP was performed with the male germ line driver line bam*GAL4*, which is active in spermatogonia and spermatocytes. Unfortunately, expression of GAL4 specifically after meiosis is not possible since there is no major transcriptional activity during spermiogenesis. Thus, we cannot interfere with Nejire translation specifically in spermatids. Although knock down of Nejire/dCBP in primary spermatocytes does not lead to obvious defects at this stage, reduced levels of *protamine* mRNA and of *protamine-like 99C* mRNA were observed. This might at least in part explain the observed sterility.

The time selective blocking of acetyl-transferases by anacardic acid after meiosis impedes H3K18 and H3K27 acetylation in late post-meiotic stages. Thus, we hypothesize that these acetylations at this time might contribute to efficient histone-to-protamine transition. Indeed, we observed co-occurrence of histones and ProtB in abnormally shaped spermatid nuclei suggesting inefficient histone degradation. Of interest, depletion of H3K9 acetylation in mice caused a prolonged retention time of histone H3 on chromatin [12].

De novo H3K18 and H3K27 acetylation takes place in the haploid phase, and the corresponding acetyl- transferase Nejire/dCBP is essential for male fertility

Enhanced deposition of post-translational histone modifications in elongating spermatids is suggested to be a consequence of prior events, such as the down-regulation of enzymes involved in their removal from histones, rather than the presence of specific enzymes generating these modifications (reviewed in [5]). Here, we show that in particular H3K18 and H3K27 acetylations appear *de novo* during the preparation and implementation of the histone-to-protamine transition during the canoe stage. Strikingly, these modifications depend directly or indirectly on the histone acetyl-transferase Nejire/dCBP. In mice, a partially depleted version of CBP led to fertile male mice [46]. In contrast, the efficient reduction of Nejire/dCBP by RNAi in male germ cells of *Drosophila* led to male sterility, underscoring the importance of this acetyl-transferase for spermatogenesis.

Conclusions

In our view, Nejire likely regulates H3K18 and H3K27 acetylation during transcription in spermatocytes. H3K18 and H3K27 are prominent also during the histone-protamine transition. We hypothesise that male sterility is directly and indirectly dependent on Nejire and caused by failure H3K18 and H3K27 acetylation in both stages.

In conclusion, with respect to the histone-to-protamine transition we propose that Nejire regulates transcript levels for sperm relevant proteins in spermatocytes and in directly or indirectly acetylation of H3K18 and H3K27 for fully efficient histone degradation. We propose that the numerous different histone modifications are required for histone degradation.

Supporting information

S1 Fig. Knocking down Nejire/dCBP *in vivo* results in failure of H3K18 acetylation. Squashed preparations of testes from ProtB-eGFP expressing wild-type flies (A-A″) in comparison to testes of ProtB-eGFP males after Nejire/dCBP knock down (B-B″). DNA was visualized with Hoechst dye (A, B). (A′, B′) H3K18ac detected with an anti-H3K18ac antibody, (A″, B″) ProtB-GFP was used to visualize protamine expression. In the wild-type, H3K18ac characterizes the spermatocyte and early canoe stage (A′), ProtB-eGFP characterizes nuclei at the late canoe stage and in individualized sperm (A″), Knock down of Nejire/dCBP led to a complete absence of individualized sperm (B-B″) and the H3K27 acetylation signal in spermatocytes and in post-meiotic spermatid stages (B′). After Nejire/dCBP knock down, residual ProtB-eGFP positive spermatid nuclei are observed (B″). Scale bar: 5 μm.
(JPG)

S1 Table. Acetyl transferases with predicted expression in the *Drosophila* testis.
(DOCX)

Acknowledgments

We thank Igor Macinkovic for advice for qPCR experiments, Rainer Renkawitz for critical reading of the manuscript. We are grateful to Mattias Mannervik for the kind gift of the dCBP-antibody. We thank Katja Gessner and Nadine Tauchen for excellent secretarial support. We thank Avril Arthur-Goettig for linguistic revision of the manuscript. This work was supported by the Deutsche Forschungsgemeinschaft (SFB TRR81 "Chromatin Changes in Differentiation and Malignancies" to C. R. and R. R.-P.).

Author Contributions

Conceptualization: Renate Renkawitz-Pohl.

Data curation: Tim Hundertmark, Stefanie M. K. Gärtner.

Funding acquisition: Christina Rathke, Renate Renkawitz-Pohl.

Investigation: Tim Hundertmark, Stefanie M. K. Gärtner.

Methodology: Tim Hundertmark, Stefanie M. K. Gärtner, Christina Rathke.

Project administration: Renate Renkawitz-Pohl.

Supervision: Christina Rathke, Renate Renkawitz-Pohl.

Visualization: Tim Hundertmark.

Writing – original draft: Stefanie M. K. Gärtner.

Writing – review & editing: Renate Renkawitz-Pohl.

References

1. Braun RE. Packaging paternal chromosomes with protamine. Nat Genet. 2001; 28(1):10–2. https://doi.org/10.1038/88194 PMID: 11326265.
2. Gaucher J, Reynoird N, Montellier E, Boussouar F, Rousseaux S, Khochbin S. From meiosis to post-meiotic events: the secrets of histone disappearance. FEBS J. 2010; 277(3):599–604. https://doi.org/10.1111/j.1742-4658.2009.07504.x PMID: 20015078.
3. Rathke C, Baarends WM, Awe S, Renkawitz-Pohl R. Chromatin dynamics during spermiogenesis. Biochim Biophys Acta. 2014; 1839(3):155–68. https://doi.org/10.1016/j.bbagrm.2013.08.004 PMID: 24091090.

4. Sassone-Corsi P. Unique chromatin remodeling and transcriptional regulation in spermatogenesis. Science. 2002; 296(5576):2176–8. https://doi.org/10.1126/science.1070963 PMID: 12077401.
5. Goudarzi A, Shiota H, Rousseaux S, Khochbin S. Genome-scale acetylation-dependent histone eviction during spermatogenesis. J Mol Biol. 2014; 426(20):3342–9. https://doi.org/10.1016/j.jmb.2014.02.023 PMID: 24613302.
6. Hazzouri M, Pivot-Pajot C, Faure AK, Usson Y, Pelletier R, Sele B, et al. Regulated hyperacetylation of core histones during mouse spermatogenesis: involvement of histone deacetylases. Eur J Cell Biol. 2000; 79(12):950–60. https://doi.org/10.1078/0171-9335-00123 PMID: 11152286.
7. Rathke C, Baarends WM, Jayaramaiah-Raja S, Bartkuhn M, Renkawitz R, Renkawitz-Pohl R. Transition from a nucleosome-based to a protamine-based chromatin configuration during spermiogenesis in Drosophila. J Cell Sci. 2007; 120(Pt 9):1689–700. https://doi.org/10.1242/jcs.004663 PMID: 17452629.
8. Sonnack V, Failing K, Bergmann M, Steger K. Expression of hyperacetylated histone H4 during normal and impaired human spermatogenesis. Andrologia. 2002; 34(6):384–90. PMID: 12472623.
9. Fenic I, Sonnack V, Failing K, Bergmann M, Steger K. In vivo effects of histone-deacetylase inhibitor trichostatin-A on murine spermatogenesis. J Androl. 2004; 25(5):811–8. PMID: 15292114.
10. Kennedy BP, Davies PL. Acid-soluble nuclear proteins of the testis during spermatogenesis in the winter flounder. Loss of the high mobility group proteins. J Biol Chem. 1980; 255(6):2533–9. PMID: 7358686.
11. Dottermusch-Heidel C, Klaus ES, Gonzalez NH, Bhushan S, Meinhardt A, Bergmann M, et al. H3K79 methylation directly precedes the histone-to-protamine transition in mammalian spermatids and is sensitive to bacterial infections. Andrology. 2014; 2(5):655–65. https://doi.org/10.1111/j.2047-2927.2014.00248.x PMID: 25079683.
12. Nair M, Nagamori I, Sun P, Mishra DP, Rheaume C, Li B, et al. Nuclear regulator Pygo2 controls spermiogenesis and histone H3 acetylation. Dev Biol. 2008; 320(2):446–55. https://doi.org/10.1016/j.ydbio.2008.05.553 PMID: 18614164; PubMed Central PMCID: PMCPMC2553271.
13. Tan M, Luo H, Lee S, Jin F, Yang JS, Montellier E, et al. Identification of 67 histone marks and histone lysine crotonylation as a new type of histone modification. Cell. 2011; 146(6):1016–28. https://doi.org/10.1016/j.cell.2011.08.008 PMID: 21925322; PubMed Central PMCID: PMCPMC3176443.
14. Doyen CM, Chalkley GE, Voets O, Bezstarosti K, Demmers JA, Moshkin YM, et al. A Testis-Specific Chaperone and the Chromatin Remodeler ISWI Mediate Repackaging of the Paternal Genome. Cell Rep. 2015; 13(7):1310–8. https://doi.org/10.1016/j.celrep.2015.10.010 PMID: 26549447.
15. Jayaramaiah Raja S, Renkawitz-Pohl R. Replacement by Drosophila melanogaster protamines and Mst77F of histones during chromatin condensation in late spermatids and role of sesame in the removal of these proteins from the male pronucleus. Mol Cell Biol. 2005; 25(14):6165–77. https://doi.org/10.1128/MCB.25.14.6165-6177.2005 PMID: 15988027; PubMed Central PMCID: PMCPMC1168805.
16. Kimura S, Loppin B. The Drosophila chromosomal protein Mst77F is processed to generate an essential component of mature sperm chromatin. Open Biol. 2016; 6(11). https://doi.org/10.1098/rsob.160207 PMID: 27810970; PubMed Central PMCID: PMCPMC5133442.
17. Kost N, Kaiser S, Ostwal Y, Riedel D, Stutzer A, Nikolov M, et al. Multimerization of Drosophila sperm protein Mst77F causes a unique condensed chromatin structure. Nucleic Acids Res. 2015; 43(6):3033–45. https://doi.org/10.1093/nar/gkv015 PMID: 25735749; PubMed Central PMCID: PMCPMC4381051.
18. Eren-Ghiani Z, Rathke C, Theofel I, Renkawitz-Pohl R. Prtl99C Acts Together with Protamines and Safeguards Male Fertility in Drosophila. Cell Rep. 2015; 13(11):2327–35. https://doi.org/10.1016/j.celrep.2015.11.023 PMID: 26673329.
19. Strahl BD, Allis CD. The language of covalent histone modifications. Nature. 2000; 403(6765):41–5. https://doi.org/10.1038/47412 PMID: 10638745.
20. Burgess RJ, Zhang Z. Histone chaperones in nucleosome assembly and human disease. Nat Struct Mol Biol. 2013; 20(1):14–22. https://doi.org/10.1038/nsmb.2461 PMID: 23288364; PubMed Central PMCID: PMCPMC4004355.
21. Pivot-Pajot C, Caron C, Govin J, Vion A, Rousseaux S, Khochbin S. Acetylation-dependent chromatin reorganization by BRDT, a testis-specific bromodomain-containing protein. Mol Cell Biol. 2003; 23(15):5354–65. https://doi.org/10.1128/MCB.23.15.5354-5365.2003 PMID: 12861021; PubMed Central PMCID: PMCPMC165724.
22. Berkovits BD, Wolgemuth DJ. The role of the double bromodomain-containing BET genes during mammalian spermatogenesis. Curr Top Dev Biol. 2013; 102:293–326. https://doi.org/10.1016/B978-0-12-416024-8.00011-8 PMID: 23287038; PubMed Central PMCID: PMCPMC3918955.
23. Awe S, Renkawitz-Pohl R. Histone H4 acetylation is essential to proceed from a histone- to a protamine-based chromatin structure in spermatid nuclei of Drosophila melanogaster. Syst Biol Reprod Med. 2010; 56(1):44–61. https://doi.org/10.3109/19396360903490790 PMID: 20170286.

24. Hime GR, Brill JA, Fuller MT. Assembly of ring canals in the male germ line from structural components of the contractile ring. J Cell Sci. 1996; 109 (Pt 12):2779–88. PMID: 9013326.

25. Lilja T, Qi D, Stabell M, Mannervik M. The CBP coactivator functions both upstream and downstream of Dpp/Screw signaling in the early Drosophila embryo. Dev Biol. 2003; 262(2):294–302. PMID: 14550792.

26. Montellier E, Rousseaux S, Zhao Y, Khochbin S. Histone crotonylation specifically marks the haploid male germ cell gene expression program: post-meiotic male-specific gene expression. Bioessays. 2012; 34(3):187–93. https://doi.org/10.1002/bies.201100141 PMID: 22170506.

27. Gartner SM, Rathke C, Renkawitz-Pohl R, Awe S. Ex vivo culture of Drosophila pupal testis and single male germ-line cysts: dissection, imaging, and pharmacological treatment. J Vis Exp. 2014;(91):51868. https://doi.org/10.3791/51868 PMID: 25286189; PubMed Central PMCID: PMCPMC4828063.

28. Balasubramanyam K, Swaminathan V, Ranganathan A, Kundu TK. Small molecule modulators of histone acetyltransferase p300. J Biol Chem. 2003; 278(21):19134–40. https://doi.org/10.1074/jbc.M301580200 PMID: 12624111.

29. Mai A, Massa S, Pezzi R, Simeoni S, Rotili D, Nebbioso A, et al. Class II (IIa)-selective histone deacetylase inhibitors. 1. Synthesis and biological evaluation of novel (aryloxopropenyl)pyrrolyl hydroxyamides. J Med Chem. 2005; 48(9):3344–53. https://doi.org/10.1021/jm049002a PMID: 15857140.

30. Yoshida M, Kijima M, Akita M, Beppu T. Potent and specific inhibition of mammalian histone deacetylase both in vivo and in vitro by trichostatin A. J Biol Chem. 1990; 265(28):17174–9. PMID: 2211619.

31. Petruk S, Sedkov Y, Smith S, Tillib S, Kraevski V, Nakamura T, et al. Trithorax and dCBP acting in a complex to maintain expression of a homeotic gene. Science. 2001; 294(5545):1331–4. https://doi.org/10.1126/science.1065683 PMID: 11701926.

32. Fuller M. Spermiogenesis. In: Bate M, Martinez-Arias A, editors. The Development of Drosophila melanogaster. Cold Spring Harbor, New York: Cold Spring Harbor Laboratory Press; 1993. p. 71–147.

33. Barckmann B, Chen X, Kaiser S, Jayaramaiah-Raja S, Rathke C, Dottermusch-Heidel C, et al. Three levels of regulation lead to protamine and Mst77F expression in Drosophila. Dev Biol. 2013; 377(1):33–45. https://doi.org/10.1016/j.ydbio.2013.02.018 PMID: 23466740; PubMed Central PMCID: PMCPMC4154633.

34. Leser K, Awe S, Barckmann B, Renkawitz-Pohl R, Rathke C. The bromodomain-containing protein tBRD-1 is specifically expressed in spermatocytes and is essential for male fertility. Biol Open. 2012; 1 (6):597–606. https://doi.org/10.1242/bio.20121255 PMID: 23213453; PubMed Central PMCID: PMCPMC3509448.

35. Theofel I, Bartkuhn M, Boettger T, Gartner SMK, Kreher J, Brehm A, et al. tBRD-1 and tBRD-2 regulate expression of genes necessary for spermatid differentiation. Biol Open. 2017; 6(4):439–48. https://doi.org/10.1242/bio.022467 PMID: 28235844; PubMed Central PMCID: PMCPMC5399552.

36. Theofel I, Bartkuhn M, Hundertmark T, Boettger T, Gartner SM, Leser K, et al. tBRD-1 selectively controls gene activity in the Drosophila testis and interacts with two new members of the bromodomain and extra-terminal (BET) family. PLoS One. 2014; 9(9):e108267. https://doi.org/10.1371/journal.pone.0108267 PMID: 25251222; PubMed Central PMCID: PMCPMC4177214.

37. Govin J, Caron C, Lestrat C, Rousseaux S, Khochbin S. The role of histones in chromatin remodelling during mammalian spermiogenesis. Eur J Biochem. 2004; 271(17):3459–69. https://doi.org/10.1111/j.1432-1033.2004.04266.x PMID: 15317581.

38. Dottermusch-Heidel C, Gartner SM, Tegeder I, Rathke C, Barckmann B, Bartkuhn M, et al. H3K79 methylation: a new conserved mark that accompanies H4 hyperacetylation prior to histone-to-protamine transition in Drosophila and rat. Biol Open. 2014; 3(6):444–52. https://doi.org/10.1242/bio.20147302 PMID: 24795146; PubMed Central PMCID: PMCPMC4058078.

39. Song N, Liu J, An S, Nishino T, Hishikawa Y, Koji T. Immunohistochemical Analysis of Histone H3 Modifications in Germ Cells during Mouse Spermatogenesis. Acta Histochem Cytochem. 2011; 44(4):183–90. https://doi.org/10.1267/ahc.11027 PMID: 21927517; PubMed Central PMCID: PMCPMC3168764.

40. Rathke C, Barckmann B, Burkhard S, Jayaramaiah-Raja S, Roote J, Renkawitz-Pohl R. Distinct functions of Mst77F and protamines in nuclear shaping and chromatin condensation during Drosophila spermiogenesis. Eur J Cell Biol. 2010; 89(4):326–38. https://doi.org/10.1016/j.ejcb.2009.09.001 PMID: 20138392.

41. Doyen CM, Moshkin YM, Chalkley GE, Bezstarosti K, Demmers JA, Rathke C, et al. Subunits of the histone chaperone CAF1 also mediate assembly of protamine-based chromatin. Cell Rep. 2013; 4(1):59–65. https://doi.org/10.1016/j.celrep.2013.06.002 PMID: 23810557.

42. Gartner SM, Rothenbusch S, Buxa MK, Theofel I, Renkawitz R, Rathke C, et al. The HMG-box-containing proteins tHMG-1 and tHMG-2 interact during the histone-to-protamine transition in Drosophila spermatogenesis. Eur J Cell Biol. 2015; 94(1):46–59. https://doi.org/10.1016/j.ejcb.2014.10.005 PMID: 25464903.

43. Zeng L, Zhou MM. Bromodomain: an acetyl-lysine binding domain. FEBS Lett. 2002; 513(1):124–8. PMID: 11911891.

44. Barreau C, Benson E, Gudmannsdottir E, Newton F, White-Cooper H. Post-meiotic transcription in Drosophila testes. Development. 2008; 135(11):1897–902. https://doi.org/10.1242/dev.021949 PMID: 18434411.

45. White-Cooper H, Davidson I. Unique aspects of transcription regulation in male germ cells. Cold Spring Harb Perspect Biol. 2011; 3(7). https://doi.org/10.1101/cshperspect.a002626 PMID: 21555408; PubMed Central PMCID: PMCPMC3119912.

46. Boussouar F, Goudarzi A, Buchou T, Shiota H, Barral S, Debernardi A, et al. A specific CBP/p300-dependent gene expression programme drives the metabolic remodelling in late stages of spermatogenesis. Andrology. 2014; 2(3):351–9. https://doi.org/10.1111/j.2047-2927.2014.00184.x PMID: 24522976.

Chapter 7: Stage-specific proteomes of the *Drosophila melanogaster* testes

Gärtner, S.M.K.*, Hundertmark, T.*, Nolte, H., Tetzner, C., Theofel, I., Eren-Ghiani, Z., Duchow, T.B., Rathke, C., Krüger, M. and Renkawitz-Pohl, R. (under review in EJCB).

* These authors contributed equally to this work

Candidate's contribution:

- Production of microscopic images and figures (Figures 5, 7, S5)
- Generation of a part of the transgenic fly lines in collaboration with B.Sc. Timothy B. Duchow (co-supervision of associated Bachelor thesis)
- Proofreading the manuscript
- Evaluation of proteome data regarding example proteins

Stage-specific testes proteomics of *Drosophila melanogaster* identifies essential proteins for male fertility

Stefanie M. K. Gärtner[a,*], Tim Hundertmark[a,*], Hendrik Nolte[b], Ina Theofel[a,d], Zeynep Eren-Ghiani[a], Carolin Tetzner[a], Timothy B. Duchow[a], Christina Rathke[a], Marcus Krüger[b,#] and Renate Renkawitz-Pohl[a,#,†]

[a] Philipps-Universität Marburg, Fachbereich Biologie, Entwicklungsbiologie, Karl-von-Frisch Str. 8, 35043 Marburg, Germany

[b] Institute for Genetics and Cologne Excellence Cluster on Cellular Stress Responses in Aging-Associated Diseases (CECAD), University of Cologne, Joseph-Stelzmann-Strasse 26, 50931 Cologne, Germany. Center for Molecular Medicine (CMMC), University of Cologne, 50931 Cologne, Germany

[c] MRC London Institute of Medical Sciences (LMS), Du Cane Road, London W120NN, UK

Institute of Clinical Sciences (ICS), Faculty of Medicine, Imperial College London, Du Cane Road, London W12 0NN, UK

[*] shared first authorship

[#] joint last authors

[†] corresponding author

phone: +49-6421-28-21502

fax: +49-6421-28-21538

E-mail: renkawit@biologie.uni-marburg.de

Running title: *Drosophila* testis proteomes

Declarations of conflict of interest: none

Abstract

Spermiogenesis in *Drosophila melanogaster* is a highly conserved process and essential for male fertility. In this haploid phase of spermatogenesis, motile sperm are assembled from round cells, flagella and needle-shaped nuclei with highly compacted genomes are formed. We aimed at identifying proteins relevant for the maturation phase from spermatids to sperm. As transcription takes place mainly in spermatocytes and transcripts with relevance for post-meiotic sperm development are translationally repressed for days, we comparatively analysed the proteome of larval testes (stages before meiotic divisions), testes of 1-2 day-old pupae (meiotic and early spermatid stages) and adult flies (late spermatids and sperm). We identified 6171 proteins, with 61 solely detectable in larval testes, 77 in pupal testes and 214 in adult testes. To substantiate our mass spectrometric data we analysed a number of so far uncharacterized proteins with respect to stage specific expression and importance for male fertility. For example, Mst84B (gene *CG1988*), a very basic cysteine- and lysine-rich nuclear protein, was present in the phase of transition from a histone-based to a protamine-based chromatin structure. *CG6332* encodes d-Theg, which is related to the mouse tHEG and human THEG proteins and mutants of *d-Theg* were sterile due to lack of sperm in the seminal vesicles. Collectively, we are confident that our catalogue of proteins for different stages of testis development in flies will pave the road for future analyses of spermatogenesis.

Keywords: transition-like protein, Proteasome Assembly Chaperone 1, microtubule-binding protein, nuclear shaping, THEG, Y chromosome.

46 **Introduction**

47 In spermatogenesis, functional motile spermatozoa develop from an initially undifferentiated germ cell
48 and the characteristic features of this process are highly conserved between *Drosophila melanogaster*
49 and mammals (Rathke et al., 2014). Stem cells divide to form new stem cells and spermatogonia, i.e.
50 differentiating germ cells. These spermatogonia proceed first through a mitotic amplification phase
51 and then enter the extended meiotic prophase as spermatocytes (Fuller, 1993). After meiotic divisions,
52 spermatids differentiate within days (*Drosophila*) or weeks (mammals) to form motile sperm with
53 highly condensed chromatin (Rathke et al., 2014).

54 It is obvious that during germ cell differentiation, a plethora of proteins have to be newly
55 synthesized in a temporal and stage-specific manner. However, data on protein expression in the testis
56 is scarce due to technological and methodical limitations. Until recently, proteomic research on whole
57 testis tissue of different species entailed 2-D gels and subsequent mass spectrometry of excised protein
58 spots. With this technique, 232 proteins were identified in testes of *Drosophila* (Takemori and
59 Yamamoto, 2009), 1108 were identified in *Drosophila* sperm (Wasbrough et al. 2010; Dorus et al.,
60 2006; for a review, see Karr 2007), 447 proteins were observed in pig testes (Huang et al., 2005), 504
61 proteins were identified in mouse testes (Zhu et al., 2006), 725 proteins were found in human testes
62 (Li et al., 2011), and 6198 proteins were identified in human sperm (in 30 studies, summarized in
63 Amaral et al., 2014). Together, these proteomes provides a comprehensive reference map for
64 differentiated testis under normal conditions. However, the number of so far identified proteins in
65 *Drosophila* does not come close to reflecting the number of genes that are transcribed during
66 spermatogenesis. For example, over 2000 genes are transcribed in *Drosophila* spermatocytes, many
67 for the first time in the life cycle (Lu and Fuller, 2015; Theofel et al., 2014, 2017; White-Cooper and
68 Davidson, 2011), and in a random mutagenesis study of *Drosophila* (Wakimoto et al., 2004), mutation
69 of at least 2000 genes led to male infertility. Furthermore, the proteomic datasets of whole testis tissue
70 provide only limited information about the expression profiles of proteins at different developmental

stages of germ cells, which is needed to further broaden the understanding of the process of spermatogenesis and pinpoint the protein function to specific cell types.

Several approaches have been used to generate mRNA expression profiles specific to certain stages of spermatogenesis and studies in mice made use of the observation that at a given day after birth, certain germ cell types are enriched in the testis (Schultz et al., 2003; Xiao et al., 2008). An earlier transcriptomics study in flies took advantage of the almost chronological arrangement of the germ cells in the adult testis, which could be divided into three regions enriched with mitotic, meiotic or post-meiotic cells (Vibranovski et al., 2009). Furthermore, isolated and enriched testicular cell populations were used to generate genetic databases of rats and mice (http://mrg.genetics.washington.edu/). These methods greatly facilitated the assignment of transcripts to mitotic, meiotic, and post-meiotic stages of spermatogenesis and helped to identify yet uncharacterized transcripts that likely encode factors involved in spermatogenesis and fertility. Nevertheless, the proteins - usually the final products of gene expression - are considered to be more relevant markers for gene function. This becomes even more obvious, since mRNA levels does not necessarily predict the protein expression, in particular during male germ cell development.

Spermatogenesis is one of the finest examples illustrating the importance of post-transcriptional regulation of gene expression. A common feature of mammalian and fly germ cell development is an almost complete shut-down of transcription in post-meiotic stages. This block of transcription occurs at the round spermatid stage in mammals, and even earlier in flies - at the end of the primary spermatocyte stage (for a review, see Rathke et al., 2014). Consequently, transcripts whose products are needed in later stages of spermatogenesis have to be translationally repressed (for a review, see Renkawitz-Pohl et al., 2005; Rathke et al., 2014) and this causes a clear discrepancy between the transcriptome and the proteome of a certain stage. Many mRNAs are translationally repressed for days until the late steps of sperm maturation. Typical examples in *Drosophila* are proteins of sperm chromatin, which are deposited between 50 and 60 h after meiotic divisions (Jayaramaiah Raja and Renkawitz-Pohl, 2005; Awe and Renkawitz-Pohl, 2010; Barckmann et al.,

2013, Eren-Ghiani et al., 2015). Thus, transcriptomic research has to be complemented by proteomic approaches to evaluate the function of genes in spermatogenesis. To date, two studies in pigs and mice have aimed at identifying differentially synthesized proteins in the developing testes (Huang et al., 2011; Paz et al., 2006).

Today, proteomic approaches allow the rapid identification of proteins in complex mixtures. Peptides are separated via liquid chromatography (LC), followed by tandem mass spectrometry (MS/MS) and with this approach, the human and mouse testis proteome was expanded to over 5000 proteins (Liu et al., 2013); Huttlin et al, 2010). However, this approach has not yet been applied to the *Drosophila* model organism of spermatogenesis. Here, it needs to consider that the fly testis contains less somatic cell types than the mammalian testes.

In this study, we used single-shot proteomics to extend the number of identified proteins in the *Drosophila* testis proteome and to investigate differential protein expression in the developing testis by analysing larval, pupal and adult testis proteomes.

Material and methods

Fly stocks and maintenance

We used an H2AvD-RFP; ProtamineB-eGFP double-transgenic *Drosophila melanogaster* strain (Awe and Renkawitz-Pohl, 2010). Fly strains CG2046^{f01807} (BL 18477), Df(3R)Exel6145, Df(3R)Exel7283 and Df(3R)Exel7284 were obtained from the Bloomington *Drosophila* Stock Center.

The fly strains were maintained at 25 °C on standard medium. Prior to isolation of the testes for proteome analysis, the flies were cultured for one generation on standard medium containing 0.003% tetracycline to avoid *Wolbachia* sp. infection (Hoffmann et al., 1988). Flies were controlled by PCR for infection with *Wolbachia* sp. using *wsp*-forward TGGTCCAATAAGTGATGAAGAAAC and *wsp*-reverse AAAAATTAAACGCTACTCCA primers (Zheng et al., 2011). Primers for *Tpl94D*

positive control were Tpl-RT-sen GAGTGCATCACGTGAATGGG and Tpl-RT-as GCCACGCTGATCCGCATTC.

Isolation of testes for proteome analysis

Testes were isolated from 3rd instar larvae, from pupae at approximately 24 h after puparium formation (APF), from pupae at approximately 48 h APF and from newly eclosed flies. Isolated testes were placed in PBS containing protease inhibitor cocktail (Roche) and stored on ice for the duration of the dissection. Testes isolated from larvae and pupae were checked for the presence of ProtamineB-eGFP, which is characteristic from 48 h APF onward, with a Zeiss Axio Observer Z1 inverted microscope. The testes were carefully transferred to microcentrifuge tubes and washed three times with PBS. The PBS supernatants were discarded, and the testes samples were snap-frozen in liquid nitrogen and stored at -80 °C until processing for one-dimensional SDS-PAGE. Three replicates of each sample were prepared.

Preparation of protein extracts for mass spectrometry

The frozen testes pellets were thawed and solubilized in sample buffer containing 4% SDS, 0.1 M Tris-HCl (pH 7.6). After shaking for 5 min at 95 °C, the samples were sonicated. The sonicated samples were incubated with shaking for 5 min at 95 °C and then centrifuged for 10 min at 10000 x g in a microcentrifuge at room temperature. The supernatant was transferred to a new microcentrifuge tube. Protein concentration was estimated using the DC protein assay (Bio-Rad).

One-dimensional SDS-PAGE

For one-dimensional SDS-PAGE, 40 µg of each testes sample, prepared as described above, was separated on a Novex NuPAGE 4-12% acrylamide gradient gel (Invitrogen). Following electrophoresis, gels were fixed in 40% methanol/10% acetic acid for 10 min and stained with the Colloidal Blue staining kit by Invitrogen according to the manufacturer's manual. The gel lanes were cut vertically and horizontally into ten fractions. For subsequent mass spectrometry analysis, proteins

147 in the gel slices were proteolytically digested with trypsin. The resulting tryptic peptides were
148 extracted with acetonitrile, desalted and purified using stop-and-go extraction (STAGE) tips
149 (Rappsilber et al., 2003).
150 *Protein identification by LC-mass spectrometry*
151 Peptides were separated on an Easy nano-flow HPLC system (Thermo Fisher Scientific) using a
152 binary buffer system consisting of buffer A (0.1% formic acid or 0.5% acetic acid) and buffer B (80%
153 acetonitrile, 0.1% formic acid or 0.5% acetic acid). This system was coupled to a Orbitrap based mass
154 spectrometer via a nano-electrospray ionization source (Velos or QExactive). Peptides were eluted
155 from in-house packed 20 cm (3 µm beads, 75 µm ID, Dr. Maisch Germany) or 50 cm (1.8 µm beads,
156 75 µm ID, Dr. Maisch Germany) column by linearly increasing the relative amount of buffer B from
157 7% to 38% in buffer B within 40 min and further increase to 65 % buffer B within 10 min, followed
158 by 5 min at 95% buffer B and then re-equilibration for 5 min to 5% buffer B. Column temperature was
159 kept constant at 50°C using an in-house build column oven.
160 MS spectra in a mass range of 350-1650 *m/z* were acquired using an AGC target of 3E6 at a
161 resolution of 70,000 at 200 *m/z*. The instrument worked in data-dependent mode; the ten most intense
162 peaks for fragmentation (HCD or CID) in a 100-1650 *m/z* mass range were isolated. The AGC target
163 was set to 5E5, combined with a resolution of 35,000 at 200 *m/z*, and a maximum injection time was
164 set to 60 ms.
165
166 *Proteome dataset composition and analysis*
167 The complete set of raw files was processed using MaxQuant (1.5.3.8) and the implemented
168 Andromeda search engine (Cox and Mann, 2008; Cox et al., 2011). For protein assignment, ESI-
169 MS/MS fragmentation spectra were correlated to the UniProt fruit fly database (*Drosophila*
170 *melanogaster*, complete proteome, June 2017) as well as a list of contaminants. A maximum of two
171 missed cleavages and a mass tolerance of 4.5 ppm and 7 ppm were set for the first and main MS/MS
172 search, respectively. Carbamidomethyl at cysteine residues was defined as a fixed modification, and

oxidation at methionine and acetylation at the N-terminus of proteins were set as variable modifications. A minimal peptide length of seven amino acids was required for identification. For quantification, a minimal ratio count of 2 was selected. The FDR was controlled to 0.01 by a target-decoy approach at the peptide-spectrum-match and protein level using the implemented reverse-algorithm. MaxQuant output text files were filtered for contaminants and reverse entries. Gene ontology based on Uniprot identifiers was annotated in the Perseus software (Tyanova et al., 2016). Data visualization and analysis was done in the in-house developed software Instant Clue (www.instantclue.uni-koeln.de, Nolte et al., 2018).

Protein extraction

Protein was extracted from adult *Drosophila* testes as described in Leser et al. (2012).

For western blots, proteins were separated on 10% SDS-polyacrylamide gels following standard methods. Anti-CG2046 (dPSMG1) antibody from rabbit was used at a dilution of 1:1000, and anti-Actin (Biomeda) was used at a dilution of 1:1000 in 5% dry milk in Tris Buffered Saline with Tween (TBST). POD-conjugated anti-rabbit antibody was subsequently applied at a dilution of 1:5000 (Jackson Immunology). Novex ECL chemiluminescent substrate reagent kit (Invitrogen) was applied to detect the signals according to the manufacturer's recommendation.

Establishment of transgenic flies

We established fly constructs carrying *CG31907-eGFP*, *CG5089-eGFP*, *CG8701-eGFP* and *CG6332-eGFP*. To do this, we PCR amplified the corresponding genomic regions from 1045, 1066, 982 and 1145 bp upstream of the translation initiation codon until the last codon, the sequence encoding eGFP were fused in frame at the end of the respective open reading frame. *CG31907* and *CG6332* were cloned into pChapΔSalΔLacZ-eGFP, and transgenic flies were established by injecting constructs into w^{1118} embryos. *CG5089* and *CG8701* were cloned into pUAST-attB-rfa-eGFP using the Gateway

198 system, and transgenic flies were established by injecting constructs into *Drosophila* stock 24749
199 (Bloomington *Drosophila* Stock Center).
200
201

202 *Fertility tests*

203 Batches of 20 flies were tested for fertility. Each adult male (0-1 day old) was placed with three wild-
204 type virgin females in a separate vial at 25 °C. After 6 days, the parental generation was removed.
205 After 2 weeks, the number of vials with and without progeny was counted.

206

207 *RT-PCR and in situ hybridization*

208 RNA was isolated from 60 testes of adult males using TRIzol (Invitrogen). Primers for *CG6332*
209 (*dtheg*) transcripts were as follows: 5′-primers for amplifying a 274 bp fragment by RT-PCR were
210 CG6332-5Fw (GGGGAGTCCATACTGAACAGAT) and CG6332-Rv
211 (CCCACTTGGGTTTGATCTCCT); 3′-primers for amplifying a 240 bp fragment by RT-PCR were
212 CG6332-Fw (GTGCGCGATAATGTCCACAT) and CG6332-3Rv
213 (GATATGCGTGTTCTCGAACTC). As a control, a 372-bp fragment of β3 tubulin transcripts was
214 amplified (fw primer: ATCATTTCCGAGGAGCACGGC, rev primer:
215 GCCCAGCGAGTGCGTCAATTG). DIG-labelled antisense RNA probes were generated using the
216 *CG2046* open reading frame (without introns) cloned into pCR®II-TOPO® Vector (Invitrogen) as
217 template. Whole-mount adult testes were hybridized *in situ* according to Morris et al. (2009).

218

219 *Antibody generation and immunofluorescence*

220 Antibodies were raised in rabbits against peptides of CG2046 (dPSMG1)
221 CKPKVEFKSEDIQLYRDH), CG6332 (dTheg: CLAKPKKAPKVPKPDRGAGE) and *CG1988*
222 (Mst84B: CDTLSHRLDQPLRSAFLEDLEKRLNQR) (Pineda Antibody Service; http://www.pineda-
223 abservice.de). The affinity-purified antibodies were applied in immunofluorescence stainings at a
224 dilution of 1:1000 anti-CG2046 (dPSMG1) 1:1000 antiCG6332 (dTheg) and 1:10000 anti-CG1988
225 (Mst84B). Squash preparations of testes, anti-histone, anti-ProtB (Doyen et al., 2013) and secondary
226 antibodies were applied as described in Gärtner et al. (2015). F-actin was visualized by rhodamine-
227 phalloidin, and DNA was visualized with Hoechst 33258 dye. Immunofluorescence was monitored

228 using a Zeiss AxioPlan2 microscope equipped with appropriate fluorescence filters. Recorded images
229 were processed with Adobe PhotoshopCS2.
230
231 *Data Availability*
232 The mass spectrometry proteomics data have been deposited to the ProteomeXchange Consortium via
233 the PRIDE partner repository with the dataset identifier PXD010627 (Vizcaino et al., 2016).
234 Submission details:
235 **Project Name:** Drosophila Testis Proteome
236 **Project accession:** PXD010627
237 **Project DOI:** Not applicable
238 Reviewer account details:
239 **Username:** reviewer04988@ebi.ac.uk
240 **Password:** dLW6igaA

241 **Results and Discussion**

242 In *Drosophila*, spermatogenesis starts from a primordial primary spermatogonium in early larval
243 stages and this process continues uninterrupted throughout the life of the fly. The primary
244 spermatogonia, located at the anterior end of the testis tube, undergo four cycles of mitotic divisions
245 with incomplete cytokinesis to produce 16 primary spermatocytes enclosed by two cyst cells. The unit
246 of the germ cells and the cyst cells is called a cyst. After the meiotic divisions, each cyst contains 64
247 haploid spermatids that undergo dramatic morphological changes during spermiogenesis, which leads
248 to the formation of mature sperm (Fuller et al., 1993). The appearance of new cell types at specific
249 times during development has to be accompanied by changes in the expression of proteins.

250 Here, we comparatively studied the proteomes of larval, pupal and adult testis, taking advantage
251 of the known composition of cell types in the different stages (Gärtner et al., 2014). Larval testes
252 contain mainly mitotic cells and cells in meiotic prophase (spermatogonia and spermatocytes). With
253 progression of spermatogenesis, the testes gradually become enriched with later germ-cell stages.
254 Pupal testes at 24 h APF are enriched in meiotic stages and early spermatid stages; the first
255 protamine-positive nuclei are visible in pupal testes at 36 h APF (Gärtner et al., 2014). Adult testes are
256 enriched in post-meiotic stages (late spermatids and spermatids ready for individualization with their
257 long flagella). Besides germ cells and cyst cells, *Drosophila* testes also contain a thin sheath of
258 pigment cells throughout their development. In larval testes, pigment cells enclose a single lumen
259 almost entirely filled with the developing germ cells. Nascent myotubes start to cover the testes from
260 36 h APF onwards, while the testes of adult flies contain a tight sheath of mature muscles between the
261 pigment cells and the germ cells (Susic-Jung et al., 2012; Rothenbusch-Fender et al., 2017). The
262 formation of the muscle sheath is accompanied by differentiation and growth of the testis from an
263 ovoid-shaped organ in larvae to the coiled tubular shape of the testes in adult flies (Fig. 1).

264 *Comprehensive proteome analysis of larval, pupal and adult testes of Drosophila by LC-MS/MS.*

265 We used wild-type *Drosophila* grown on medium containing tetracycline to inhibit growth of
266 *Wolbachia* sp., a bacterium that infects germ cells and that might inhibit spermatogenesis (Zheng et
267 al., 2011). The lack of Wolbachia DNA/transcripts was controlled by RT-PCR (Supplemantary Fig. 1).
268 To unravel the stage-specific testes proteome signature, we isolated larval testes (L3), pupal testes at
269 24 and 48 h APF, and adult testes (Fig. 1). Proteins were separated by SDS-PAGE and in-gel digested
270 followed by LC-MS/MS using an Orbitrap mass spectrometer (Fig. 1).
271 In total, more than 6000 protein groups were identified and of which more than 5000 proteins were
272 quantified in at least 3 replicates and greatly expands the number of testis proteins compared to an
273 earlier study that identified 232 proteins in flies (Takemori and Yamamoto, 2009). Quantification and
274 identification data as well as Flybase IDs and CG numbers are reported in the Appendix. Technical
275 reproducibility was assessed by determining the Pearson correlation coefficient between all replicates.
276 We found almost linear correlation between biological replicates ($r > 0.87$) and we visualized this
277 correlation matrix by using hierarchical clustering. The clustering showed clear separation between
278 biological replicates of larvae, pupal and adult testes indicating unique stage specific proteomes. Small
279 distances were obtained between the protein signatures of 24h and 48h treated pupal samples,
280 indicating that the technical variance of independent sample preparation was higher than the biological
281 variance between 24 h und 48 h treatment. Therefore, the samples were pooled for the following
282 analysis (Supplementary Fig. S2). Furthermore, a principal component analysis revealed a clear
283 separation of larval, pupal and adult proteomes indicating unique proteomic expression profiles at
284 investigated developmental states (Fig. 2A).

285 We quantified 5359 proteins in larval testes, 5798 proteins in pupal testes, and 5738 proteins in adult
286 testes indicating robust sample preparation and instrument performance. In addition to the class of
287 proteins that were exclusively identified in larval (61), pupal (77) and adult (214) testes**,** we observed
288 4905 proteins in all developmental stages (Fig. 2B; Appendix). Moreover, 295 proteins were found in
289 both larval and pupal testes but not in adult testes, 537 proteins were found in both pupal and adult

testes but not in larval testes, and 82 proteins were found in both larval and adult testes but not in pupal testes (Fig. 2B).

In agreement with the high transcriptional activity during the growth of spermatocytes and translational activity throughout spermatogenesis, we found the poly(A) binding protein pAbp and the translational elongation factors Efalpha48D and Ef2B among the 20 most abundant proteins in larval, pupal and adult testes. Exu, a protein that binds single-stranded RNA, was particularly abundant in pupal testes. In addition, in pupal and adult testis, tubulins were the second most abundant class of proteins, which is consistent with the beginning of the growth of long spermatid flagella in pupal testes. Important to note, the vertebrate testes express high levels of structural proteins, including tubulins, actins, and histones (Martyniuk and Alvarez, 2012), which reflects the high number of somatic cells compared to the *Drosophila* testes.

Identification of proteins that are known to be stage-specifically synthesized confirmed the specificity of the testes proteomes of the different stages.

The spermatocyte stage is the only stage in which Y-chromosomal genes of *Drosophila* are transcribed (for review Piergentili (2010)). We identified several proteins encoded by the Y-chromosome, which showed an accumulation from larval to adult stages (Fig. 2C). The Y chromosome is essential for male fertility and encodes male fertility factors. Here, we identified WDY (FBgn0267449), kl-2 (FBgn0001313), kl-3 (FBgn0267432) and kl-5 (Fbgn0267433) enriched in the proteome of pupal and adult testes (Fig. 2C). WDY, which contains a WD40 repeat domain, was predicted based on expressed sequence tags, and it has been suggested that its encoding gene is *kl-1* (Vibranovski et al., 2008). The male fertility factors encoded by the *kl-2*, *kl-3* and *kl-5* genes encode outer dynein heavy chains of the axoneme (Golbstein et al, 1982; Gepner and Hays, 1993 for a review, see Carvalho et al., 2002). Thus, the abundance of these proteins in pupal and adult testes correlates with the post-meiotic assembly of the axoneme. The Y chromosome transcribes the Mst77Y pseudogenes (Krsticevic et al., 2010; 2015) and the corresponding predicted proteins are very similar to Mst77F which is an essential

316 sperm chromatin protein (Jayaramaiah Raja and Renkawitz-Pohl, 2005; Doyen et al., 2015, Kimura
317 and Loppin, 2016). Here we detected for the first time a corresponding protein to one of the Mst77Y
318 transcripts, Mst77Y-13 (FBgn0267491).

319 Mature sperm consist of a head with a length of ca.10 µm, whereas the tail is much longer with
320 ca. 1.8 mm (Fuller, 1993); thus, we expected that the abundant proteins are mainly part of the
321 flagellum. Accordingly, the outer dense fibre protein of the flagellum Mst98Ca (FBgn0002865;
322 Appendix) was detected enriched in adult testes (Schäfer et al., 1993). However, also proteins of the
323 sperm head were observed enriched in adult proteomes, e.g. Protamine B (FBgn0013301, Appendix)
324 encoded by *Mst35Bb* and another known sperm chromatin component, Mst77F (FBgn0086915,
325 Appendix), was identified (Jayaramaiah Raja and Renkawitz-Pohl, 2005). Furthermore, the detection
326 of several myosin heavy chain isoforms (Mhc, FBgn0264695, Appendix) in adult testes reflects the
327 presence of the fully developed muscle sheath of the mature organ (Susic-Jung et al., 2012 and
328 references therein).

329

330 *Cellular and subcellular distribution of newly identified components of nuclei and flagella*
331 Significantly regulated proteins were identified by an analysis of variance using a FDR < 5% resulting
332 in approximately 1850 proteins. This subset of proteins was then subjected to hierarchical clustering
333 (Fig. 3A). We defined 8 clusters and calculated by a Fisher Exact test for overrepresented terms in
334 each cluster using Gene Ontology (GO) Annotations compared to all proteins. The adult proteome is
335 for example enriched for components involved in sperm individualization (Fig. 3B), while larval and
336 pupal proteomes are enriched for mRNA splicing components (Fig. 3C) in agreement with the
337 enrichment of transcriptionally active stages before meiotic divisions.

338

339 *CG2046 is present at all stages of testis development and is essential for male fertility*.
340 Before concentrating on stage specifically expressed proteins, we analysed one so far uncharacterized
341 protein (encoded by CG2046) detected in all stages in more detail. It has been predicted that *CG2046*

342 (FBgn0037378) encodes a 25.8 kDa protein; the C-terminal region is conserved with the proteasome
343 assembly chaperone 1 (PSMG1) of mice (Flybase, Gramates et al., 2017; InterPro, Jones et al., 2014).
344 This chaperone in mice binds to the proteasome (for a review see Murata et al., 2009) and is associated
345 with a proteasome complex (Guruharsha et al., 2011). We propose to name the *CG2046*-encoded
346 protein *Drosophila* Proteasome Assembly Chaperone 1 (dPSMG1). dPSMG1 was identified in the
347 proteome of all analysed testes stages (Fig. 4A, Appendix). We analysed a $CG2046^{F01807}$ mutant,
348 which bears a PiggyBac transposon insertion 85 bp downstream of the translation initiation codon of
349 *dPsmg1* that thus interrupts the open reading frame (Fig. 4B). Homozygous flies were viable. In testes
350 of heterozygous $CG2046^{F01807}$ males, dPSMG1 transcripts were observed from the spermatocyte stage
351 until elongating spermatid stages (Fig. 4C), whereas the transcripts were barely detectable in
352 homozygous $CG2046^{F01807}$ mutants (Fig. 4D). We raised an antibody against a peptide of dPCMG1.
353 This antibody detected a protein of ca. 25 kDa (25.8 kDa predicted, Flybase, Gramates et al., 2017). In
354 agreement with the lack of *CG2046* transcripts, the CG2046 protein was not detected in immunoblots
355 using protein extracts of *CG2046* mutant testes (Fig. 4F; actin loading control shown in Fig. 4E).
356 Notably, our customized anti-dPCMG1 antibody was suitable for immunoblot analysis but
357 immunofluorescence staining revealed no difference between *CG2046* mutants and controls (data not
358 shown).

359 In testes of *CG2046* mutants, the phenotype manifested very late during spermiogenesis. We
360 found no individualized sperm (compare Fig. 4G and H), cysts with elongated spermatids shortly
361 before individualization varied in phenotype; some nuclei were similar to those of the wild type (Fig.
362 4H), some were doughnut shaped (Fig. 4I) and some were bent at one end like a walking stick (Fig.
363 4J). We asked whether protamines are deposited at the late canoe stage and whether individualization
364 complexes are formed. Protamine B (Fig. 4K′) and the actin-rich individualization cones (visualized
365 by phalloidin staining; Fig. 4K″; merged image in Fig. 4K‴) were clearly present in homozygous
366 $CG2046^{F01807}$ mutants. Protamine B was detected in homozygous $CG2046^{01807}$ mutants (Fig. 4L′), but
367 individualization cones were not detected at the doughnut-shaped nuclei (Fig. 4L″; merged image in

368 Fig. 4L‴). However, we cannot exclude that this aberrant form of nuclei is generated after
369 individualization. In accordance with the strong post-meiotic phenotype, homozygous *CG2046*^{F01807}
370 mutants and *CG2046*^{F01807} *in trans* to the deletion Exel6145 (where *CG2046* and 15 other genes are
371 deleted) were male sterile (Fig. 4M). *CG2046* ^{F01807} *in trans* to other deletions excluding *CG2046* were
372 fertile, which indicated that the sterility is due to disruption of the *CG2046* gene and not due to second
373 hit events. Thus, we conclude that dPSGM1 is essential for male fertility, and that this is manifested in
374 the nuclear-shaping defects and arrest at the individualization stage.
375
376 *Mst27D marks spermatid nuclei during nuclear shaping.*
377 We found CG31907 (FBgn0051907, Appendix) in the testes proteome of pupae and adult males and
378 strongly reduced in that of larval males (Fig. 5A), which indicates a limited protein expression to post-
379 meiotic stages. As the gene is solely transcribed in males and localized at 27D on polytene
380 chromosomes, we named this gene *Male specific transcript 27D (Mst27D)*. It is predicted that *Mst27D*
381 encodes a microtubule-binding protein (Flybase, Gramates et al., 2017). Microtubules are involved in
382 many cellular structures during the development of male germ cells. For example, microtubules are
383 associated to the formation of mitotic and meiotic spindles, the centrosomes and the axonemes, and
384 are involved in nuclear shaping of the sperm head (Fuller et al., 1988). Here we constructed a gene
385 encoding an Mst27D-eGFP fusion protein and the established transgenic *Drosophila* strain showed a
386 strong eGFP signal shortly after meiotic divisions (Fig. 5B; arrow). In addition, Mst27D-eGFP was
387 clearly visible along round nuclei of spermatids (Fig. 5B, arrowhead; D, arrow) and prominent during
388 the stages of nuclear elongation (Fig. 5B, arrowhead). We did not observe labelled sperm nuclei in
389 seminal vesicles (Fig. 5B). A closer inspection confirmed that the first clear presence of Mst27D-
390 eGFP was along round spermatid nuclei (Fig. 5D) and it accumulated on one side of the nucleus of
391 early elongating spermatids (Fig. 5E). Early and late canoe stages (Fig. 5F, G) showed Mst27D-eGFP
392 on one side of the elongated nucleus, and Mst27D-eGFP was not detected when nuclei were fully
393 elongated (Fig. 5H). Microtubules play an essential role in nuclear shaping (Fuller et al., 1988).

394 Furthermore, β2 tubulin (Tub85D, FBgn0003889, Appendix), is highly abundant, it is a component of
395 the axoneme and also essential for nuclear shaping (Fuller et al., 1987; Rathke et al., 2010). Sperm
396 head shaping is also a feature in mammals (for review see Wei and Yang, 2018). Mst27D is related to
397 the human microtubule associated protein MAPRE1, a member of the EB1 family proteins (Su and Qi,
398 2001).

399

400 *Mst84B contains C-terminal lysine-rich regions and characterizes the spermatid chromatin during the*
401 *histone-to-protamine transition.*

402 We have quantified CG1988 (FBgn0037464) exclusively in adult testes but not in larval and pupal
403 testes (Fig. 6A, Appendix). The protein is rich in cysteine and lysine resulting in a basic pI value of
404 10.48. Such a high pI is typical for transition proteins and sperm packaging proteins. It contains
405 multiple putative nuclear localization sites (Fig. 6B) and we considered this protein as a potential
406 candidate for a post-meiotic chromosomal protein. The *CG1988* transcripts are limited to males in
407 adult stages and we named this protein *Male specific transcript 84B (Mst84B)* (Flybase, Gramates et
408 al., 2017). Mst84D protein expression was observed in a dotted pattern over the spermatid chromatin
409 during the histone-to-protamine transition (Fig. 6C, D). The timing of Mst84B protein expression
410 overlapped with that of histones and the transition protein-like 94D (Tpl94D) in early canoe stage
411 (Fig. 6C). Both Tpl94D and Mst84B were also detected in the late canoe stage (Fig. 6D). At this stage,
412 the exchange of histones starts with transient chromatin components, such as Tpl94D and dimers of
413 tHMG-1 and tHMG-2 (Gärtner et al., 2015) and ends with ProtA (Mst35Ba, FBgn0013300), ProtB
414 (Mst35Bb, FBgn0013301), Mst77F (FBgn0086915) and Prtl99C (FBgn0039707) (Eren-Ghiani et al.,
415 2015). Hence, the similar expression of Mst84B suggests that Mst84B is also a transient component of
416 chromatin during the transition from a histone-based chromatin to a protamine-based chromatin (for a
417 review on chromatin dynamics during spermiogenesis, see Rathke et al., 2014). This stage is
418 characterized by multiple DNA breaks, (Rathke et al., 2007) which might facilitate the opening of the
419 chromatin and thus the release of histones, followed by the deposition of transition proteins and

420 protamines (for a review, see Rathke et al., 2014). The expression of Mst84B coincided with DNA
421 breaks, but the signals hardly co-localized (Supplementary Fig. 3B, C). A P-element mutation results
422 in a truncated protein; flies homozygous for this mutation are fertile (Flybase, Gramates et al., 2017).
423 Mutants of Tpl94D were also fertile, as were mutants that lost both tHMG-1 (CG7048) and tHMG-2
424 (CG7046), which form a transient chromatin component dimer (Gärtner et al., 2015). Thus, we
425 propose that either transition-protein-like proteins are functionally redundant or their loss is
426 compensated by up-regulation of related proteins, as has been suggested to occur at the transcriptional
427 level for HMGZ after loss of tHMG-1 and tHMG-2 (Gärtner et al., 2015).
428
429 *In adult testes, CG5089-eGFP and CG8701-eGFP are detected in elongated flagella.*
430 We exemplarily studied other small basic proteins that were solely detected or showed a significant
431 up-regulation in adult flies compared to pupa and larvae (Fig. 7A), as this stage might be enriched in
432 proteins associated with flagella or sperm chromatin. For example, *CG5089* (FBgn0034144) has the
433 coding capacity for a basic protein (Table 1 and Appendix). We established transgenic *Drosophila*
434 lines that synthesize a CG5089-eGFP fusion protein. Pupal testes at 48 h APF showed no GFP signal
435 (Fig. 7B), in agreement with the results obtained from the pupal proteome. In adult testes, CG5089-
436 eGFP was detected in some but not all bundles of flagella (Fig. 7C) and the nuclei of elongated
437 spermatids showed no CG5089-eGFP signal (Fig. 7D).
438 We detected the cysteine-rich protein CG8701 (FBgn0033287) only in the proteome of adult testes
439 (Fig. 7A, Appendix), as described in Dorus et al. (2006) and Wasbrough et al. (2010) and the tagged
440 version of CG8701-eGFP protein was restricted to some flagella in adult testes (Fig. 7E-G).
441
442 *dTheg is a component of the flagellum and essential for male fertility*.
443 Another protein with a restricted and abundant expression in the adult testes is CG6332
444 (FBgn0038921, Fig. 8A, Appendix). This candidate is related to the Theg (testicular haploid expressed

445 gene) protein of mice, known as THEG in humans. We detected the characteristic repeats of human
446 THEG protein in the *Drosophila* protein (Fig. 8B) and named this protein dTheg.
447 Earlier, Yanaka et al. (2000) observed abnormally elongated spermatids and spermatids lacking
448 flagella in an insertional Theg mutant mouse model, whereas Mannan et al. (2003) reported a nuclear
449 localization of Theg in spermatids. However, the *Theg* knockout mouse models demonstrated that
450 Theg might be dispensible for mouse spermatogenesis. Here, we established transgenic flies with a
451 gene encoding the fusion protein CG6332-eGFP. The GFP signal was detected in the flagella of very
452 late elongated spermatids and in the flagella of sperm in the seminal vesicles (Supplementary Fig. 4B).
453 We analysed the *CG6332* minos insertion mutant *Mi{ET1}CG6332*^{MB01798} (Flybase, Gramates et al.,
454 2017), for which a C-terminal truncated protein (CG6223-ΔC, 236 aa instead of 353 aa) was predicted
455 (Fig. 8B). We verified the shorter transcript of *Mi{ET1}CG6332*^{MB01798} by RT-PCR. Primers that
456 amplified the 5′ region of the transcripts detected both the full-length and the truncated transcript (Fig.
457 8C), whereas the primers that amplified the 3′ region only detected in the full-length transcript (Fig.
458 8C). A specific antibody raised against a dTheg epitope (anti-CG6332; Fig. 8B) revealed the presence
459 of dTheg in flagella of elongated spermatids (Fig. 8E); DNA co-staining showed at higher
460 magnification that the nuclei are free of dTheg (Fig. 8F). Testes of homozygous
461 *Mi{ET1}CG6332*^{MB01798} mutants contained bundles of elongated spermatids but lacked dTheg (Fig.
462 8E′), indicating that the truncated protein is unstable. Moreover, the loss of dTheg caused complete
463 male sterility (n = 20). In agreement with the observed sterility, the seminal vesicles lacked mature
464 sperm (Fig. 8D). Thus, the *Drosophila* dTheg protein is deposited during very late stages in the
465 flagella, suggesting a function during the formation of the mature flagellum.
466
467 **Concluding remarks**
468 The stage-specific testes proteomes of *Drosophila* identified hundreds of proteins that are enriched
469 before meiotic divisions (larval proteome), in round spermatids and spermatids during elongation of
470 nuclei and flagella (pupal proteome) and in late steps of spermiogenesis, such as protamine deposition

and formation of outer dense fibres (adult proteome). Our biological data of some of these proteins confirm the results of proteome analysis and underscore the high potential of testes proteome analysis for future studies of spermatogenesis in *Drosophila*. Together, our comprehensive quantitative proteome study of the *Drosophila* sperm development represents a public repository and will be of great importance to study the sperm development in flies in more detail.

Acknowledgements

We thank Sylvia Jeratsch and Ellen Borowski (Max-Planck-Institut für Herz- und Lungenforschung) for advice and technical assistance on sample preparation for mass spectrometry analysis. We are grateful to Rainer Renkawitz and Katharina Fritzen for critical reading, Karen A. Brune for competent language revision of this manuscript and Katja Gessner for excellent secretarial assistance. We thank Christopher Feldewert for technical help, and Ruth Hyland and Ljubinka Cigoja for taking care of our fly facility and establishment of transgenic *Drosophila* lines. This work was supported by grants from Deutsche Forschungsgemeinschaft (TRR81 "Chromatin Changes in Differentiation and Malignancies" to R.R.-P. and C.R.) and by REPRO-TRAIN Marie Curie Initial Training Network (Z.E.-G, PITN-2011-289880 to R.R.-P.) and the DFG Excellence Cluster Cardio-Pulmonary System (ECCPS), and the Cologne *Cluster* of Excellence on Cellular Stress Responses in Aging-associated Diseases (CECAD to M. K).

489 **References**

490 Amaral, A., Castillo, J., Ramalho-Santos, J., Oliva, R., 2014. The combined human sperm proteome:
491 cellular pathways and implications for basic and clinical science. Hum Reprod Update 20, 40-62.

492 Awe, S., Renkawitz-Pohl, R., 2010. Histone H4 acetylation is essential to proceed from a histone- to a
493 protamine-based chromatin structure in spermatid nuclei of *Drosophila* melanogaster. Syst Biol
494 Reprod Med 56, 44-61.

495 Barckmann, B., Chen, X., Kaiser, S., Jayaramaiah-Raja, S., Rathke, C., Dottermusch-Heidel, C.,
496 Fuller, M.T., Renkawitz-Pohl, R., 2013. Three levels of regulation lead to protamine and Mst77F
497 expression in *Drosophila*. Dev Biol 377, 33-45.

498 Cox, J., Mann, M., 2008. MaxQuant enables high peptide identification rates, individualized p.p.b.-
499 range mass accuracies and proteome-wide protein quantification. Nat Biotechnol 26, 1367-1372.

500 Cox, J., Neuhauser, N., Michalski, A., Scheltema, R.A., Olsen, J.V., Mann, M., 2011. Andromeda: a
501 peptide search engine integrated into the MaxQuant environment. J Proteome Res 10, 1794-1805.

502 Dorus, S., Busby, S.A., Gerike, U., Shabanowitz, J., Hunt, D.F., Karr, T.L., 2006. Genomic and
503 functional evolution of the *Drosophila melanogaster* sperm proteome. Nat Genet 38, 1440-1445.

504 Doyen, C.M., Chalkley, G.E., Voets, O., Bezstarosti, K., Demmers, J.A., Moshkin, Y.M., Verrijzer,
505 C.P., 2015. A Testis-Specific Chaperone and the Chromatin Remodeler ISWI Mediate Repackaging of
506 the Paternal Genome. Cell Rep 13, 1310-1318.

507 Doyen, C.M., Moshkin, Y.M., Chalkley, G.E., Bezstarosti, K., Demmers, J.A., Rathke, C., Renkawitz-
508 Pohl, R., Verrijzer, C.P., 2013. Subunits of the histone chaperone CAF1 also mediate assembly of
509 protamine-based chromatin. Cell Rep 4, 59-65.

510 Eren-Ghiani, Z., Rathke, C., Theofel, I., Renkawitz-Pohl, R., 2015. Prtl99C acts together with
511 protamines and safeguards male fertility in *Drosophila*. Cell Rep 13, 2327-2335.

512 Fuller, M.T., 1993. Spermatogenesis, in: Bate, M., Martinez-Arias, A. (Eds.), The development of
513 *Drosophila melanogaster*. Cold Spring Harbor Laboratory Press, Cold Spring Harbor, New York, pp.
514 71-147.

515 Fuller, M.T., Caulton, J.H., Hutchens, J.A., Kaufman, T.C., Raff, E.C., 1987. Genetic analysis of
516 microtubule structure: a beta-tubulin mutation causes the formation of aberrant microtubules in vivo
517 and in vitro. J Cell Biol 104, 385-394.

518 Fuller, M.T., Caulton, J.H., Hutchens, J.A., Kaufman, T.C., Raff, E.C., 1988. Mutations that encode
519 partially functional beta 2 tubulin subunits have different effects on structurally different microtubule
520 arrays. J Cell Biol 107, 141-152.

521 Gärtner, S.M., Rathke, C., Renkawitz-Pohl, R., Awe, S., 2014. Ex vivo culture of *Drosophila* pupal
522 testis and single male germ-line cysts: dissection, imaging, and pharmacological treatment. J Vis Exp,
523 51868.

524 Gärtner, S.M., Rothenbusch, S., Buxa, M.K., Theofel, I., Renkawitz, R., Rathke, C., Renkawitz-Pohl,
525 R., 2015. The HMG-box-containing proteins tHMG-1 and tHMG-2 interact during the histone-to-
526 protamine transition in *Drosophila spermatogenesis*. Eur J Cell Biol 94, 46-59.

527 Gepner, J., Hays, T.S., 1993. A fertility region on the Y chromosome of *Drosophila melanogaster*
528 encodes a dynein microtubule motor. Proc Natl Acad Sci U S A 90, 11132-11136.

529 Goldstein, L.S., Hardy, R.W., Lindsley, D.L., 1982. Structural genes on the Y chromosome of
530 *Drosophila melanogaster*. Proc Natl Acad Sci U S A 79, 7405-7409.

531 Gramates, L.S., Marygold, S.J., Santos, G.D., Urbano, J.M., Antonazzo, G., Matthews, B.B., Rey,
532 A.J., Tabone, C.J., Crosby, M.A., Emmert, D.B., Falls, K., Goodman, J.L., Hu, Y., Ponting, L.,
533 Schroeder, A.J., Strelets, V.B., Thurmond, J., Zhou, P., the FlyBase, C., 2017. FlyBase at 25: looking
534 to the future. Nucleic Acids Res 45, D663-D671.

535 Guruharsha, K.G., Rual, J.F., Zhai, B., Mintseris, J., Vaidya, P., Vaidya, N., Beekman, C., Wong, C.,
536 Rhee, D.Y., Cenaj, O., McKillip, E., Shah, S., Stapleton, M., Wan, K.H., Yu, C., Parsa, B., Carlson,
537 J.W., Chen, X., Kapadia, B., VijayRaghavan, K., Gygi, S.P., Celniker, S.E., Obar, R.A., Artavanis-
538 Tsakonas, S., 2011. A protein complex network of Drosophila melanogaster. Cell 147, 690-703.

539 Hoffmann, A.A., Turelli, M., 1988. Unidirectional incompatibility in *Drosophila simulans*:
540 inheritance, geographic variation and fitness effects. Genetics 119, 435-444.

541 Huang, S.Y., Lin, J.H., Chen, Y.H., Chuang, C.K., Lin, E.C., Huang, M.C., Sunny Sun, H.F., Lee,
542 W.C., 2005. A reference map and identification of porcine testis proteins using 2-DE and MS.
543 Proteomics 5, 4205-4212.

544 Huang, S.Y., Lin, J.H., Teng, S.H., Sun, H.S., Chen, Y.H., Chen, H.H., Liao, J.Y., Chung, M.T., Chen,
545 M.Y., Chuang, C.K., Lin, E.C., Huang, M.C., 2011. Differential expression of porcine testis proteins
546 during postnatal development. Anim Reprod Sci 123, 221-233.

547 Huttlin, E.L., Jedrychowski, M.P., Elias, J.E., Goswami, T., Rad, R., Beausoleil, S.A., Villen, J., Haas,
548 W., Sowa, M.E., Gygi, S.P., 2010. A tissue-specific atlas of mouse protein phosphorylation and
549 expression. Cell 143, 1174-1189.

550 Jayaramaiah Raja, S., Renkawitz-Pohl, R., 2005. Replacement by *Drosophila melanogaster*
551 protamines and Mst77F of histones during chromatin condensation in late spermatids and role of
552 sesame in the removal of these proteins from the male pronucleus. Mol Cell Biol 25, 6165-6177.

553 Jones, P., Binns, D., Chang, H.Y., Fraser, M., Li, W., McAnulla, C., McWilliam, H., Maslen, J.,
554 Mitchell, A., Nuka, G., Pesseat, S., Quinn, A.F., Sangrador-Vegas, A., Scheremetjew, M., Yong, S.Y.,
555 Lopez, R., Hunter, S., 2014. InterProScan 5: genome-scale protein function classification.
556 Bioinformatics 30, 1236-1240.

557 Karr, T.L., 2007. Fruit flies and the sperm proteome. Hum Mol Genet 16 Spec No. 2, R124-133.

558 Kimura, S., Loppin, B., 2016. The Drosophila chromosomal protein Mst77F is processed to generate
559 an essential component of mature sperm chromatin. Open Biol 6.

560 Krsticevic, F.J., Santos, H.L., Januario, S., Schrago, C.G., Carvalho, A.B., 2010. Functional copies of
561 the Mst77F gene on the Y chromosome of *Drosophila melanogaster*. Genetics 184, 295-307.

562 Krsticevic, F.J., Schrago, C.G., Carvalho, A.B., 2015. Long-Read Single Molecule Sequencing to
563 Resolve Tandem Gene Copies: The Mst77Y Region on the *Drosophila melanogaster* Y Chromosome.
564 G3 (Bethesda) 5, 1145-1150.

565 Leser, K., Awe, S., Barckmann, B., Renkawitz-Pohl, R., Rathke, C., 2012. The bromodomain-
566 containing protein tBRD-1 is specifically expressed in spermatocytes and is essential for male fertility.
567 Biol Open 1, 597-606.

568 Li, J., Liu, F., Liu, X., Liu, J., Zhu, P., Wan, F., Jin, S., Wang, W., Li, N., Liu, J., Wang, H., 2011.
569 Mapping of the human testicular proteome and its relationship with that of the epididymis and
570 spermatozoa. Mol Cell Proteomics 10, M110 004630.

571 Liu, M., Hu, Z., Qi, L., Wang, J., Zhou, T., Guo, Y., Zeng, Y., Zheng, B., Wu, Y., Zhang, P., Chen,
572 X., Tu, W., Zhang, T., Zhou, Q., Jiang, M., Guo, X., Zhou, Z., Sha, J., 2013. Scanning of novel
573 cancer/testis proteins by human testis proteomic analysis. Proteomics 13, 1200-1210.

574 Lu, C., Fuller, M.T., 2015. Recruitment of Mediator Complex by Cell Type and Stage-Specific Factors
575 Required for Tissue-Specific TAF Dependent Gene Activation in an Adult Stem Cell Lineage. PLoS
576 Genet 11, e1005701.

577 Mannan, A.U., Nayernia, K., Mueller, C., Burfeind, P., Adham, I.M., Engel, W., 2003. Male mice
578 lacking the Theg (testicular haploid expressed gene) protein undergo normal spermatogenesis and are
579 fertile. Biol Reprod 69, 788-796.

580 Martyniuk, C.J., Alvarez, S., 2013. Proteome analysis of the fathead minnow (Pimephales promelas)
581 reproductive testes. J Proteomics 79, 28-42.

582 Morris, C.A., Benson, E., White-Cooper, H., 2009. Determination of gene expression patterns using in
583 situ hybridization to *Drosophila* testes. Nat Protoc 4, 1807-1819.

584 Murata, S., Yashiroda, H., Tanaka, K., 2009. Molecular mechanisms of proteasome assembly. Nat Rev
585 Mol Cell Biol 10, 104-115.

586 Nayernia, K., von Mering, M.H., Kraszucka, K., Burfeind, P., Wehrend, A., Kohler, M., Schmid, M.,
587 Engel, W., 1999. A novel testicular haploid expressed gene (THEG) involved in mouse spermatid-
588 sertoli cell interaction. Biol Reprod 60, 1488-1495.

589 Nolte, H., MacVicar, T.D., Tellkamp, F., Kruger, M., 2018. Instant Clue: A Software Suite for
590 Interactive Data Visualization and Analysis. Sci Rep 8, 12648.

591 Paz, M., Morin, M., Del Mazo, J., 2006. Proteome profile changes during mouse testis development.
592 Comp Biochem Physiol Part D Genomics Proteomics 1, 404-415.

593 Piergentili, R., 2010. Multiple roles of the Y chromosome in the biology of Drosophila melanogaster.
594 ScientificWorldJournal 10, 1749-1767.

595 Rappsilber, J., Ishihama, Y., Mann, M., 2003. Stop and go extraction tips for matrix-assisted laser
596 desorption/ionization, nanoelectrospray, and LC/MS sample pretreatment in proteomics. Anal Chem
597 75, 663-670.

598 Rathke, C., Baarends, W.M., Awe, S., Renkawitz-Pohl, R., 2014. Chromatin dynamics during
599 spermiogenesis. Biochim Biophys Acta 1839, 155-168.

600 Rathke, C., Baarends, W.M., Jayaramaiah Raja, S., Bartkuhn, M., Renkawitz, R., Renkawitz-Pohl, R.,
601 2007. Transition from a nucleosome-based to a protamine-based chromatin configuration during
602 spermiogenesis in *Drosophila*. J Cell Sci 120, 1689-1700.

603 Rathke, C., Barckmann, B., Burkhard, S., Jayaramaiah Raja, S., Roote, J., Renkawitz-Pohl, R., 2010.
604 Distinct functions of Mst77F and protamines in nuclear shaping and chromatin condensation during
605 *Drosophila* spermiogenesis. Eur J Cell Biol 89, 326-338.

606 Renkawitz-Pohl, R., Hollmann, M., Hempel, L., Schäfer, M.A., 2005. Spermatogenesis, in: Gilbert,
607 L.I., Iatrou, K., Gill, S.S. (Eds.), Comprehensive Molecular Insect Science. Elsevier BV, pp. 157-177.

608 Rothenbusch-Fender, S., Fritzen, K., Bischoff, M.C., Buttgereit, D., Oenel, S.F., Renkawitz-Pohl, R.,
609 2017. Myotube migration to cover and shape the testis of *Drosophila* depends on Heartless,
610 Cadherin/Catenin, and myosin II. Biol Open 6, 1876-1888.

611 Schäfer, M., Börsch, D., Hülster, A., Schäfer, U., 1993. Expression of a gene duplication encoding
612 conserved sperm tail proteins is translationally regulated in *Drosophila melanogaster*. Mol Cell Biol
613 13, 1708-1718.

614 Schultz, N., Hamra, F.K., Garbers, D.L., 2003. A multitude of genes expressed solely in meiotic or
615 postmeiotic spermatogenic cells offers a myriad of contraceptive targets. Proc Natl Acad Sci U S A
616 100, 12201-12206.

617 Shevchenko, A., Tomas, H., Havlis, J., Olsen, J.V., Mann, M., 2006. In-gel digestion for mass
618 spectrometric characterization of proteins and proteomes. Nat Protoc 1, 2856-2860.

619 Su, L.K., Qi, Y., 2001. Characterization of human MAPRE genes and their proteins. Genomics 71,
620 142-149.

621 Susic-Jung, L., Hornbruch-Freitag, C., Kuckwa, J., Rexer, K.H., Lammel, U., Renkawitz-Pohl, R.,
622 2012. Multinucleated smooth muscles and mononucleated as well as multinucleated striated muscles
623 develop during establishment of the male reproductive organs of *Drosophila melanogaster*. Dev Biol
624 370, 86-97.

625 Takemori, N., Yamamoto, M.T., 2009. Proteome mapping of the *Drosophila melanogaster* male
626 reproductive system. Proteomics 9, 2484-2493.

627 Theofel, I., Bartkuhn, M., Boettger, T., Gartner, S.M.K., Kreher, J., Brehm, A., Rathke, C., 2017.
628 tBRD-1 and tBRD-2 regulate expression of genes necessary for spermatid differentiation. Biol Open
629 6, 439-448.

630 Theofel, I., Bartkuhn, M., Hundertmark, T., Boettger, T., Gartner, S.M., Leser, K., Awe, S., Schipper,
631 M., Renkawitz-Pohl, R., Rathke, C., 2014. tBRD-1 selectively controls gene activity in the *Drosophila*
632 testis and interacts with two new members of the bromodomain and extra-terminal (BET) family.
633 PLoS One 9, e108267.

634 Tyanova, S., Temu, T., Cox, J., 2016a. The MaxQuant computational platform for mass spectrometry-
635 based shotgun proteomics. Nat Protoc 11, 2301-2319.

636 Tyanova, S., Temu, T., Sinitcyn, P., Carlson, A., Hein, M.Y., Geiger, T., Mann, M., Cox, J., 2016b.
637 The Perseus computational platform for comprehensive analysis of (prote)omics data. Nat Methods
638 13, 731-740.

639 Vibranovski, M.D., Koerich, L.B., Carvalho, A.B., 2008. Two new Y-linked genes in *Drosophila*
640 *melanogaster*. Genetics 179, 2325-2327.

641 Vibranovski, M.D., Lopes, H.F., Karr, T.L., Long, M., 2009. Stage-specific expression profiling of
642 *Drosophila* spermatogenesis suggests that meiotic sex chromosome inactivation drives genomic
643 relocation of testis-expressed genes. PLoS Genet 5, e1000731.

644 Vizcaino, J.A., Csordas, A., del-Toro, N., Dianes, J.A., Griss, J., Lavidas, I., Mayer, G., Perez-Riverol,
645 Y., Reisinger, F., Ternent, T., Xu, Q.W., Wang, R., Hermjakob, H., 2016. 2016 update of the PRIDE
646 database and its related tools. Nucleic Acids Res 44, D447-456.

647 Wakimoto, B.T., Lindsley, D.L., Herrera, C., 2004. Toward a comprehensive genetic analysis of male
648 fertility in *Drosophila melanogaster*. Genetics 167, 207-216.

649 Wasbrough, E.R., Dorus, S., Hester, S., Howard-Murkin, J., Lilley, K., Wilkin, E., Polpitiya, A.,
650 Petritis, K., Karr, T.L., 2010. The *Drosophila melanogaster* sperm proteome-II (DmSP-II). J
651 Proteomics 73, 2171-2185.

652 Wei, Y.L., Yang, W.X., 2018. The acroframosome-acroplaxome-manchette axis may function in
653 sperm head shaping and male fertility. Gene 660, 28-40.

654 White-Cooper, H., Davidson, I., 2011. Unique aspects of transcription regulation in male germ cells.
655 Cold Spring Harb Perspect Biol 3.

656 Xiao, P., Tang, A., Yu, Z., Gui, Y., Cai, Z., 2008. Gene expression profile of 2058 spermatogenesis-
657 related genes in mice. Biol Pharm Bull 31, 201-206.

658 Yanaka, N., Kobayashi, K., Wakimoto, K., Yamada, E., Imahie, H., Imai, Y., Mori, C., 2000.
659 Insertional mutation of the murine kisimo locus caused a defect in spermatogenesis. J Biol Chem 275,
660 14791-14794.

661 Zheng, Y., Wang, J.L., Liu, C., Wang, C.P., Walker, T., Wang, Y.F., 2011. Differentially expressed
662 profiles in the larval testes of Wolbachia infected and uninfected *Drosophila.* BMC Genomics 12, 595.

663 Zhu, Y.F., Cui, Y.G., Guo, X.J., Wang, L., Bi, Y., Hu, Y.Q., Zhao, X., Liu, Q., Huo, R., Lin, M.,
664 Zhou, Z.M., Sha, J.H., 2006. Proteomic analysis of effect of hyperthermia on spermatogenesis in adult
665 male mice. J Proteome Res 5, 2217-2225.

Figure legends

Figure 1. Experimental design for the identification of proteins in *Drosophila* larval, pupal and adult testes by LC-MS/MS. Larval, pupal and adult testes of tetracycline-treated flies were isolated. Blue, third instar larval testis (L3); red, pupal testes at 24 h and 48 h APF; green, adult testis. Corresponding protein extracts were separated on SDS-polyacrylamide gels and processed for mass spectrometric analysis.

Figure 2. Proteome analysis of *Drosophila* testes at selected stages of development. (A) PCA score plot showing clear segregation between biological developmental states. B) Venn diagram showing the overlap of quantified proteins between biological conditions. C) Pointplot of proteins/genes encodes on the Y-chromosome. The log2 LFQ intensities were Z-score transformed. Gene names are colour coded.

Figure 3. Changes in the proteome during testis development. (A) Log2 LFQ intensities of significantly regulated proteins (ANOVA - FDR < 5%) were Z-Score transformed and subjected to hierarchical clustering (Euclidean, complete method). 8 Clusters were identified (rows) and tested for enriched GO terms against all quantified proteins. The complete list with enriched GO terms can be found in the Appendix. (B-C) Highlighting Cluster 2 and 5 in a line plot colour encoding the members of the distinct clusters. Next to the plot, enriched GO terms are listed.

Figure 4. *CG2046* encodes a predicted proteasome assembly chaperone 1 in larval, pupal and adult testes. (A) Presence of the CG2046 protein in the proteome of testes developmental stages. (B) PiggyBac insertion in the coding region of the first exon of *CG2046* in the *Drosophila* fly line $CG2046^{f01807}$ (Flybase, Gramates et al., 2017). (C) Detection of *CG2046* transcripts (arrowhead) in the wild-type germ line from spermatogonia to elongated spermatids by *in situ* hybridization with an antisense probe against *CG2046.* (D) Lack of signal (arrowhead) in the male germ line of homozygous $CG2046^{f01807}$ mutants ($CG2046^{f01807}$-/-). (E) Western blot of proteins from testes of wild type and homozygous $CG2046^{f01807}$ -/- males using anti-Actin. (F) Western blot of proteins from testes of

691 (*CG2046*^{f01807}+/-) and homozygous *CG2046*^{f01807} -/- males using anti-CG2046. (G) Nuclei of post-
692 meiotic germ cell stages from heterozygous *CG2046*^{f01807} males and (H) homozygous *CG2046*^{f01807}
693 males visualized by Hoechst staining. (I) Elongated, ring-shaped nuclei of spermatids in some cysts of
694 homozygous *CG2046*^{f01807} testes. (J) Elongated, bent nuclei of spermatids in some cysts of
695 homozygous *CG2046*^{f01807} testes. (K-K‴) Nuclei in a cyst of heterozygous *CG2046*^{f01807} males; (K)
696 DNA visualized by Hoechst staining; (K′) Protamine B staining (green); (K″) Phalloidin staining of
697 individualized actin cones (red); (K‴) merged image of K, K′ and K″. (L-L‴) Misshaped spermatid
698 nuclei of homozygous *CG2046*^{01807} mutants; (L) DNA visualized by Hoechst staining; (L′) Protamine
699 B staining (green); (L″) phalloidin staining of actin (red); (L‴) merged image of L, L′ and L″. (M)
700 Fertility test of homozygous *CG2046* ^{f01807} mutant males, wild-type males and males carrying the
701 *CG2046* mutant allele *in trans* to a deficiency in which *CG2046* is deleted (Df(3R)Exel6145) or not
702 (Df(3R)Exel7283, 7284). The number of fertile males is given. n = 20. Asterisk marks the hub. Scale
703 bars 5 µm.

704 **Figure 5. Mst27D-eGFP (CG31907) is detected close to nuclei during nuclear shaping.** (A)
705 Presence of CG31907 (Mst27D) in the proteome of testes developmental stages. (B) Detection of
706 Mst27D-eGFP combined with differential interference contrast (DIC) image of adult testes; arrow,
707 shortly after meiosis; arrowhead, close to nuclei of elongated spermatid Asterisk, testis hub; SV,
708 seminal vesicle. (C-H) Analysis of different stages of spermatogenesis in testes squash preparations;
709 (C) spermatocytes; (D) round nuclei; (E) oval nuclei; (F) early canoe stage nuclei; (G) late canoe stage
710 nuclei; (H) nuclei of elongated spermatids. Blue, DNA visualized by Hoechst staining; green,
711 Mst27D-eGFP. Scale bars 5 µm.

712 **Figure 6. Mst84B (CG1988) is synthesized during histone-to-protamine transition.** (A) Presence
713 of Mst84B in the proteome of testes developmental stages. (B) Amino acid sequence of Mst84B.
714 Green, putative mitochondrial import signal; red underline, mitochondrial peptidase consensus
715 sequence; purple underline, peptide used as antigen for antibody generation; blue, putative nuclear

716 localization signals. (C, D) Localization of Mst84D (red), Tpl94D-eGFP (green), and histones (white)
717 in (C) early and (D) late canoe stages. Scale bar 5 μm.

718 **Figure 7. CG5089-eGFP and CG8701-eGFP are synthesized in flagella of late elongating**
719 **spermatids.** (A) Presence of CG5089 and CG8701 in the proteome of testes developmental stages. (B,
720 E) Lack of detection of (B) CG5089-eGFP and (E) CG8071-eGFP in pupal testes 48 h APF in
721 differential interference contrast (DIC) images; arrow, elongating unlabelled flagella. (C, F) Detection
722 of (C) CG5089-eGFP and (F) CG8071-eGFP in adult testes in DIC image; arrowhead, late elongated
723 spermatids; arrow, other unlabelled spermatid bundles. (D, G) Detection of (D) CG5089-eGFP and
724 (G) CG8701-eGFP in adult testes squash preparations; blue, DAPI staining of nuclei; arrowhead,
725 eGFP-labelled flagella. Scale bars 10 μm.

726 **Figure 8. CG6332 (dTheg) is synthesized in flagella in adult testes and resembles the testicular**
727 **haploid expressed gene protein (THEG) of human.** (A) Presence of CG6332 in the proteome testes
728 developmental stages. (B) Schematic comparison of human THEG protein, the *Drosophila* CG6332
729 protein and its truncated version CG6332-ΔC. Pink, characteristic human THEG repeat regions; black
730 bar, epitope (CLAKPKKAPKVPKPDRGAGE) used for generating antibody against CG6332. (C) RT-
731 PCR analysis of *CG6332* in wild type and *Mi{ET1}CG6332*^{MB01798} (*CG6332*-Δ*C*) transcripts using
732 RNA isolated from adult testes, and a 5′ primer pair and a 3′ primer pair; transcript of the β3 tubulin
733 gene served as control. (D) Whole-mount of testes isolated from homozygous *Mi{ET1}CG6332*^{MB01798}
734 (*CG6332*-Δ*C*) males; arrow SV, empty seminal vesicles; arrowheads, elongated flagella; asterisk,
735 testis hub. (E, E′) Differential interference contrast images of (E) heterozygous and (E′) homozygous
736 *Mi{ET1}CG6332*^{MB01798} (*CG6332*-Δ*C*) males stained with anti-CG6332 (red). Blue, Hoechst, (F)
737 Higher magnification of E. Scale bar 20 μm (E-E′) or 10 μm (F).

738 **Table 1. Predicted basic proteins expressed at a high level in *Drosophila* testes**

Gene	pI (predicted)	Molecular mass (kDa; predicted)	Domain/motif (predicted)	Transcript level in adult testes (Fly Atlas)
CG12860	9.76	36.6	Cysteine rich	Very high
CG4691	10.38	30.8	Cysteine rich	Very high
CG1988	10.48	60.2	Cysteine and lysine rich	Very high
CG17377	8.45	18.6	-	Very high
CG31542	8.63	21.2	-	Very high
CG31907	9.82	49.0	Calponin homology domain, microtubule-associated protein Rp/EB, CH domain superfamily	Very high
CG6332	10.60	40.5	Testicular haploid expressed repeat	Very high
CG5089	10.48	51.7	-	Very high
CG8701	9.66	27.6	Cysteine rich	Very high

739

740 **Supplementary Figure 1. *Drosophila* testes are free of *Wolbachia* sp. infection.** RT-PCR of RNA
741 extracts and genomic DNA of pooled larva, pupa and adult flies used for subsequent testes isolation
742 (MS flies, tet+), and of a laboratory fly line infected with *Wolbachia* sp. (wsp+ flies) as positive con
743 trol. MS: flies raised for mass spectroscopic (MS) analysis M, markers. *wsp* primer: *Wolbachia* sp.-
744 specific primers (Zheng et al., 2011) amplified a prominent cDNA fragment (*wsp*) in infected flies
745 (wsp+ flies), whereas no PCR product was detected in samples of tetracycline-treated flies (MS flies,
746 tet+). *Tpl* primer: Control RT-PCR reactions with a testis-specific primer pair for *Tpl94D*, which spans
747 the intron of *Tpl94D*; both the gene and the transcript of *Tpl94* (cDNA) were amplified in MS flies,
748 tet+ but no *wsp* amplification was detected.

749 **Supplementary Figure 2. High reproducibility of the biological replicates.** Correlation matrix
750 using the Pearson correlation coefficient. Biological sample matrix was arranged by hierarchical
751 clustering (Euclidian distance, complete method).

752 **Supplementary Figure 3. Mst84B and DNA breaks are distinctly localized in chromatin of**
753 **spermatids. (A)** Presence of Mst84B in the proteome of testes developmental stages. (B, C) Squash
754 preparation of adult testes analysed with anti-Mst84D. Green, Mst84D; red, DNA breaks (TUNEL
755 assay), white, histones in (B) early and (C) late spermatid stages; merge, overlay of red and green
756 images. Scale bar 5 µm.

757 **Supplementary Figure 4. CG6332-eGFP is mainly synthesized in flagella of late spermatids and**
758 **mature sperm.** (A) Presence of CG6332 in the proteome of testes developmental stages. (B)
759 Differential interference contrast (DIC) image of CG6332-eGFP in adult testes; arrow, late spermatid
760 bundles; SV, seminal vesicles; asterisk, hub.

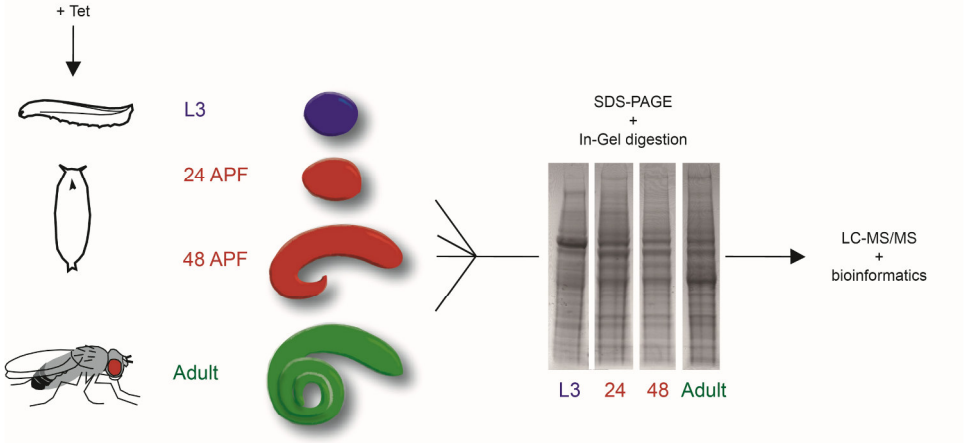
+ Tet
L3
24 APF
48 APF
Adult
SDS-PAGE
+
In-Gel digestion
L3
24
48
Adult
LC-MS/MS
+
bioinformatics

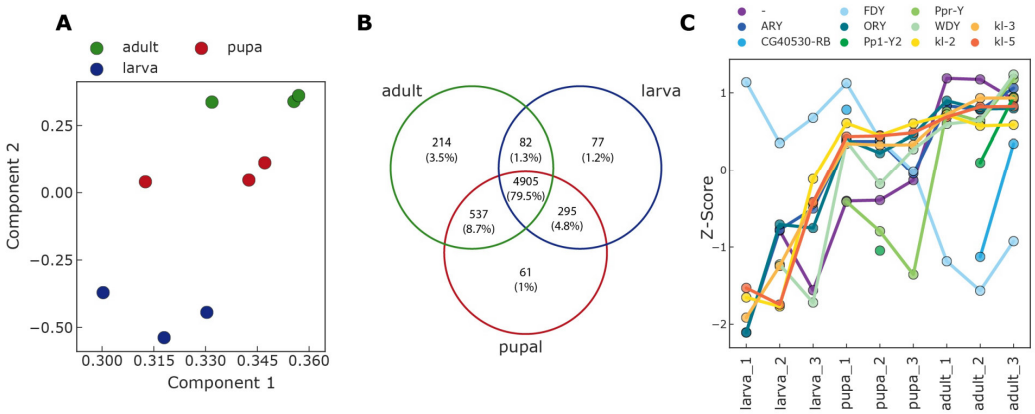
A
adult
pupa
larva
Component 2
0.25
0.00
−0.25
−0.50
0.300 0.315 0.330 0.345 0.360
Component 1
B
adult
larva
pupal
214
(3.5%)
82
(1.3%)
77
(1.2%)
4905
(79.5%)
537
(8.7%)
295
(4.8%)
61
(1%)
C
-
ARY
CG40530-RB
FDY
ORY
Pp1-Y2
Ppr-Y
WDY
kl-2
kl-3
kl-5
Z-Score
1
0
−1
−2
larva_1
larva_2
larva_3
pupa_1
pupa_2
pupa_3
adult_1
adult_2
adult_3

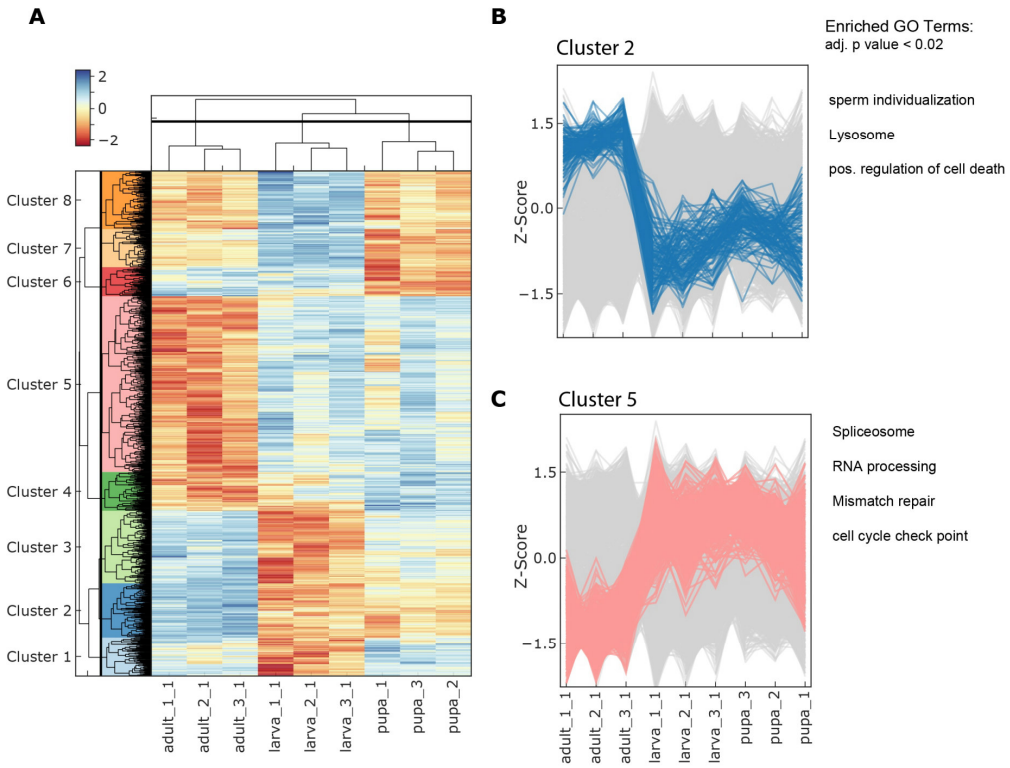
A
2
0
−2
Cluster 8
Cluster 7
Cluster 6
Cluster 5
Cluster 4
Cluster 3
Cluster 2
Cluster 1
adult_1_1
adult_2_1
adult_3_1
larva_1_1
larva_2_1
larva_3_1
pupa_1
pupa_3
pupa_2
B
Cluster 2
Z-Score
1.5
0.0
−1.5
Enriched GO Terms:
adj. p value < 0.02
sperm individualization
Lysosome
pos. regulation of cell death
C
Cluster 5
Z-Score
1.5
0.0
−1.5
Spliceosome
RNA processing
Mismatch repair
cell cycle check point
adult_1_1
adult_2_1
adult_3_1
larva_1_1
larva_2_1
larva_3_1
pupa_3
pupa_2
pupa_1

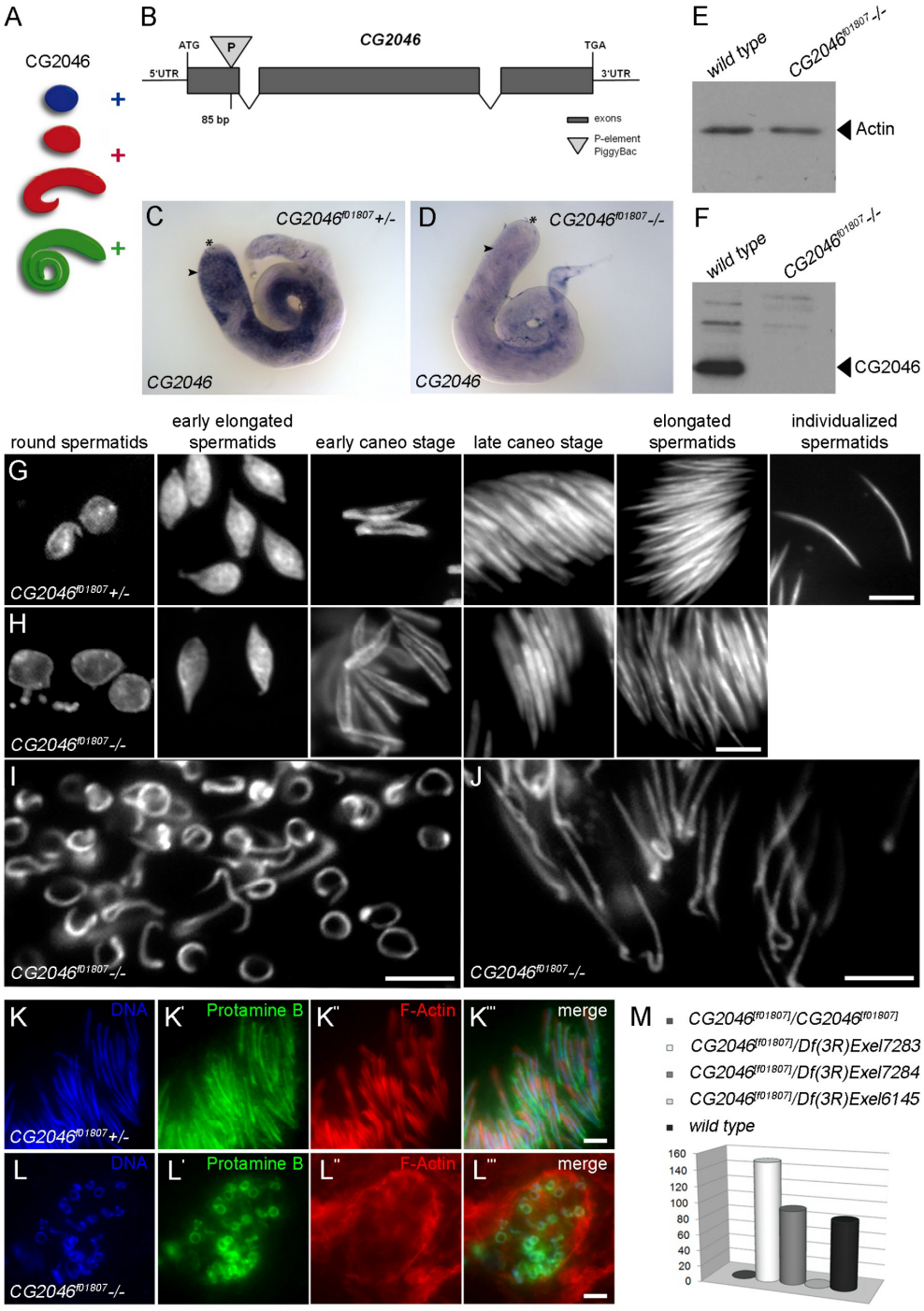
A
CG2046
B
CG2046
ATG
P
TGA
5'UTR
3'UTR
85 bp
exons
P-element
PiggyBac
E
wild type
CG2046f01807 -/-
Actin
C
CG2046f01807 +/-
CG2046
D
CG2046f01807 -/-
CG2046
F
wild type
CG2046f01807 -/-
CG2046
round spermatids
early elongated spermatids
early caneo stage
late caneo stage
elongated spermatids
individualized spermatids
G
CG2046f01807 +/-
H
CG2046f01807 -/-
I
CG2046f01807 -/-
J
CG2046f01807 -/-
K
DNA
K'
Protamine B
K''
F-Actin
K'''
merge
CG2046f01807 +/-
L
DNA
L'
Protamine B
L''
F-Actin
L'''
merge
CG2046f01807 -/-
M
CG2046f01807/CG2046f01807
CG2046f01807/Df(3R)Exel7283
CG2046f01807/Df(3R)Exel7284
CG2046f01807/Df(3R)Exel6145
wild type
160
140
120
100
80
60
40
20
0

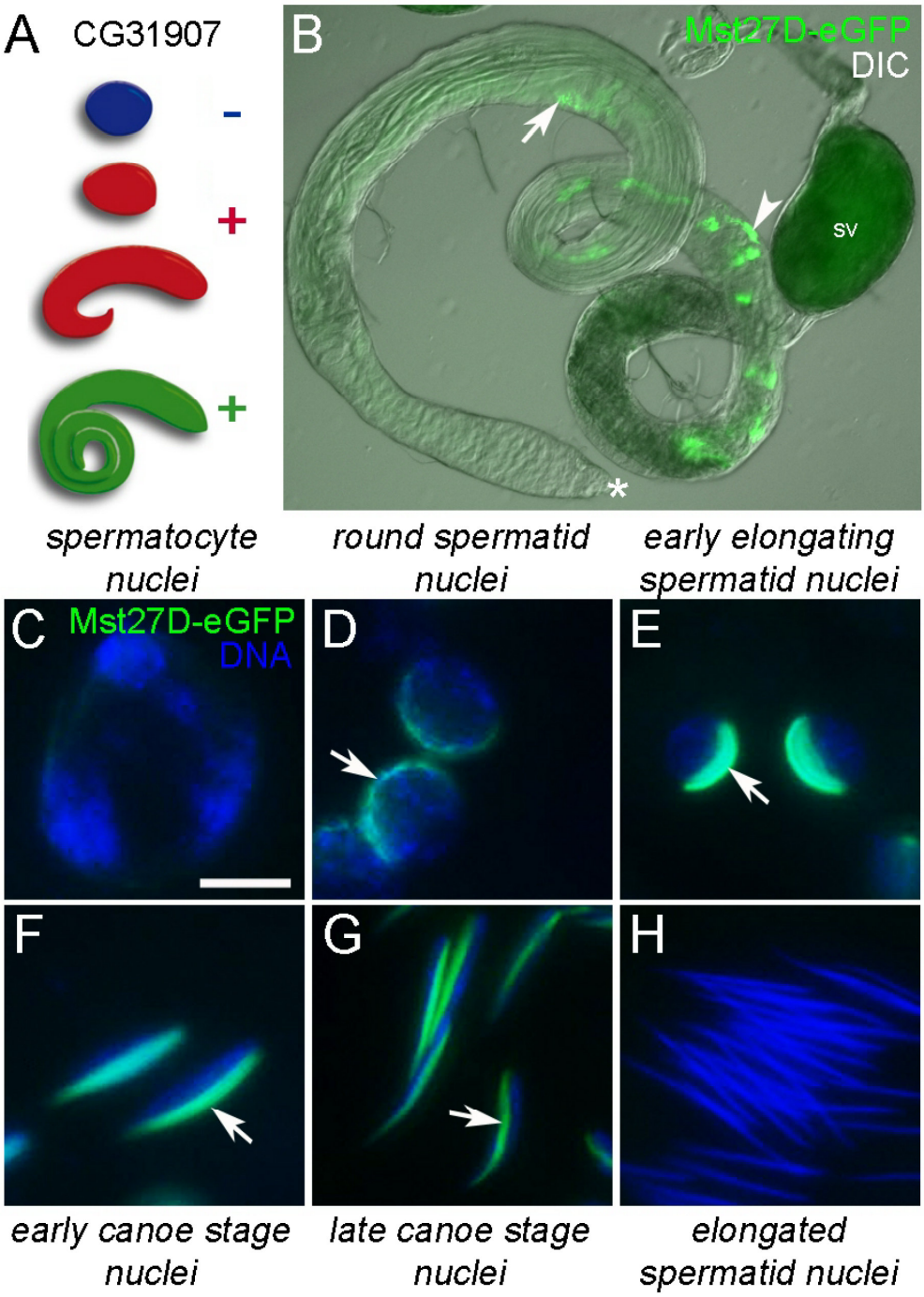
A
CG31907
-
+
+
B
Mst27D-eGFP
DIC
sv
*
spermatocyte nuclei
round spermatid nuclei
early elongating spermatid nuclei
C
Mst27D-eGFP
DNA
D
E
F
G
H
early canoe stage nuclei
late canoe stage nuclei
elongated spermatid nuclei

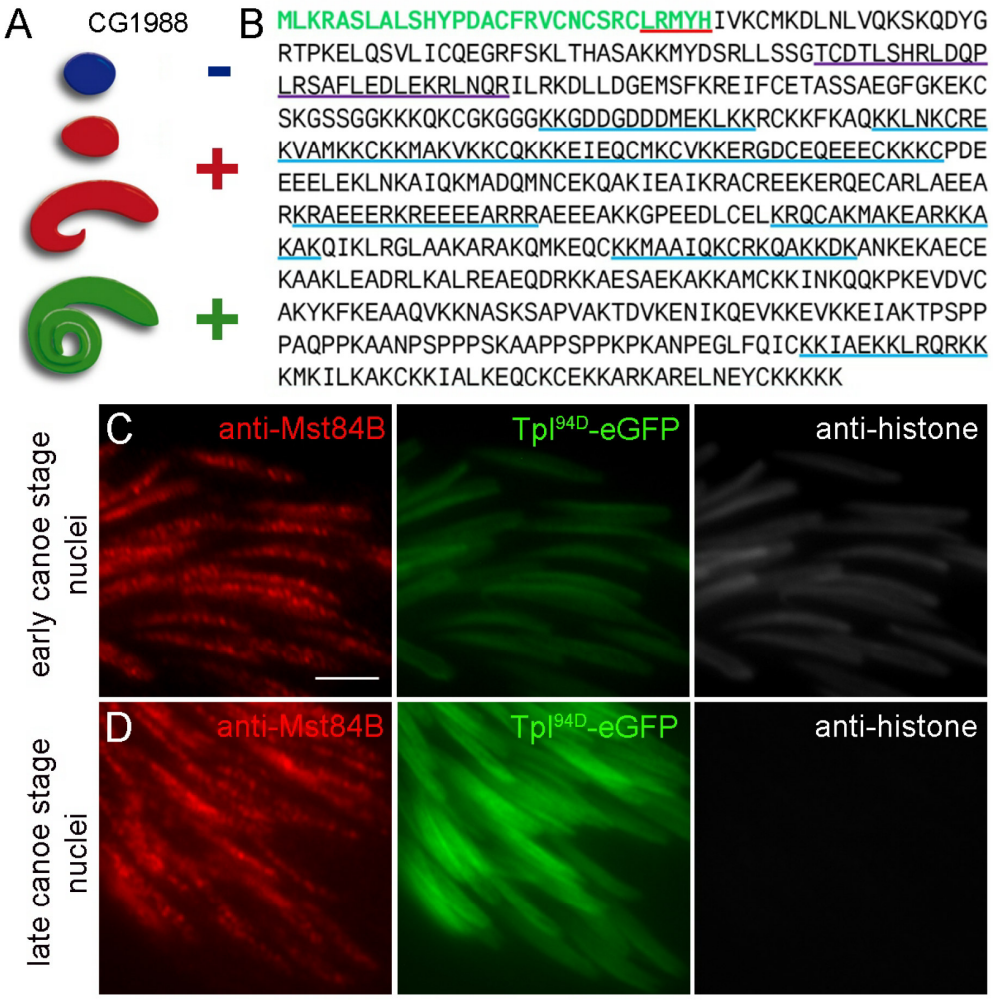
A
CG1988
-
+
+
B
MLKRASLALSHYPDACFRVCNCSRCLRMYHIVKCMKDLNLVQKSKQDYG
RTPKELQSVLICQEGRFSKLTHASAKKMYDSRLLSSGTCDTLSHRLDQP
LRSAFLEDLEKRLNQRILRKDLLDGEMSFKREIFCETASSAEGFGKEKC
SKGSSGGKKKQKCGKGGGKKGDDGDDDMEKLKKRCKKFKAQKKLNKCRE
KVAMKKCKKMAKVKKCQKKKEIEQCMKCVKKERGDCEQEEECKKKCPDE
EEELEKLNKAIQKMADQMNCEKQAKIEAIKRACREEKERQECARLAEEA
RKRAEEERKREEEEARRRAEEEAKKGPEEDLCELKRQCAKMAKEARKKA
KAKQIKLRGLAAKARAKQMKEQCKKMAAIQKCRKQAKKDKANKEKAECE
KAAKLEADRLKALREAEQDRKKAESAEKAKKAMCKKINKQQKPKEVDVC
AKYKFKEAAQVKKNASKSAPVAKTDVKENIKQEVKKEVKKEIAKTPSPP
PAQPPKAANPSPPPSKAAPPSPPKPKANPEGLFQICKKIAEKKLRQRKK
KMKILKAKCKKIALKEQCKCEKKARKARELNEYCKKKKK
C
anti-Mst84B
Tpl94D-eGFP
anti-histone
early canoe stage nuclei
D
anti-Mst84B
Tpl94D-eGFP
anti-histone
late canoe stage nuclei

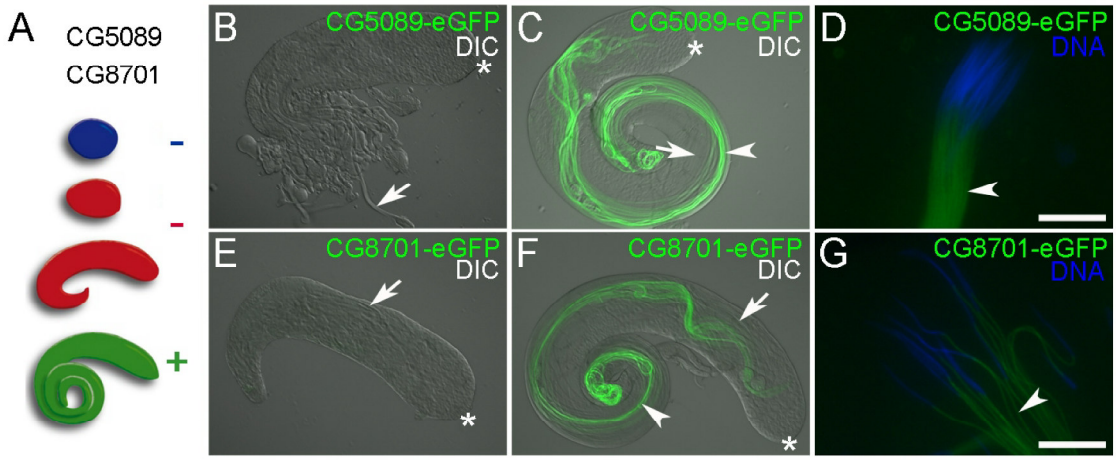
A
CG5089
CG8701
B
CG5089-eGFP
DIC
C
CG5089-eGFP
DIC
D
CG5089-eGFP
DNA
E
CG8701-eGFP
DIC
F
CG8701-eGFP
DIC
G
CG8701-eGFP
DNA

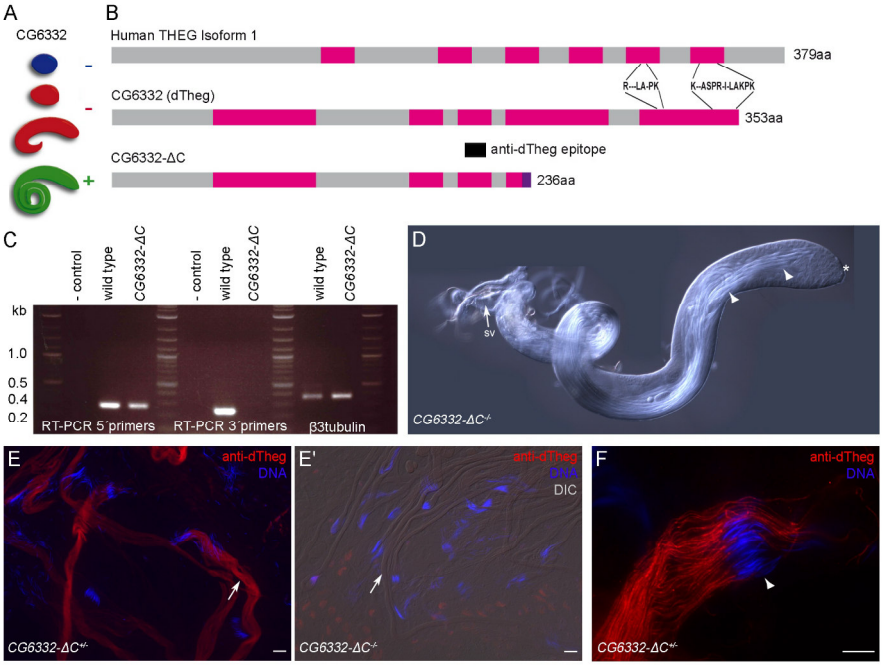
A
CG6332
B
Human THEG Isoform 1
379aa
CG6332 (dTheg)
R--LA-PK
K--ASPR-I-LAKPK
353aa
anti-dTheg epitope
CG6332-ΔC
236aa
C
- control
wild type
CG6332-ΔC
kb
1.0
0.5
0.4
0.2
RT-PCR 5´primers
RT-PCR 3´primers
β3tubulin
D
sv
CG6332-ΔC-/-
E
anti-dTheg
DNA
CG6332-ΔC+/-
E'
anti-dTheg
DNA
DIC
CG6332-ΔC-/-
F
anti-dTheg
DNA
CG6332-ΔC+/-

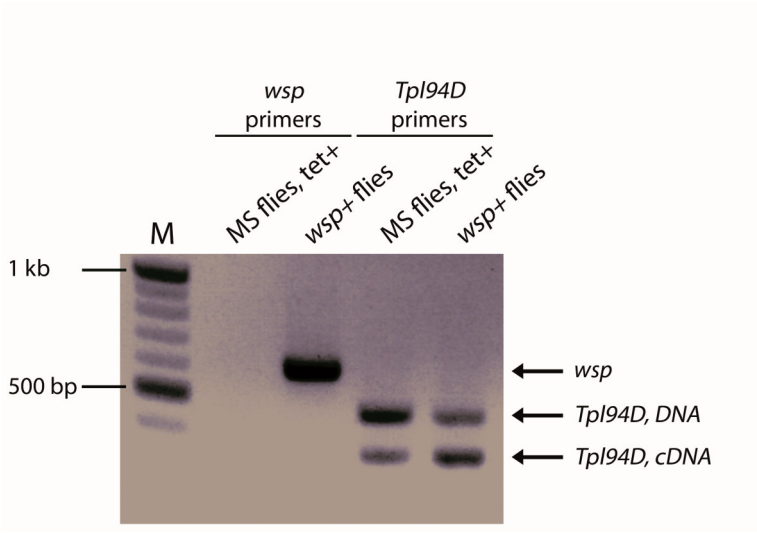
wsp
primers
Tpl94D
primers
M
MS flies, tet+
wsp+ flies
MS flies, tet+
wsp+ flies
1 kb
500 bp
wsp
Tpl94D, DNA
Tpl94D, cDNA

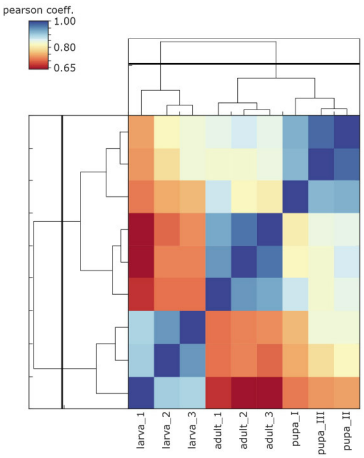
pearson coeff.
1.00
0.80
0.65
larva_1
larva_2
larva_3
adult_1
adult_2
adult_3
pupa_I
pupa_III
pupa_II

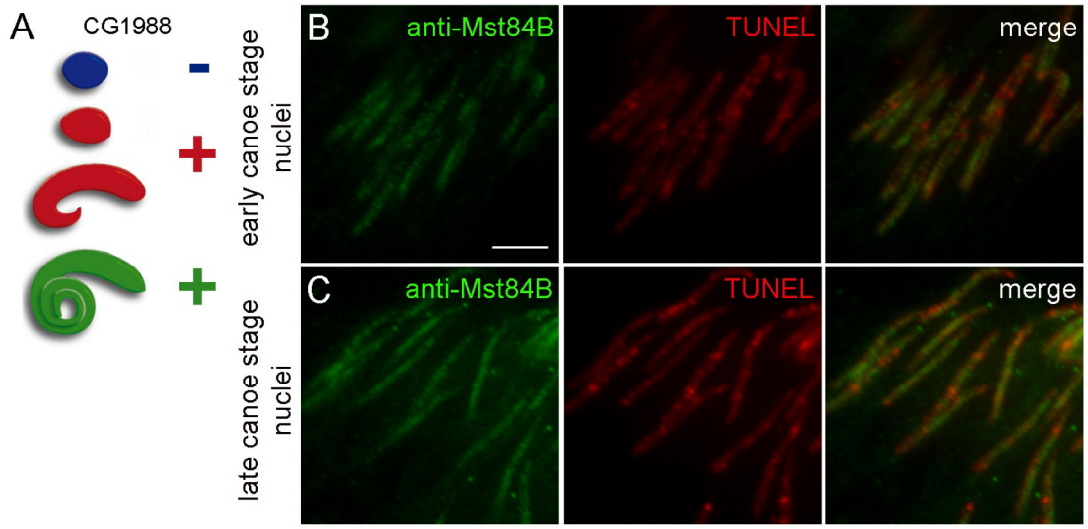
A
CG1988
-
+
+
B
anti-Mst84B
TUNEL
merge
early canoe stage nuclei
C
anti-Mst84B
TUNEL
merge
late canoe stage nuclei

Chapter 8: tBRD-1 selectively controls gene activity in the *Drosophila* testis and interacts with two new members of the bromodomain and extra-terminal (BET) family

Theofel, I.*, Bartkuhn, M.*, Hundertmark, T., Boettger, T., Gärtner, S.M.K., Leser, K., Awe, S., Schipper, M., Renkawitz-Pohl, R. and Rathke, C. (2014). Published in PLoS One, 2014 Sep 24;9(9):e108267

* These authors contributed equally to this work

Candidate's contribution:

- Yeast Two-Hybrid experiments (Figure 7)
- Proofreading the manuscript

OPEN ACCESS Freely available online

PLOS ONE

tBRD-1 Selectively Controls Gene Activity in the *Drosophila* Testis and Interacts with Two New Members of the Bromodomain and Extra-Terminal (BET) Family

Ina Theofel[1☯], Marek Bartkuhn[2☯], Tim Hundertmark[1], Thomas Boettger[3], Stefanie M. K. Gärtner[1], Katja Leser[1], Stephan Awe[1¤a], Michael Schipper[1¤b], Renate Renkawitz-Pohl[1], Christina Rathke[1]*

1 Philipps-University Marburg, Department of Biology, Marburg, Germany, **2** Institute for Genetics, Justus-Liebig-University, Giessen, Germany, **3** Department of Cardiac Development and Remodeling, Max-Planck-Institute for Heart and Lung Research, Bad Nauheim, Germany

Abstract

Multicellular organisms have evolved specialized mechanisms to control transcription in a spatial and temporal manner. Gene activation is tightly linked to histone acetylation on lysine residues that can be recognized by bromodomains. Previously, the testis-specifically expressed bromodomain protein tBRD-1 was identified in *Drosophila*. Expression of tBRD-1 is restricted to highly transcriptionally active primary spermatocytes. tBRD-1 is essential for male fertility and proposed to act as a co-factor of testis-specific TATA box binding protein-associated factors (tTAFs) for testis-specific transcription. Here, we performed microarray analyses to compare the transcriptomes of *tbrd-1* mutant testes and wild-type testes. Our data confirmed that tBRD-1 controls gene activity in male germ cells. Additionally, comparing the transcriptomes of *tbrd-1* and tTAF mutant testes revealed a subset of common target genes. We also characterized two new members of the bromodomain and extra-terminal (BET) family, tBRD-2 and tBRD-3. In contrast to other members of the BET family in animals, both possess only a single bromodomain, a characteristic feature of plant BET family members. Immunohistology techniques not only revealed that tBRD-2 and tBRD-3 partially co-localize with tBRD-1 and tTAFs in primary spermatocytes, but also that their proper subcellular distribution was impaired in *tbrd-1* and tTAF mutant testes. Treating cultured male germ cells with inhibitors showed that localization of tBRD-2 and tBRD-3 depends on the acetylation status within primary spermatocytes. Yeast two-hybrid assays and co-immunoprecipitations using fly testes protein extracts demonstrated that tBRD-1 is able to form homodimers as well as heterodimers with tBRD-2, tBRD-3, and tTAFs. These data reveal for the first time the existence of single bromodomain BET proteins in animals, as well as evidence for a complex containing tBRDs and tTAFs that regulates transcription of a subset of genes with relevance for spermiogenesis.

Citation: Theofel I, Bartkuhn M, Hundertmark T, Boettger T, Gärtner SMK, et al. (2014) tBRD-1 Selectively Controls Gene Activity in the *Drosophila* Testis and Interacts with Two New Members of the Bromodomain and Extra-Terminal (BET) Family. PLoS ONE 9(9): e108267. doi:10.1371/journal.pone.0108267

Editor: Helen White-Cooper, Cardiff University, United Kingdom

Received May 13, 2014; **Accepted** August 4, 2014; **Published** September 24, 2014

Data Availability: The authors confirm that all data underlying the findings are fully available without restriction. The GEO accession number for our microarray data is: GSE52511.

Funding: This work was supported by the German Research Foundation (DFG) (http://www.dfg.de/) within a research grant to CR (RA 2150/2-1) and within the TRR81 to MB and RR-P. The funders had no role in study design, data collection and analysis, decision to publish, or preparation of the manuscript.

Competing Interests: The authors have declared that no competing interests exist.

* Email: rathke@biologie.uni-marburg.de

¤a Current address: Institut für Molekularbiologie und Tumorforschung, Philipps-Universität Marburg, Marburg, Germany
¤b Current address: Weatherall Institute of Molecular Medicine, MRC Molecular Haematology Unit, University of Oxford, John Radcliffe Hospital, Headington, Oxford, United Kingdom

☯ These authors contributed equally to this work.

Introduction

During spermatogenesis male germ cells must pass through a highly organized differentiation process to produce haploid sperm. Spermatogenesis is characterized by three main phases: a mitotic amplification phase, a meiotic phase and a post-meiotic phase also known as spermiogenesis. Within the *Drosophila* testis 50% of the protein coding genes become activated, and among them many in a testis-specific or testis-enriched manner [1,2]. Since most transcription ceases with entry into the meiotic divisions, spermiogenesis is mainly based on translationally repressed and stored mRNAs (e.g. mRNAs that encode protamines) transcribed in a prolonged meiotic prophase in primary spermatocytes [3–5]. Primary spermatocytes are highly transcriptionally active cells that produce two different types of mRNAs: those required for the primary spermatocytes themselves and those that encode proteins necessary for spermiogenesis [2]. Transcription of spermiogenesis-relevant genes depends on the "meiotic arrest" genes that belong to the *aly*-class or the *can*-class [6]. Proteins of the *aly*-class exhibit a broader range of target genes and are part of the testis-specific meiotic arrest complex (tMAC) [7]. The *can*-class comprises proteins specifically expressed in the testis and homologous to the TATA box binding protein-associated factors (TAFs). To date, five testis-specific TAFs (tTAFs) have been described: Cannonball (Can; dTAF5 homolog), No hitter (Nht; dTAF4 homolog), Meiosis I arrest (Mia; dTAF6 homolog), Spermatocyte arrest (Sa; dTAF8 homolog) and Ryan express (Rye; dTAF12 homolog) [8,9]. In

addition, TAF1-2, an isoform of TAF1 is expressed in primary spermatocytes and together with tTAFs and other factors might form a testis-specific TFIID complex [10].

In primary spermatocytes, large amounts of tTAFs and TAF1 localize to the nucleolus [10,11]. In addition to gene activation, a second function for tTAFs as a repressor of the Polycomb Repression Complex 1 (PRC1) by recruitment of PRC1 to the nucleolus has been proposed [11]. However, recently published genome-wide and cell-specific analyses argue against a model where Polycomb displacement is involved in gene activation in spermatogenesis [12]. In primary spermatocytes, the "meiotic arrest" genes are known to activate directly or indirectly about 1500–2000 spermiogenesis-relevant genes whose mRNAs become translationally repressed until post-meiotic stages. In addition, the "meiotic arrest" genes are essential for cell cycle progression and mutant males show a meiotic arrest phenotype [1]. Based on the fact that these mutants lack post-meiotic stages, the impact of the "meiotic arrest" genes for spermiogenesis is difficult to address. To date, the tMAC and the testis-specific TFIID complex are the only two described transcription complexes in *Drosophila* spermatogenesis. Hence, many open questions remain, e.g. the transcriptional co-factors are not known, it is not known if and how both complexes interact, or whether additional transcription complexes exist in primary spermatocytes. Our aim was to discover which epigenetic "reader" proteins cooperate with tTAFs in primary spermatoyctes.

Acetylation of N-terminal histone tails by histone acetyltransferases (HATs) plays an important role in gene regulation [13]. Acetylation of lysine residues on histone tails is linked to gene activation and can be recognized by bromodomain-containing proteins (BRDs) [14–16]. The bromodomain is a module of about 110 amino acids that is conserved in many chromatin-associated proteins including HATs and ATP-dependent chromatin-remodeling factors [17]. Nearly all HAT-associated transcriptional co-factors, such as GCN5, p300/CBP, p300/CBP-associated factors, as well as TAF1 contain bromodomains [18].

Previously, we identified the testis-specifically expressed double bromodomain-containing protein tBRD-1 that is essential for male fertility [19]. In primary spermatocytes, tBRD-1 partially co-localizes with tTAFs and TAF1 in a tTAF dependent manner. Although, tBRD-1 expression is restricted to primary spermatocytes, *tbrd-1* mutants passed through meiosis and only exhibit a post-meiotic phenotype. This is in clear contrast to tTAF mutants that show a meiotic arrest phenotype and completely lack post-meiotic germ cells. A more detailed investigation of *tbrd-1* mutants showed that post-meiotic spermatid nuclei failed to elongate. In addition, the typical clustered arrangement of 64 spermatid nuclei within one cyst was disturbed in *tbrd-1* mutant testes and spermatids failed to individualize. However, spermiogenesis was not completely disturbed since for example the histone-to-protamine transition took place in *tbrd-1* mutants and elongated flagella could be observed. This indicated that tBRD-1 plays an important role in primary spermatocytes that is crucial for specific steps during spermiogenesis. We previously proposed that in primary spermatoyctes, tBRD-1 might act together with tTAFs to activate transcription of a subset of genes that encode proteins with relevance for spermiogenesis [19].

A special group of bromodomain proteins is the bromodomain and extra-terminal (BET) family characterized by having one (plants) or two (animals/yeast) N-terminal bromodomains and a poorly characterized extra-terminal (ET) domain assumed to function as a protein-protein interaction motif. The ET domain comprises three different regions: a conserved NET domain (for N-terminal ET), an intervening sequence and a C-terminal SEED motif. Plant BET proteins often lack the SEED domain.

After bromodomain-mediated association of BET proteins with acetylated chromatin, the ET domain may function as an interface to localize different complexes or proteins to chromatin. BET proteins associate with chromatin and with the basal transcriptional machinery to modulate chromatin structure and influence transcription in a sequence-independent manner [20,21]. In mammals, BRD2 is involved in gene activation, e.g. by binding to and recruiting the TATA box binding protein (TBP) [22]. The ET domain of BRD4 regulates transcriptional activity by e.g. recruiting specific factors to chromatin [23]. In *Drosophila*, the only known BET gene so far is *female sterile (1) homeotic* (*fs(1)h*) that encodes a multifunctional transcriptional regulator crucial for establishing and maintaining cell fates [24].

To confirm that tBRD-1 is involved in gene expression, we performed microarray analyses and showed that in *tbrd-1* mutant testes hundreds of transcripts are indeed significantly down-regulated compared to levels in wild-type testes. Additionally, we show that a *tbrd-1-eGFP* transgene constructed from the genomic region not only reverses the male sterile phenotype of *tbrd-1* mutants but also the effects on gene activity. Subsequently, we compared the transcriptomes of *tbrd-1* mutant testes with those of *sa* mutants and demonstrate a significant overlap of target genes. Furthermore, we identified two new BET genes in *Drosophila*: *tbrd-2* and *tbrd-3*. Both encoded proteins are testis-specifically expressed and partially co-localize with tTAFs and tBRD-1 in primary spermatocytes. The subcellular localization of tBRD-2 and tBRD-3 is dependent on the acetylation status within the cell. Moreover, similar to plant BET proteins, tBRD-2 and tBRD-3 exhibit only one bromodomain. Thus, we present here for the first time existence of BET family proteins containing a single bromodomain in animals. In addition, we demonstrate that tBRD-1 is able to homodimerize and form heterodimers with tBRD-2, tBRD-3 and tTAFs. These data confirm our hypothesis that tBRD-1 controls gene activity in male germ cells and we propose a model of how tBRDs together with tTAFs might control gene expression in primary spermatocytes.

Results

tBRD-1 is required for gene expression in the testis

Previously, we showed that tBRD-1 partially co-localizes with tTAFs in primary spermatocytes. While tBRD-1 expression is restricted to primary spermatocytes, the lack of tBRD-1 function only has consequences in post-meiotic stages. Therefore, we proposed that tBRD-1 acts together with tTAFs to initiate transcription of a special subset of genes with relevance for spermiogenesis [19].

To analyze whether tBRD-1 is indeed involved in gene expression, we performed microarray analyses, and compared the testes transcriptomes of homozygous *tbrd-1* mutants (*tbrd-1*^{1}) and wild-type flies (Figure 1). Five independent wild-type and five independent *tbrd-1* mutant hybridizations were carried out using Affymetrix *Drosophila* Genome 2.0 arrays. For each array, independent RNA from whole testes pooled from 25 animals was used. After quality control and normalization the expression values for each probe set from the five arrays of the same genotype were averaged and the log2-fold change between mutant and wild-type was calculated. A positive log2-fold change corresponds to elevated transcription in *tbrd-1* mutants. Genes with a log2-fold change $\geq +1$ or ≤ -1 were considered to have altered expression. Probe set specific P-values were corrected for testing multiple hypotheses (corrPVal) and used in place of P-value to assess the

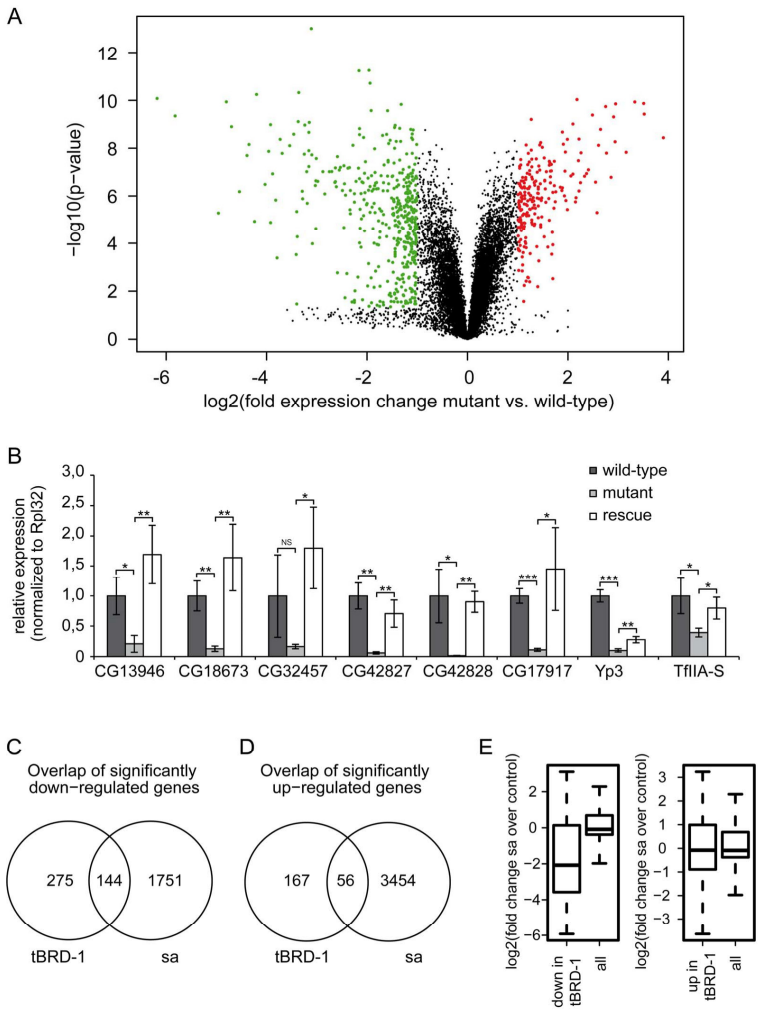

Figure 1. tBRD-1 is required for gene activity in the testis. (A) Distribution of gene expression changes observed when comparing wild-type and *tbrd-1* mutant testis. The volcano plot shows the logarithm of the probability of the t-test as a function of the logarithm of fold change for each reporter on the microarray. Reporter with an absolute log2-fold change ≥1 and a corrected p-value ≤0.05 are plotted in red (up-regulated) and green (down-regulated). (B) Quantitative real-time PCR (qPCR) using cDNA of wild-type, *tbrd-1*^{1} and *tbrd-1-eGFP; tbrd-1*^{1} testes. Transcript levels of *CG13946, CG18673, CG32457, CG42827, CG42828, CG17917, Yp3* and *TfIIA-S* were significantly reduced in *tbrd-1* mutant testes compared to wild-type and *tbrd-1-eGFP; tbrd-1*^{1} testes. P-values for significance: * p≤0.05, ** p≤0.01 and *** p≤0.001. NS: not significant. (C,D) Significantly changed genes in *tbrd-1* mutants and *sa* mutants. (C) 144 genes were significantly down-regulated in both *tbrd-1* and *sa* mutants. (D) 56 genes were significantly up-regulated in *tbrd-1* and *sa* mutants. (E) Genes down-regulated (left boxplot) and up-regulated (right boxplot) in *tbrd-1* mutant tested were analyzed for the associated transcriptional changes observed in *sa* mutant testes (all: all genes).
doi:10.1371/journal.pone.0108267.g001

significance of altered gene expression. At a corrPVal of ≤0.05 642 probe sets showed a statistically relevant change in expression. Of those, 223 genes were up-regulated and 419 genes were down-regulated (Figure S1A and Dataset S1). Raw data were deposited in the GEO database (accession number GSE52511).

Obviously, tBRD-1 can function in either way: gene activation and repression. The *tbrd-1*^{1} allele was generated by remobilization

and subsequent integration of P(EPgy2)^{EY02323} into the *tbrd-1* gene [19]. As expected *tbrd-1* itself was significantly down-regulated in *tbrd-1* mutant testes. In addition, in *tbrd-1* mutant testes a significant up-regulation of the *white* gene was detectable due to the integration of P(EPgy2)^{EY02323} (bearing the *white* gene) in *tbrd-1*^{1} (Dataset S1). Quantitative real-time PCR (qPCR) using cDNA of wild-type and *tbrd-1*^{1} testes was carried out to validate the results of the microarray experiments (Figure 1B and Figure S1B).

Recently, we showed that *tbrd-1*^{1} homozygous males and *tbrd-1*^{1}*/Df(3R)ED10893* or *tbrd-1*^{1}*/Df(3R)Exel9014* trans-heterozygous males shared the same phenotype. In addition, we showed that expression of the fusion protein tBRD-1-eGFP in *tbrd-1*^{1} mutants rescues male sterility [19]. Nevertheless, to exclude a "second hit" on the *tbrd-1*^{1} mutant chromosome, qPCRs using cDNA from *tbrd-1-eGFP*; *tbrd-1*^{1} testes were also performed here. Transcript levels of *CG13946*, *CG18673*, *CG32457*, *CG42827*, *CG42828* (note: annotation *CG6784* split into *CG42827* and *CG42828* in release 5.30 of the genome annotation FlyBase Genome Annotators, 2010), *CG17917*, *Yp3*, and *TfIIA-S* were significantly reduced in *tbrd-1* mutant testes compared to wild-type and *tbrd-1-eGFP*; *tbrd-1*^{1} testes (Figure 1B). Clearly, the reduced transcript levels are the result of the *tbrd-1* mutation since testes of *tbrd-1-eGFP*; *tbrd-1*^{1} flies exhibit similar or even higher transcript levels than wild-type testes.

TfIIA-S is the neighboring gene of *tbrd-1* and encodes a transcription factor. We thus performed qPCRs to exclude that the *TfIIA-S* gene region itself is affected (by remobilization and subsequent integration of P(EPgy2)^{EY02323}) in *tbrd-1* mutants. However, the transcript levels of *TfIIA-S* were reduced in *tbrd-1*^{1} testes but not in *tbrd-1-eGFP*; *tbrd-1*^{1} testes (Figure 1B). Apparently remobilization and subsequent integration of P(EPgy2)^{EY02323} in *tbrd-1*^{1} flies did not affect the *TfIIA-S* gene itself. In addition, qPCRs revealed that the transcript levels of up-regulated genes such as *CG31750* (note: formerly known as *Gr36d*; FlyBase curator comment: Gene symbol reverted back to CG symbol because this gene is no longer considered a member of the gustatory receptor (Gr) superfamily [25]), *cutlet*, *TwdlV* and *CG1441* were enriched in *tbrd-1* mutant testes compared to wild-type and *tbrd-1-eGFP*; *tbrd-1*^{1} testes (Figure S1B).

Our microarray analyses showed that tBRD-1 is directly or indirectly involved in gene expression within the testis. Here, we concentrated on the down-regulated probe sets that reflect genes directly or indirectly activated by tBRD-1. 391 of the 419 down-regulated probe sets matched annotated protein-coding genes in FlyBase [26]. Among these 391 probe sets 157 (40.2%) corresponded to a characterized gene having a specific name, while 234 (59.8%) matched only to CG numbers. To determine when the corresponding transcripts are detectable during spermatogenesis the 391 probe sets were analyzed using the "*Drosophila spermatogenesis expression database*" (http://mnlab.uchicago.edu/sppress/) [27]. This analysis revealed that 66.2% of the transcripts were enriched in post-meiotic male germ cells and 21.2% in meiotic cells. A few transcripts (8.7%) were enriched in mitotic cells and 3.8% could not be found in this database.

Our microarray data nicely demonstrated that tBRD-1 is indeed involved in gene activation in the testis and the majority of the corresponding transcripts accumulated in post-meiotic cells. Since tBRD-1 expression is restricted to primary spermatocytes we propose that in these cells tBRD-1 is mainly required to activate genes whose transcripts become translationally repressed until post-meiotic stages. This fits well with the post-meiotic phenotype of *tbrd-1* mutants.

Next, we compared our microarray data with available data sets of *sa* mutant testes (GSE48837) [28]. We observed big differences between both transcriptomes, but also a subset of common target genes (Figure 1C,D). In *tbrd-1* mutant testes, 419 genes were significantly down-regulated. Of these 144 (34.4%) were also down-regulated in *sa* mutant testis (Figure 1C). In contrast, among the 223 significantly up-regulated *tbrd-1* target genes only 56 genes (24.1%) were also up-regulated in *sa* mutant testes (Figure 1D). We determined the significance of the observed overlaps using the hypergeometric probability distribution. In case of the up-regulated genes we only found a modest albeit significant enrichment of the observed overlap over the expected overlap (1.3-fold, $p<1.22e-05$). In contrast, we observed a 3.4-fold enrichment in case of the down-regulated genes ($p<3.55e-41$). Similarly, we analyzed the relationship between genes down-regulated in *tbrd-1* and *sa* mutant testes in a more quantitative fashion (Figure 1E). In general, genes down-regulated in *tbrd-1* mutant testes were also down-regulated in *sa* mutant testes (Figure 1E, left). In contrast, genes up-regulated in *tbrd-1* mutant testes were not specifically de-regulated in *sa* mutant testes (Figure 1E, right). Indeed, tBRD-1 and Sa share a subset of common target genes, implying that tBRD-1 acts together with tTAFs to activate a subset of genes with relevance for spermiogenesis.

tBRD-2 and tBRD-3 constitute two new types of BET proteins in *Drosophila*

Besides tBRD-1 with two widely spaced bromodomains (amino acid 55 to 127 and 336 to 409) (Figure 2A and [19]) the *Drosophila* genome encodes two further as yet uncharacterized testis-specific bromodomain containing proteins. The *Drosophila CG7229* gene encodes a 674 amino acid protein of 74.6 kDa (Flybase) [26] with a predicted N-terminal bromodomain (amino acid 47 to 119), a NET domain (amino acid 362 to 443) (Prosite database) [29] and a SEED motif (amino acid 580 to 660) [20] (Figure 2B). The *Drosophila CG30417* gene encodes a 268 amino acid protein of 30.6 kDa (Flybase) [26] with a predicted N-terminal bromodomain (amino acid 28 to 100) and a NET domain (amino acid 181 to 261) (Prosite database) [29] (Figure 2C). Beyond the N-terminal bromodomains and the NET domains all three tBRD proteins show no sequence similarity.

RT-PCR analyses revealed that *CG7229* and *CG30417* transcripts are predominantly detectable in male gonads (Figure S2A,B). Affymetrix expression data also indicate an enrichment of both transcripts in the testis (Flyatlas: the *Drosophila* gene expression atlas) [30]. Consequently, we renamed CG7229 tBRD-2 and CG30417 tBRD-3 (testis-specifically expressed bromodomain-containing protein-2 and 3) and the corresponding genes *tbrd-2* and *tbrd-3*. In animals, proteins of the BET family have two bromodomains and an ET domain [20]. tBRD-2 and tBRD-3 are different since both have only a single N-terminal bromodomain. Additionally, tBRD-2 has a typical ET domain comprising a NET domain, an intervening sequence and a C-terminal SEED motif, whereas tBRD-3 has only the conserved NET domain of the ET domain. Beyond the bromodomains and the ET domains, tBRD-2 and tBRD-3 proteins show no sequence similarity to human or plant BET protein family members. We propose that tBRD-2 and tBRD-3 constitute two new members of the BET protein family in *Drosophila* that more resemble BET proteins in plants.

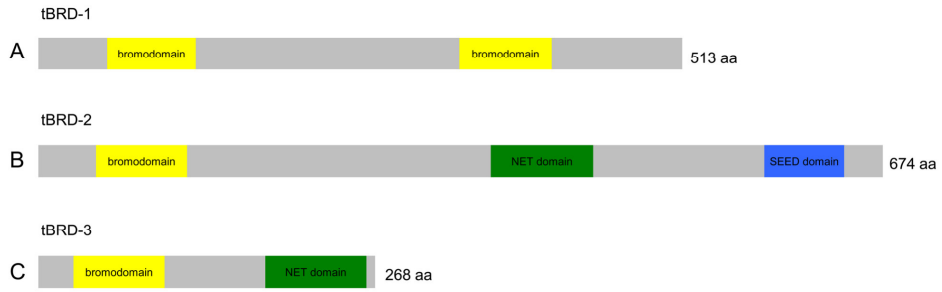

Figure 2. tBRD-2 and tBRD-3 represent two new types of BET proteins. Scheme of full-length tBRD-1 (A), tBRD-2 (B) and tBRD-3 (C) proteins. Bromodomains are indicated in yellow, NET domains in green and the SEED domain in blue.
doi:10.1371/journal.pone.0108267.g002

tBRD-1, tBRD-2 and tBRD-3 largely co-localize at the chromosome territories in primary spermatocytes

Recently, we showed that tBRD-1 is specifically expressed in primary spermatocytes, strongly localizing to the nucleolus, with lower amounts distributed over the partially condensed chromosomes [19] (Figure 3A′). Within the nucleoplasm tBRD-1 localizes to several nuclear speckles of unknown function. Within the scope of the experiments described here we focused on the chromosomal localization of tBRD-1, tBRD-2 and tBRD-3 in primary spermatocytes. To analyze the subcellular localization of tBRD-2 we generated *tbrd-2-eGFP* transgenic flies that express the fusion protein under the control of the endogenous gene regulatory regions. To analyze tBRD-3 we raised a peptide antibody (aa 175 to aa 189). The specificity of the antibody was confirmed by a peptide-blocking assay (Figure S3).

Examination of mature spermatocytes expressing tBRD-2-eGFP (Figure 3A,B) or immunostained with anti-tBRD-3 (Figure 3B′) revealed that, like tBRD-1, tBRD-2 and tBRD-3 localize to the partially condensed chromosomes (Figure 3A,B,B′, arrows). Thus, in primary spermatocytes tBRD-1, tBRD-2 and tBRD-3 largely co-localize and might cooperate in transcription of spermatogenesis-relevant genes. Recently, we could show that proper protein distribution of tBRD-1 in spermatocytes required wild-type function of tTAFs [19]. Likewise, immunofluorescence staining of sa^2 mutant testes showed that localization of tBRD-2-eGFP and tBRD-3 is altered in homozygous sa^2 mutant spermatocytes (Figure S4B and Figure 4B′). The localization to the nucleolus was strongly reduced, increased signals were visible within chromosome territories and nuclear speckles were hardly detectable. However, despite the altered distribution of tBRD-1, tBRD-2 and tBRD-3, co-localization of tBRD-2 and tBRD-3 with tBRD-1 was still detectable over the chromosomes in homozygous sa^2 mutant testes (Figure S4B″ and Figure 4B″, arrows). Clearly, tTAF Sa is not required for recruiting tBRD-1, tBRD-2 or tBRD-3 to chromosomes.

Analyses of homozygous *tbrd-1* mutant testes demonstrated that protein distributions of tBRD-2 and tBRD-3 are altered in primary spermatocytes (Figure 5B,B′). As above, localization to the nucleolus was strongly reduced and nuclear speckles were hardly detectable. However, both proteins continued to co-localize

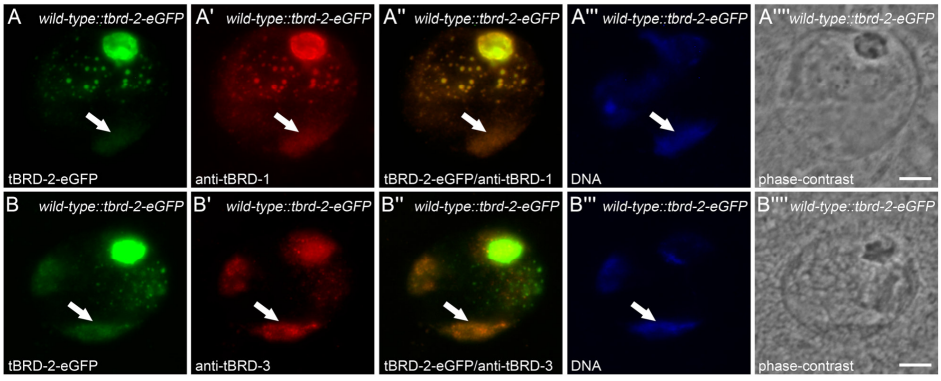

Figure 3. In primary spermatocytes tBRD-2 co-localizes with tBRD-1 and tBRD-3. Single primary spermatocyte nuclei of flies expressing tBRD-2-eGFP stained with anti-tBRD-1 (A panels) or anti-tBRD-3 (B panels). (A,B) tBRD-2-eGFP was visible over the chromosome territories (arrows). tBRD-2-eGFP partially co-localizes with tBRD-1 (A″) and tBRD-3 (B″) over the chromosomes (arrows). (A‴,B‴) Hoechst DNA staining. (A⁗,B⁗) Phase-contrast images. Scale bars: 5 µm.
doi:10.1371/journal.pone.0108267.g003

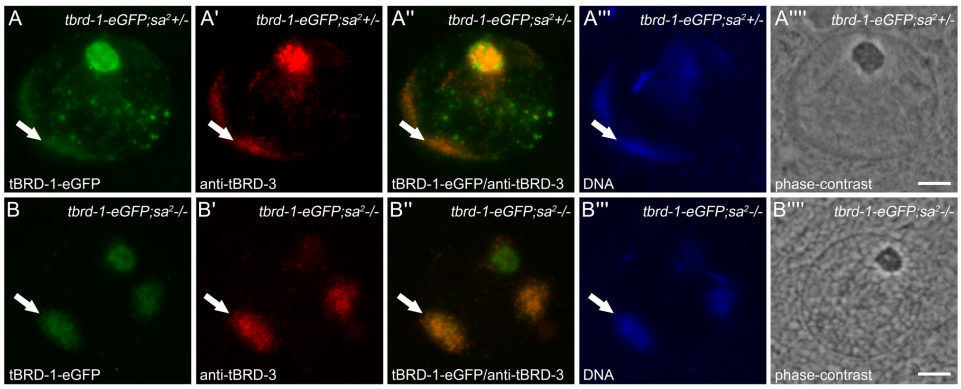

Figure 4. Recruitment of tBRD-1 and tBRD-3 to chromatin is independent of tTAF Sa. Single primary spermatocytes from heterozygous (A panels) and homozygous *sa*^{2} (B panels) mutants that express tBRD-1-eGFP stained with anti-tBRD-3 antibody. (A″,B″) In heterozygous and homozygous *sa*^{2} mutant spermatocytes tBRD-3 partially co-localizes with tBRD-1-eGFP over the chromosomes (arrows). (A‴,B‴) Hoechst DNA staining. (A⁗,B⁗) Phase-contrast images. Scale bars: 5 μm.
doi:10.1371/journal.pone.0108267.g004

over the chromosomes, although in a severely reduced manner (Figure 5B–B″, arrows) (note: *tbrd-2* and *tbrd-3* transcripts are not significantly down-regulated in *tbrd-1* mutant testes). Obviously, tBRD-1 is not absolutely essential for recruitment of tBRD-2 and tBRD-3 to chromosomes and their co-localization, but might increase and/or stabilize their binding to chromatin.

The acetylation status influences the localization of tBRD-1, tBRD-2 and tBRD-3 in primary spermatocytes

Previously, we could show that the distribution of tBRD-1 in primary spermatocytes changed after inhibitor treatment of cultured germ cells with trichostatin A (TSA) or anachardic acid (AA) [19]. Treatment of cells with TSA inhibits histone deacetylases (HDACs) and leads to a significant increase of histone H4 acetylation in primary spermatocytes, while AA leads to a dramatic decrease in acetylation by inhibiting histone acetyltransferases (HATs) [19,31,32]. Here, we treated pupal testes of *tbrd-2-eGFP* transgenic flies with either TSA or AA and subsequently performed immunofluorescence staining using an anti-tBRD-1 antibody (Figure 6). Increased or decreased acetylation was confirmed by an anti-histone H4ac antibody (Figure S5).

After treatment with AA, tBRD-2-eGFP and tBRD-1 distribution at the chromosomes was dramatically altered (Figure 6B,B′, arrows) compared to control spermatocytes (Figure 6A,A′, arrows). Treatment with TSA led to increased tBRD-2-eGFP and tBRD-1 localization to the chromosomes (Figure 6D,D′, arrows).

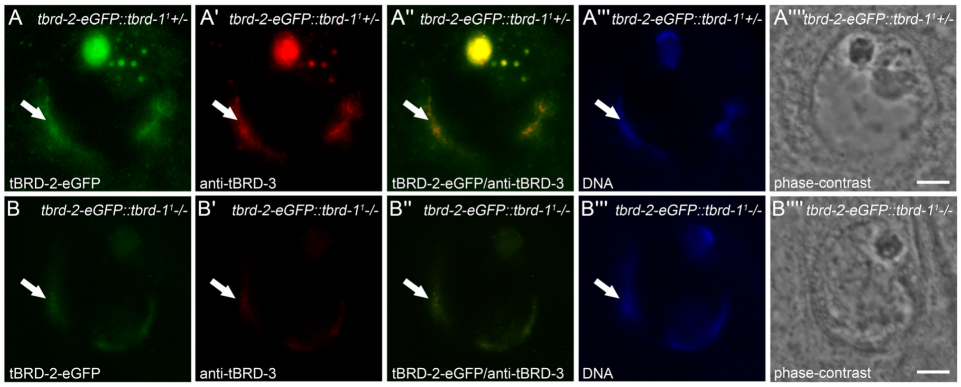

Figure 5. tBRD-1 is not essential for co-localization of tBRD-2 and tBRD-3. Single primary spermatocytes from heterozygous (A panels) and homozygous *tbrd-1*^{1} (B panels) mutants that express tBRD-2-eGFP stained with anti-tBRD-3 antibody. (B″) Partial co-localization of tBRD-2-eGFP and tBRD-3 over the chromosomes (arrows) was still detectable in homozygous *tbrd-1*^{1} mutant spermatocytes. (A‴,B‴) Hoechst DNA staining. (A⁗,B⁗) Phase-contrast images. Scale bars: 5 μm.
doi:10.1371/journal.pone.0108267.g005

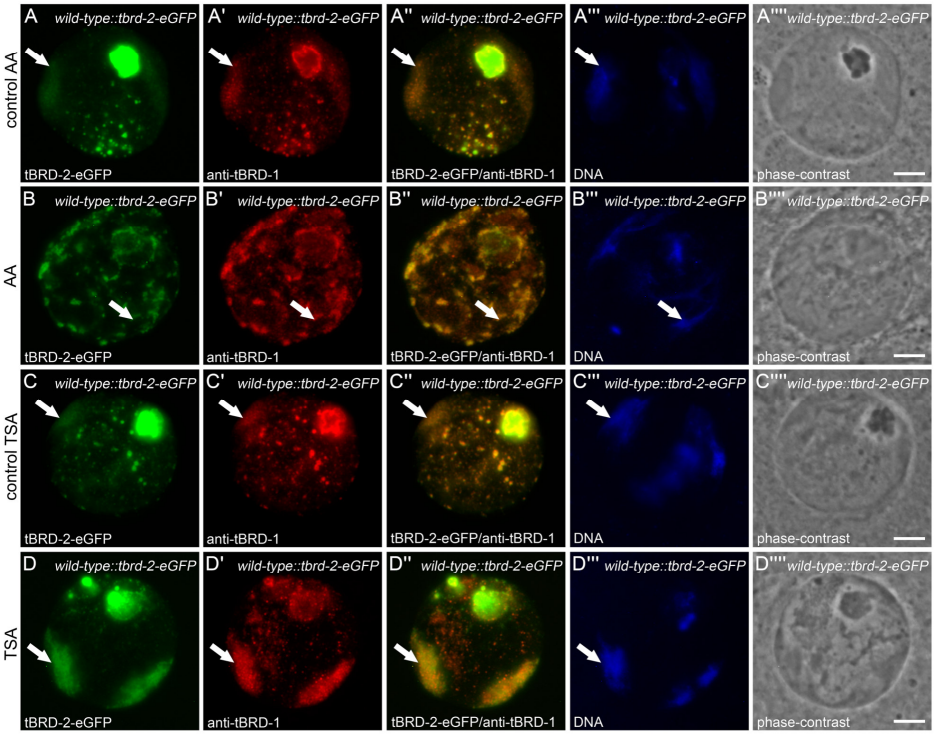

Figure 6. Acetylation levels in primary spermatocytes influences tBRD-2-eGFP localization. Pupal testis of tBRD-2-eGFP expressing flies were treated with anacardic acid (AA) (B panels) or TSA (D panels) for 24 hours in culture and afterwards spermatoyctes were stained with an antibody against tBRD-1. (A and C panels) Untreated control. (B) Incubation of testis with AA led to a spotted pattern of tBRD-2-eGFP at chromosome territories (arrow) compared to the control (A). (D) TSA treatment led to increased localization of tBRD-2-eGFP to the chromosomes (arrow) compared to the control (C). (B″,D″) Partial co-localization of tBRD-2-eGFP and tBRD-1 was not affected by AA or TSA treatment. (A‴,B‴,C‴,D‴) Hoechst DNA staining. (A⁗,B⁗,C⁗,D⁗) Phase-contrast images. Scale bars: 5 μm.
doi:10.1371/journal.pone.0108267.g006

Interestingly, an increase or decrease in acetylation had no effect on the overall co-localization of tBRD-1 and tBRD-2-eGFP (Figure 6B″,D″). This indicates that tBRD-1 and tBRD-2 interact in primary spermatocytes independently from the acetylation level.

Immunofluorescence staining using an anti-tBRD-3 antibody after TSA treatment of pupal testes from *tbrd-1-eGFP* transgenic flies led to similar results (Figure S6); tBRD-3 localization to the chromosomes increased (Figure S6D′, arrow) and co-localization with tBRD-1-eGFP was still visible (Figure S6D″). However, after AA treatment co-localization between tBRD-3 and tBRD-1 was no longer detectable (Figure S6B″). This implies that co-localization of tBRD-1 and tBRD-3 is acetylation dependent. These data indicate that proper recruitment of tBRD-1, tBRD-2 and tBRD-3 to chromatin depends on defined acetylation levels in primary spermatocytes.

tBRD-1 can interact with tBRD-2, tBRD-3 and tTAFs

The data above point to an interdependency of several tBRDs and tTAFs. Hence, we reasoned that they might interact with each other at the protein level. To analyze whether tBRD-1, tBRD-2, tBRD-3 and the five tTAFs can form homodimers or heterodimers among each other, we performed yeast two-hybrid analyses. Every coding region was inserted into both the pGBKT7 expression vector (expresses a fusion protein of the GAL4 DNA-binding domain (DBD) and a bait protein) and the pGADT7 expression vector (expresses a fusion protein of the GAL4 activation domain (AD) and a prey protein). This enabled us to test each protein acting either as bait or prey. When bait and the prey fusion proteins interact, the DBD and AD are brought into close proximity and subsequently activate reporter genes, e.g. *lacZ*, leading to colony growth and blue color. Some proteins also possess intrinsic DNA-binding and/or transcriptional activating properties (self-activity). Therefore, each DBD-bait and AD-prey fusion protein was also tested in combination with an empty pGADT7 or pGBKT7 expression vector (Figure 7C–F,J,K and Figure S7).

Additionally, a positive (DBD-53+AD-T) and a negative (DBD-Lam+AD-T) control was included on each plate (Figure 7 and Figure S7). DBD-53 encodes a fusion protein between the DBD and murine p53, AD-T encodes a fusion protein between the AD

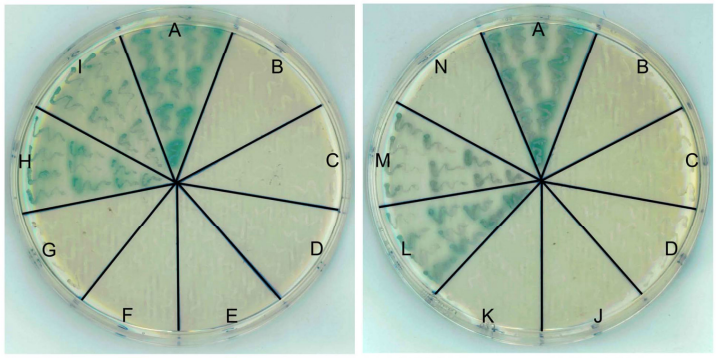

A: AD-T	+ DBD-53	H: AD-tBRD-1	+ DBD-tBRD-2
B: AD-T	+ DBD-Lam	I: AD-tBRD-2	+ DBD-tBRD-1
C: AD-tBRD-1	+ DBD	J: AD-Sa	+ DBD
D: AD	+ DBD-tBRD-1	K: AD	+ DBD-Sa
E: AD-tBRD-2	+ DBD	L: AD-tBRD-1	+ DBD-tBRD-1
F: AD	+ DBD-tBRD-2	M: AD-tBRD-1	+ DBD-Sa
G: AD-tBRD-2	+ DBD-tBRD-2	N: AD-Sa	+ DBD-tBRD-1

Figure 7. tBRD-1 interacts with tBRD-2 and the tTAF Sa in yeast two-hybrid experiments. (A) Positive control (DBD-53+AD-T). (B) Negative control (DBD-Lam+AD-T). (C–F, J,K) tBRD-1, tBRD-2 and Sa fusion proteins showed no self-activity. (G) No homodimerization of tBRD-2 was detectable. (H,I) tBRD-1 and tBRD-2 heterodimer formation was visible. (L) tBRD-1 was able to homodimerize. (M,N) tBRD-1 and Sa could only interact when Sa was acting as the bait.
doi:10.1371/journal.pone.0108267.g007

and the SV40 large T-antigen, and DBD-Lam encodes a fusion protein between the DBD and human lamin C. SV40 large T-antigen is known to interact in yeast two-hybrid assays with murine p53 [33,34] but not with Lamin C [35,36]. With the exception of DBD-Can (Figure S7E) no self-activity was observed (Figure 7C F,J,K and Table S1 and Figure S7).

tBRD-1 was able to form homodimers (Figure 7L and Table S2) as well as heterodimers with tBRD-2 (Figure 7H,I and Table S2), tBRD-3 (Figure S7A and Table S2), Sa (Figure 7M and Table S3), Rye (Figure S7D and Table S3) and Can (Figure S7E,G and Table S3). Although we observed self-activity potential for DBD-Can the growth of blue colonies was much lower for DBD-Can in combination with AD than with AD-tBRD-1 (Figure S7E). In addition, heterodimer formation was detectable between tBRD-2 and tBRD-3 as well as between tBRD-3 and Sa (Figure S7B,F and Table S2, S3) and both could interact with the tTAF Rye (Figure S7H and Table S3).

Among the tTAFs homodimerization was only demonstrated for Rye (Figure S7K,L and Table S4). An interaction between Rye and Nht has already been reported [9] and served here as an additional control (Figure S7N and Table S4). An interaction between other tTAFs was not observed (Figure S7 and Table S4). We never observed interactions with Mia fusion proteins. However, some fusion proteins are not stably expressed in yeast. Therefore, we do not know if Mia does not interact with tBRDs and/or other tTAFs or if Mia fusion proteins are not stably expressed.

To examine whether homo- and heterodimerization occur within the testis, we performed co-immunoprecipitations (Co-IPs) with testes protein extracts from *tbrd-1-eGFP* and *tbrd-2-eGFP* transgenic flies using the GFP-Trap A Kit. Subsequent immunoblotting revealed that tBRD-1 co-immunoprecipitated with tBRD-1-eGFP and tBRD-2-eGFP (Figure 8). Based on our co-localization studies, inhibitor experiments and protein interaction analyses we hypothesized that a complex comprising tBRD-1, tBRD-2, tBRD-3 and tTAFs exists that controls gene activity in primary spermatocytes (see Figure 9).

Discussion

Within the testis more than 50% of the *Drosophila* protein coding genes become activated and most of them are transcribed in primary spermatocytes. However, as yet we are far from understanding how gene activation, in particular synthesis of translationally repressed mRNAs, is achieved in male germ cells. Another question is how tTAFs might be connected to chromatin modifications, in particular to acetylated histones recognized by bromodomains. Here, we address the questions of whether tBRD-1 is the only relevant bromodomain protein, whether bromodomain proteins physically interact with tTAFs, whether the recruitment of bromodomain proteins depends on tTAFs and the acetylation status of histones, how many genes depend on the function of tBRD-1 and finally whether common tBRD-1 and tTAF target genes exist.

tBRD-1, tBRD-2 and tBRD-3 localize to chromatin in primary spermatocytes

Here, we identified two new bromodomain-containing proteins in *Drosophila*. In contrast to tBRD-1, tBRD-2 and tBRD-3 each contain only one bromodomain. However, both exhibit a NET domain a characteristic feature of BET protein family members. We described here for the first time BET proteins in animals that contain only one bromodomain. In primary spermatocytes, both tBRD-2 and tBRD-3 were predominantly expressed in the testis and largely co-localized with tBRD-1 over the chromosomal regions in an acetylation dependent manner. Therefore, we

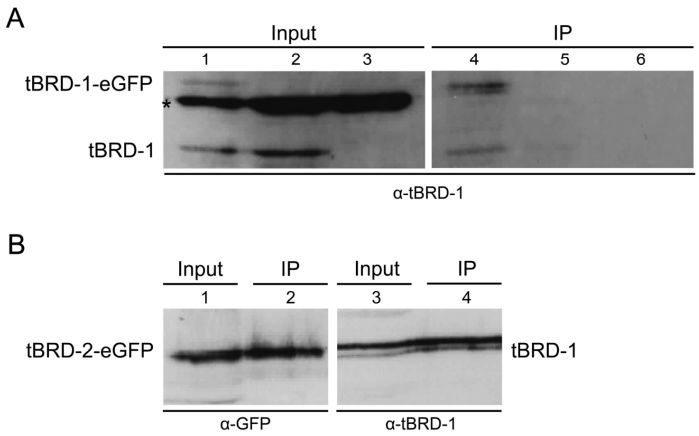

Figure 8. tBRD-1 co-precipitates with tBRD-1-eGFP and tBRD-2-eGFP from testes protein extracts. (A) Proteins were analyzed by SDS-PAGE and immunoblotting using anti-tBRD-1 antibody. Lanes 1–3: testes extracts before immunoprecipitation (Input). The anti-tBRD-1 antibody detected a protein at about 56 kDa (tBRD-1 predicted molecular mass: 59.2 kDa) in protein extracts of *tbrd-1-eGFP* (lane 1) and wild-type (lane 2), but not in *tbrd-1* mutant testis (lane 3). Additionally, a protein at about 90 kDa was detected in protein extracts of *tbrd-1-eGFP* testes (lane 1) that represents the tBRD-1-eGFP fusion protein. An unspecific protein at about 76 kDa was visible in all three extracts (asterisk). Lanes 4–6: eGFP-tagged tBRD-1 was immunoprecipitated (IP) with the GFP-Trap A Kit from testes protein extracts of *tbrd-1-eGFP* transgenic flies (lane 4), wild-type flies (lane 5) or *tbrd-1* mutants (lane 6). tBRD-1 was detected in the IP from *tbrd-1-eGFP* testes (lane 4) but not from wild-type (lane 5) or *tbrd-1* mutant testis. (B) Input and immunoprecipitates (IP performed as in A) from testes protein extracts of *tbrd-2-eGFP* transgenic flies were analyzed by SDS-PAGE and immunoblotting using anti-GFP and anti-tBRD-1 antibodies. tBRD-2-eGFP and tBRD-1 were detected in both immunoprecipitates (lanes 2 and 4).
doi:10.1371/journal.pone.0108267.g008

hypothesize that in primary spermatocytes, tBRD-2 and tBRD-3 can act together with tBRD-1 and tTAFs to activate transcription of a subset of spermatogenesis-relevant genes (Figure 9).

tBRD-1 interact with tBRD-2, tBRD-3 and with tTAFs

Our protein-protein interaction studies indicated that the tTAF Sa, which binds to DNA [11], interacts with tBRD-1. Additionally, we found that tBRD-1 interacts with itself, the tTAFs Rye and Can as well as with tBRD-2 and tBRD-3. We observed that the tTAF Rye can exist as homodimer and is able to form heterodimers with Nht (the Rye and Nht interaction was already shown in [9]) and all three bromodomain proteins. Additionally, interaction of the tTAF Sa with tBRDs was indicated by immunohistology. The overall distribution of tBRDs was altered in *sa* mutant testes. However, despite the altered distribution, co-localization of tBRDs was still detectable. Hence, we propose that Sa function is required for proper subcellular localization of tBRDs, but not essential for their co-localization and principal recruitment of tBRDs to chromatin.

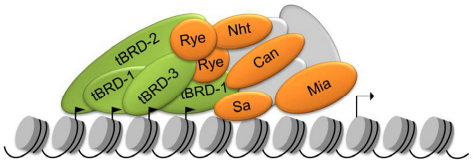

Figure 9. Model for tBRD-1, tBRD-2, tBRD-3 and tTAF function in primary spermatocytes. Scheme of a complex of tBRDs (green), tTAFs (orange) and so far unknown proteins (grey) that may activate transcription of a specific set of genes in primary spermatocytes. In our model tBRDs recognize and bind to acetylated histones (little black flags). This binding could in turn lead to the recruitment of tTAFs and additional transcription factors and subsequently gene activation.
doi:10.1371/journal.pone.0108267.g009

We propose the existence of a transcriptional activating complex that includes all three tBRDs and the TAFs Sa, Can, Rye, Nht and Mia. Additionally, we suggest that the tBRDs, by binding to acetylated chromatin, might act as a scaffold to bundle these proteins for transcriptional activation (Figure 9). However, in the case of Mia we could not observe an interaction with tBRDs or other tTAFs, possibly due to lack of stable Mia fusion proteins in yeast.

tBRD-1 regulates hundreds of genes

Our microarray analyses showed that tBRD-1 is indeed directly or indirectly involved in gene activation within the testis. In contrast to tTAF mutants, *tbrd-1* mutant testes clearly have post-meiotic cells with elongated flagella [19]. Correspondingly, 66.2% of the tBRD-1 dependent transcripts are enriched in spermatids. Since tBRD-1 expression is restricted to spermatocytes these transcripts likely reflect translationally repressed mRNAs that accumulate in post-meiotic stages, although they are synthesized in primary spermatocytes. This strengthens our hypothesis that in primary spermatocytes, tBRD-1 regulates a subset of the putative 1500–2000 tTAF target genes.

In tTAF mutant testes, genes are affected on a massive scale and several reasons argue against a direct comparison between *tbrd-1* and tTAF mutant testes. tTAF mutant testes are smaller in size and show a meiotic arrest phenotype. Hence, tTAF mutant testes accumulate primary spermatocytes and lack post-meiotic cells [37,12]. In contrast, *tbrd-1* mutant testes clearly have post-meiotic cells with elongated flagella [19]. The transcriptomes of *tbrd-1*

mutant and tTAF mutant testes are likely not directly comparable. Nevertheless, we showed that tBRD-1 and Sa share a common subset of target genes. Among these genes, 144 were significantly down-regulated in *tbrd-1* and *sa* mutant testes. These genes represent a promising starting point for future studies on gene activation in the testis.

Bromodomain proteins and TAF variants in mammalian spermatogenesis

Developmental differentiation processes based on stored mRNAs or mRNAs synthesized by tissue-specific isoforms of general transcription factors is not a unique feature of *Drosophila* spermatogenesis. Also in mammals, spermiogenesis is programmed by repressed and stored mRNAs. TAF4b, a paralog of TAF4, is highly expressed in mouse testes as well as in ovaries, and is required for male and female fertility [38,39,40]. Initially, TAF4b was discovered in a human B-cell line as the first cell-type-specific TFIID subunit [41]. The testis-linked paralog of TAF7, TAF7L, can interact with TBP and other TAFs, and is thought to be part of an alternative TFIID-like complex [42].

Recently, it has been suggested that TAF7L directly cooperates with TBP-related factor 2 (TRF2) to activate a subset of spermiogenesis-relevant genes [43]. The bromodomain protein BRDT (bromodomain testis-specific) is highly enriched in mice testes and essential for male germ cell differentiation and fertility [44,45]. BRDT specifically binds hyperacetylated histone H4 and exhibits acetylation-dependent chromatin remodeling activity [46]. BRDT can interact with Smarce1, a member of the SWI/SNF family and hyperacetylation of histones increases this interaction [47]. In mice testes, the bromodomain protein BRDT is involved in transcription of a large number of genes [48,49]. Additionally, the other members of the BET family, BRD2, BRD3 and BRD4, are expressed in mammalian male germ cells [50]. However, it is yet not known whether these BRD proteins interact among each other or with tissue-specifically expressed TAFs.

Our data provide important information and new insights into gene activation in male germ cells that may be relevant to other organisms. We believe that a complex of tBRDs, tTAFs and so far unknown proteins exists that activates transcription of a specific set of genes in primary spermatocytes (Figure 9). In our model tBRDs recognize and bind to acetylated histones, leading to recruitment of tTAFs and additional transcription factors to mediate gene activation.

Many tBRD-1 and Sa target genes overlapped; however, we observed many tBRD-1 targets that do not depend on Sa function and *vice versa*. Therefore, complexes containing either tBRD-1, or tBRD-2 or tBRD-3 in combination with different tTAFs are conceivable. Likewise, complexes containing tBRD-1 and tBRD-2 or tBRD-1 and tBRD-3 or tBRD-2 and tBRD-3 in combination with different tTAFs are possible. These different complexes could further subdivide the many thousands of genes and thus each might activate a certain set of spermatogenesis-relevant genes.

Materials and Methods

Fly strains and culture

Drosophila melanogaster strains were maintained on standard medium at 25°C. w^{1118} was used as the wild-type strain. The *tbrd-1* mutant allele, and tBRD-1-eGFP expressing flies were described previously [19]. sa^2 mutants [8] were kindly provided by M.T. Fuller (Palo Alto).

RT-PCR

Total RNA was prepared using TRIzol (Invitrogen) from 80 testes, 40 carcass of males, 40 adult females, and 40 third instar larvae. The OneStep RT-PCR Kit (Qiagen) was used to amplify a 319 bp cDNA fragment from the open reading frame of *tbrd-2*. The chosen primers (*tbrd-2-fw GTCGAACGGCAAAAGTGTTC* and *tbrd-2-rv GGCTCCAAGAAGTCCAAGG*) flank an intron of 54 bp to distinguish between RNA and DNA. To amplify a 462 bp cDNA fragment from the intronless *tbrd-3* polyA$^+$-mRNA was prepared from total RNA using Oligotex mRNA Mini Kit (Qiagen). For RT-PCR the following primers were used: *tbrd-3-fw TGGGTTTTCTACGAGCCACT* and *tbrd-3-rv CTGCTCCGAAGTTTCCAAAG*. Primers for the ubiquitously transcribed *β3-tubulin* gene (*b3-tubulin-fw ATCATTTCCGAG-GAGCACGGC* and *b3-tubulin-rv GCCCAGCGAGTGCGT-CAATTG*) were used as controls. These primers amplify a 372 bp fragment on RNA and a 490 bp fragment on DNA.

Cloning the *tbrd-2-eGFP* construct

To generate a *tbrd-2-eGFP* construct, the open reading frame (ORF) of the *tbrd-2* gene together with a 591 bp sequence upstream of the ATG translational start was PCR amplified using genomic DNA and primers with linked *EcoRI* and *SpeI* restriction sites. The PCR fragment was inserted into *pChabΔsalΔlacZ-eGFP* in frame with the *eGFP*. Transgenic fly strains were established in a wild-type background.

RNA purification and microarray analysis

Total RNA was extracted from wild-type testes and homozygous *tbrd-1* mutant testis using TRIzol (Invitrogen). RNA quality was monitored using the Agilent Bioanalyser 2100 with the RNA 6000 Nano kit. Gene expression analysis was carried out using Affymetrix *Drosophila* Genome 2.0 arrays according to the manufacturer's recommendations. For each array, independent RNA from whole testes pooled from 25 animals was used.

Data deposition

The microarray data from this publication was deposited at NCBI's gene expression omnibus (GEO) under the accession number GSE52511.

Quantitative real-time PCR

Total RNA from 100 wild-type testes, homozygous *tbrd-1* mutant testes and *tbrd-1* mutant testes that express a tBRD-1-eGFP rescue protein was isolated using TRIzol (Invitrogen). RNA was treated with DNase (Promega) according to the manufacturer's protocol. 1 µg of RNA was reverse transcribed using Transcriptor First Strand cDNA Synthesis Kit (Roche). qPCR was performed with a Sybrgreen platform on a Bio-Rad CFX Cycler. Values were normalized to the expression of *Rpl32* as an internal control. For primer sequences see Table S5.

Yeast two-hybrid assay

For yeast two-hybrid experiments the Matchmaker GAL4 Two-Hybrid System 3 from Clontech was used. To generate yeast constructs the ORFs were PCR amplified using specific primers with linked restriction sites (Table S6). To amplify *tbrd-1*, *tbrd-3* and *nht* genomic DNA was used. To exclude introns, cDNA was used to amplify *tbrd-2*, *sa*, *can*, *mia* and *rye*. cDNA was synthesized using innuScript Reverse Transcriptase (analytik jena) or iScript cDNA Synthesis Kit (BIO-RAD). The PCR fragments were inserted into pCRII-TOPO Vector (Invitrogen). Subsequently, the ORFs were ligated in frame into *pGBKT7* (*bait*

vector) and *pGADT7* (*prey* vector) that were opened with the appropriate restriction enzymes. Yeast two-hybrid experiments were performed according to the manufacturer's manual.

Co-immunoprecipitation

Co-IPs were carried out using the GFP-Trap A Kit (Chromo-Tek). Protein extracts were made from 200 adult testes (in case of *tbrd-1-eGFP*, *wild-type* and *tbrd-1* mutants) or 400 adult testes (in case of *tbrd-2-eGFP*). Testes were homogenized in 200 µl lysis buffer (supplied with the GFP-Trap A Kit) that include 2 µl 100× protease inhibitor (Thermo Scientific). Protein extracts were recovered following the manufacturer's advice. After adding 500 µl dilution buffer 4% (*tbrd-1-eGFP* and *wild-type*) or 8% (*tbrd-2-eGFP*) of the extract was retained as the input control. The remaining extract was incubated with 30 µl of GFP trap-A beads for 2.5 h at 4°C. Beads were washed twice and bound proteins were eluted by boiling in 100 µl SDS sample buffer for 10 min at 95°C. The whole supernatant was applied to a 10% SDS-gel. Western blots were performed using standard methods. Anti-tBRD-1 [19] was used at 1:1000 in 5% dry milk in TBST. Anti-GFP (polyclonal rabbit antiserum was raised against full length GFP; unpublished; kindly provided by Joerg Leers) was used at a 1:2000 dilution in 5% dry milk in TBST. POD-conjugated anti-rabbit antibody was subsequently applied at 1:5000 (Jackson Immunology). Novex ECL Chemiluminescent Substrate Reagent Kit (Invitrogen) was used according to the manufacturer's recommendation.

Immunofluorescence staining

Hoechst staining was used to visualize chromatin. All antibodies were used in immunofluorescence stainings of squashed testis carried out essentially as described before [51] and [52,53]. We raised a peptide antibody (aa 175 to aa 189) against tBRD-3 in rabbit. The peptide sequence showed no sequence homology to tBRD-1 or tBRD-2. The affinity-purified antibody was applied in a dilution 1:1000 (Pineda-Antibody-Service; http://www.pineda-abservice.de). Anti-tBRD-1 was used in a dilution 1:5000 [19]. For peptide-blocking experiments the anti-tBRD-3 and anti-tBRD-1 antibodies were incubated with different concentrations of the tBRD-3 peptide (2–20 µg/ml) before carrying out the immunofluorescence stainings. To analyze the acetylation level after inhibitor treatment an anti-histone H4 acetyl-antibody (Millipore 06-598; 1:200) was used. Cy3-conjugated anti-rabbit (Dianova; 1:100) and Cy5-conjugated anti-rabbit (Dianova; 1:100) were used as secondary antibodies. Immunofluorescence, eGFP and Hoechst signals were examined using a Zeiss microscope (AxioPlan2) equipped with appropriate fluorescence filters. Images were individually recorded and processed with Adobe Photoshop 7.0.

Culture of pupal testis and inhibitor treatment

Pupal testis were dissected, cultured and treated with inhibitors as previously described [31], [19] and [32].

Supporting Information

Figure S1 tBRD-1 is required for gene repression in the testis. (A) Gene expression was measured in wild-type and *tbrd-1*^{1} mutant testis by Affymetrix microarrays in 5 replicates. Differentially expressed genes were identified after normalization RMA [54] using limma [55]. Of the genes with a p-value ≤0.05 (after Benjamini-Hochberg correction [56]) and an absolute log2-fold change ≥1, 419 genes were down-regulated and 223 were up-regulated. (B) Quantitative real-time PCR (qPCR) using cDNA of wild-type, *tbrd-1*^{1} and *tbrd-1-eGFP*; *tbrd-1*^{1} testes. Transcript levels of *CG31750*, *cutlet*, *twdlV* and *CG1441* were enriched in *tbrd-1* mutant testes compared to wild-type and *tbrd-1-eGFP*; *tbrd-1*^{1} testes. P-values for significance: ** p≤0.01 and *** p≤0.001.
(TIF)

Figure S2 tBRD-2 and tBRD-3 are predominantly transcribed in the testis. (A) The *tbrd-2*-specific primers amplified a 319 bp cDNA fragment from the open reading frame of *tbrd-2* in testes (t) but not in carcass males (c) or in adult females (f). Additionally, in testes (t), in carcass males (c) and in adult females (f) a 373 bp fragment due to DNA contamination was amplified. (B) The *tbrd-3*-specific primers amplified a 462 bp cDNA fragment from the open reading frame of *tbrd-3* in testes (t) and in larvae (l). (A′,B′) A 372 bp cDNA fragment of the *β3-tubulin* gene amplified as a control was visible in all samples. Total RNA was used in A and A′, polyA^{+}-mRNA was used in B and B′. +RT: with reverse transcriptase. −RT: without reverse transcriptase.
(TIF)

Figure S3 The tBRD-3 peptide specifically blocks the anti-tBRD-3 antibody. Single primary spermatocytes from wild-type testis stained with anti-tBRD-3 antibody (A), peptide-neutralized anti-tBRD-3 antibody (B), anti-tBRD-1 antibody (C) or anti-tBRD-1 antibody pre-incubated with the tBRD-3 peptide (D). tBRD-3 was no longer detectable with peptide-neutralized anti-tBRD-3 antibody (B) whereas blocking the tBRD-1 antibody with the tBRD-3 peptide did not affect the detection of tBRD-1 (D). (A′,B′,C′,D′) Hoechst DNA staining. (A″,B″,C″,D″) Phase-contrast images. Scale bars: 5 µm.
(TIF)

Figure S4 Recruitment of tBRD-2 to the chromosomes is independent of the tTAF Sa. Single primary spermatocytes from heterozygous (A panels) and homozygous *sa*^{2} (B panels) mutants that express tBRD-2-eGFP stained with anti-tBRD-1 antibody. (A″,B″) In both heterozygous and homozygous *sa*^{2} mutant spermatocytes tBRD-2-eGFP partially co-localized with tBRD-1 over the chromosomes (arrows). (A‴,B‴) Hoechst DNA staining. (A⁗,B⁗) Phase-contrast images. Scale bars: 5 µm.
(TIF)

Figure S5 Localization of tBRD-1-eGFP and tBRD-2-eGFP is acetylation dependant. Pupal testis of tBRD-1-eGFP (A-C″) or tBRD-2-eGFP (D–F″) expressing flies were treated with TSA or anacardic acid (AA) for 24 hours in culture and afterwards spermatoyctes were stained with an antibody against acetylated histone H4 (H4ac) (A′,B′,C′,D′,E′,F′). (A and D panels) Untreated control. (A,B,C,D,E,F) Hoechst DNA staining. (B and E panels) Incubation of testis with TSA led to increased histone H4 acetylation (B′,E′) and increased localization of tBRD-1-eGFP (B″) and tBRD-2-eGFP (E″) to the chromosomes (arrowheads) in comparison to the control (A″,D″). (C and F panels) Incubation of testis with AA led to a decrease in histone H4 acetylation (C′,F′) and altered localization of tBRD-1-eGFP (C″) and tBRD-2-eGFP (F″) to the chromosome territories (arrowheads). Scale bars: 20 µm in A–C″, 5 µm in D–F″.
(TIF)

Figure S6 Co-localization of tBRD-1-eGFP and tBRD-3 is acetylation dependant. Pupal testis of tBRD-1-eGFP expressing flies were treated with anacardic acid (AA) (B panels) or TSA (D panels) for 24 hours in culture and afterwards spermatoyctes were stained with an antibody against tBRD-3. (A and C panels) Untreated control. (B′,B″) Incubation of testis with AA led to a loss of tBRD-3 localization to the chromosome

territories and co-localization between tBRD-3 and tBRD-1-eGFP was no longer detectable (arrows). (D′) TSA treatment led to increased localization of tBRD-3 to the chromosomes (arrow) in comparison to the control (C′). (D″) Partial co-localization of tBRD-1-eGFP and tBRD-3 was not affected by TSA treatment. (A′″, B′″, C ′″,D′″) Hoechst DNA staining. (A″″,B″″,C″″,D″″) Phase-contrast images. Scale bars: 5 μm.
(TIF)

Figure S7 Overview of yeast two-hybrid experiments. Positive (DBD-53+AD-T) and negative (DBD-Lam+AD-T) controls are shown on each plate. (A) Interaction of tBRD-1 and tBRD-3. tBRD-1 and tBRD-3 fusion proteins showed no self-activity. No homodimerization of tBRD-3 was detectable. (B) Interaction of tBRD-2 and tBRD-3. tBRD-2 and tBRD-3 fusion proteins showed no self-activity. (C) Interaction of tBRD-1 and tBRD-2. tBRD-2 was not able to interact with itself, tBRD-3 or Sa. tBRD-3 showed no interaction with Sa. (D) Interaction of tBRD-1 and Rye. tBRD-1 and Rye fusion proteins showed no self-activity. (E) Interaction of tBRD-1 and Can when Can is acting as the bait. Both tBRD-1 fusion proteins and AD-Can showed no self-activity. Weak self-activity was detectable for DBD-Can. Nevertheless, a clear difference between the self-activity of DBD-Can compared to DBD-Can+AD-tBRD-1 was visible. (F) tBRD-3 and Sa could interact when tBRD-3 acts as the bait. tBRD-3 and Sa fusion proteins showed no self-activity. (G) Interaction of tBRD-1 and Can when Can acts as the bait. Can was not able to interact with tBRD-2 or tBRD-3. A few blue colonies were detectable for DBD-Can+AD-tBRD-2 and DBD-Can+AD-tBRD-3 and resulted from the self-activity of DBD-Can (shown on plate E). (H) Interaction of Rye with tBRD-1, tBRD-2 and tBRD-3. Rye was not able to interact with Sa. (I) Nht showed no interaction with tBRD-1, tBRD-2 or tBRD-3. (J) Mia showed no interaction with tBRD-1, tBRD-2 or tBRD-3. However, a control that shows expression of Mia fusion proteins in yeast is missing. (K) Homodimerization of Rye. Mia, Sa and Nht were not able to form homodimers. Blue colonies were detectable for DBD-Can+AD-Can that might result from the self-activity of DBD-Can. (L) Homodimerization of Rye. Mia, Sa and Nht were not able to form homodimers. Sa and Nht showed no interaction. (M) Mia showed no interaction with Sa, Rye or Nht. Mia fusion proteins showed no self-activity. As above, a control that shows expression of Mia fusion proteins in yeast is missing. (N) Interaction of Rye and Nht. Rye and Nht fusion proteins showed no self-activity. (O) Can was not able to interact with Sa, Nht or Rye. A few blue colonies were detectable that might result from the self-activity of DBD-Can (shown on plate E and P). (P) Weak self-activity was detectable for DBD-Can but not for AD-Can. Can was not able to interact with Rye or Mia. A few blue colonies were detectable that might result from the self-activity of DBD-Can.
(TIF)

Table S1 Summary of self-activity tests of the different plasmids used for yeast two-hybrid experiments.
(PDF)

Table S2 Summary of yeast two-hybrid experiments for the three bromodomain proteins tBRD-1, tBRD-2 and tBRD-3.
(PDF)

Table S3 Summary of yeast two-hybrid experiments for tBRD-1, tBRD-2, tBRD-3 and tTAFs.
(PDF)

Table S4 Summary of yeast two-hybrid experiments for the five tTAFs.
(PDF)

Table S5 Primers used for qPCRs.
(PDF)

Table S6 Oligonucleotids used for yeast constructs.
(PDF)

Dataset S1 (XLSX)

Acknowledgments

We thank Rainer Renkawitz for helpful discussions and support, Margaret Fuller for fly strains, Joerg Leers for the anti-GFP antibody, Ruth Hyland, Corinna Kilger and Christiane Rohrbach for excellent technical assistance and Katja Gessner for graphical design and competent secretarial assistance.

Author Contributions

Conceived and designed the experiments: IT CR. Performed the experiments: IT MB TH TB SMKG KL SA MS CR. Analyzed the data: IT MB CR. Contributed reagents/materials/analysis tools: MB TB RR CR. Wrote the paper: CR.

References

1. White-Cooper H (2010) Molecular mechanisms of gene regulation during Drosophila spermatogenesis. Reproduction 139: 11–21.
2. White-Cooper H, Davidson I (2011) Unique aspects of transcription regulation in male germ cells. Cold Spring Harb Perspect Biol 3.
3. Rathke C, Baarends WM, Awe S, Renkawitz-Pohl R (2014) Chromatin dynamics during spermiogenesis. Biochim Biophys Acta 1839:155–168.
4. Jayaramaiah Raja S, Renkawitz-Pohl R (2005) Replacement by Drosophila melanogaster protamines and Mst77F of histones during chromatin condensation in late spermatids and role of sesame in the removal of these proteins from the male pronucleus. Mol Cell Biol 25: 6165–6177.
5. Barckmann B, Chen X, Kaiser S, Jayaramaiah-Raja S, Rathke C, et al. (2013) Three levels of regulation lead to protamine and Mst77F expression in Drosophila. Dev Biol 377: 33–45.
6. White-Cooper H, Schäfer M, Alphey L, Fuller M (1998) Transcriptional and post-transcriptional control mechanisms coordinate the onset of spermatid differentiation with meiosis I in Drosophila. Development 125: 125–134.
7. Beall EL, Lewis PW, Bell M, Rocha M, Jones DL, et al. (2007) Discovery of tMAC: a Drosophila testis-specific meiotic arrest complex paralogous to Myb-Muv B. Genes Dev 21: 904–919.
8. Hiller MA, Lin TY, Wood C, Fuller MT (2001) Developmental regulation of transcription by a tissue-specific TAF homolog. Genes Dev 15: 1021–1030.
9. Hiller M, Chen X, Pringle M, Suchorolski M, Sancak Y, et al. (2004) Testis-specific TAF homologs collaborate to control a tissue-specific transcription program. Development 131: 5297–5308.
10. Metcalf C, Wassarman D (2007) Nucleolar colocalization of TAF1 and testis-specific TAFs during Drosophila spermatogenesis. Dev Dyn 236: 2836–2843.
11. Chen X, Hiller M, Sancak Y, Fuller M (2005) Tissue-specific TAFs counteract Polycomb to turn on terminal differentiation. Science 310: 869–872.
12. El-Sharnouby S, Redhouse J, White RA (2013) Genome-wide and cell-specific epigenetic analysis challenges the role of polycomb in Drosophila spermatogenesis. PLoS Genet 9: e1003842.
13. Marushige K (1976) Activation of chromatin by acetylation of histone side chains. Proc Natl Acad Sci U S A 73: 3937–3941.
14. Dhalluin C, Carlson JE, Zeng L, He C, Aggarwal AK, et al. (1999) Structure and ligand of a histone acetyltransferase bromodomain. Nature 399: 491–496.
15. Jacobson RH, Ladurner AG, King DS, Tjian R (2000) Structure and function of a human TAFII250 double bromodomain module. Science 288: 1422–1425.
16. Owen DJ, Ornaghi P, Yang JC, Lowe N, Evans PR, et al. (2000) The structural basis for the recognition of acetylated histone H4 by the bromodomain of histone acetyltransferase gcn5p. EMBO J 19: 6141–6149.
17. Jeanmougin F, Wurtz JM, Le Douarin B, Chambon P, Losson R (1997) The bromodomain revisited. Trends Biochem Sci 22: 151–153.
18. Barlev NA, Poltoratsky V, Owen-Hughes T, Ying C, Liu L, et al. (1998) Repression of GCN5 histone acetyltransferase activity via bromodomain-mediated binding and phosphorylation by the Ku-DNA-dependent protein kinase complex. Mol Cell Biol 18: 1349–1358.

19. Leser K, Awe S, Barckmann B, Renkawitz-Pohl R, Rathke C (2012) The bromodomain-containing protein tBRD-1 is specifically expressed in spermatocytes and is essential for male fertility. Biology Open 1:597–606.
20. Florence B, Faller DV (2001) You bet-cha: a novel family of transcriptional regulators. Front Biosci 6: D1008–1018.
21. Florence BL, Faller DV (2008) Drosophila female sterile (1) homeotic is a multifunctional transcriptional regulator that is modulated by Ras signaling. Dev Dyn 237: 554–564.
22. Peng J, Dong W, Chen L, Zou T, Qi Y, et al. (2007) Brd2 is a TBP-associated protein and recruits TBP into E2F-1 transcriptional complex in response to serum stimulation. Mol Cell Biochem 294: 45–54.
23. Rahman S, Sowa ME, Ottinger M, Smith JA, Shi Y, et al. (2011) The Brd4 extraterminal domain confers transcription activation independent of pTEFb by recruiting multiple proteins, including NSD3. Mol Cell Biol 31: 2641–2652.
24. Kockmann T, Gerstung M, Schlumpf T, Xhinzhou Z, Hess D, et al. (2013) The BET protein FSH functionally interacts with ASH1 to orchestrate global gene activity in Drosophila. Genome Biol 14: R18.
25. Robertson HM, Warr CG, Carlson JR (2003) Molecular evolution of the insect chemoreceptor gene superfamily in Drosophila melanogaster. Proc Natl Acad Sci U S A 100 Suppl 2: 14537–14542.
26. Marygold SJ, Leyland PC, Seal RL, Goodman JL, Thurmond J, et al. (2013) FlyBase: improvements to the bibliography. Nucleic Acids Res 41: D751–757.
27. Vibranovski MD, Lopes HF, Karr TL, Long M (2009) Stage-specific expression profiling of Drosophila spermatogenesis suggests that meiotic sex chromosome inactivation drives genomic relocation of testis-expressed genes. PLoS Genet 5: e1000731.
28. Lu C, Kim J, Fuller MT (2013) The polyubiquitin gene Ubi-p63E is essential for male meiotic cell cycle progression and germ cell differentiation in Drosophila. Development 140: 3522–3531.
29. Sigrist CJ, de Castro E, Cerutti L, Cuche BA, Hulo N, et al. (2013) New and continuing developments at PROSITE. Nucleic Acids Res 41: D344–347.
30. Chintapalli V, Wang J, Dow J (2007) Using FlyAtlas to identify better Drosophila melanogaster models of human disease. Nat Genet 39: 715–720.
31. Awe S, Renkawitz-Pohl R (2010) Histone H4 acetylation is essential to proceed from a histone- to a protamine-based chromatin structure in spermatid nuclei of Drosophila melanogaster. Syst Biol Reprod Med 56: 44–61.
32. Gärtner SMK, Rathke C, Renkawitz-Pohl R, Awe S (2014) *Ex vivo* Culture of *Drosophila* Pupal Testis and Single Male Germ-line Cysts: Dissection, Imaging, and Pharmacological Treatment. J Vis Exp (), e51868, doi:10.3791/51868 (2014).
33. Li B, Fields S (1993) Identification of mutations in p53 that affect its binding to SV40 large T antigen by using the yeast two-hybrid system. FASEB J 7: 957–963.
34. Iwabuchi K, Li B, Bartel P, Fields S (1993) Use of the two-hybrid system to identify the domain of p53 involved in oligomerization. Oncogene 8: 1693–1696.
35. Bartel P, Chien CT, Sternglanz R, Fields S (1993) Elimination of false positives that arise in using the two-hybrid system. Biotechniques 14: 920–924.
36. Ye Q, Worman HJ (1995) Protein-protein interactions between human nuclear lamins expressed in yeast. Exp Cell Res 219: 292–298.
37. Lin TY, Viswanathan S, Wood C, Wilson PG, Wolf N, et al. (1996) Coordinate developmental control of the meiotic cell cycle and spermatid differentiation in Drosophila males. Development 122: 1331–1341.
38. Freiman RN, Albright SR, Zheng S, Sha WC, Hammer RE, et al. (2001) Requirement of tissue-selective TBP-associated factor TAFII105 in ovarian development. Science 293: 2084–2087.
39. Falender AE, Shimada M, Lo YK, Richards JS (2005) TAF4b, a TBP associated factor, is required for oocyte development and function. Dev Biol 288: 405–419.
40. Falender AE, Freiman RN, Geles KG, Lo KC, Hwang K, et al. (2005) Maintenance of spermatogenesis requires TAF4b, a gonad-specific subunit of TFIID. Genes Dev 19: 794–803.
41. Dikstein R, Zhou S, Tjian R (1996) Human TAFII 105 is a cell type-specific TFIID subunit related to hTAFII130. Cell 87: 137–146.
42. Pointud J, Mengus G, Brancorsini S, Monaco L, Parvinen M, et al. (2003) The intracellular localisation of TAF7L, a paralogue of transcription factor TFIID subunit TAF7, is developmentally regulated during male germ-cell differentiation. J Cell Sci 116: 1847–1858.
43. Zhou H, Grubisic I, Zheng K, He Y, Wang PJ, et al. (2013) Taf7l cooperates with Trf2 to regulate spermiogenesis. Proc Natl Acad Sci U S A 110: 16886–16891.
44. Jones MH, Numata M, Shimane M (1997) Identification and characterization of BRDT: A testis-specific gene related to the bromodomain genes RING3 and Drosophila fsh. Genomics 45: 529–534.
45. Shang E, Nickerson HD, Wen D, Wang X, Wolgemuth DJ (2007) The first bromodomain of Brdt, a testis-specific member of the BET sub-family of double-bromodomain-containing proteins, is essential for male germ cell differentiation. Development 134: 3507–3515.
46. Pivot-Pajot C, Caron C, Govin J, Vion A, Rousseaux S, et al. (2003) Acetylation-dependent chromatin reorganization by BRDT, a testis-specific bromodomain-containing protein. Mol Cell Biol 23: 5354–5365.
47. Dhar S, Thota A, Rao MR (2012) Insights into role of bromodomain, testis-specific (Brdt) in acetylated histone H4-dependent chromatin remodeling in mammalian spermiogenesis. J Biol Chem 287: 6387–6405.
48. Berkovits BD, Wang L, Guarnieri P, Wolgemuth DJ (2012) The testis-specific double bromodomain-containing protein BRDT forms a complex with multiple spliceosome components and is required for mRNA splicing and 3′-UTR truncation in round spermatids. Nucleic Acids Res 40: 7162–7175.
49. Gaucher J, Boussouar F, Montellier E, Curtet S, Buchou T, et al. (2012) Bromodomain-dependent stage-specific male genome programming by Brdt. EMBO J 31: 3809–3820.
50. Shang E, Salazar G, Crowley T, Wang X, Lopez R, et al. (2004) Identification of unique, differentiation stage-specific patterns of expression of the bromodomain-containing genes Brd2, Brd3, Brd4, and Brdt in the mouse testis. Gene Expr Patterns 4: 513–519.
51. Hime G, Brill J, Fuller M (1996) Assembly of ring canals in the male germ line from structural components of the contractile ring. J Cell Sci 109 (Pt 12): 2779–2788.
52. Rathke C, Baarends WM, Jayaramaiah-Raja S, Bartkuhn M, Renkawitz R, et al. (2007) Transition from a nucleosome-based to a protamine-based chromatin configuration during spermiogenesis in Drosophila. J Cell Sci 120: 1689–1700.
53. Rathke C, Barckmann B, Burkhard S, Jayaramaiah-Raja S, Roote J, et al. (2010) Distinct functions of Mst77F and protamines in nuclear shaping and chromatin condensation during Drosophila spermiogenesis. Eur J Cell Biol 89: 326–338.
54. Irizarry RA, Hobbs B, Collin F, Beazer-Barclay YD, Antonellis KJ, et al. (2003) Exploration, normalization, and summaries of high density oligonucleotide array probe level data. Biostatistics 4: 249–264.
55. Smyth GK (2004) Linear models and empirical bayes methods for assessing differential expression in microarray experiments. Stat Appl Genet Mol Biol 3: Article3.
56. Benjamini Y, Hochberg Y (1995) Controlling the False Discovery Rate: A Practical and Powerful Approach to Multiple Testing. J R Statist Soc B 57: 289–300.

Chapter 9: *Drosophila melanogaster* tPlus3a and tPlus3b ensure full male fertility by regulating transcription of Y-chromosomal, sperm fluidity, and heat shock genes

Hundertmark, T., Kreutz, S., Merle, N., Nist, A., Lamp, B., Stiewe, T., Brehm, A., Renkawitz-Pohl, R. and Rathke, R. (under review in Plos One).

Candidate's contribution:

- Generation of CRISPR/Cas9 mutants
- Characterisation of mutants
- Fertility tests
- Preparation of RNA for RNAseq
- qPCR validation
- Generation of transgenic fly lines, *in situ* hybridisation and Yeast Two-Hybrid experiments in collaboration with M.Sc. Sabrina Kreutz (co-supervision of associated Bachelor thesis)
- Immunofluorescence stainings and Western Blot in collaboration with B.Sc. Nastasja Merle (co-supervision of associated Bachelor thesis)
- Writing of the manuscript in collaboration with Renate Renkawitz-Pohl

Drosophila melanogaster tPlus3a and tPlus3b ensure full male fertility by regulating transcription of Y-chromosomal, sperm fluidity, and heat shock genes

Tim Hundertmark[1], Sabrina Kreutz[1], Nastasja Merle[1], Andrea Nist[2], Boris Lamp[2], Thorsten Stiewe[2,3], Alexander Brehm[4], Renate Renkawitz-Pohl[1,*], Christina Rathke[1]

[1]Department of Biology, Developmental Biology, Philipps-Universität Marburg, Marburg, Germany

[2]Genomics Core Facility, Center for Tumor- and Immunobiology, Philipps-Universität Marburg, Marburg, Germany

[3]Institute of Molecular Oncology, Center for Tumor- and Immunobiology, Philipps-Universität Marburg, Marburg, Germany

[4]Institute of Molecular Biology and Tumor Research (IMT), Biomedical Research Centre (BMFZ), Philipps-Universität Marburg, Marburg, Germany

*Corresponding author:

Department of Biology, Developmental Biology, Philipps-Universität Marburg, Karl-von-Frisch Str. 8, 35043 Marburg, Germany

Email: renkawit@biologie.uni-marburg.de

Tel.: +49-6421-2823498 and +49-6421-2823474

Fax: +49-6421-2821538

Short title: tPlus3a and tPlus3b regulate transcription to ensure full male fertility of *Drosophila melanogaster*

Key words: Spermatogenesis, Plus3 domain, tBRD-1, transcriptional regulation, kl3, kl-5, Hsp67Bc, Hsp70Aa

Abstract

Spermatogenesis in *Drosophila melanogaster* is characterized by a specific transcriptional program during the spermatocyte stage. Transcription of thousands of genes is regulated by the interaction of several proteins or complexes, including a tTAF-containing TFIID variant, tMAC, Mediator, and chromatin interactors, e.g., bromodomain proteins. We addressed how distinct subsets of target genes are selected. We characterized the highly similar proteins tPlus3a and tPlus3b, which contain a Plus3 domain and are enriched in the testis, mainly in spermatocytes. In tPlus3a/tPlus3b deletion mutants generated using the CRISPR/Cas9 system, fertility was severely reduced and sperm showed defects during individualization. tPlus3a/tPlus3b heterodimerized with the bromodomain protein tBRD-1. To elucidate the role of the tPlus3a/tPlus3b proteins in transcriptional regulation, we determined the transcriptomes of *tplus3a/tplus3b* and *tbrd-1* deletion mutants using next-generation sequencing (RNAseq) and compared them to that of the wild-type. tPlus3a/tPlus3b positively or negatively regulated the expression of nearly 400 genes; tBRD1 regulated 1,500 genes. Nearly 200 genes were regulated by both tPlus3a/tPlus3b and tBRD-1. tPlus3a/tPlus3b activated the Y-chromosomal genes *kl-3* and *kl-5*, which indicates that tPlus3a/tPlus3b are required for the function of distinct classes of genes. tPlus3a/tPlus3b and tBRD-1 repress genes relevant for sperm fluid and heat shock. We hypothesize that the tPlus3a and tPlus3b proteins are required to specify the general transcriptional program in spermatocytes.

Introduction

In mammals and in *Drosophila melanogaster*, regulation of transcription during spermatogenesis is complex. The germ cell transcriptional program covers various processes, including meiosis, post-meiotic formation of flagella, nuclear shaping, and chromatin reorganization. In flies, the majority of transcripts needed in spermatogenesis are produced in the prolonged meiotic prophase of the spermatocyte stage. Therefore, most transcripts required for post-meiotic sperm development (spermiogenesis) are translationally repressed until they are needed in later stages [1-4]. About 50% of the *D. melanogaster* genome is expressed in the testis [5] and a large portion of the transcripts are testis enriched or even testis specific. The complexity of transcriptional regulation is high as sperm development occurs in different stages at different time points.

One complex that plays a pivotal role in transcriptional regulation during spermatogenesis is a germ-line-specific variant of the general transcription factor TFIID. This complex is composed of somatic TATA-binding protein (TBP)-associated factors (TAFs) and the testis-specific paralogues tTAFs [6-7]. tTAFs are recruited by the Mediator complex to chromatin, where they activate genes [8]. Mediator regulates several hundred genes, and some of its subunits are recruited to gene regions by the testis meiotic arrest complex (tMAC), which is involved in regulation of spermiogenesis-relevant genes [8-9]. Together, tTAFs, tMAC, and Mediator regulate thousands of genes [3].

It is assumed that other factors target gene expression more specifically. Bromodomain-containing proteins (tBRDs), which are synthesized specifically in the testis, heterodimerize with some of the tTAFs and partly with each other [10-11]. In general, bromodomain proteins bind to acetylated lysine residues [12], which suggests that tBRDs might serve as a platform to guide parts of the transcriptional machinery to chromatin. The well-characterized tBRD-1 and tBRD-2 proteins regulate smaller sets of target genes than tTAFs and tMAC, and both depend on tTAF function. Loss of *tbrd-1* or knock-down of *tbrd-2* lead to post-meiotic phenotypes [10-11, 13], whereas *tTAF* mutants show an earlier meiotic arrest phenotype [6]. Despite heterodimerization of tBRD-1 and tBRD-2 and a

similar phenotype of *tbrd-1*- and *tbrd-2*-deficient flies, microarray analyses suggest that both proteins are also part of different subcomplexes, as they regulate partially non-overlapping sets of target genes [11].

Another complex that is conserved in yeast, mouse, human, and fly is the RNA-polymerase-II-associated factor complex (Paf1C) [14]. Subunits of Paf1C co-purify with RNA polymerase II subunits in yeast [15] and higher eukaryotes [14, 16]. Many studies have suggested that Paf1C plays a role in transcriptional regulation and several mechanisms have been proposed how the effect on transcription might be achieved, including transcription elongation, RNA polymerase II pausing, or maintenance of co-transcriptional histone modifications [17]. Some subunits of Paf1C are conserved, namely Paf1, Cdc73, Leo1, Ctr9, and Rtf1 [14]. Rtf1 can also function outside of the Paf1C complex in humans and *D. melanogaster* [16, 18-20]. Rtf1 contains several functional domains, including a histone modification domain, a Plus3 domain, and a protein interaction domain that mediates Paf1C interaction. It has been suggested that in yeast, the histone modification domain mediates co-transcriptional histone modifications and the Plus3 domain is needed for Paf1C recruitment to chromatin [14, 21]. Strikingly, the Plus3 domain is highly conserved in yeast, human, and fly. Structural homology and *in vitro* experiments using recombinant Rtf1 indicate that the Plus3 domain binds nucleic acids, especially single-stranded DNA. This feature suggests a supportive role in transcription through stabilization of the transcription machinery during transcript elongation [22]. However, evidence for an interplay between the complexes involved in transcriptional regulation is fragmentary. In *D. melanogaster*, Rtf1 is ubiquitously transcribed [5]. In a search for proteins that might play a role in refining the transcriptional program of spermatocytes in *D. melanogaster*, we investigated proteins carrying the Plus3 domain that are mainly synthesized in the testes. Here, we characterized two such proteins, tPlus3a and tPlus3b, and show that they are essential for spermiogenesis and full male fertility.

Results

Identification of three genes specifically expressed in the male germ line that encode Plus3-domain proteins

During spermatogenesis in *D. melanogaster,* transcription mainly takes place in spermatocytes, where distinct complexes regulate thousands of genes. We aimed at identifying testes-specific regulators responsible for distinct subsets of genes. One of the known general complexes that are involved in transcriptional regulation is Paf1C [14]. A prominent subunit of Paf1C is the Plus3 domain protein Rtf1, which is conserved in *Saccharomyces cerevisiae*, *D. melanogaster,* and *Homo sapiens*, especially regarding its Plus3 domain [22]. In *D. melanogaster*, the gene is ubiquitously expressed and is highly expressed in the testis. In a search for genes of other proteins with a Plus3 domain that are specifically expressed in the *D. melanogaster* testis, we identified three genes, namely *CG12498*, *CG31702,* and *CG31703*. According to RNAseq and microarray analyses, all three genes are mostly expressed in the testis [5, 23]. The nucleotide sequences of *CG31702* and *CG31703* are approximately 99% identical. Based on their testis-specific transcription and their encoded Plus3 domain, we named the *CG31702* and *CG31703* genes *tplus3a* and *tplus3b* (testis-specifically transcribed *plus3* genes), respectively. The Plus3 domains of tPlus3a, tPlus3b, and CG12498 contain the three positively charged eponymous amino acids and many other amino acids that are crucial for domain conformation [22]. We used Clustal Omega [24] to align the amino acid sequences of Rtf1, tPlus3a, tPlus3b, and CG12498 (Fig 1A). The histone modification domain of Rtf1 is not present in the other Plus3-domain proteins. All four proteins have a conserved sequence near the C-terminus; in Rtf1, this sequence serves as a protein interaction domain. This domain is truncated in CG12498. The Plus3-domain sequence in tPlus3a and tPlus3b is slightly shorter than that in Rtf1 and CG12498.

Fig 1. tPlus3a/tPlus3b proteins are limited to the spermatocyte stage.

We unsuccessfully attempted to generate flies that synthesized CG12498-mCherry to analyze subcellular localization of CG12498 (data not shown). However, we were able to generate transgenic *tplus3b-eGFP* flies; *tplus3b-eGFP* was weakly expressed in spermatocytes (Fig S1). We therefore concentrated on the functional characterization of *tplus3a* and *tplus3b*. Because of their high sequence identity, we refer to them as *tplus3a/tplus3b*.

tplus3a/tplus3b transcripts are expressed and their proteins are synthesized in male germ cells

We used RNA *in situ* hybridization to examine the distribution of *tplus3a/tplus3b* transcripts in the testis of wild-type flies. Transcripts were detected from the spermatocyte stage onward (Fig 1B), but late stages of spermatogenesis did not show any signal (Fig 1B). Thus, *tplus3a/tplus3b* transcripts characterize the spermatocyte and early spermatid stage. A control probe containing the sense sequence did not yield any signal (Fig 1C).

We raised a peptide antibody that could detect both tPlus3a and tPlus3b. In immunofluorescence stainings of squash preparations of wild-type testes, tPlus3a/tPlus3b were detected only in the nuclei of spermatocytes. The signal was fairly homogenously distributed in the nucleus and slightly concentrated in chromosomal regions (Fig. 1D–D'') and in distinct areas between the chromosomal regions in the nucleus (Fig 1D, D''). This region between the Hoechst-positive chromosomal regions contains large lampbrush loops, which correspond to three of the Y-chromosomal fertility loci [25]. We conclude that *tplus3a/tplus3b* expression is characteristic for the highly transcriptionally active spermatocyte phase.

tPlus3a and tPlus3b are required for full male fertility

To determine whether tPlus3a and tPlus3b are essential for male fertility, we generated deletion mutants using the CRISPR/Cas9 system. We established transgenic flies carrying a construct coding for a single guide RNA able to detect both *tplus3a* and *tplus3b* and crossed these with flies expressing

Cas9 in the germ line [26]. We screened 50 independent single crossings of putative mutants via PCR and identified the deletion mutant Δ*tplus3a/tplus3b* in which large parts of the open reading frame (ORF) of both *tplus3a* and *tplus3b* were deleted. The deletions led to a fusion of *tplus3a* within its ORF to *CR31700*, an inactive pseudogene approximately 4,000 base pairs (bp) upstream of *tplus3a* [5, 23] and yielded a null allele of *tplus3a*. In addition, it was possible to PCR amplify regions flanking *tplus3b* but not its ORF, which indicated that most of the *tplus3b* ORF was deleted. Thus, this mutant likely carries loss-of-function mutations for both genes; the genes neighboring *tplus3a* and *tplus3b*, other than *CR31700,* remained intact (Fig 2A).

Fig 2. Deletion of *tplus3a* and *tplus3b* leads to severely reduced male fertility and defects during sperm individualization.

In situ hybridization detected transcripts in testis of heterozygous Δ*tplus3a/tplus3b* mutants (Fig. 2B, arrow) but not in homozygous mutants (Fig. 2C). Analogous results were obtained in anti-tPlus3a/tPlus3b immunofluorescence stainings. Anti-tPlus3a/tPlus3b proteins were detected in spermatocytes of heterozygous Δ*tplus3a/tplus3b* mutant flies (Fig 2D) but not in homozygous Δ*tplus3a/tplus3b* mutants (Fig 2E).

In western blots using protein extracts from testes and probed with anti-tPlus3a/tPlus3b, a prominent band at approximately 60 kDa was detected in the wild-type (predicted molecular mass of tPlus3a/tPlus3b ca. 50 kDa). The signal of protein extracts of heterozygous Δ*tplus3a/tplus3b* testes was lower, and no signal was detected when protein extracts of homozygous Δ*tplus3a/tplus3b* testes were probed (Fig 2F).

To exclude off-target effects arising during CRISPR/Cas9 mutagenesis, we crossed Δ*tplus3a/tplus3b/CyO* with *Df(2L)BSC151/CyO*, which is a fly line deficient in *tplus3a* and *tplus3b*. All further phenotypic analyses were carried out with *trans*-heterozygous Δ*tplus3a/tplus3b/Df(2L)BSC151* flies. These flies were mildly defective in sperm individualization

compared to wild-type flies; in wild-type flies, the nuclei of spermatids in an individual cyst with synchronously developing spermatids are arranged strictly parallel, as visualized with *protB-eGFP* transgene expression (Fig 2G). In Δ*tplus3a/tplus3b/Df(2L)BSC151* flies, many sperm bundles were arranged in parallel, but some sperm were dispersed in the testis and lost their cyst organization (Fig 2H). In wild-type testis squash preparations, many cysts appeared and the individualization complex formed normally, as visualized with TRITC-phalloidin (Fig 2I). In Δ*tplus3a/tplus3b/Df(2L)BSC151* testis squash preparations, a number of sperm bundles were disorganized (not shown). In some cases, the individualization complex formed was abnormal in that one end was thickened (Fig. 2J). The seminal vesicles of wild-type flies were already filled with sperm 1 day after hatching (Fig 2K), whereas the seminal vesicles of Δ*tplus3a/tplus3b/Df(2L)BSC151* males of the same age were empty (Fig 2L). Two days after hatching, also seminal vesicles of Δ*tplus3a/tplus3b/Df(2L)BSC151* males contained sperm and some motile flagella were detected (not shown). However, in sterility tests comparing 4-day-old wild-type, *Df(2L)BSC151/CyO*, Δ*tplus3a/tplus3b/CyO,* and Δ*tplus3a/tplus3b/Df(2L)BSC151* males, the fertility of Δ*tplus3a/tplus3b/Df(2L)BSC151* males was reduced to ca. 12% of that of the wild-type control (Fig. 2M). As 2-day-old Δ*tplus3a/tplus3b/Df(2L)BSC151* males started to have sperm in the seminal vesicles, the reduced fertility after 4 days suggests that most of the sperm found in the seminal vesicles after 2 days are not motile. Sterility tests with 8-day-old Δ*tplus3a/tplus3b/Df(2L)BSC151* males revealed that fertility is partially restored after several days (Fig. 2M). We conclude that defects in late sperm development result in delayed fertility of Δ*tplus3a/tplus3b/Df(2L)BSC151* males and that the proportion of motile sperm in Δ*tplus3a/tplus3b/Df(2L)BSC151* males increases with age.

tPlus3a/tPlus3b heterodimerize with the bromodomain protein tBRD-1

We then addressed whether tPlus3a/tPlus3b interact with other known proteins of transcription complexes in spermatocytes. We previously observed a late arrest in spermatogenesis and infertility of *tbrd-1* mutants and after *tbrd-2* knock-down in male germ cells [11, 13]. We analyzed tPlus3a/tPlus3b immunofluorescence stainings at high magnification in flies synthesizing tBRD-1-eGFP to determine whether tPlus3a/tPlus3b co-localize with tBRD-1 in nuclei of spermatocytes (Fig 3A–A'''). The tBRD-1-eGFP signal was concentrated in the chromosomal regions (Fig 3A') and overlapped with the tPlus3a/tPlus3b staining in this region (Fig 3A, A'''). The tBRD-1-eGFP signal also concentrated in speckles widely distributed in the nucleus (Fig 3A'), but these areas did not overlap significantly with the prominent tPlus3a/tPlus3b staining between the chromosomal regions (Fig 3A, A''').

Fig 3. tPlus3a/tPlus3b partially co-localize with tBRD-1 and interacts with tBRD-1 but not with tBRD-2 in yeast two-hybrid experiments.

The partial co-localization of tPlus3a/tPlus3b and tBRD-1 in the chromosomal regions prompted us to test whether tBRD-1 and also tBRD-2, whose synthesis overlaps with that of tBRD-1, interact with tPlus3a/tPlus3b. We analyzed whether tPlus3a/tPlus3b heterodimerize with tBRD-1 or tBRD-2 using yeast two-hybrid assays. The coding regions of tPlus3a/tPlus3b, tBRD-1, and tBRD-2 were fused to the GAL4 DNA binding domain (DBD), which represented the bait protein, and to the GAL4 activation domain (AD), which represented the prey protein. Interaction of bait and prey fusion proteins leads to activation of a MEL1 reporter gene, which stains yeast colonies blue. The positive control, with DBD-p53 as bait protein and the large T antigen (AD-T) as prey protein, activated the reporter gene (Fig 3B), whereas the negative control, with Lamin C as bait protein and the large T antigen as prey protein, did not (Fig 3C).

In the assay, the bait fusion DBD-tPlus3a/tPlus3b heterodimerized with the prey fusion AD-tBRD-1 (Fig 3D). To exclude auto-activation of reporter genes that might be caused by bait or prey fusion proteins, we tested DBD-tPlus3a/tPlus3b with an unfused activation domain; the reporter gene was not activated (not shown). We did not detect heterodimerization of DBD-tBRD-1 with AD-tPlus3a/tPlus3b (Fig 3E), possibly because of conformational changes in the tPlus3a/tPlus3b structure caused by the fusion to the activation domain or insufficient synthesis of the AD-tPlus3a/tPlus3b fusion. DBD-tPlus3a/tPlus3b did not heterodimerize with AD-tBRD-2 (Fig 3F), and DBD-tBRD-2 did not heterodimerize with AD-tPlus3a/tPlus3b (Fig 3G). As a control for the functionality of the yeast two-hybrid constructs, we tested the previously described heterodimerization of tBRD-1 and tBRD-2 [10]; the proteins formed a heterodimer (Fig 3H, I).

tPlus3a/tPlus3b and tBRD-1 activate and repress transcription individually and together

Next, we addressed whether tPlus3a/tPlus3b are important for gene activation and/or repression. As our yeast two-hybrid results showed that tPlus3a/tPlus3b and tBRD-1 form a heterodimer, we asked whether tPlus3a/tPlus3b and tBRD-1 share target genes. We sequenced testis RNA from Δ*tplus3a/tplus3b/Df(2L)BSC151* flies, *tbrd-1*^{1} mutants, and wild-type flies in parallel and identified differentially expressed genes (log2 FC ≥ 1 and ≤ −1). In Δ*tplus3a/tplus3b/Df(2L)BSC151* testes, 398 transcripts were differentially expressed of which 209 were down-regulated and 189 were up-regulated compared to the wild-type (Fig 4A). In *tbrd-1*^{1} mutant flies, 1,499 genes were differentially expressed, of which 1,196 were down-regulated and 303 were up-regulated compared to the wild-type.

The number of genes down-regulated in both Δ*tplus3a/tplus3b/Df(2L)BSC151* and *tbrd-1*^{1} mutants, namely 141, represents about two-thirds of the genes that are activated by tPlus3a/tPlus3b (Fig 4A). On the other hand, only 12% of the differentially expressed genes in *tbrd-1*^{1} mutants overlap with genes expressed in Δ*tplus3a/tplus3b/Df(2L)BSC151*, which suggests that most genes regulated by

tPlus3a/tPlus3b are also targeted by tBRDa-1, but that tBRD-1 itself activates a much larger set of genes. Of the up-regulated genes in Δ*tplus3a/tplus3b/Df(2L)BSC151* and *tbrd-1*^{1} mutants, 56 overlap, which corresponds to about 30% of the tPlus3a/tPlus3b up-regulated genes and 17% of the genes up-regulated in *tbrd-1*^{1} mutants. As our results suggested that bromodomain proteins specifically synthesized in the testis serve as regulators of different sets of target genes in the germ line transcription machinery. Therefore, we also compared our RNAseq data of Δ*tplus3a/tplus3b/Df(2L)BSC151* and *tbrd-1*^{1} mutants to RNA microarray data from *tbrd-2* knock-down testes [11]. In contrast to the large number of target genes common to tPlus3a/tPlus3b and tBRD-1, the expression of only six genes changed in both the absence of tPlus3a/tPlus3b and upon knock-down of tBRD-2. Four of these genes are also regulated by tBRD-1; 66 genes are regulated by both tBRD-1 and tBRD-2 (Fig 4B). These findings suggest a role for tPlus3a/tPlus3b in defining a subset of genes regulated by tBRD-1.

Fig 4. tPlus3a/tPlus3b and tBRD-1 regulate a common set of genes.

To validate our RNAseq results, we performed real-time quantitative PCR (qPCR) with cDNA from wild-type and Δ*tplus3a/tplus3b/Df(2L)BSC151* and *tbrd-1*^{1} mutants. We first validated down-regulation of *tbrd-1* and *tplus3a/tplus3b* in the respective mutants and observed a clear decrease in the number of the transcripts expressed. There was also a down-regulation visible for *tplus3a/tplus3b* in *tbrd-1*^{1} mutants. *tplus3a* and *tplus3b* transcripts are reduced by 40-45% in *tbrd-1*^{1} mutants according to our RNAseq analysis and do not appear in the results due to a decrease of the log2 fold change less than twofold (Fig 4C). We determined the transcript levels of the down-regulated target genes *CG7543*, *CG2772,* and *kl-3*. Our results confirmed that *CG7543* is down-regulated in both mutants, and *CG2772* and *kl-3* are down-regulated only in Δ*tplus3a/tplus3b/Df(2L)BSC151* testes (Fig 4C). We then validated the results for the up-regulated genes *Sox21b*, *Hsp67Bc*, *Hsp70Aa*, *CG13428,* and *AstCC* (Fig 4C). *Hsp67Bc* was slightly up-regulated

only in Δ*tplus3a/tplus3b/Df(2L)BSC151, Sox21b* was up-regulated and *Hsp70Aa* was strongly up-regulated in both Δ*tplus3a/tplus3b/Df(2L)BSC151* and *tbrd-1*^{1} mutants.

The top 40 most down- or up-regulated genes in both Δ*tplus3a/tplus3b/Df(2L)BSC151* and *tbrd-1*^{1} mutant testes or in only Δ*tplus3a/tplus3b/Df(2L)BSC151* testes are given in Table 1.

Table 1. Genes regulated by tPlus3a/tPlus3b and tBRD-1, and by tPlus3a/tPlus3b but not tBRD-1.

Down-regulated genes		Up-regulated genes	
Δ*tplus3a/tplus3b/ Df(2L)BSC151* only	Δ*tplus3a/tplus3b/ Df(2L)BSC151* and *tbrd-1*[1]	Δ*tplus3a/tplus3b/ Df(2L)BSC151* only	Δ*tplus3a/tplus3b/ Df(2L)BSC151* and *tbrd-1*[1]
CG31703	salt	CG34436	Sfp87B
CG31702	CG14245	CG13428	Peb
Muc30E	CG31703	AstCC	Sfp24Bb
CG2772	Muc11A	CG12990	Sox21b
CG43401	CG7542	Elo68alpha	PebII
Dh31-R	CG31702	CG10764	Obp56g
CG9259	Mur18B	CG43320	Sfp60F
CG42370	CG16762	Uro	CG17572
CG6293	CG8028	CG18180	CG14304
CG12017	CG3285	CG12268	CG3868
CG12009	CG18095	Acp24A4	ppk19
CG43707	CG34426	CG34113	CG30427
dpr7	CG32023	Eip63F-1	Hsp70Aa
CG41434	CG45072	GstZ2	Hsp70Ab
IM23	CG14292	CG42313	AttB
kl-3	CG31198	CG11951	Hsp70Ba
CG34393	CG3290	kek3	Hsp70Bb
CG8641	Irk3	ninaC	Hsp70Bc
Ory	CG42235	CG4267	Hsp70Bbb
CG8093	Smvt	CG14535	CG11893
mthl8	Muc30E	rho-6	CG2065
IM1	unc80	CG13038	Hsp67Bc
CG31897	CG2187	CG2663	CG18278
CG31600	Scp2	Snoo	CG1441
l(2)34Fc	CG34284	CG5697	CG30059
CG6967	CG11626	CG11598	CG10550
CG14982	CG13309	CG31710	CG10096
CG8301	CG2772	asparagine-synthetase	CG10097
CG8145	CG2736	CG10657	fd102C
CG12869	CG14219	CG7214	CG5337
CG42368	Oatp58Da	NimC2	CG31157
CG17162	CG7882	TwdlT	CG13285
CG16898	NaPi-T	CG16820	GstD5
CG11634	CG10560	SA-2	sisA
CG13748	CG34043	CG12780	Cyp4e3
stum	CG9512	CG45546	Arr1
CG34166	CG43401	Adh	Adgf-D
CG17159	CG3690	Adhr	CG6488
H15	CG31202	CG13516	CG31300
CG11629	Dh31-R	Rdl	CG31777

tPlus3a/tPlus3b activate the Y chromosomal fertility factors *kl-3* and *kl-5*

The set of genes down-regulated in Δ*tplus3a/tplus3b/Df(2L)BSC151,* i.e., regulated by tPlus3a/tPlus3b, includes *kl-3* and *kl-5*, which encode Y chromosomal fertility factors. These genes were not co-regulated by tBRD-1. As *kl-3* and *kl-5* encode dynein heavy chains of the axoneme, their down-regulation could contribute to the severely reduced fertility in Δ*tplus3a/tplus3b/Df(2L)BSC151* flies that we observed.

tPlus3a/tPlus3b and tBRD-1 negatively regulate heat shock genes and seminal fluid protein genes in the germ line

Strikingly, many heat-shock-related genes, e.g., *Hsp70Aa,* are among the genes up-regulated in both mutants (Table 1). Therefore, tPlus3a/tPlus3b and tBRD-1 might fulfill a repressive function for this gene class by limiting the activation of heat shock genes during the spermatocyte phase. Another class that appears to be regulated by both factors is represented by genes such as *Sfp87B* and *Sfp24Bb*, which encode seminal fluid proteins. These are synthesized by somatic parts of the reproductive tract and are first needed after sperm development [27]. *Acp24A4*, which encodes a male accessory gland protein [28], was only regulated by tPlus3a/tPlus3b. These findings suggest that transcriptional repression of *Sfp87B*, *Sfp24Bb,* or *Acp24A* in spermatocytes is required.

Discussion

D. melanogaster spermatogenesis is characterized by a unique transcriptional program in spermatocytes. Thousands of transcripts are synthesized in this germ cell stage, but most are only needed much later in post-meiotic development [1-3]. Jiang et al. [29] reported that one-third of the tTAF-dependent genes is regulated by Modulo or Acj6. In our previous studies, we described a possible interplay between tBRDs and the testis transcription machinery and a role of tBRDs in guiding the complexes Mediator, tMAC, and TFIID to specific subsets of target genes [10-11]. We hypothesize that in addition to tBRD-1 and tBRD-2, other factors are required for fine-tuning gene expression during spermatogenesis. In the current study, we characterized synthesis and function of tPlus3a and tPlus3b. We show that tPlus3a/tPlus3b and the bromodomain protein tBRD-1 co-regulate distinct groups of target genes, which underscores their potential for fine-tuning the transcriptional regulatory network in spermatocytes. *tplus3a* and *tplus3b* are target genes of Aly und Med22 [8, 30] and are also slightly down-regulated in *tbrd-1*^{1} mutants indicating that regulators of transcription are interdependent.

Plus3-domain proteins are synthesized in the testis and might be functionally redundant

The genome of *D. melanogaster* has the potential to synthesize only a few proteins containing a Plus3 domain. Here, we showed that the Plus3-domain proteins tPlus3a/tPlus3b are essential for full male fertility. In male germ cells, tPlus3a/tPlus3b were limited to nuclei of spermatocytes and localize in the chromosomal regions. tPlus3a/tPlus3b also localizes to distinct spots in some regions of the nucleus, which might correspond to areas of Y chromosomal lampbrush loops. The lampbrush loops harbor genes encoding male fertility factors, e.g., *kl-3* and *kl-5*. In contrast to the Plus3-domain protein Rtf1, tPlus3a/tPlus3b lack the histone modification domain, which suggests that tPlus3a/tPlus3b are not able to directly modify histones by themselves. The Plus3 domain might be

needed for DNA binding, as described for human Rtf1 [22]. Therefore, tPlus3a/tPlus3b could be required as a platform to recruit other histone-modifying enzymes. Based on a C-terminal consensus sequence in Rft1 and tPlus3a/tPlus3b, we conclude that a Paf1C interaction domain like that in Rtf1 is also present in tPlus3a/tPlus3b, but interaction between tPlus3a/tPlus3b and members of Paf1C remains to be examined. Interestingly, all homologues of Paf1C subunits in *D. melanogaster* are also synthesized in the testis [5], which might point to an interaction of at least one of the Paf1C components with tPlus3a/tPlus3b. In addition, a role in spermatogenesis for the remaining Plus3-domain protein-coding gene, *CG12498*, should be considered. Based on structural homologies between tPlus3a/tPlus3b and CG12498, it seems likely that these proteins would be able to functionally replace each other to a certain degree. Functional redundancy between tPlus3a/tPlus3b and CG12498 might be the reason for the increasing fertility of 8-day-old Δ*tplus3a/tplus3b/Df(2L)BSC151* males and could also explain why younger Δ*tplus3a/tplus3b/Df(2L)BSC151* males are not completely sterile.

tPlus3a and tPlus3b regulate Y chromosomal genes essential for full male fertility

Generation of Δ*tplus3a/plus3b* deletion mutants resulted in cysts with abnormal individualization during sperm individualization. The inefficient individualization of sperm likely contributes to the reduced fertility of males. In our RNAseq data of Δ*tplus3a/tplus3b/Df(2L)BSC151,* the *kl-3* and *kl-5* genes were down-regulated. Both of these targets encode axonemal outer arm dynein heavy chains, which suggests a role in assembly of the axoneme and motility of sperm [31-33]. As flies bearing *kl-3* or *kl-5* deletions lose the outer dynein arm of the flagellar axoneme [34], down-regulation of *kl-3* and *kl-5* might explain our finding that Δ*tplus3a/tplus3b/Df(2L)BSC151* testes contain sperm with reduced motility. In addition, as *kl-3* and *kl-5* mutants have a reduced fertility [35-36], this might also explain the reduced fertility of *tplus3a/tplus3b*-deficient flies. *kl-3* and *kl-5* are both transcribed in the spermatocyte Y-loops [37]. Three of these loop structures can be observed in spermatocytes during

spermatocyte development [25]. According to our RNAseq data, *kl-3* and *kl-5* are regulated by tPlus3a/tPlus3b but not by tBRD-1. This might point to a specific function of tPlus3a/tPlus3b in the regulation of these male fertility factors. Along these lines, co-localization of tBRD-1 and tPlus3a/tPlus3b was only observed in chromosomal regions, whereas speckles of tBRD-1 and distinct spots of tPlus3a/tPlus3b did not overlap.

tPlus3a/tPlus3b and tBRD-1 co-repress heat shock genes in spermatocytes

Our RNAseq data also suggest a repressor function of tPlus3a/tPlus3b as many genes were up-regulated in Δ*tplus3a/tplus3b/Df(2L)BSC151*. Strikingly, several genes seemed to be up-regulated also in *tbrd-1*^{1} mutant testes. One group of genes (*Sfp87B*, *Sfp24Bb,* and *Sfp60F*) encode several seminal fluid proteins (Sfp). These are needed for fertilization and can found in the ejaculate of male flies [38]. *Peb* (*Ebp*, *Peb-me*) and *PebII* (*EbpII*), which encode proteins of the ejaculatory bulb, are likewise not expressed in germ cells of wild-type flies. Their proteins are transferred together with sperm in the ejaculate of males to female flies during mating to prevent early remating [39-40]. As these protein classes are first needed during fertilization, it is not surprising that a repression mechanism controls these genes in germ cells. As the general transcription rate is extremely high in the spermatocyte phase, tPlus3a/tPlus3b and tBRD-1 might prevent untimely transcription of sperm fluid genes.

Interestingly, *AstCC* and *CG13428* were upregulated in Δ*tplus3a/tplus3b/Df(2L)BSC151* but strongly down-regulated in *tbrd-1*^{1} mutants. This might indicate that these genes are regulated contrarily by tPlus3a/tPlus3b and tBRD-1.

Another gene group repressed by both tPlus3a/tPlus3b and tBRD-1 are heat shock genes. Many *Hsp70* genes as well as *Hsp67Bc* were up-regulated in Δ*tplus3a/tplus3b/Df(2L)BSC151* and *tbrd-1*^{1}.

This finding might explain why primary spermatocytes were reported to poorly respond to heat shock in spermatocytes [41].

tPlus3a/tPlus3b share a large subset of target genes with tBRD-1 but not with tBRD-2

As previously reported, the transcription machinery in spermatocytes is supported by several interactions between various complexes, such as TFIID, tMAC, and Mediator [8]. Recent findings indicate how the specificity for different sets of genes might be achieved by cooperation of general transcription factors with bromodomain proteins [10-11]. Our RNAseq results for *tplus3a/tplus3b*-deficient fly testes and *tbrd-1*^{1} mutant testes suggest a role for Plus3-domain proteins in transcription regulation. Comparative analyses of our Δ*tplus3a/tplus3b/Df(2L)BSC151* and *tbrd-1*^{1} RNAseq datasets with microarray data from *tbrd-2* knock-down testis revealed that many genes are co-regulated by tPlus3a/tPlus3b and tBRD-1, whereas only a few genes are commonly regulated by tPlus3a/tPlus3b and tBRD-2. However, a direct comparison of microarray data and RNAseq data should be handled with caution. A potential cooperation between tPlus3b and tBRD-1 is supported by their heterodimerization in the yeast two-hybrid system. We hypothesize that tPlus3a/tPlus3b either activate (Fig 5A) or repress (Fig 5B) sets of target genes, and in doing so probably also interacts with some factors of the general or testis-specific transcription machinery. Indeed, tBRD-1 heterodimerizes with the tTAF Sa [10].

Fig 5. Model of the complex formation of tPlus3a/tPlus3b, tBRD-1, and other factors.

tPlus3a/tPlus3b and tBRD-1 together likely also activate or repress genes (Fig 5C, D). There is also a small overlap of genes regulated by tPlus3a/tPlus3b and tBRD-1 and genes regulated in the tTAF mutant *sa* [42]. The genes regulated by all three proteins comprise ca. 12% of tPlus3a/tPlus3b regulated genes, ca. 3% of tBRD-1 regulated genes and ca. 1% of Sa regulated genes. Similar results indicating minor overlaps for regulated genes are obtained in comparison of our RNAseq data with

405 microarray data for other tTAFs or tMAC components [8]. This might speak for a refinement of
406 transcription activity by tPlus3a/tPlus3b during spermatogenesis.

407

408 Material and Methods

409 Fly strains and cultures

410 Flies were maintained at 25 °C on standard medium. w^{1118} or w^{1118}*;CyO/Sp;ProtB-eGFP* [43] flies were
411 used as the wild-type control. *tbrd-1*^{1} mutants and flies synthesizing tBRD-1-eGFP [13] were used for
412 RNAseq and analysis of co-localization with tPlus3a/tPlus3b, respectively. w^{1118}*;Df(2L)BSC151/CyO*
413 (Bloomington stock number: 9510) was used as deficiency fly line for *tplus3a* and *tplus3b*.
414 Δ*tplus3a/*Δ*tplus3b* (Δ*tplus3a/tplus3b*) mutants were maintained in a $y^{1}cho^{2}v^{1}$ background, and
415 Δ*tplus3a/tplus3b/Df(2L)BSC151* trans-heterozygotes were maintained in a w^{1118} background.
416 w^{1118}*;*Δ*tplus3a/tplus3b/Df(2L)BSC151;ProtB-eGFP* was used for visualization of nuclei phenotypic
417 analyses.

418 Generation of *tplus3b-eGFP* flies

419 The *tplus3b-eGFP* fusion construct was generated by PCR amplification of the *tplus3b* putative
420 promoter region, 5'-UTR, and open reading frame (ORF) on w^{1118} genomic DNA with primers 5'-
421 GGTACCTCGTGTAGCTCTTTTTAGC-3' and 5'-ACTAGTGCCTTTCATTATCTCGTCCC-3'. The PCR product
422 was subcloned into the pCR®II-TOPO® vector (Invitrogen). The recombinant plasmid was digested
423 with KpnI and SpeI and ligated into pChabΔ*sal*Δ*lacZ* (modified after [44]), which carries the gene
424 encoding eGFP, yielding a construct with eGFP at the C-terminus. Transgenic flies were established
425 by injection into the w^{1118} strain.

426

427

In situ hybridization

In situ hybridization of w^{1118}, $y^1cho^2v^1$;Δ*tplus3a/tplus3b* and $y^1cho^2v^1$; Δtplus3a/tplus3b/CyO was performed as described in Morris et al. [45]. *tplus3a/tplus3b* RNA probes were synthesized by PCR amplification of 610 bp of the tplus3b ORF with primers 5'-CAAATAAACTGGAGTCTGGTGG-3' and 5'-TTGGCGATGTCATTAAGCGTTG-3'. The amplified product was cloned into the pCR®II-TOPO® vector (Invitrogen). *In vitro* transcription for probe synthesis was performed with SP6 and T7 Polymerase (Roche) after linearization of the vector with KpnI or EcoRI, respectively. Probes where then EtOH precipitated and solved in hybridization solution [45].

Immunofluorescence staining and antibody generation

Immunofluorescence stainings were performed according to Hime et al. [46] with modifications [47] DNA was stained with Hoechst, and actin components, e.g., the individualization complex, were stained with TRITC-phalloidin. A tPlus3a/tPlus3b peptide antibody was raised against peptide KRTAKPEQHELEKYMRRKY (aa 329 to aa 347 of tPlus3a/tPlus3b) in rabbit, affinity purified (Pineda Antibody Service, http://www.pineda-abservice.de), and diluted 1:500. The secondary antibody anti-rabbit-Cy3 (Dianova) was diluted 1:100. Stainings were analyzed with an AxioPlan2 microscope (Zeiss). Images were processed using Photoshop (Adobe).

CRISPR/Cas9 mutant generation and analysis

$y^1cho^2v^1$;Δ*tplus3a/tplus3b* mutants were generated using a single target construct in the CRISPR/Cas9 system as described by Kondo and Ueda [26]. For cloning of the target construct, primers 5'-CTTCGCAGAATGGATGAGCGCTTA-3' and 5'-AAACTAAGCGCTCATCCATTCTGC-3' were used, and the product was ligated to *pBFv-U6.2*. The target construct was injected into $y^2cho^2v^1$*P{nos-phiC31\int.NLS}X;attP2(III),* and established transgenic flies were crossed with $y^2cho^2v^1$*;attP40{nos-Cas9}/CyO* flies for mutagenesis. Fifty founder flies were crossed with $y^2cho^2v^1$*;Sco/CyO* flies to

451 establish potential mutants. Genomic regions next to the target sequence of homozygous offspring
452 were analyzed by PCR for and screened for deletions.

453 Western blotting

454 Protein extracts for western blots were prepared from 20 testes of w^{1118},
455 $y^1cho^2v^1;\Delta tplus3a/tplus3b/CyO$ and $y^1cho^2v^1;\Delta tplus3a/tplus3b$ flies. Testes were homogenized with
456 20 µl 2×SDS sample buffer by sonication for 20 min at 4 °C. Protein extracts were incubated for 5 min
457 at 95 °C and separated on SDS-10% polyacrylamide gels. Western blotting followed standard
458 procedures. Anti-tPlus3a/tPlus3b was diluted 1:1,000 in 5% dry milk powder/1×TBS. HRP-conjugated
459 anti-rabbit (Jackson Immunology) was diluted 1:1,000 in 5% dry milk powder/1×TBS. Enhanced
460 chemiluminescence (ECL, Invitrogen) was detected on an Odyssey® Fc Imaging System (Licor)
461 following the manufacturer's instructions.

462 Sterility tests

463 For sterility tests, individual 1-day (after hatching)-old males (w^{1118}, $w^{1118};Df(2L)BSC151/CyO$,
464 $y^1cho^2v^1;\Delta tplus3a/tplus3b/CyO$ and $w^{1118};\Delta tplus3a/tplus3b/Df(2L)BSC151$) and 5-day (after hatching)-
465 old $w^{1118};\Delta tplus3a/tplus3b/Df(2L)BSC151$ males were placed with two virgin w^{1118} females in separate
466 vials at 25 °C and were allowed to mate for three days. The final age of the flies was 4 days and 8
467 days, respectively. The number of offspring per vial was counted after 2 weeks. Statistical analysis
468 was performed using One-way ANOVA with Tukey's multiple comparison test and Graph Pad Prism
469 Version 5.

470 Yeast two-hybrid experiments

471 Yeast two-hybrid experiments were carried out using the Matchmaker™ GAL4 Two-Hybrid System 3
472 (Takara Clontech) according to the manufacturer's instructions. For construct generation, the *tplus3b*
473 ORF of genomic w^{1118} DNA was PCR amplified with primers 5'-CCATGGCGATGGATGAGCGCTTAC-3'
474 and 5'-GTCGACCTAGCCTTTCATTATCTCGTC-3'; the products were cloned into the pCR®II-TOPO®

vector (Invitrogen). The prey vector pGBKT7 was digested with NcoI and SalI, and the bait vector pGADT7 was digested with NcoI and XhoI. The *tplus3b* ORF was excised from pCR®II-TOPO® with NcoI and SalI and ligated into pGBKT7 for synthesis of the DBD-tPlus3b fusion protein (fusion with GAL4-DNA- binding domain) and into pGADT7 for synthesis of the AD-tPlus3b fusion protein (fusion with GAL4-activation domain). Yeast two-hybrid constructs for *tbrd-1* and *tbrd-2* are described in Theofel et al. [10].

RNA isolation and RNAseq

Total RNA from 200 testes of w^{1118}, $tbrd\text{-}1^{1}$ and w^{1118};Δ*tplus3a/tplus3b/Df(2L)BSC151* flies was isolated using TRIzol (Invitrogen). DNA was digested with TURBO™ DNase (Invitrogen) and purified with the RNeasy Mini Kit (Qiagen) according to the manufacturer's instructions. Transcriptomes were analyzed using next-generation sequencing (RNAseq) in three replicates. Prior to library preparation, RNA quality was assessed using the Experion RNA StdSens Analysis Kit (BioRad). Libraries were prepared using the TruSeq Stranded mRNA LT Kit (Illumina) according to the manufacturer's instructions. The quality of libraries was controlled using a Bioanalyzer 2100 and the Agilent High Sensitivity DNA Kit (Agilent). Pooled libraries were quantified with digital PCR (QuantStudio 3D, Thermo Fisher) and sequenced on the HiSeq 1500 platform (Illumina) in rapid-run mode with 50-base single reads. Reads were aligned to the *D. melanogaster* genome retrieved from Ensembl revision 89 (BDGP6) with STAR 2.4.1a [48]. Default parameters were used, except for outFilterScoreMin and outFilterMatchNmin, which were set to 60% of the read length. For analysis of RNAseq data, tag counts were calculated and normalized to one million mapped exonic reads and gene length (FPKM). To generate the set of expressed genes, only genes with a minimum read count of 50 and a minimum FPKM of 0.3 were kept. Fold change was calculated between the technical replicates of two conditions. Differential expression was assessed using the log2 of the median fold change. Only genes with an increase or decrease of at least twofold were considered to be differentially expressed.

qPCR

RNA from 200 testes of *w*^{1118}, *tbrd-1*^{1} and w^{1118};Δ*tplus3a/tplus3b/Df(2L)BSC151* was isolated using TRIzol (Invitrogen). DNA was digested with TURBO™ DNase (Invitrogen) and purified with RNeasy Mini Kit (Qiagen) according to the manufacturer's instructions. RNA (1 µg) was used for reverse transcription with random hexamer primers using the Transcriptor First Strand cDNA Synthesis Kit (Roche). The qPCR reaction (20 µl) contained 10 µl iTaq™ Universal SYBR® Green Supermix (Bio-Rad), 12.5 ng cDNA, and 10 µM gene-specific forward and reverse primers (Table S1), and was run on an Agilent Stratagene Mx3000P cycler with an annealing temperature of 60 °C. Ct-values for three technical replicates were normalized to the expression level of Rpl32. Depicted is the mean value and SD of three replicates using GraphPad PRISM version 5.03. Statistical analysis was calculated with student's t-test and Bonferroni correction.

ArrayExpress accession data

RNAseq data were deposited in the ArrayExpress [49] database at EMBL-EBI (www.ebi.ac.uk/arrayexpress) under accession number E-MTAB-7013.

Acknowledgements

We thank Rainer Renkawitz and Christian Bökel for helpful discussions and support, and Igor Macinkovic, Stephan Awe, and Julia Seiz for help with qPCR experiments and evaluation. We thank Ruth Hyland, Ljubinka Cigoja, and Sabina Huhn for excellent technical assistance, and Katja Gessner for support with graphic programs. We thank Karen A. Brune for linguistic revision of the manuscript. We are grateful to Ryu Ueda and the NIG Japan for sending us the CRISPR/Cas9 flies.

Funding

This work was supported by the Deutsche Forschungsgemeinschaft (SFB TRR81 "Chromatin Changes in Differentiation and Malignancies" to C. R. and R. R.-P.).

Author contributions

T.H. generated *tplus3a/tplus3b* mutants and carried out subsequent immunofluorescence, sterility tests, phenotypic analyses, RNA isolation for RNAseq, and qPCR, and wrote the first draft of the manuscript. S.K. performed yeast two-hybrid interaction tests and *in situ* hybridization. N.M. carried out immunofluorescence of *tplus3a/tplus3b* mutants and western blots. A.N. prepared the RNAseq library. B.L. analyzed the raw data of RNAseq experiments. T.S. supervised the Genomics Unit, A.B. supervised the qPCR experiments and participated manuscript preparation. C.R. designed the project. C.R. and R.R-P. supervised the project including manuscript preparation.

References

1. Olivieri G, Olivieri A. Autoradiographic study of nucleic acid synthesis during spermatogenesis in *Drosophila melanogaster*. Mutat Res. 1965 Aug;2(4):366-80.

2. White-Cooper H, Schäfer MA, Alphey LS, Fuller MT. Transcriptional and post-transcriptional control mechanisms coordinate the onset of spermatid differentiation with meiosis I in *Drosophila*. Development. 1998 Jan;125(1):125-34.

3. White-Cooper H, Davidson I. Unique aspects of transcription regulation in male germ cells. Cold Spring Harb Perspect Biol. 2011 Jul 1;3(7).

4. Rathke C, Baarends WM, Awe S, Renkawitz-Pohl R. Chromatin dynamics during spermiogenesis. Biochim Biophys Acta. 2014 Mar;1839(3):155-68.

5. Chintapalli VR, Wang J, Dow JAT. Using FlyAtlas to identify better *Drosophila* models of human disease. Nat Genet. 2007 Jun;39(6):715-20.

6. Hiller MA, Lin TY, Wood C, Fuller MT. Developmental regulation of transcription by a tissue-specific TAF homolog. Genes Dev. 2001 Apr 15;15(8):1021-30.

7. Hiller MA, Chen X, Pringle MJ, Suchorolski M, Sancak Y, Viswanathan S, et al. Testis-specific TAF homologs collaborate to control a tissue-specific transcription program. Development. 2004 Nov;131(21):5297-308.

8. Lu C, Fuller MT. Recruitment of mediator complex by cell type and stage-specific factors required for tissue-specific TAF dependent gene activation in an adult stem cell lineage. PLoS Genet. 2015 Dec 1;11(12):e1005701.

9. Beall EL, Lewis PW, Bell M, Rocha M, Jones DL, Botchan MR. Discovery of tMAC: a *Drosophila* testis-specific meiotic arrest complex paralogous to Myb-Muv B. Genes Dev. 2007 Apr 15;21(8):904-19.

10. Theofel I, Bartkuhn M, Hundertmark T, Boettger T, Gärtner SM, Leser K, et al. tBRD-1 selectively controls gene activity in the *Drosophila* testis and interacts with two new members of the bromodomain and extra-terminal (BET) family. PLoS One. 2014 Sep 24;9(9):e108267.

11. Theofel I, Bartkuhn M, Boettger T, Gärtner SMK, Kreher J, Brehm A et al. tBRD-1 and tBRD-2 regulate expression of genes necessary for spermatid differentiation. Biol Open. 2017 Apr 15;6(4):439-448.

12. Dhalluin C, Carlson JE, Zeng L, He C, Aggarwal AK, Zhou M-M. Structure and ligand of a histone acetyltransferase bromodomain. Nature. 1999 Jun 3;399(6735):491-6.

13. Leser K, Awe S, Barckmann B, Renkawitz-Pohl R, Rathke C. The bromodomain-containing protein tBRD-1 is specifically expressed in spermatocytes and is essential for male fertility. Biol Open. 2012 Jun 15;1(6):597-606.

14. Tomson BN, Arndt KM. The many roles of the conserved eukaryotic Paf1 complex in regulating transcription, histone modifications, and disease states. Biochim Biophys Acta. 2013 Jan;1829(1):116-26.

15. Wade PA, Werel W, Fentzke RC, Thompson NE, Leykam JF, Burgess RR, et al. A novel collection of accessory factors associated with yeast RNA polymerase II. Protein Expr Purif. 1996 Aug;8(1):85-90.

16. Kim J, Guermah M, Roeder RG. The human PAF1 complex acts in chromatin transcription elongation both independently and cooperatively with SII/TFIIS. Cell. 2010 Feb 19;140(4):491-503.

17. Van Oss SB, Cucinotta CE, Arndt KM. Emerging insights into the roles of the Paf1 Complex in gene regulation. Trends Biochem Sci. 2017 Oct;42(10):788-798.

18. Rozenblatt-Rosen O, Hughes CM, Nannepaga SJ, Shanmugam KS, Copeland TD, Guszczynski T, et al. The parafibromin tumor suppressor protein is part of a human Paf1 complex. Mol Cell Biol. 2005 Jan;25(2):612-20.

19. Adelman K, Wei W, Ardehali MB, Werner J, Zhu B, Reinberg D, et al. *Drosophila* Paf1 modulates chromatin structure at actively transcribed genes. Mol Cell Biol. 2006 Jan;26(1):250-60.

20. Cao QF, Yamamoto J, Isobe T, Tateno S, Murase Y, Chen Y, et al. Characterization of the Human Transcription Elongation Factor Rtf1: Evidence for Nonoverlapping Functions of Rtf1 and the Paf1 Complex. Mol Cell Biol. 2015 Oct;35(20):3459-70.

21. Warner MH, Roinick KL, Arndt KM. Rtf1 is a multifunctional component of the Paf1 complex that regulates gene expression by directing cotranscriptional histone modification. Mol Cell Biol. 2007 Sep;27(17):6103-15.

22. De Jong RN, Truffault V, Diercks T, Eiso AB, Daniels MA, Kaptein R, et al. Structure and DNA Binding of the Human Rtf1 Plus3 Domain. Structure. 2008 Jan;16(1):149-59.

23. Brown JB, Boley N, Eisman R, May GE, Stoiber MH, Duff MO, et al. Diversity and dynamics of the *Drosophila* transcriptome. Nature. 2014 Aug 28;512(7515):393-9.

24. Sievers F, Wilm A, Dineen D, Gibson TJ, Karplus K, Li W, et al. Fast, scalable generation of high-quality protein multiple sequence alignments using Clustal Omega. Mol Syst Biol. 2011 Oct 11;7:539.

25. Bonaccorsi S, Pisano C, Puoti F, Gatti M. Y chromosome loops in *Drosophila melanogaster*. Genetics. 1988 Dec;120(4):1015-34.

26. Kondo S, Ueda R. Highly Improved Gene Targeting by Germline-Specific Cas9 Expression in *Drosophila*. Genetics. 2013 Nov;195(3):715-21.

27. Adams EM, Wolfner MF. Seminal proteins but not sperm induce morphological changes in the *Drosophila melanogaster* female reproductive tract during sperm storage. J Insect Physiol. 2007 Apr;53(4):319-31.

28. Kubli E. Sex-peptides: seminal peptides of the *Drosophila* male. Cell Mol Life Sci. 2003 Aug;60(8):1689-704.

29. Jiang M, Gao Z, Wang J, Nurminsky DI. Evidence for a hierarchical transcriptional circuit in *Drosophila* male germline involving testis-specific TAF and two gene-specific transcription factors, Mod and Acj6. FEBS Lett. 2018 Jan;592(1):46-59.

30. Doggett K, Jiang J, Aleti G, White-Cooper H. Wake-up-call, a lin-52 paralogue, and Always early, a lin-9 homologue physically interact, but have opposing functions in regulating testis-specific gene expression. Dev Biol. 2011 Jul 15;355(2):381-93.

31. Goldstein LS, Hardy RW, Lindsley DL. Structural genes on the Y chromosome of *Drosophila melanogaster*. Proc Natl Acad Sci U S A. 1982 Dec;79(23):7405-9.

614 32. Gepner J, Hays TS. A fertility region on the Y chromosome of *Drosophila melanogaster*
615 encodes a dynein microtubule motor. Proc Natl Acad Sci U S A. 1993 Dec 1;90(23):11132-6.

616 33. Carvalho AB, Dobo BA, Vibranovski MD, Clark AG. Identification of five new genes on the Y
617 chromosome of *Drosophila melanogaster*. Proc Natl Acad Sci U S A. 2001 Nov
618 6;98(23):13225-30.

619 34. Hardy RW, Tokuyasu KT, Lindsley DL. Analysis of spermatogenesis in *Drosophila*
620 *melanogaster* bearing deletions for Y-chromosome fertility genes. Chromosoma.
621 1981;83(5):593-617.

622 35. Kennison JA. The Genetic and Cytological Organization of the Y Chromosome of *Drosophila*
623 *melanogaster*. Genetics. 1981 Jul;98(3):529-48.

624 36. Zhang P, Stankiewicz RL. Y-linked male sterile mutations induced by P-Element in *Drosophila*
625 *melanogaster*. Genetics. 1998 Oct;150(2):735-44.

626 37. Ceprani F, Raffa GD, Petrucci R, Piergentili R. Autosomal mutations affecting Y chromosome
627 loops in *Drosophila melanogaster*. BMC Genet. 2008 Apr 11;9:32.

628 38. Findlay GD, Yi X, MacCoss MJ, Swanson WJ. Proteomics reveals novel *Drosophila* seminal fluid
629 proteins transferred at mating. PLoS Biol. 2008 Jul 29;6(7):e178.

630 39. Bretman A, Lawniczak MK, Boone J, Chapman T. A mating plug protein reduces early female
631 remating in *Drosophila* melanogaster. J Insect Physiol. 2010 Jan;56(1):107-13.

632 40. Avila FW, Cohen AB, Ameerudeen FS, Duneau D, Suresh S, Mattei AL, et al. Retention of
633 ejaculate by *Drosophila melanogaster* females requires the male-derived mating plug protein
634 PEBme. Genetics. 2015 Aug;200(4):1171-9.

635 41. Bendena WG, Ayme-Southgate A, Garbe JC, Pardue ML. Expression of heat-shock locus *hsr-*
636 *omega* in nonstressed cells during development in *Drosophila* melanogaster. Dev Biol. 1991
637 Mar;144(1):65-77.

638 42. Lu C, Kim J, Fuller MT. The polyubiquitin gene Ubi-p63E is essential for male meiotic cell cycle
639 progression and germ cell differentiation in *Drosophila*. Development. 2013
640 Sep;140(17):3522-31.

641 43. Jayaramaiah Raja S, Renkawitz-Pohl R. Replacement by *Drosophila* melanogaster protamines
642 and Mst77F of histones during chromatin condensation in late spermatids and role of sesame
643 in the removal of these proteins from the male pronucleus. Mol Cell Biol. 2005
644 Jul;25(14):6165-77.

645 44. Thummel CS, Boulet AM, Lipshitz HD. Vectors for *Drosophila* P-element-mediated
646 transformation and tissue culture transfection. Gene. 1988 Dec 30;74(2):445-56.

647 45. Morris CA, Benson E, White-Cooper H. Determination of gene expression patterns using *in*
648 *situ* hybridization to *Drosophila* testes. Nat Protoc. 2009;4(12):1807-19.

649 46. Hime GR, Brill JA, Fuller MT. Assembly of ring canals in the male germ line from structural
650 components of the contractile ring. J Cell Sci. 1996 Dec;109 (Pt 12):2779-88.

651 47. Hundertmark T, Theofel I, Eren-Ghiani Z, Miller D, Rathke C. Analysis of chromatin dynamics
652 during *Drosophila* spermatogenesis. Methods Mol Biol. 2017;1471:289-303.

653 48. Dobin A, Davis CA, Schlesinger F, Drenkow J, Zaleski C, Jha S, et al. STAR: ultrafast universal
654 RNA-seq aligner. Bioinformatics. 2013 Jan 1;29(1):15-21.

655 49. Kolesnikov N, Hastings E, Keays M, Melnichuk OY, Tang A, Williams E, et al. ArrayExpress
656 update—simplifying data submissions. Nucleic Acids Res. 2015 Jan;43(Database
657 issue):D1113-6.

658

659

660

Figure legends

Fig 1. tPlus3a/tPlus3b proteins are limited to the spermatocyte stage.

(A) Schematic of the alignment of the *D. melanogaster* Plus3-domain-containing proteins Rtf1, tPlus3a, tPlus3b, and CG12498. aa, length of protein in amino acids; HMD, histone modification domain; Plus3, Plus3 domain; PI, protein interaction domain. (B, C) *In situ* hybridization of wild-type testis with (B) *tplus3a/tplus3b* antisense (as) probe and (C) *tplus3a/tplus3b* sense (se) probe. Asterisk, hub region; arrow, detection of *tplus3a* and *tplus3b* mRNA in spermatocytes; arrowhead, lack of detection in late stages. (D) Spermatocyte from wild-type testes stained with anti-tPlus3a/tPlus3b antibody. Arrowhead, tPlus3a/tPlus3b distributed throughout nucleus, but slightly concentrated in chromosomal regions; arrow, tPlus3a/tPlus3b in distinct areas between chromosomal regions. (D') DNA visualized with Hoechst. (D'') Merged image of D and D'. Scale bar = 5 μm.

Fig 2. Deletion of *tplus3a* and *tplus3b* leads to severely reduced male fertility and defects during sperm individualization.

(A) Schematic view of the *tplus3a/tplus3b* genomic region and the CRISPR/Cas9-mediated generation of deletions (red boxes), which resulted in the fusion of *tplus3a* and pseudogene *CR31700* and a deletion of most of the *tplus3b* ORF. Dashed lines, regions not fully depicted. (B, C) *In situ* hybridization of testis of (B) heterozygous Δ*tplus3a/tplus3b* mutant (arrow, *tplus3a/tplus3b* signal detected) and (C) homozygous Δ*tplus3a/tplus3b* mutant. Asterisk, hub region. (D, E) Spermatocytes of (D) heterozygous and (E) homozygous Δ*tplus3a/tplus3b* mutant testes stained with anti-tPlus3a/tPlus3b. Scale bar = 10 μm. (F) Western blot of protein extracts from wild-type and homozygous and heterozygous Δ*tplus3a/tplus3b* mutant testes probed with anti-tPlus3a/tPlus3b. Asterisk, lack of signal at ca. 60 kDa. (G, H) Whole-mount preparations of (G) wild-type and (H) Δ*tplus3a/tplus3b/Df(2L)BSC151* testes. Sperm nuclei visualized with ProtB-eGFP. Arrow, sperm nuclei

aligned in tight bundles; arrowhead, sperm nuclei distributed across the testis. Scale bar = 10 μm. (I, J) Squash preparations of (I) wild-type and (J) Δ*tplus3a/tplus3b/Df(2L)BSC151* testes. Sperm nuclei visualized with ProtB-eGFP, DNA stained with Hoechst, and individualization complex stained with TRITC-Phalloidin. Arrow, sperm nuclei aligned in tight bundles; arrowhead, disturbed individualization complex formation with one end thickened. Scale bar = 10 μm. (K, L) Whole-mount preparations of (K) wild-type and (L) Δ*tplus3a/tplus3b/Df(2L)BSC151* seminal vesicles (sv) of 1-day-old males. Sperm nuclei visualized with ProtB-eGFP. Arrow, seminal vesicles filled with sperm; arrowhead, empty seminal vesicles. (M) Fertility of wild-type, *Df(2L)BSC151/CyO,* and 4- and 8-day-old Δ*tplus3a/tplus3b/CyO* flies. *, $p < 0.05$; ***, $p < 0.005$.

Fig 3. tPlus3a/tPlus3b partially co-localize with tBRD-1 and interacts with tBRD-1 but not with tBRD-2 in yeast two-hybrid experiments.

(A–A’’’) Anti-tPlus3a/tPlus3b immunofluorescence staining of the spermatocytes of flies synthesizing tBRD-1-eGFP. (A) tPlus3a/tPlus3b signal present throughout the nucleus but concentrated in chromosomal regions (double arrowhead) and in distinct spots (arrows). (A’) tBRD-1 found mainly in the nucleolus, in chromosomal regions (double arrowhead), and in a speckled pattern (arrowhead). (A’’) DNA stained with Hoechst. Double arrowhead, chromosomal regions. (A’’’) Merged image of A, A’, and A’’ showing co-localization of tPlus3a/tPlus3b and tBRD-1-eGFP in the chromosomal regions (double arrowhead). Scale bar = 5μm. (B–I) Yeast two-hybrid interaction assay. (B) Positive control. (C) Negative control. (D) Heterodimerization of tPlus3a/tPlus3b bait and tBRD-1 prey. (E) Lack of heterodimerization of tPlus3a/tPlus3b prey and tBRD-1 bait. (F, G) Lack of heterodimerization of tPlus3a/tPlus3b as bait or prey and tBRD-2 as prey or bait. (H, I) Heterodimerization of tBRD-1 and tBRD-2 as prey or bait.

712 **Fig 4. tPlus3a/tPlus3b and tBRD-1 regulate a common set of genes.**

713 Transcript expression was measured with RNAseq in three replicates each of testes RNA of the wild-
714 type, Δ*tplus3a/tplus3b/Df(2L)BSC151,* and *tbrd-1*^{1} mutants. Expression levels in mutants are relative
715 to those in the wild-type, which were set to 1. Differentially expressed genes were identified using a
716 log2 FC ≥ 1 and ≤ −1. (A) Venn diagrams showing the overlap between down-regulated and up-
717 regulated genes in Δ*tplus3a/tplus3b/Df(2L)BSC151* (tPlus3a/tPlus3b regulated) and *tbrd-1*^{1} (tBRD-1
718 regulated) mutants relative to the wild-type. (B) Venn diagram showing the overlap of similarly
719 regulated genes in Δ*tplus3a/tplus3b/Df(2L)BSC151, tbrd-1*^{1} and *tbrd-2* knock-down testes (tBRD-2
720 regulated). (C) Validation of RNAseq results using qPCR, normalized to Rpl32. As controls, no
721 *tplus3a/tplus3b* and *tbrd-1* transcripts were expressed in the respective mutants. P-values for
722 significance Δ*tplus3a/tplus3b/Df(2L)BSC151* or *tbrd-1*^{1} compared to wild-type: * $p < 0.025$, ** $p <$
723 0.005 and *** $p < 0.0025$.
724
725 **Fig 5. Model of the complex formation of tPlus3a/tPlus3b, tBRD-1, and other factors.**
726 Numbers indicate the number of genes that were shown to be regulated. (A) tPlus3a/tPlus3b
727 function in gene activation (arrow) or (B) repression (STOP). (C) tPlus3a/tPlus3b and tBRD-1 co-
728 activate and (D) co-repress genes.
729
730 **Fig S1. *tplus3b-eGFP* is expressed in the nucleus and nucleolus of spermatocytes.**
731 Whole-mount preparations of testis from flies weakly expressed *tplus3b-eGFP* in spermatocytes.
732 Signals are visible in the nucleus (arrow) and concentrated in the nucleolus (arrowhead). Asterisk
733 marks the hub region. Scale bar = 20 μm.

Figure 1

Click here to download Figure Fig 1.tif

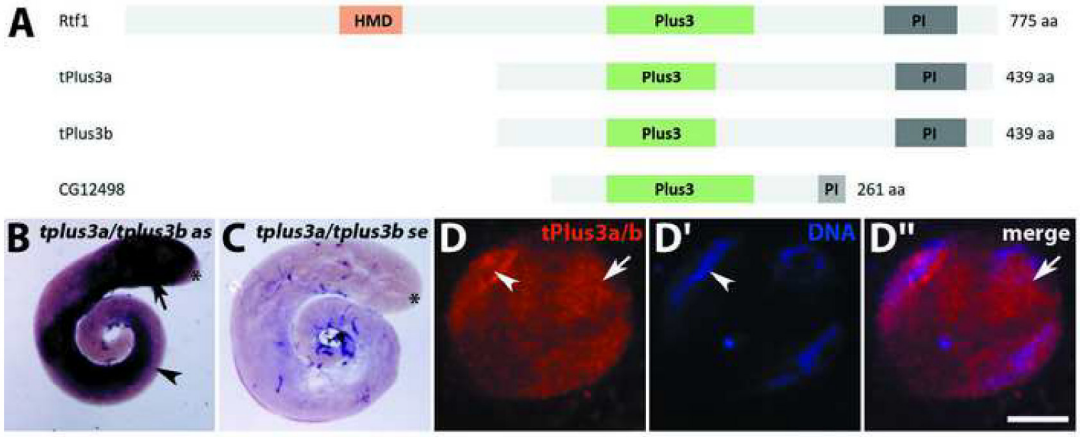

Figure 2

Click here to download Figure Fig 2.tif

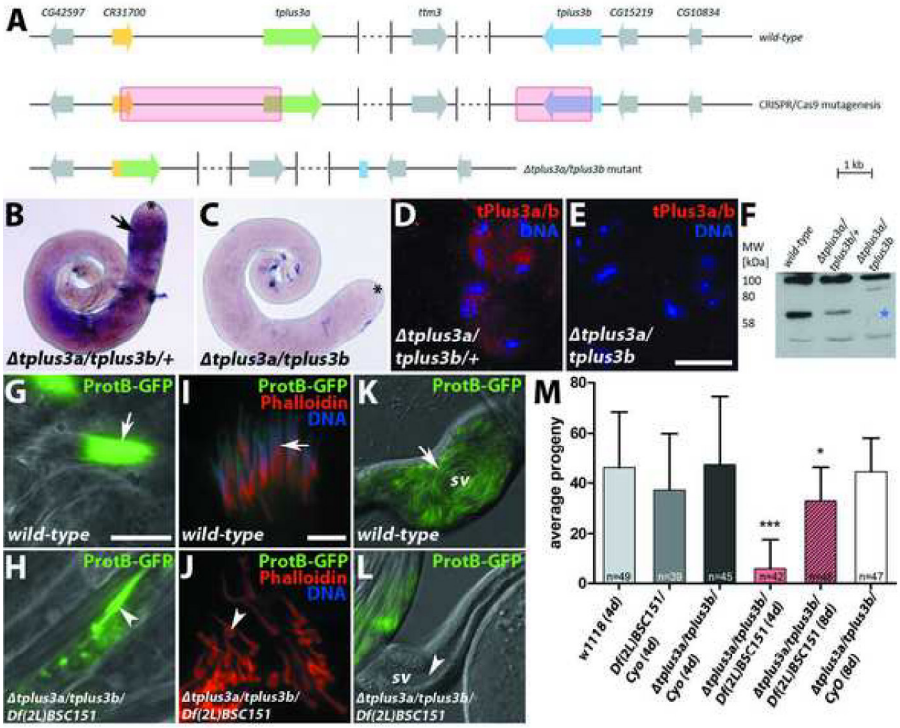

Figure 3

Click here to download Figure Fig 3.tif

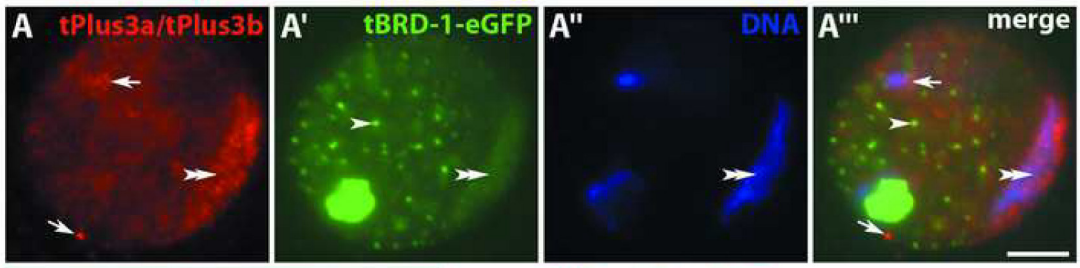

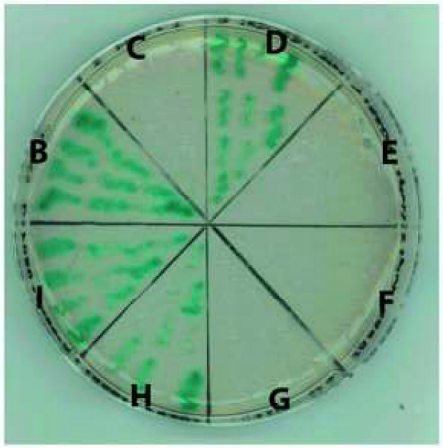

B DBD-p53 + AD-T

C DBD-Lam + AD-T

D DBD-tPlus3a/tPlus3b + AD-tBRD-1

E DBD-tBRD-1 + AD-tPlus3a/tPlus3b

F DBD-tPlus3a/tPlus3b + AD-tBRD-2

G DBD-tBRD-2 + AD-tPlus3a/tPlus3b

H DBD-tBRD-1 + AD-tBRD-2

I DBD-tBRD-2 + AD-tBRD-1

Figure 4

Click here to download Figure Fig 4.tif

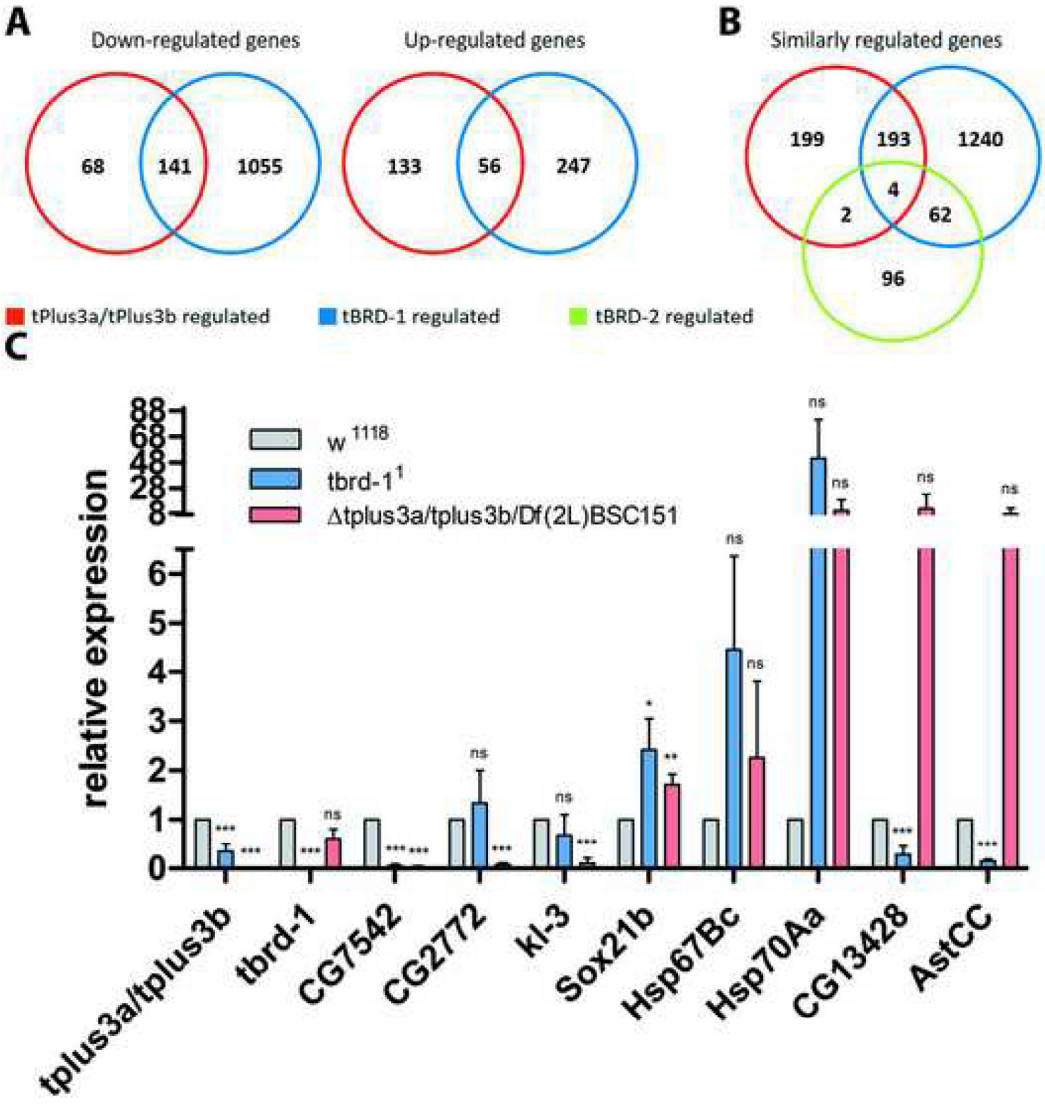

Figure 5

Click here to download Figure Fig 5.tif

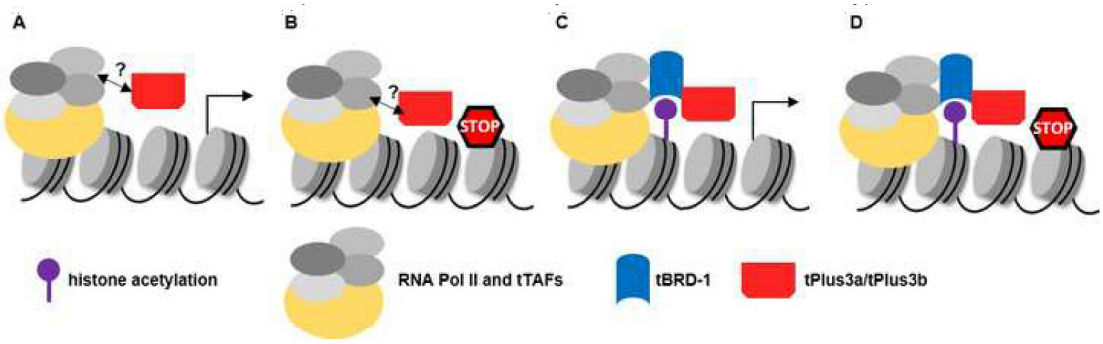

Chapter 10: Discussion

10 Discussion

Many aspects of *Drosophila* spermatogenesis can contribute to a better understanding of cellular and developmental processes. The testes of flies are easy to access and can also be used in *in vitro* culture systems for pharmacological studies on whole testes or even on isolated cysts (Gärtner et al., 2014). This enabled us to study the impact of inhibitors for HATs and HDACs on histone acetylations in post-meiotic germ cells (Chapter 6; Hundertmark, et al., in press) as discussed in Chapter 10.2 along with the role of a specific HAT - Nejire/dCBP - for distinct histone marks. These studies can only be carried out by visualising proteins or modifications, e.g. by using immunofluorescence stainings. Therefore, a reproducible protocol for this method (Chapter 5; Hundertmark et al., 2017) is a valuable tool and might also help to visualise proteins, which are difficult to access as discussed below (Chapter 10.1). In our large-scale proteomic approach, we identified thousands of proteins expressed in different developmental stages. We validated these findings for some of the identified proteins (Chapter 7; Gärtner et al., under review). Discussion concerning the expression and function of these proteins is given in Chapter 10.3. The transcriptional programme driving spermatogenesis is a special one compared to somatic tissues. Flies and mammals almost completely cease synthesis of new transcripts at certain points in male germ cell development. Transcripts that are synthesised in *Drosophila* spermatocytes are very diverse, as they are needed in different developmental stages and biological processes. Testis-specific components of transcription factors are suggested to take part in the regulation of transcription in male germ cells (reviewed in White-Cooper and Davidson, 2011). We describe testis-specifically expressed BRD proteins and show that tBRD-1 functions in transcriptional regulation in spermatocytes (Chapter 8; Theofel et al., 2014). This might specify a subset of target genes regulated by tTAFs. Further unpublished experiments examining the function of tBRD-3 are additionally discussed in Chapter 10.4. In addition to BRD proteins, other factors might influence transcriptional regulation in spermatocytes. We identified two Plus3 domain proteins enriched in spermatocytes, tPlus3a and tPlus3b. Their interaction with tBRD-1 indicates that they might as well be part of the testis transcription machinery (Chapter 9; Hundertmark et al., under review). Discussion on identified target genes and unpublished observations on a third Plus3 domain protein enriched in the testis can be found in Chapter 10.5.

10.1 Decondensation of chromatin enables detection of previously undetectable proteins in sperm

In the context of this thesis, a protocol for immunofluorescence-based detection of proteins in male germ cells is developed (Chapter 5; Hundertmark et al., 2017). It provides assistance for setting up first stainings and covers different germ cell stages. The spermatocyte stage is characterised by clearly separated chromosomal areas, which are visible in the nucleus with Hoechst staining. Proper staining and magnification can visualise proteins located over the chromosomal areas. The nucleolus and other

structures like nuclear speckles can likewise be detected this way and enable to distinguish protein expression in different compartments within the nucleus. Post-meiotic chromatin components, like Tpl94D, tHMG-1 and tHMG-2, are detectable transiently until the late canoe stage (Gärtner et al., 2015). Using standard immunofluorescence protocols transient expression until the canoe stage could also be observed for Prtl99C, which is suggested to compact post-meiotic chromatin. However, transgenic flies expressing Prtl99C-eGFP controlled by its own regulatory region revealed a persisting signal in mature sperm (Eren-Giani et al., 2015). This indicates that the antibody for Prtl99C might not be able to recognise the epitope due to the high compaction of the chromatin in mature sperm. In such cases, a variation of the standard immunofluorescence protocol can help to open the chromatin structure and therefore expose the epitope of Prtl99C, which was previously undetectable (Eren-Ghiani et al., 2015). Similar problems with detection of proteins in a highly compact chromatin environment were reported for other proteins as well (Miller et al., 2010). A variation in protocol with regard to decondensation of sperm chromatin is described in our study. It is unclear how many proteins in post-meiotic germ cell development could be affected by the strong compaction of chromatin and are therefore hard to detect. The formation of disulphide bridges between cysteines in the very basic sperm compacting proteins is one of the main factors for the chromatin stability (reviewed in Björndahl and Kvist, 2011). Release of disulphide bridges is required after fertilisation in order to decondense sperm chromatin, requiring a specific thioredoxin (Tirmarche et al., 2016). The above-mentioned examples suggest that the decondensation protocol developed in our study should accompany every analysis of post-meiotic chromatin component. An alternative could be the generation of transgenic flies expressing tagged fusion proteins or reporter lines expressing *lacZ* or fluorescent tags controlled by the regulatory region of a certain protein. The question if some chromatin components might not be detectable in sperm due to highly compact chromatin has also been asked for human spermatogenesis. Using chromatin decondensation, Li et al. could show that histone expression was partially overlapping with protamines in human sperm nuclei, although both were localised to different compartments of the nucleus (Li et al., 2008). Another publication describing the expression of key players during mouse and human spermatogenesis also discusses the possibility whether different fixation methods for immunohistology might yield aberrant expression patterns for some proteins (Klaus et al., 2016). These studies emphasise the importance of elaborated protocols for antibody staining on tissues with dynamic chromatin content.

10.2 Efficient synthesis of sperm chromatin packaging proteins depends on H3K18 and H3K27 acetylation

The histone-to-protamine transition during spermatogenesis implicates a compaction of chromatin. Although the exact reason for such a drastic alteration of the chromatin configuration is not fully understood, several functions for protamination have been proposed (reviewed in Rathke et al., 2014). It is still unclear what molecular mechanisms are required to accomplish the exchange of histones. A

remarkable wave of histone hyperacetylation can be observed directly before the histone-to-protamine switch in mammals (Meistrich et al., 1993) as well as in *Drosophila* (Rathke et al., 2007). Most propably, the acetylation status of histones is an essential factor for the incorporation of protamines. This was shown by *in vitro* studies using isolated nucleosomes (Oliva et al., 1987) and by inhibitor treatment of testes in an *in vitro* culture system (Awe and Renkawitz-Pohl, 2010; Gärtner et al., 2014). Treatment with the HAT inhibitor anacardic acid prevents maturation of sperm and incorporation of protamines. Notably, the inhibition of HDACs leads to an increased acetylation status yet in early spermiogenesis but not to a premature exchange of histones (Gärtner et al., 2014). Our study provides a detailed map of single histone acetylations, especially on histones H3 and H4, occurring during spermiogenesis as well as in the spermatocyte stage (Chapter 6; Hundertmark et al., 2018). While H4K5, H4K8 and H4K12 were acetylated continuously from spermatocytes until early canoe stage, H3 acetylation seemed to be generated *de novo* in post-meiotic stages. H3K9ac was detectable in spermatocytes and again in young elongating spermatids, which corresponds to the findings of Hennig and Weyrich (2013), who also detected H3K9ac in early spermatocytes and - after being absent - again in young spermatids. For the first time, we describe that acetylations on H3K14, H3K18, H3K23 and H3K27 occur in spermatocytes and later in canoe stage nuclei during *Drosophila* spermatogenesis. H3K9, H3K18 and H3K23 acetylation are also known features from post-meiotic spermatogenesis in mammals (Song et al., 2011).

Treatment with anacardic acid revealed that all of these acetylations are affected by inhibition of HATs. Anacardic acid inhibits a wide range of HATs, covering p300, PCAF and MYST families (Balasubramanyam et al., 2003; Sun et al., 2006). Unspecific inhibition by anacardic acid and the fact that few candidate enzymes have been identified to play a role in regulating histone acetylations in germ cells makes it difficult to evaluate the impact of HATs on specific histone acetylations. This thesis contributed to the characterisation of Nejire/dCBP, which belongs to the p300 HAT family, as a contributor to acetylation of H3K18 and H3K27 in spermatocytes and in canoe stage spermatids. Upon knock-down of *nejire* in germ cells both acetylations were not detectable anymore. A direct acetylation of H3K18 and H3K27 through Nejire/dCBP in the spermatocyte stage seems likely as the modifications could be detected simultaneously with Nejire/dCBP in this stage. H3K18ac and H3K27ac set by Nejire/dCBP were shown to be connected with transcriptional regulation in *Drosophila* embryos (Tie et al., 2016). This might be also a possible function in transcriptional highly active spermatocytes. Indeed, reduction of Nejire/dCBP in spermatocytes led to loss of H3K18ac and H3K27ac in spermatocytes and reduced transcript levels of *protA* and *prtl99C*. The *nejire/dCBP* transcript level after RNAi treatment is reduced to about one third of the wild-type level, which might explain the residual transcripts of *protA* and *prtl99C* (Hundertmark et al., 2018). However, the reduced transcript levels could also represent *nejire* transcripts in somatic cells, which are not affected by the RNAi knock-down. Clearly, we need further investigations to decide if Nejire/dCBP directly or indirectly regulates *protA* and *prtl99C* transcripts.

The post-meiotic function of Nejire/dCBP remains unclear because it is detected in late canoe stage spermatids while H3K18ac and H3K27ac were only visible in early canoe stage spermatids. This raises the question if another HAT expressed in post-meiotic germ cell stages might be responsible for acetylation of H3K18 and H3K27 in early canoe stage. Our proteome analysis revealed that, besides Nejire/dCBP, the HAT Hat1 is also expressed in *Drosophila* testes (Chapter 7; Gärtner et al., in preparation). Hat1 was shown to have a binding specificity for histone H4 (Boltengagen et al., 2016), suggesting that it is not directly involved in modifying H3. Thus, Hat1 can be considered as a potential candidate for acetylation of H4K5, H4K8 and H4K12 in germ cells rather than H3K18 and H3K27 acetylation. Nejire/dCBP remains the only enzyme with proven target specificity for H3K18 and H3K27 acetylation. In *Drosophila* embryogenesis, chromatin occupancy by Nejire/dCBP does not always entail an acetylation of histones at the respective sites. Nejire/dCBP was observed at sites of inactive genes but respective acetylation marks were missing in some cases. Instead, H3K27 tri-methylation was detected at these sites, which led to the assumption that histone acetylation by Nejire/dCBP might be repressed by H3K27 tri-methylation (Holmqvist et al., 2012). This might be an explanation for Nejire/dCBP detection in late canoe stage where it could represent a functionally repressed form of the enzyme, which is not able to acetylate histones due to presence of histone tri-methylation. However, presence of histones has not been described for late germ cell stages so far. Here, a sensitive antibody would be needed to detect potentially remaining amounts of histones or histone modifications.

An active form of Nejire/dCBP might not be detectable in early canoe stage due to a masked antibody epitope caused by stable integration of Nejire/dCBP in a protein complex. However, this explanation would then raise the question which function Nejire/dCBP performs in spermatocytes, as we are able to detect Nejire/dCBP in in this stage. There is still the possibility left that we only detect a functionally repressed form of Nejire/dCBP in spermatocytes as well while an active form is masked. It can also not be excluded that a yet undescribed HAT is expressed in germ cells to specifically modify H3K18 and H3K27 in post-meiotic germ cells.

Other candidates for post-meiotic acetylation of histones are given as supplementary information (Chapter 6; Table S1, Hundertmark et al., 2018). Taking into account our proteome data, the family of GNAT HATs is strongly represented in the testis (San, Naa20A, Naa20B, Naa30A, Naa30B, Naa40, Naa60, San, L(1)G0020, CG12560, Vnc, Gnpnat, CG4210, CG31730 and AANATL2). A well-known GNAT family member in *Drosophila* is Gcn5/PCAF. This protein is not detected in our testis proteome data but was shown to have HAT activity for histone H3 and H4 (Suganuma et al., 2008). Furthermore, a crosstalk between mammalian Gcn5/PCAF and CBP-mediated histone modifications has been described by Kornacki et al. (2015). Thus, HATs of the GNAT family could on the one hand influence modification of histones in cooperation with Nejire/dCBP and on the other hand directly set histone modifications themselves. Especially CG31730 and Naa60 might be candidates for enzymes

that catalyse histone modifications in post-meiotic stages as they are exclusively found in the adult or the pupal proteome, respectively.

Mof is a member of the MYST family, which comprises several HATs, and is known for acetylation of H4K16 (Schiemann et al., 2010). Our proteome data suggest that Mof is also expressed in the *Drosophila* testis, representing the only detected MYST family protein. Strikingly, apart from HAT activity, a recent study described a crotonylation activity for mammalian Mof as well as for CBP (Liu et al., 2017). Therefore, Nejire/dCBP and Mof are promising candidates for catalysing the post-meiotic histone crotonylation wave described in our study. CG1894 is a further HAT candidate, which might play a role in spermatogenesis. We could not detect CG1894 in the testes proteome but Heseding et al. (2017) described its presence in germ cells.

Combining our proteome data with the histone modification map in germ cells might yield new insights into the histone-to-protamine transition. Further proteins for the regulation of these histone modifications have to be postulated, as knock-down of *nejire* does not lead to a decreased incorporation of post-meiotic chromatin components while inhibition of global histone acetylation ceases protamination completely.

10.3 The *Drosophila melanogaster* testis proteome comprises several thousand proteins

Many studies deal with the analysis of expression in *Drosophila*, covering different tissues or developmental processes. The testis is a challenging tissue to study, nevertheless there is a wide range of transcriptome and proteome data available. A common problem for examination of testis tissue is often the presence of somatic cells, which are connected to the germ cells. Beside the testis sheath, the germ cell bundles are surrounded by somatic cyst cells. These are first removed during individualisation.

A large portion of transcripts is not directly translated in the transcriptional highly active spermatocyte phase but gradually during post-meiotic spermatogenesis. Therefore, transcriptome data provide an indication of protein expression throughout the testis, but it is difficult to predict protein expression at various stages of spermatogenesis. We generated proteome data for three different stages of testes development, enabling identification of proteins along with proceeding germ cell differentiation. Taken together the proteome data from all three stages we identified over 6000 proteins (Chapter 7; Table S1; Gärtner et al., under review). This widely expands existing proteome data from previous studies (Takemori et al., 2009; Wasbrough et al., 2010) and adds the utility of a staged proteome. So far, only a staged transcriptome exists for *Drosophila* testes. Vibranovski et al., (2009; SpermPress database) fractioned whole adult testes in three parts, representing mitotic germ cells until the spermatocyte stage, meiotic germ cells with dividing germ cells and finally post-meiotic germ cells

comprising mostly spermatid stages. However, RNA extracted with this method might be contaminated with other germ cell stages in the separated testis parts and should be handled carefully. Nevertheless, a comparison of these transcriptome data with our proteome data might yield new insights into transcripts that are translationally repressed.

RNAseq data generated by the modENCODE consortium might be a good source of information on the transcriptome of different developmental stages as well (Graveley et al., 2011). We identified CG8701 as part of the adult testes proteome but not of larval or pupal testes. Developmental RNAseq data already give a hint on the expression of *CG8701* transcripts, which are highly enriched in adult flies and hardly detectable in larval testes. This kind of comparison between transcriptome and proteome data might be useful, especially for germ cell-specifically expressed genes, as there will be no overlay of transcripts from germ cells with transcripts from somatic cells like cyst cells. For *CG8701*, a similar result can be observed in comparison to transcript data from the SpermPress database where its transcripts are enriched in the post-meiotic fraction (Vibranovski et al., 2009). Our proteome data will therefore contribute to the clarification of expression patterns of many transcripts and proteins.

10.4 Testis-specifically expressed BRD proteins regulate expression of a subset of target genes in cooperation with tTAFs

More than half of all annotated *Drosophila* genes are expressed in the testis (Chintapalli et al., 2007). So far, several multiprotein complexes have been described to regulate transcription for a large portion of the testis-expressed genes. A tTAF-containing TFIID complex together with the tMAC and the Mediator complex regulate thousands of genes. Meiotic arrest mutants as well as mutants for components of the Mediator complex terminate germ cell development in the spermatocyte stage, indicating that the regulated genes are already needed in a very early phase of spermatogenesis (reviewed in White-Cooper and Davidson, 2011; Lu and Fuller, 2015). It seems unlikely that such a large number of genes is regulated only by a few complexes and therefore, other proteins are suggested to play a role in the recognition of target genes. This thesis contributed to the identification of target genes for the BRD protein tBRD-1 and to the characterisation of two other testis-specifically expressed BRD proteins, tBRD-2 and tBRD-3 (Chapter 8; Theofel et al., 2014). *tbrd-1* mutants exhibit a phenotype different from the meiotic arrest mutant phenotype as the germ cells reach post-meiotic stages but do not further develop to mature sperm (Leser et al., 2012). Several hundred genes are up- or down-regulated in *tbrd-1* mutants and a comparison with genes regulated by the tTAF Sa revealed a set of 200 common target genes. We therefore suggest tBRD-1 as a further regulator of transcription in germ cells recognising acetylated histones via its bromodomains. Binding of acetylated histones is a common feature of bromodomain proteins. The affinity of proteins containing two bromodomains for acetylated histones is higher than of proteins featuring a single bromodomain (Dhalluin et al., 1999,

reviewed in Florence and Faller, 2001). BRDT is a mammalian bromodomain protein containing two bromodomains similar to tBRD-1; it was shown to regulate transcription in mouse germ cells (Gaucher et al., 2012). BRDT also comprises an ET domain and thus belongs to the BET family. Even though tBRD-1 does not have an ET domain, the two other BRD proteins expressed in the *Drosophila* testis, tBRD-2 and tBRD-3, contain a single bromodomain as well as an ET domain. In general, BET family members in animals contain more than one bromodomain whereas BET family members in plants are characterised by a single bromodomain (Florence and Faller, 2001). We concluded that tBRD-2 and tBRD-3 might represent a special variant of animal BET proteins. Strikingly, tBRD-1 and tBRD-2 are able to physically interact with each other providing a possible functional dependency between the two proteins. By their interaction, tBRD-1 and tBRD-2 could even display a heterodimer with all features of a BET family member as it was also suggested by Kimura and Loppin (2015). Indeed, in a subsequent study, it was shown that tBRD-2 co-regulates a subset of genes together with tBRD-1; more than half of the potential tBRD-2 target genes are shared with tBRD-1 (Theofel et al., 2017). This further strengthens the hypothesis that the BRDs contribute to a testis-specific mechanism of gene regulation. In the course of this study, it was also validated that tBRD-1 is able to bind acetylated histones tails *in vitro*. Interestingly, the opposite result was observed for tBRD-2, indicating that the tBRD-2 protein might need further interacting proteins to fulfil a function as a reader of histone acetylations (Theofel et al., 2017). We already observed that the subcellular localisation of tBRD-2 is depending on tBRD-1 function (Theofel et al., 2014). tBRD-1 might therefore be required for the recruitment of tBRD-2 to target sites. As both proteins seem to regulate a subset of genes also independent of each other, an interaction of tBRD-1 and tBRD-2 could be considered as transient until tBRD-2 has been directed to chromatin. It also seems possible that tBRD-1 has a higher affinity for some chromatin regions than tBRD-2, which is supported by the increased binding capacity of tBRD-1 to acetylated histone peptides *in vitro*. Additional interaction between tBRD-2 and tBRD-1 might further increase the binding affinity to even more histone acetylation sites.

However, the exact mechanism how the testis-specifically expressed BRD proteins in *Drosophila* regulate transcription is still unclear. They might bind acetylated histones in order to guide other proteins to specific target sites in the genome; this is supported by the interaction of tBRD-1 with some of the tTAFs (Theofel et al., 2014). Other functions for the BRDs cannot be excluded, since mammalian BRDT was shown to interact with components of the spliceosome and its N-terminal bromodomain is an essential feature for a testis-specific splicing mechanism (Berkovits et al., 2012). This might also apply for the BRDs in the *Drosophila* testis. It should be kept in mind that in *tbrd-1* mutants and in *tbrd-2* knock-down several genes are activated, indicating that transcription of these genes is usually repressed by the BRD proteins (Theofel et al., 2017). As some of these repressed targets are also shared with tTAFs, this might be a mechanism to silence genes which are not needed for germ cell development.

10.4.1 Unpublished observation: tBRD-3 might be dispensable for spermatogenesis

The least described protein of the three identified testis-specific expressed BRDs is tBRD-3. In the beginning of this thesis the elucidation of tBRD-3 function was prioritised. Beforehand, a P-element mobilisation had been carried out to generate loss-of-function mutants for *tbrd-3*. These mutants were fertile and anti-tBRD-3 immunofluorescence staining did not show any significant change in protein expression (Theofel PhD thesis, 2016). However, the P-element mobilisation might have been insufficient to generate a loss-of-function mutant. Additionally, the genome region in the *tbrd-3* mutant left the possibility of an alternative start codon, which would lead to a truncated form of tBRD-3. This thesis aimed to generate a *tbrd-3* mutant, which represents a loss-of-function mutant. Therefore, the CRISPR/Cas9 system was used to generate several *tbrd-3* mutant lines. Generation of transgenic flies for sgRNA strains and crossing to Cas9 strain was carried out as described in Kondo and Ueda (2013). The resulting mutants were screened for mutations within the region of the target construct via PCR and sequenced to determine the exact genomic situation. An alignment of mutant *tbrd-3* lines to the wild-type sequence is given in Appendix A. Two different sgRNA lines were used, each resulting in a mutation within the open reading frame. All generated mutations should result in a frame shift and therefore in nonsense translation for the downstream sequence. Line 2.30 yielded a STOP codon near the mutated site. The fly lines were analysed with anti-tBRD-3 immunofluorescence staining and in Western Blot experiments to see if a differential signal for tBRD-3 would be detectable. All of the examined mutant lines showed a wild-typic phenotype of the germ cells, the anti-tBRD-3 signal was still detectable in spermatocytes and was only slightly weaker in rare cases. Western Blot signals were comparable to the wild-type and flies were fertile. These results suggest that the antibody used for detection of tBRD-3 in immunofluorescence staining and Western Blot might be insufficient to properly detect the tBRD-3 protein. The described mutations should clearly result in a loss-of-function for *tbrd-3* as the region coding for its bromodomain was always affected. As the flies were still fertile and did not exhibit an obvious phenotype we concluded that tBRD-3 might not be essential for spermatogenesis. It cannot be excluded that the other bromodomain proteins are able to replace the function of tBRD-3. Other studies carried out for tBRD-3 could not identify the protein in mass spectrometric data for tBRD-1 pulldown experiments, suggesting that it is not part of a complex with tBRD-1 (Kimura and Loppin, 2015). However, our proteome data revealed low levels for tBRD-3 in larval and pupal testes, indicating that the protein is expressed in germ cells (Chapter 7). The results for the *tbrd-3* mutant generation let us to assume that the *tbrd-3* gene could be the product of a gene duplication, which might have either lost its functionality for spermatogenesis over time or might have never had one.

10.5 Plus3 domain proteins support transcriptional regulation in *Drosophila* spermatocytes

We aimed to identify further proteins besides BRD proteins which might act as transcription factors or as interaction partners of such in *Drosophila* germ cells. The Paf1 complex is a promising candidate as its role in transcription has been described for many species (reviewed in Tomson and Arndt, 2013). In our large-scale proteomic approach we found components of Paf1C in the testis (Chapter 7). Rtf1, Cdc73 (Hyrax) and Ctr9 were present from larval to adult testes, while Leo1 (Another transcription unit) and Paf1 (Antimeros) were not detected in any stage. Leo1 and Paf1 might not have been detected due to low expression levels of the proteins in testis tissue. Furthermore, it cannot be excluded that yet undescribed paralogues exist in the testis as it was observed for the tTAFs or the tMAC complex (Hiller et al., 2004; Beall et al., 2007). However, previous studies on *Drosophila* Rtf1 described that it can also be observed while not associated with other Paf1C components (Adelman et al., 2006). These findings indicate that Rtf1 might be able to fulfil a function without other Paf1C components; this is further supported by results for human Rtf1 (Kim et al., 2010).

A database search (Flybase) identified further genes with coding capacity for Plus3 domain proteins and enrichment of corresponding transcripts in the testis. *In situ* hybridisation indeed revealed transcripts in the spermatocyte phase for *CG12498* (Dottermusch-Heidel and Renkawitz-Pohl unpublished). In agreement with that, our proteome data suggested that, apart from ubiquitously expressed Rtf1, further Plus3 domain-containing proteins are expressed in the *Drosophil*a testis, tPlus3a, tPlus3b, and CG12498. tPlus3b was detected in larval and pupal testes while tPlus3a was not observed in any stage. Due to the nearly identical amino acid sequence it is not clear if both proteins could be discriminated from each other in a proteome analysis. Main objective of this thesis was the analysis of expression and function of *tplus3a* and *tplus3b* as testis enriched Plus3 domain protein coding genes (Chapter 9; Hundertmark et al., under review). tPlus3a/tPlus3b share a conserved Plus3 domain with Rtf1 featuring all amino acids which are important for the secondary structure of the domain. In contrast, the histone modification domain of Rtf1 cannot be found in tPlus3/tPlus3b, suggesting that the testis-enriched Plus3 domain proteins are not directly involved in the modification of histones. Nevertheless, they might still be part of a protein complex performing this function. The Plus3 domain structure has been analysed best for human Rtf1. De Jong et al. (2008) described the *in vitro* formation of a protein-DNA complex using either single stranded DNA or by mimicking a transcription bubble in addition with a recombinant Rtf1 Plus3 domain. This experiment indicates that the Plus3 domain of Rtf1 might have a function in binding single-stranded DNA, possibly in order to associate with open reading frames on active transcription sites. A deletion of parts of the Plus3 domain in yeast Rtf1 was reported to cause dissociation of Rtf1 from open reading frames (Warner et al., 2007). Furthermore, the Plus3 domain of Rtf1 was shown to be important for recruitment of Spt5,

a general factor involved in transcription elongation (Wier et al., 2013). These studies on Rtf1 function and especially its Plus3 domain led us to consider a similar function for tPlus3a/tPlus3b.

In our RNAseq data for *tplus3a/tplus3b*-deficient flies we found many up- and down-regulated genes. Among the down-regulated genes, *kl-3* and *kl-5* are male fertility factors, which are coded on the *Drosophila* Y-chromosome (Brosseau, 1959). This is also the case for *ory*, coding for an Occludin-related protein (Carvalho et al., 2000). While *kl-3* and *kl-5* genes are transcribed, distinct structures, the so-called lampbrush loops, are formed and represent the respective gene activation (Bonaccorsi et al., 1988). The Y-chromosomal fertility factors are encoded in huge genomic loci, spanning millions of base pairs with large introns (Gatti and Pimpinelli, 1983). We observed tPlus3a/tPlus3b localisation in the nucleus of spermatocytes; some spots seemed to contrast from other areas of the nucleus. These spots might represent tPlus3a/tPlus3b localisation at the lampbrush loops. We therefore hypothesise that tPlus3a/tPlus3b regulate transcription of the Y-chromosomal fertility factors *kl-3* and *kl-5* by association with the large area reflecting the active transcription of these genes. As described above, the Plus3 domain of Rtf1 is presumably able to bind single-stranded DNA and specifically associates with transcriptional active open reading frames. This mechanism could also serve for gene regulation by tPlus3a/tPlus3b. The extremely extensive transcriptional areas might be stabilised by binding of tPlus3a/tPlus3b to the open reading frames of the fertility factors.

Another possible option how tPlus3a/tPlus3b could regulate gene expression is the participation in the 3'-end formation as reported by Nordick et al. (2008) for yeast Rtf1. Rtf1 was shown to be crucial for the recruitment of other proteins to RNA Pol II during transcription elongation. However, this hypothesised function for tPlus3a/tPlus3b requires further investigations as Rtf1 is a constant part of the Paf1C while, so far, tPlus3a/tPlus3b were only shown to interact with tBRD-1 in our study. However, we did not test interaction of tPlus3a/tPlus3b with Paf1C components. The partial conservation of the C-terminal protein interaction domain of tPlus3a/tPlus3b suggests that it might share interaction partners of Rtf1. De Jong et al. (2008) raised the question how stable human Rtf1 association with other Paf1C components is and how this influences its function. They proposed a transient role for Rtf1 in transcription regulation as Paf1C is still able to interact with RNA Pol II when Rtf1 is absent. A mechanism of transcription regulation, which is rather focussed on a small and specific gene set, could also be conceivable for tPlus3a/tPlus3b. The gene set regulated by tPlus3a/tPlus3b is much smaller than the ones regulated by tBRD-1 or other testis-specific transcription complexes, like the tTAF-containing TFIID or tMAC, indicating that tPlus3a/tPlus3b might fulfil a specified function for only a few genes. In general, many transcipts of germ line expressed genes are down-regulated and those of genes expressed in the soma of the reproductive system are up-regulated in *tplus3a/tplus3b* mutant testes. If these genes are directly or indirectly regulated by tPlus3a/tPlus3b needs to be determined by biochemical assays.

10.5.1 Unpublished observation: testis-enriched CG12498 might complement the function of tPlus3a/tPlus3b

CG12498 is a fourth gene coding for a Plus3 domain-containing protein in *Drosophila*. Our protein alignment revealed that the Plus3 domain of CG12498 is conserved as well (Chapter 9). Previous experiments aimed to identify the expression of CG12498. *In situ* hybridisation revealed that *CG12498* transcripts are expressed in early germ cell stages. Unfortunately, the generation of transgenic flies expressing CG12498-mCherry under the control of its own regulatory region yielded no observable signal in spermatocytes or other germ cells (Dottermusch-Heidel and Renkawitz-Pohl unpublished data). However, we found CG12498 in our proteome data as part of all examined testis stages, indicating that the protein is indeed expressed and might as well play a role for germ cell development.

To fully understand the function of Plus3 domain-containing proteins in the testis, the generation of *CG12498* mutants was the next step, aiming to get a loss-of-function mutant for further analysis. Making use of the CRISPR/Cas9 system (Kondo and Ueda, 2013) we first generated transgenic flies for three individual sgRNAs of which only one turned out to be functional for mutagenesis. The screening of the resulting offspring after crossing with a Cas9 fly strain revealed several different mutant lines, representative examples of deletions and insertions are depicted in Appendix B. Most of the deletions would result in a frame shift shortly after the start codon of *CG12498* yielding nonsense information for the downstream open reading frame. This was the case for line 1.1, which carried a deletion of 14 base pairs and was used for further experiments. *CG12498* mutant line 1.1 was analysed with fertility tests, revealing that the flies were male fertile. However, when line 1.1 was crossed together with Δ*tplus3a/tplus3b* mutants *in trans* with *Df(2L)BSC151* the resulting males, deficient for all three Plus3 domain-containing protein coding genes, were completely sterile. A first analysis of these flies showed no obvious change in phenotype compared to Δ*tplus3a/tplus3b/Df(2L)BSC151* males that exhibit reduced fertility (described in chapter 9). These results suggest that tPlus3a/tPlus3b function in Δ*tplus3a/tplus3b/Df(2L)BSC151* males might be partially replaced by CG12498, while flies deficient for all three genes are sterile. CG12498 alone does not seem to be essential for spermatogenesis as mutant flies do not have a mutant phenotype.

It has to be kept in mind that off-target effects can occur using the CRISPR/Cas9 system. We minimised the risk for an influence of off-target effects on further experiments for Δ*tplus3a/tplus3b* mutants by keeping Δ*tplus3a/tplus3b in trans* with *Df(2L)BSC151* deficiency. However, this is hardly possible for *CG12498* mutants as this gene is located on the X chromosome. A generation of CG12498 transgenic flies and a subsequent rescue experiment might be able to rule out off-target effects. In summary, Plus3 domain-containing proteins seem to play a vital role for spermatogenesis, guaranteeing efficient transcription in spermatocytes and contributing to the male germ line specific transcriptional programme.

10.6 References

Adelman, K., Wei, W., Ardehali, M.B., Werner, J., Zhu, B., Reinberg, D. and Lis, J.T. (2006). *Drosophila* Paf1 modulates chromatin structure at actively transcribed genes. Mol Cell Biol. 2006 Jan; 26(1):250-60

Awe, S. and Renkawitz-Pohl R. (2010). Histone H4 acetylation is essential to proceed from a histone- to a protamine-based chromatin structure in spermatid nuclei of *Drosophila melanogaster*. Syst. Biol. Reprod. Med. 2010 Feb; 44–61

Balasubramanyam, K., Swaminathan, V., Ranganathan, A. and Kundu, T.K. (2003). Small molecule modulators of histone acetyltransferase p300. J Biol Chem. 2003 May; 278(21):19134-40

Beall, E.L., Lewis, P.W., Bell, M., Rocha, M., Jones, D.L. and Botchan, M.R. (2007). Discovery of tMAC: a *Drosophila* testis-specific meiotic arrest complex paralogous to Myb-Muv B. Genes Dev. 2007 Apr; 21(8):904-19

Berkovits, B.D. and Wolgemuth, D.J. (2011). The first bromodomain of the testis-specific double bromodomain protein Brdt is required for chromocenter organization that is modulated by genetic background. Dev Biol. 2011 Dec; 360(2):358-68. doi: 10.1016/j.ydbio.2011.10.005

Björndahl, L. and Kvist, U. (2011). A model for the importance of zinc in the dynamics of human sperm chromatin stabilization after ejaculation in relation to sperm DNA vulnerability. Syst Biol Reprod Med. 2011 Feb; 57(1-2):86-92. doi: 10.3109/19396368.2010.516306

Boltengagen, M., Huang, A., Boltengagen, A., Trixl, L., Lindner, H., Kremser, L., Offterdinger, M. and Lusser, A. (2016). A novel role for the histone acetyltransferase Hat1 in the CENP-A/CID assembly pathway in *Drosophila melanogaster*. Nucleic Acids Res. 2016 Mar; 44(5):2145-59. doi: 10.1093/nar/gkv1235

Bonaccorsi S., Pisano C., Puoti F. and Gatti M. (1988). Y chromosome loops in *Drosophila melanogaster*. Genetics. 1988 Dec; 120(4):1015-34

Brosseau, G.E.Jr. (1959). Genetic analysis of the male fertility factors on the Y chromosome of *Drosophila melanogaster*.

Carvalho, A.B., Dobo, B.A., Vibranovski, M.D. and Clark, A.G. (2000). Identification of five new genes on the Y chromosome of *Drosophila melanogaster*. Proc Natl Acad Sci USA. 2001 Nov; 98(23):13225-30

Chintapalli, V.R., Wang, J. and Dow, J.A. (2007). Using FlyAtlas to identify better *Drosophila* models of human disease. Nature Genetics. 2007 Jun; 39:715–720,

De Jong, R.N., Truffault, V., Diercks, T., Ab, E., Daniels, M.A., Kaptein, R. and Folkers, G.E. (2008). Structure and DNA binding of the human Rtf1 Plus3 domain. Structure. 2008 Jan; 16(1):149-59. doi: 10.1016/j.str.2007.10.018

Dhalluin, C., Carlson, J.E., Zeng, L., He, C., Aggarwal, A.K. and Zhou, M.M. (1999). Structure and ligand of a histone acetyltransferase bromodomain. Nature. 1999 Jun; 399(6735):491-6

Eren-Ghiani, Z., Rathke, C., Theofel, I. and Renkawitz-Pohl, R. (2015). Prtl99C Acts Together with Protamines and Safeguards Male Fertility in *Drosophila*. Cell Rep. 2015 Dec; 13(11):2327-2335. doi: 10.1016/j.celrep.2015.11.023

Florence, B. and Faller, D.V. (2001). You bet-cha: a novel family of transcriptional regulators. Front Biosci. 2001 Aug; 6:D1008-18. Review

Gärtner, S.M.K., Hundertmark, T., Nolte, H., Tetzner, C., Theofel, I., Eren-Ghiani, Z., Duchow, T.B., Rathke, C., Krüger, M. and Renkawitz-Pohl, R. (under review). Stage-specific proteomes of the *Drosophila melanogaster* testes. Manuscript under review.

Gärtner, S.M., Rathke, C., Renkawitz-Pohl, R. and Awe, S. (2014). Ex vivo culture of *Drosophila* pupal testis and single male germ-line cysts: dissection, imaging, and pharmacological treatment. J Vis Exp. 2014 Sep; (91):51868. doi: 10.3791/51868

Gärtner, S.M., Rothenbusch, S., Buxa, M.K., Theofel, I., Renkawitz, R., Rathke, C. and Renkawitz-Pohl, R. (2015). The HMG-box-containing proteins tHMG-1 and tHMG-2 interact during the histone-to-protamine transition in *Drosophila* spermatogenesis. Eur J Cell Biol. 2015 Jan; 94(1):46-59. doi: 10.1016/j.ejcb.2014.10.005

Gatti, M. and Pimpinelli, S. (1983). Cytological and genetic analysis of the Y chromosome of *Drosophila melanogaster*. 1983 Nov; (88)5, pp349-373

Gaucher, J., Boussouar, F., Montellier, E., Curtet, S., Buchou, T., Bertrand, S., Hery, P., Jounier, S., Depaux, A., Vitte, A.L., Guardiola, P., Pernet, K., Debernardi, A., Lopez, F., Holota, H., Imbert, J., Wolgemuth, D.J., Gérard, M., Rousseaux, S. and Khochbin, S. (2012). Bromodomain-dependent stage-specific male genome programming by Brdt. EMBO J. 2012 Oct; 31(19):3809-20. doi: 10.1038/emboj.2012.233

Graveley, B.R., Brooks, A.N., Carlson, J.W., Duff, M.O., Landolin, J.M., Yang, L., Artieri, C.G., van Baren, M.J., Boley, N., Booth, B.W., Brown, J.B., Cherbas, L., Davis, C.A., Dobin, A., Li, R., Lin, W., Malone, J.H., Mattiuzzo, N.R., Miller, D., Sturgill, D., Tuch, B.B., Zaleski, C., Zhang, D., Blanchette, M., Dudoit, S., Eads, B., Green, R.E., et al. (2011). The developmental transcriptome of *Drosophila melanogaster*. Nature. 2011 Mar; 471(7339):473-9. doi: 10.1038/nature09715

Hennig, W. and Weyrich, A. (2013). Histone modifications in the male germ line of *Drosophila*. BMC Dev Biol. 2013 Feb; 13:7. doi: 10.1186/1471-213X-13-7

Heseding, C., Saumweber, H., Rathke, C. and Ehrenhofer-Murray, A.E. (2017). Widespread colocalization of the *Drosophila* histone acetyltransferase homolog MYST5 with DREF and insulator proteins at active genes. Chromosoma. 2017 Feb; 126(1):165-178. doi: 10.1007/s00412-016-0582-9

Hiller, M., Chen, X., Pringle, M.J., Suchorolski, M., Sancak, Y., Viswanathan, S., Bolival, B., Lin, T.Y., Marino, S. and Fuller, M.T. (2004). Testis-specific TAF homologs collaborate to control a tissue-specific transcription program. Development. 2004 Nov; 131(21):5297-308

Holmqvist, P.H., Boija, A., Philip, P., Crona, F., Stenberg, P. and Mannervik, M. (2012). Preferential genome targeting of the CBP co-activator by Rel and Smad proteins in early Drosophila melanogaster embryos. PLoS Genet. 2012; 8(6):e1002769. doi: 10.1371/journal.pgen.1002769

Hundertmark, T., Gärtner, S.M.K., Rathke, C. and Renkawitz-Pohl, R. (in press). Nejire/dCBP-mediated histone H3 acetylation during spermatogenesis is essential for male fertility in *Drosophila melanogaster*. Manuscript in press in PlosOne.

Hundertmark, T., Kreutz, S., Merle, N., Nist, A., Lamp, B., Stiewe, T., Brehm, A., Renkawitz-Pohl, R. and Rathke, R. (under review). *Drosophila melanogaster* tPlus3a and tPlus3b ensure full male fertility by regulating transcription of Y-chromosomal, sperm fluidity, and heat shock genes. Manuscript under review.

Hundertmark, T., Theofel, I., Eren-Ghiani, Z., Miller, D. and Rathke, C. (2017). Analysis of chromatin dynamics during *Drosophila* spermatogenesis. Methods Mol Biol. 2017; 1471:289-303. doi: 10.1007/978-1-4939-6340-9_17

Kim, J., Guermah, M. and Roeder, R.G. (2010). The human PAF1 complex acts in chromatin transcription elongation both independently and cooperatively with SII/TFIIS. Cell. 2010 Feb; 140(4):491-503. doi: 10.1016/j.cell.2009.12.050

Kimura, S. and Loppin, B. (2015). Two bromodomain proteins functionally interact to recapitulate an essential BRDT-like function in *Drosophila* spermatocytes. Open Biol. 2015 Feb; 5(2):140145. doi: 10.1098/rsob.140145Klaus, E.S., Gonzalez, N.H., Bergmann, M., Bartkuhn, M., Weidner, W., Kliesch, S. and Rathke, C. (2016). Murine and human spermatids are characterized by numerous, newly synthesized and differentially expressed transcription factors and bromodomain-containing proteins. Biol Reprod. 2016 Jul; 95(1):4. doi: 10.1095/biolreprod.115.137620

Kondo, S. and Ueda, R. (2013). Highly improved gene targeting by germline-specific Cas9 expression in *Drosophila*. Genetics. 2013 Nov; 195(3):715-21. doi: 10.1534/genetics.113.156737

Kornacki, J.R., Stuparu, A.D. and Mrksich, M. (2015). Acetyltransferase p300/CBP associated Factor (PCAF) regulates crosstalk-dependent acetylation of histone H3 by distal site recognition. ACS Chem Biol. 2015 Jan; 10(1):157-64. doi: 10.1021/cb5004527

Leser, K., Awe, S., Barckmann, B., Renkawitz-Pohl, R. and Rathke, C. (2012). The bromodomain-containing protein tBRD-1 is specifically expressed in spermatocytes and is essential for male fertility. Biol Open. 2012 Jun; 1(6):597-606. doi: 10.1242/bio.20121255

Li, Y., Lalancette, C., Miller, D. and Krawetz, S.A. (2008). Characterization of nucleohistone and nucleoprotamine components in the mature human sperm nucleus. Asian J Androl. 2008 Jul; 10(4):535-41. doi: 10.1111/j.1745-7262.2008.00410.x

Liu, X., Wei, W., Liu, Y., Yang, X., Wu, J., Zhang, Y., Zhang, Q., Shi, T., Du, J.X., Zhao, Y., Lei, M., Zhou, J.Q., Li, J. and Wong, J. (2017). MOF as an evolutionarily conserved histone crotonyltransferase and transcriptional activation by histone acetyltransferase-deficient and crotonyltransferase-competent CBP/p300. Cell Discov. 2017 May; 3:17016. doi: 10.1038/celldisc.2017.16

Lu, C. and Fuller, M.T. (2015). Recruitment of Mediator complex by cell type and stage-specific factors required for tissue-specific TAF dependent gene activation in an adult stem cell lineage. PLoS Genet. 2015 Dec; 11(12):e1005701. doi: 10.1371/journal.pgen.1005701

Matangkasombut, O., Buratowski, R.M., Swilling, N.W. and Buratowski, S. (2000). Bromodomain factor 1 corresponds to a missing piece of yeast TFIID. Genes Dev. 2000 Apr; 14(8):951-62

Meistrich, M.L., Trostle-Weige, P.K., Lin, R., Bhatnagar, Y.M. and Allis, C.D. (1993). Highly acetylated H4 is associated with histone displacement in rat spermatids. Mol Reprod Dev. 1992 Mar; 31(3):170-81

Miller, D., Brinkworth, M. and Iles, D. (2010). Paternal DNA packaging in spermatozoa: more than the sum of its parts? DNA, histones, protamines and epigenetics. Reproduction. 2010 Feb; 139(2):287-301. doi: 10.1530/REP-09-0281

Nordick, K., Hoffman, M.G., Betz, J.L. and Jaehning, J.A. (2008). Direct interactions between the Paf1 complex and a cleavage and polyadenylation factor are revealed by dissociation of Paf1 from RNA polymerase II. Eukaryot Cell. 2008 Jul; 7(7):1158-67. doi: 10.1128/EC.00434-07

Oliva, R., Bazett-Jones, D., Mezquita, C. and Dixon, G.H. (1987). Factors affecting nucleosome disassembly by protamines *in vitro*. Histone hyperacetylation and chromatin structure, time dependence, and the size of the sperm nuclear proteins. J Biol Chem. 1987 Dec 15; 262(35):17016-25

Rathke, C., Baarends, W.M., Awe, S. and Renkawitz-Pohl, R. (2014). Chromatin dynamics during spermiogenesis. Biochim Biophys Acta. 2014 Mar; 1839(3):155-68. doi:10.1016/j.bbagrm. 2013.08.004

Rathke, C., Baarends, W.M., Jayaramaiah-Raja, S., Bartkuhn, M., Renkawitz, R. and Renkawitz-Pohl, R. (2007). Transition from a nucleosome-based to a protamine-based chromatin configuration during spermiogenesis in *Drosophila*. J Cell Sci. 2007 May; 120(Pt 9):1689-700

Schiemann, A.H., Li, F., Weake, V.M., Belikoff, E.J., Klemmer, K.C., Moore, S.A. and Scott, M.J. (2010). Sex-biased transcription enhancement by a 5' tethered Gal4-MOF histone acetyltransferase fusion protein in *Drosophila*. BMC Mol Biol. 2010 Nov; 11:80. doi: 10.1186/1471-2199-11-80

Song, N., Liu, J., An, S., Nishino, T., Hishikawa, Y. and Koji, T. (2011). Immunohistochemical analysis of histone H3 modifications in germ cells during mouse spermatogenesis. Acta Histochem Cytochem. 2011 Aug; 44(4):183-90. doi: 10.1267/ahc.11027

Suganuma, T., Gutiérrez, J.L., Li, B., Florens, L., Swanson, S.K., Washburn, M.P., Abmayr, S.M. and Workman, J.L. (2008). ATAC is a double histone acetyltransferase complex that stimulates nucleosome sliding. Nat Struct Mol Biol. 2008 Apr; 15(4):364-72. doi: 10.1038/nsmb.1397

Sun, Y., Jiang, X., Chen, S. and Price, B.D. (2006). Inhibition of histone acetyltransferase activity by anacardic acid sensitizes tumor cells to ionizing radiation. FEBS Lett. 2006 Aug; 580(18):4353-6

Takemori, N. and Yamamoto, M.T. (2009). Proteome mapping of the *Drosophila melanogaster* male reproductive system. Proteomics. 2009 May; 9(9):2484-93. doi: 10.1002/pmic.200800795

Theofel, I. (2016). The bromodomain protein tBRD-1 interacts with the BET family members tBRD-2 and tBRD-3 and is required for gene activation in *Drosophila* male germ cells. Phillips-Universität Marburg

Theofel, I., Bartkuhn, M., Boettger, T., Gärtner, S.M.K., Kreher, J., Brehm, A. and Rathke, C. (2017). tBRD-1 and tBRD-2 regulate expression of genes necessary for spermatid differentiation. Biol Open. 2017 Apr; 6(4):439-448. doi: 10.1242/bio.022467.

Theofel, I., Bartkuhn, M., Hundertmark, T., Boettger, T., Gärtner, S.M., Leser, K., Awe, S., Schipper, M., Renkawitz-Pohl, R. and Rathke, C. (2014). tBRD-1 selectively controls gene activity in the *Drosophila* testis and interacts with two new members of the bromodomain and extra-terminal (BET) family. PLoS One. 2014 Sep; 9(9):e108267. doi: 10.1371/journal.pone.0108267

Tie, F., Banerjee, R., Fu, C., Stratton, C.A., Fang, M. and Harte, P.J. (2016). Polycomb inhibits histone acetylation by CBP by binding directly to its catalytic domain. Proc Natl Acad Sci USA. 2016 Feb; 113(6):E744-53. doi: 10.1073/pnas.1515465113

Tirmarche, S., Kimura, S., Dubruille, R., Horard, B. and Loppin, B. (2016). Unlocking sperm chromatin at fertilization requires a dedicated egg thioredoxin in *Drosophila*. Nat Commun. 2016 Nov 23; 7:13539. doi: 10.1038/ncomms13539

Tomson, B.N. and Arndt, K.M. (2013). The many roles of the conserved eukaryotic Paf1 complex in regulating transcription, histone modifications, and disease states. Biochim Biophys Acta. 2013 Jan; 1829(1):116-26. doi: 10.1016/j.bbagrm.2012.08.011. Review

Vibranovski, M.D., Lopes, H.F., Karr, T.L. and Long, M. (2009). Stage-specific expression profiling of *Drosophila* spermatogenesis suggests that meiotic sex chromosome inactivation drives genomic relocation of testis-expressed genes. PLoS Genet. 2009 Nov; 5(11):e1000731. doi: 10.1371/journal.pgen.1000731

Warner, M.H., Roinick, K.L. and Arndt, K.M. (2007). Rtf1 is a multifunctional component of the Paf1 complex that regulates gene expression by directing cotranscriptional histone modification. Mol Cell Biol. 2007 Sep; 27(17):6103-15

Wasbrough, E.R., Dorus, S., Hester, S., Howard-Murkin, J., Lilley, K., Wilkin, E., Polpitiya, A., Petritis, K. and Karr, T.L. (2010). The *Drosophila melanogaster* sperm proteome-II (DmSP-II). J Proteomics. 2010 Oct; 73(11):2171-85. doi: 10.1016/j.jprot.2010.09.002

White-Cooper, H. and Davidson, I. (2011). Unique aspects of transcription regulation in male germ cells. Cold Spring Harb Perspect Biol. 2011 Jul; 3(7). pii: a002626. doi: 10.1101/cshperspect.a002626. Review

Wier, A.D., Mayekar, M.K., Héroux, A., Arndt, K.M. and VanDemark, A.P. (2003). Structural basis for Spt5-mediated recruitment of the Paf1 complex to chromatin. Proc Natl Acad Sci USA. 2013 Oct; 110(43):17290-5. doi: 10.1073/pnas.1314754110

Chapter 11

Erklärung

Ich versichere hiermit, dass ich die vorliegende Dissertation „Nejire/dCBP-mediated control of H3 acetylation and transcriptional regulation by testis-specific Plus3 domain proteins during *Drosophila* spermatogenesis" unter der Leitung von Frau Professor Dr. Renate Renkawitz-Pohl und Frau Dr. Christina Pütz-Rathke (Fachbereich Biologie, Philipps-Universität Marburg) selbst und ohne fremde Hilfe verfasst und keine anderen als die in ihr angegebenen Quellen oder Hilfsmittel benutzt habe. Alle den Quellen wörtlich oder sinngemäß übernommenen Zitate wurden als solche kenntlich gemacht.

Die Dissertation wurde in der vorliegenden oder einer ähnlichen Form noch bei keiner anderen in- oder ausländischen Hochschule anlässlich eines Promotionsgesuchs eingereicht und hat noch keinen sonstigen Prüfungszwecken gedient.

Marburg, den

(Tim Hundertmark)

Appendices

Appendix A

```
                                    TARGET SEQUENCE PAM
WT    ACTGAACGGTCCTCGCCGGAAATTAATGCCTGCAAGGTGATTATTAAAAGGT WT
2.1   ACTGAACGGTCCTCGCCGGAAATTAATGC----AAGGTGATTATTAAAAGGT -4
2.9   ACTGAACGGTCCTCGCCGGAAATTAATGCaaggCTGCAAGGTGATTATTAAA +4
2.20  ACTGAACGGTCCTCGCCGGAAATTAATGCC-GCAAGGTGATTATTAAAAGGT -1
2.22  ACTGAACGGTCCTCGCCGGAA----------GGTGATTATTAAAAGGT -14
2.30  ACTGAACGGTCCTCGCCGGAAATTAAT---T--AAGGTGATTATTAAAAGGT -3,-2
2.46  ACTGAACGGTCCTCGCCGGAAATTAATGC--GCAAGGTGATTATTAAAAGGT -2

WT    AAGGTTGTTTTCCAGTACCTATAAGAATATTGCTTGGGTTTTCTACGAGCCA WT
3.10  AAGGTTGTTTTCCAGTACCTATAAGAATA-cGacgGGGTTTTCTACGAGCCA -1,+4
3.36  AAGGTTGTTTTCCAGTACCTATAAGAAT-TTGCTTGGGTTTTCTACGAGCCA -1
3.49  AAGGTTGTTTTCCAGTACCTATAAGAATAT----aGGGTTTTCTACGAGCCA -4,+1
```

Appendix A: CRISPR/Cas9-mediated mutagenesis of *tbrd-3*. Depicted are two *tbrd-3* sequences containing the target sequence (green) and the PAM sequence (blue) for guidance of Cas9. Wild-type (WT) sequence aligned to sequences of different mutants. Orange letters indicate an insertion. Numbers preceding the sequence (highlighted in yellow) indicate the name of the respective mutant line. Highlighted in grey are the numbers of the deleted (-) or inserted (+) base pairs in the respective mutant.

Appendix B

```
                                    TARGET SEQUENCE PAM
WT    AAAATTGTTCGAATGTTGATTGAGGAAACCTTTTTGGCGAAGCTCACATAAG WT
1.1   AAAATTGTTCGAATGTTGATT----------GGCGAAGCTCACATAAG -14
1.2   AAAATTGTTCGAATGTTGATTGAGGAAA--TgTtgaTTTGGCGAAGCTCACA -2,+4
1.3   AAAATTGTTCGAATGTTGATTGAGGAA-----TTTGGCGAAGCTCACATAAG -5
1.4   AAAATTGT--------------------TTTTTGGCGAAGCTCACATAAG -22
1.7   AAAATTGTTCGAATGTTGATTGAGGAAA--TTgaTTTGGCGAAGCTCACATA -2,+2
1.9   AAAATTGTTCGAATGTTGATTGAG-------TTTTGGCGAAGCTCACATAAG -7
1.10  AAAATTG-------------------------TTGGCGAAGCTCACATAAG -26
1.11  AAAATTGTTCGAATGTTGATT------------TGGCGAAGCTCACATAAG -13
1.12  AAAATTGTT----TccTGATTG----------TTTGGCGAAGCTCACATAAG -4,+2,-10
1.15  AAAATTGTTCGAATGTTGATTGAGGAA----------GCTCACATAAG -14
1.16  AAAATTGTTCGAATGTTGATTGAGGAAACC---ccGGCGAAGCTCACATAAG -3,+2
1.18  AAAATTGT-----------------------------TCACATAAG -35
1.19  AAAATTGTTCGAATG----------------TTGGCGAAGCTCACATAAG -18
1.20  AAAATTGTTCGAATGTTGATTGAGGA-----TTTTGGCGAAGCTCACATAAG -5
```

Appendix B: CRISPR/Cas9-mediated mutagenesis of *CG12498*. Depicted is the *CG12498* sequence containing the target sequence (green) and the PAM sequence (blue) for guidance of Cas9. Wild-type (WT) sequence aligned to sequences of different mutants. Orange letters indicate an insertion. Numbers preceding the sequence (highlighted in yellow) indicate the name of the respective mutant line. Highlighted in grey are the numbers of the deleted (-) or inserted (+) base pairs in the respective mutant